Hydrological modelling in the meso scale semiarid region of Wadi Kafrein / Jordan

-The use of innovative techniques under data scarcity-

Dissertation
zur Erlangung des Doktorgrades
der Mathematisch-Naturwissenschaftlichen Fakultäten
der Georg-August-Universität zu Göttingen

vorgelegt von

William Alkhoury

aus Amman

Göttingen 2011

D 7

Referentin/Referent: Prof. Dr. M. Sauter
Korreferentin/Korreferent: Prof. Dr. E. Salameh
Tag der mündlichen Prüfung: 18. April 2011

Acknowledgment

Most of all, I am grateful to God, who was a source of inspiration and blessing to me all through my PhD. The first person I want to thank is my supervisor Prof. Dr. Martin Sauter, to whom I am so much indebted for his invaluable support over the course of my PhD research. Prof. Sauter not only supported me from the scientific point of view but he also believed in my work and when I faced critical obstacles and challenges he gave a great support, especially at the start of my thesis. His enthusiasm and our valuable scientific discussions were of great importance for the development of my research. His continuous support from the beginning until the end of my research is highly appreciated.

I am also very indebted to another scientific legend who never hesitated to support me in all available means, starting from the valuable scientific discussions and ending with the support in contacting official and governmental institutions. Prof. Dr. Elias Salameh was the main scientific and administrative support who helped me in my scientific research and field work in Jordan over a period of several months. I am grateful to Prof. Salameh for being my second supervisor and for reviewing my manuscript.

Another key individual who helped guide me during my journey of my PhD is Dr. Mathias Toll. Dr. Toll was not only a friend but also a tremendous technical advisor who dedicated a lot of his time to discuss the topic of my research and contribute very effectively in the methodology of data acquisition and analysis.

As my research involved a lot of hydrological modelling, it is necessary to thank those who helped me with the model. I would like to express my gratitude and appreciation to Dr. Jens Lange from the Institute of Hydrology at Freiburg University, who guided me and received me for a month to build up the hydrological model. Also I thank my friend Anne Gunkel who did not hesitate in supporting me despite being a PhD student in a situation similar to myself. Her support in addition to the support from Matthias Ritter during my stay in Freiburg played an essential role in building the hydrological model. The support of Anne was not limited to my stay in Freiburg but continued on until the end of the modelling process, which I very much appreciate.

Next, I want to express my gratitude to those that helped me in Göttingen, the city where I spent the last few years conducting my scientific research within the great Department of Applied Geology. I enjoyed working here not only for the many friends I've made here but also for the scientifically fertile ground and scientifically rigorous and healthy environment which is conducive to proper research and creative solutions. Among many, I would like to express my sincere gratitude to my friend Dr. Bianca Wagner for her support and supervision in analyzing the satellite images and in her scientific and technical support in GIS and remote sensing analysis. My gratitude also extends to my friends Eng. Mohammad Azizur Rahman, Dipl.-Geol. Torsten Lange and Eng. Enayatollah Ranjineh Kojasteh for several fruitful discussions had over the course of my time here. I am also indebted to my friend and office mate Dipl.-Geol. Sebastian Schmidt for the fruitful scientific discussions and for reviewing a part of my manuscript.

From beloved Palestine I would like to thank my friend Eng. Muath Abu Saadah for his continuous support and for the constructive discussions and advice which effectively enhanced and improved my research. Also, I thank him for reviewing a part of my manuscript.

From my beloved country Jordan, I am grateful to my friends Dr. Marwan Alraggad and Dr. Alsharifa Hind Alsharif Mohammed Jasem for data provision and for the productive discussions we used to have during my stay in Jordan. As my research included a lot of instrumentation and field measurements, I would like to thank Alshaykh Khalid Abu Khusah from the Kafrein Dam operation office and Eng. Na'em Dabour from Dam control Unit for data provision and the continuous support. My gratitude also extends to Mr. Omar Yahya from Wadi Es Sir WWTP and all his kind colleagues for support in installing and caring after the weather station. My thanks also go to the manager and employees of King Hussein Gardens, the general director Eng. Abu Yazan also Eng. Ahmad Alamori and Mr. Yassin Alhayek, for their cooperation and caring for our instruments in King Hussein Gardens. Also, I would like to thank Alshaykh Omar Mousa from Iraq Al Amir, Mohammad Beak Alabadi from Alrabahiyya Aljanoubiya, Mr. Abdelhalem Almanaser from Alkashef, and Mr. Hassan Almanaser from Wadi Bahhath for allowing me to install scientific instruments in their properties and on the roofs of their houses.

Talking about field work and instrumentation, I am so much indebted to my beloved brother Henry who helped me a lot in the field work. Also, he, together with my beloved Brother-in-law Ziad, took care of the instruments and read them out regularly, while sending me the measurements to Germany for analysis. I am also indebted to my beloved mother Buthaina and my beloved sister Jumana not only for the very delicious food they prepared during my stay in Jordan but also for being a main source of support during my PhD work.

I am so grateful to the financial support from the German Ministry of Science and Education BMBF for financing the SMART project. Also, I am grateful to the Ministry of Water and Irrigation for allowing me to install a lot of field equipment and for data provision. My gratitude goes to Eng. Ali Subuh, Dr. Khair Alhadedi, and Eng. Thair Almomani.

I also would like to thank Eng. Mohammad Samawi and Eng. Firas Abu Hazem from the Jordan Meteorological Department for the climatic data provision which were used to develop the climatic scenarios. I am so grateful to the many Bedouins and local people who helped me in many rainy days while I was conducting field measurements. They showed the real Arabian generosity and kindness. Among others, I am grateful to my friend Emad Almahamed and his family from Alhamdeya for their help in field measurements in Wadi Al Nar and for taking care of the instruments and their help in field constructions. I am also very thankful and grateful to Nicholas Ryan for reviewing the language in my manuscript.

I dedicate my thesis to my family and the soul of my father, Captain Edward, who I always kept in mind all through my study. I am sure if he were alive he would be a great source of inspiration and support, but God gives and God takes and it will be only his will. May God bless my father's soul in heaven.

Contents

Figures

Tables

Summary

In order to effectively plan and manage the water resources of a country or geographical region, available water resources must be quantitatively assessed and hydrological processes must be known. Although surface water is ordinarily considered a primary source of water, the Middle Eastern focus has been primarily on groundwater. Attention to surface water, runoff generation processes, and overall catchment modelling has typically been paid little attention. However due to hydrological conditions and population increase, countries like Jordan are considering the entire spectrum of water resources and the quantitative assessment and characterization of hydrological resources are becoming ever more important.

Hydrological modelling in the arid to semi arid catchment of Wadi Kafrein (161 km²) was the objective of this study, and in order to complete this objective, detailed hydrological investigations were performed there. The catchment is characterized by a wide range of climatic differences, topographic variations, and spatial land uses. A physically based, spatially distributed, hydrological model was prepared within the framework of this dissertation. The aim of this dissertation is a detailed quantification of the water balance of the study area with emphasis on (1) runoff generation mechanisms and (2) the resulting transmission losses. A secondary aim of this study was for the model to assist local decision makers in solving water resources management problems.

Due to the large variability in hydrological parameters of the catchment area, the model was intended to be physically based and spatially distributed. The type of physically based model which was selected for the Wadi Kafrein catchment is the TRAIN-ZIN model. In order to meet the requirements of this model, data which was of high spatial and temporal resolution was obtained and a comprehensive hydrological database was prepared. The geometry of the catchment (Digital Elevation Model, DEM) was prepared using Cartosat-1 satellite images with a resolution of 5 m. The spatial variations in land use and soils were graphically shown in respective land use and soil maps by using multi-temporal ASTER satellite images.

In order to calibrate the model, runoff measurements were required, and therefore, the topography of the surface water reservoir behind the Kafrein dam was surveyed during a dry period using high resolution differential GPS measurements. From the resulting elevation model, a rating curve for the surface water reservoir was prepared. This allowed the quantification of surface runoff by water height determination. The water height in the reservoir was measured continuously using data loggers. The monitoring period extended from November, 2007 until December, 2009. Several sub-wadis with catchment areas of 0.3 km2 to 7 km2 were instrumented for high temporal rainfall and runoff measurements.

The numerical model was parameterized, calibrated, and validated using the measured data. The model was calibrated and validated using the Differential Split Sample Test approach. The water components of the two consecutive hydrological years were quantified and spatial distribution maps were prepared for every water component on an event basis. The results of a sensitivity analysis indicate a strong effect of soil depth and soil infiltration rates on the generated runoff amounts while transmission

losses are mainly affected by channel length, channel width, and the depth to active alluvium.

Runoff generation mechanisms were quantified in detail for the monitored runoff events. The results show that Infiltration Excess Overland Flow (IEOF) is the dominant runoff mechanism in the study area, which is also known to be the dominant mechanism in other arid and semi arid regions. On the other hand, and despite that fewer events were generated due to Saturation Excess Overland Flow (SEOF), the results show that, quantitatively, runoff is mainly generated due to SEOF. For similar amounts of rainfall measured in two different storm events, the volume of the generated runoff with SEOF as the dominant runoff generation mechanism was ten times more than an earlier event with a similar measured rainfall amount. This earlier event was characterized by IEOF. This observation may be attributed to the rainfall intensity, the antecedent soil moisture, and the lag time between the storm events. Transmission losses were also quantified on an event basis and on an annual basis. Transmission losses ranged from 18-44% of the generated runoff on an event basis while the average transmission losses were 24% and 26% of the generated runoff in 2007/2008 and in 2008/2009, respectively. The maximum runoff coefficient was 4% in 2007/2008 and 11% in 2008/2009. Recharge was higher when SEOF was the dominant mechanism and lower when IEOF was the dominant mechanism.

In order to attempt to predict the impact of climatic patterns' variations and the impact of urban expansion and land use changes on the water balance components of Wadi Kafrein, a new approach has also developed within the bounds of this dissertation. This new approach takes into consideration precipitation characteristics and temperature increases, including the wettest and driest years on the available records. In total, 24 climatic scenarios were developed and the results were further validated by applying continuous modelling for the hydrological years from 2002 until 2007. The results of climatic scenarios show that runoff coefficients range from 4% in very dry years to 21% in very wet years. Furthermore, an increase in temperature of 1-3 °C will slightly decrease recharge and runoff. Urbanization expansion in Wadi Kafrein will mainly increase the volume of generated runoff and decrease the recharged water.

As a further result of the research described herein, indications are that previous estimations of runoff and recharge in the Wadi Kafrein were too low and evapotranspiration was too high. The results from this study indicate that on an average year, runoff is approximately 6.4 MCM and recharge is around 21 MCM. Recharge equations were also developed to estimate recharge based on annual rainfall.

Zusammenfassung

Die Quantifizierung der vorhandenen Wasserressourcen und das Verständnis der hydrologischen Prozesse sind entscheidend für wasserwirtschaftliche Planungen. In Jordanien besitzen wasserwirtschaftliche Fragestellungen, aufgrund der hydrologischen Rahmenbedingungen sowie der demographischen Entwicklung, eine hohe Relevanz. In der Nahostregion lag der Schwerpunkt hydrologischer Studien bisher eher auf dem Gebiet der Grundwasserforschung. Weniger Aufmerksamkeit wurde den Oberflächengewässern und Abflussbildungsprozessen sowie deren Modellierung zuteil, obwohl Oberflächenwasser ein wichtiger Teil der verfügbaren Wasserressourcen darstellt.

Der Fokus der vorliegenden Arbeit ist die hydrologischen Modellierung in ariden und semi-ariden Regionen. Im 161 km² große Einzugsgebiet des Wadi Kafrein wurden umfangreiche hydrologische Untersuchungen durchgeführt und unter Verwendung der gewonnenen Daten ein physikalisch basiertes, räumlich verteiltes hydrologisches Modell erstellt. Ziel dieser Untersuchungen ist eine detaillierte Quantifizierung (1) der Wasserhaushaltskomponenten des Untersuchungsgebietes mit Schwerpunkt auf der Analyse der Abflussbildungsprozesse und (2) der Infiltrationsverluste in das Gerinnebett. Weiterhin sollen durch die Arbeit lokale Entscheidungsträger beim Wasserressourcenmanagement unterstützt werden.

Aufgrund der großen Variabilität der hydrologischen Parameter im Einzugsgebiet und für eine fundierte Prognose der verfügbaren Wasserressourcen, ist es nötig, für die Modellierung ein physikalisch basiertes Niederschlags-Abfluss-Modell zu verwenden. Hierfür wurde das Modell TRAIN-ZIN gewählt. Aufgrund des hohen Datenbedarfs des TRAIN-ZIN-Modells wurde eine einheitliche und umfassende hydrologische Datenbank für das Untersuchungsgebiet erstellt. Im Vordergrund stand die Erhebung und Synchronisierung von Daten mit hoher räumlicher und zeitlicher Auflösung. Die Geometrie des Gebietes (Digitales Höhenmodell, DHM) wurde aus Cartosat-1-Satellitenbildern mit einer Auflösung von 5 m erstellt. Die räumliche Verteilung der Landnutzung und eine Bodenkarte wurden von multi-temporalen ASTER-Satellitenbildern abgeleitet.

Für die Kalibrierung des Modells muss der Gebietsabfluss bestimmt werden. Hierzu wurde der entleerte Oberflächenspeicher -Kafrein Damm- am Gebietsauslass während einer Trockenperiode mit einem differentiellen GPS-Gerät topographisch vermessen. Aus dem resultierenden Höhenmodell wurde eine Wasserstands-Speicherinhalt-Beziehung für den Stausee abgeleitet. Diese erlaubt die Quantifizierung des Oberflächenabflusses aus Wasserstandsmessungen. Der Wasserstand im See wurde zeitkontinuierlich mit Drucksonden und Datenloggern gemessen und aufgezeichnet. Die Messperiode erstreckte sich vom November 2007 bis zum Dezember 2009. Im Einzugsgebiet des Kafrein Damms wurden zudem mehrere Teileinzugsgebiete mit Größen von 0,3 km² bis 7 km² ausgewählt und mit Messgeräten ausgestattet, die Niederschlag und Oberflächenabfluss registrieren.

Das numerische Modell wurde mit Hilfe der aufgezeichneten Daten parametrisiert, kalibriert und validiert. Dabei wurde die gemessenen Daten in Zeitbereiche für die Kalibrierung und Modellvalidierung aufgeteilt. Die Wasserhaushaltskomponenten der

beiden gemessenen hydrologischen Jahre wurden quantifiziert und Karten ihrer räumlichen Verteilung auf Ereignisbasis erstellt. Für die Kalibrationsparameter wurde eine Sensitivitätsanalyse durchgeführt. Diese zeigt den großen Einfluss der Parameter Bodenmächtigkeit und Infiltrationsraten auf die Abflussbildung. Die Infiltrationsverluste in das trockene Gerinnebett werden hauptsächlich durch Kanallänge, Kanalbreite und die Mächtigkeit des aktiven Alluviums bestimmt.

Die Abflussbildungsprozesse wurden auf Ereignisbasis analysiert. Die Ergebnisse zeigen, dass die Überschreitung der Infiltrationskapazität des Bodens (Infiltration Excess Overland Flow, IEOF) der dominierende Abflussbildende Mechanismus in der untersuchten Region ist. Dies ist in vielen ariden und semi-ariden Regionen weltweit ähnlich. Obwohl der Sättigungsflächenabfluss (Saturation Excess Overland Flow, SEOF) bei weniger Ereignissen auftritt, wird der mengenmäßig größte Teil des Abflusses jedoch durch SEOF gebildet. Für ähnliche Niederschlagsmengen aus zwei unterschiedlichen Niederschlagsereignissen liegt das durch SEOF gebildete Abflussvolumen um ein zehnfaches über dem eines anderen Ereignisses mit bei dem IEOF der dominierende Abflussprozess darstellte. Diese Beobachtung kann auf die Niederschlagsintensität, die Vorfeuchte und den zeitlichen Abstand zwischen zwei Ereignissen zurückgeführt werden. Die Infiltrationsverluste in das Gerinnebett wurden auf Jahres- und Ereignisbasis quantifiziert. Diese betrugen bei Einzelereignissen zwischen 18-44% des gebildeten Abflusses sowie 24% und 26% des Gesamtabflusses für die hydrologischen Jahre 2007/2008 bzw. 2008/2009. Der maximale Ereignis-Abflusskoeffizient (Anteil am Gebietsniederschlag) betrug 4% in 2007/2008 und 11% in 2008/2009. Die Grundwasserneubildung ist höher wenn SEOF der dominante Abflussprozess ist und niedriger wenn IEOF der dominante Abflussprozess ist.

Um den Effekt der Veränderung klimatischer Parameter, Urbanisierung und Landnutzungsänderungen auf die Wasserhaushaltskomponenten im Wadi Kafrein vorhersagen zu können, wurde ein neuer Ansatz entwickelt. Dieser Ansatz berücksichtigt die Niederschlagseigenschaften und den Temperaturanstieg, einschließlich der trockensten und feuchtesten Zeiten der verfügbaren aufgezeichneten Daten. Insgesamt wurden 24 Klimaszenarien entwickelt, deren Ergebnisse durch die Modellierung des Gebietsabflusses für den Zeitraum 2002 bis 2007 validiert wurde. Die Ergebnisse der Klimaszenarien zeigen, dass der Abflusskoeffizient zwischen 4% in sehr trockenen Jahren bis 21% in sehr feuchten Jahren liegt. Die Grundwasserneubildung und der Abfluss wird durch einen Temperaturanstieg von 2-3 °C leicht verringert werden. Die zunehmende Urbanisierung im Einzugsgebiet des Wadi Kafrein führt zu einer Zunahme des Abflussvolumens und einer Abnahme der Grundwasserneubildung.

Die Ergebnisse dieser Arbeit belegen, dass der Oberflächenabfluss und die Grundwasserneubildung im Untersuchungsgebiet im Vorfeld unterschätzt und die Evapotranspiration überschätzt wurden. Der mittlere jährliche Oberflächenabfluss wird auf 6,4 Mio. m^3/a und die mittlere jährliche Grundwasserneubildung auf 21 Mio. m^3/a geschätzt. Auf der Grundlage von jährlichen Niederschlagsmengen wurden Gleichungen zur Grundwasserneubildung entwickelt, die einen wichtigen Beitrag für die wasserwirtschaftliche Planung darstellen.

1 Introduction

1.1 General overview

Water may be considered to be the lifeblood of all living creatures. The oldest civilizations known to man began where water was plentiful, and some civilizations ended due to issues concerning water shortages or problems. It was in southern Iraq about 5,300 BC where the Sumerian culture began depending on agriculture and irrigation from Tigris and Euphrates rivers. Due to imperfect irrigation practices and the hot and dry climate, soils easily succumbed to sodification and salinization, consequently reduced the agricultural lands, which ultimately lead to the declination of this ancient agrarian society (Thompson, 2004).

In southern Jordan, the Nabataeans constructed Petra as their capital city around 100 B.C. (Mish, 1985). Excavations have demonstrated that it was the ability of the Nabataeans to control the water supply that allowed the desert city of Petra to flourish, while in effect the Nabataeans had created a vibrant artificial oasis (Ortloff, 2005).

The Jordan of today is facing serious water resource issues which have been exasperated in the last decades due to social and industrial development. Political conflicts and the influx of refugees from neighboring countries, which is partly responsible for the ninth largest population growth rate of all countries of the world (RWC, 2009), have both added to the increased pressure on water resources and have helped to cause a drastic decrease in the annual per capita share of potable water from 3600 m^3 in 1946 to only 145 m^3 annual per capita in recent years (RWC, 2009). Today, Jordan is considered to be one of the four poorest countries worldwide with respect to available and accessible freshwater resources.

Only the highlands of northwest Jordan receive a significant amount of rainfall ranging from more than 200 mm/year up to about 600 mm/year, representing the main source of groundwater recharge in Jordan. The precipitation in all other parts of Jordan is less than 200 mm/ year and the long term average annual precipitation for the whole country is only 95 mm/ year calculated on a 40-year average (1963-2002).

Groundwater is the main water resource in Jordan and in some areas groundwater is the only available water resource. The annual average abstraction from groundwater basins of Jordan exceeds the average recharge by 159%. The over-pumping ratio ranges from 146% in minor aquifers to 235% in major aquifers (El-Naqa and Al-Shayeb, 2009).

Long-term inflow to groundwater is less than the long term outflow, which is cause for a groundwater budget deficit (Table 1.1); reflecting the unsustainable groundwater use that is taking place in Jordan right now.

Table 1.1: Mean annual budget of renewable groundwater (MWI and GTZ, 2004).

Budget Component	**Quantity** MCM/Year
Groundwater recharge from precipitation	395
Trans-boundary groundwater inflow from Syria	68
Return flows from irrigation, leaks from pipes, reservoirs, wastewater treatment plants	70
Total Inflow	**533**
Groundwater abstraction (wells, springs)	440
Baseflow	197
Total outflow	637
Change in storage (inflow - outflow)	-104

In order to reduce over-pumping and the groundwater budget deficit, Jordanian decision makers need to initiate plans to exploit alternative available water resources, including retained floodwaters. To facilitate water resource management decisions, further field-specific hydrological research and hydrological modelling are needed.

1.2 Research motivation and challenges

Due to the critical state of Jordan's water resources, many groundwater modelling and groundwater management studies have been conducted with the aim of improving freshwater yield while reducing the impact on Jordanian aquifers. Historically the focus has been greater on groundwater and less attention has been given to surface water and runoff processes modelling. This present study is a result of an analysis of field data pertaining to hydrological processes of the Wadi Kafrein catchment area in Jordan. Based on this analysis, the overall aim of the study is to make extrapolations and draw general conclusions on the driving factors of runoff generation mechanisms in arid and semiarid areas.

Field investigations were carried out in the Wadi Kafrein catchment area. The outlet of the catchment is controlled by a surface water dam, where all surface water is collected. This gives a good opportunity to control the total surface water discharge at the outlet and this advantage has been used by measuring the total volume of surface water entering the reservoir. Several geological and hydrogeological studies have been applied to Wadi Kafrein but generally unreliable data were used for hydrological predictions and estimations. Up to date, no hydrological models have been applied to this area. This can be attributed to several reasons: the lack of high quality precipitation and runoff data and/or the absence of suitable hydrological models which suit the climatological and ecological characteristics of the study area.

There is a need to identify and quantify the hydrological process components and to understand the effect of the climatic changes on the water situation. This can be achieved by building up an accurate hydrological database and by the application of a suitable hydrological model which can quantify and analyze the complicated

hydrological processes in arid and semiarid areas, which are different from the processes in humid areas.
In this research, all needed hydrological, geomorphological, and pedological data have been prepared with high accuracy in order to study the hydrological processes and investigate the driving mechanisms for runoff processes in the semiarid region of Wadi Kafrein.

Although data scarcity posed challenges during this study, all necessary data for the modelling process have been prepared either by direct measurements or by the application of innovative techniques to acquire the needed data with high quality and accuracy. A literature review has also been undertaken where results of previous studies were considered.

Most streamflow gauge stations in Jordan have been installed during the 1950's and 1960's, whereby the oldest station was installed in 1932 at the King Hussein Bridge (Agrar and Hydrotechnik GMBH, 1977). When the first National Water Master Plan was prepared in 1977, only few stations were still functioning and in most cases, time series data were incomplete. Some stations have been flushed away by strong floods, one for example being the Wadi Kafrein gauge. Generally, the available records of streamflow suffered either from short monitoring periods and/or incomplete records, which made any long-term water management plans difficult. Since that time, the water sector in Jordan has witnessed large steps forward in monitoring and gauging several wadis, mainly in the western Wadi catchments, which drain to the Jordan Valley as they account for most of the potential surface water resources. Still, the modelling of surface water has received little attention which has created a gap in this research field. The results of this present study will hopefully bridge this gap and motivate further research in this domain as it is an important key in managing the surface water amounts once the generating mechanism processes and amounts of surface water is defined and located properly.

1.3 Objectives

The multi-lateral, interdisciplinary SMART project (Sustainable Management of Available Water Resources with Innovative Technologies) funded by the German Federal Ministry for Education and Research (BMBF) aims to develop a transferable approach for Integrated Water Resources Management (IWRM) in the water scarce region of the Lower Jordan Valley. The overall objective of SMART is to develop an IWRM concept for the Lower Jordan River Basin (LJRB) and to support further developments to improve water availability. By using a multidisciplinary approach, all water resources of the LJRB, namely groundwater, wastewater, saline water, and flood water are taken into consideration. This research is part of the SMART project, and the outcomes of the hydrological modelling and the field investigations will contribute to the scientific research and cooperation in the Lower Jordan Valley area.

One of the main objectives of this study is to investigate runoff generation on a catchment scale. The study quantifies runoff amounts and does contribute to the understanding of the dynamics and processes that are involved in runoff generation.

The surface flow in the catchment is a response to rainfall events. However, several questions of special interest to hydrologists need to be answered, such as:

What is the amount of runoff that occurs due to a rainfall event?
Which path does the generated runoff take?
Where does the rain reside in the catchment area?

Answering these questions need an understanding of the dynamics of specific hydrological processes, the way runoff is generated and the types of runoff prevailing in arid and semi arid regions. Runoff, soil water storages, evapotranspiration and deep infiltration amounts have been quantified in this research, with emphasis on the runoff component due to its importance and relevance to IWRM purposes. This includes the allocation of runoff zones and runoff storages, also the usage of runoff in artificial recharge managements. By studying the water balance components such overall precipitation and more specific components like runoff in several sites with different slope, soil, parent rock material, plant cover, and land use, one will certainly gain better understanding of the driving factors generation runoff and from this knowledge one can enhance the existing water supply by knowing where to build water infrastructure aimed at capturing water that may have otherwise been lost. These investigations will be carried out on the example of Wadi Kafrein catchment in Jordan in order to apply it to other areas in Jordan and elsewhere.

The main objectives of this research can be summarized as follows:

- To improve understanding of specific characteristics of arid to semiarid hydrological systems
- To simulate hydrological processes of the Wadi Kafrein catchment area
- To create a hydrological database for the Wadi Kafrein catchment area
- To provide high quality data at low costs using innovative techniques
- To portray detailed quantified measurements and investigations on runoff with emphasis on process mechanisms
- To monitor precipitation and runoff of several small-scale wadis, in addition to the whole catchment of the study area *(These small-scale wadis were monitored in order to better understand hydrological response variations to rainfall events on a finer scale)*
- To provide a water budget of the Wadi Kafrein catchment and as an aid for selection calculating sustainable approaches to water management
- To provide future climatic scenarios and forecast potential future climatic effects on groundwater resources

1.4 Thesis structure

This thesis is divided into three main parts. **Part One**, **Chapters (1-3)**, is focused on the study area aspects and characteristics as well as the literature of available rainfall-runoff models, their developments, classification, and problems. Jordan's water crisis is discussed in **Chapter One**, as well as motivations and main objectives of this work. **Chapter Two** contains a description of all aspects of the study area, focusing on the dominant hydrological processes and climatological conditions. **Chapter Three** is a

discussion on hydrological models of arid and semiarid areas with emphasis on differences between hydrology of arid/semiarid areas and humid areas and the criteria used in selecting the hydrological model of the Wadi Kafrein catchment.
Part Two, **Chapters (4-6)**, is on methodology of data acquisition and analysis, the hydrological model of Wadi Kafrein, including a description of the modelling approach, goals of modelling, numerical model design, applications, and results. **Chapter four** gives an explanation on the methodology followed in this study and the innovative techniques followed to acquire the needed data to achieve the research objectives. **Chapter five** describes the hydrological model design process, and the numerical model of Wadi Kafrein as well as the numerical model simulations, parameterization, calibration, and validation. **Chapter six** is on model application, potential future climatic scenarios and land use changes are discussed and the model results are presented.

Part Three, **Chapter (7)**, is on conclusions with a discussion on potential future perspectives. Final all-encompassing results recommendations are discussed as well.

2 Study Area

2.1 Study area selection

In spite of the qualitative and quantitative scarcity of hydrological data, Wadi Kafrein has a suitable research environment. The geographical location of Wadi Kafrein is between the Highlands in the east and the Jordan Valley in the west. This location and also the proximity of Wadi Kafrein to Amman city on one side make the area of special interest for several researchers and academic agencies. The climate is Mediterranean in the upper eastern part and changes within a few kilometers downstream to a semi arid climate. The semi arid climate dominates most of the study area, including that area which surrounds the Kafrein Dam (Section 2.6). This variation in climate gives the opportunity to study the effects which are borne out of this unique situation. The study area is endowed with a good road network and services, making the whole area accessible for research teams who need to move equipment around and transport time sensitive samples.

Wadi is an Arabic word, which means valley, and is used to describe a dry river bed, containing water only during heavy rain events or what is known as an ephemeral water course. In spite of this definition, Wadi Kafrein has perennial baseflow which represents a vital source of water for local farmers in the catchment area. Wadi Kafrein is additionally important to agricultural lands in the Jordan Valley, which depend on the water of Kafrein reservoir for irrigation purposes.

During the 1950's, water was diverted using a concrete weirs and a concrete system of lined canals to irrigate agricultural fields. No storage basins were present to collect the water and farmers depended on gravity irrigation supplies. Macdonald and Partners (1964) reported an area of about 6,500 donums of Ghor el Kafrein was irrigated using the perennial water of Wadi Kafrein in conjunction with boreholes located downstream. In the area where the gravity irrigation was limited (flatland on the west side of the Wadi Kafrein catchment area), boreholes extracting shallow groundwater were used for irrigation. This caused a gradual decrease in groundwater level and an increase in salinity. The Central Water Authority (now the Water Authority) was therefore ready to study this problem. A comprehensive report was published in November 1964 entitled "Inventory and Ground Water Evaluation, Jordan Valley" to detail the groundwater situation in this area.

Baseflow draining to the Wadi from springs is approximately 12 MCM/yr (Section 2.5.2). One MCM/yr of Wadi As Sir Waste Water Treatment Plant effluent at approximately 3,000 m^3/day is also discharged into the catchment area. All this water is collected in a reservoir, the dam of which was constructed in 1967 at the entrance of the Wadi Kafrein to the Jordan Valley with a present capacity of 8 MCM. The presence of Kafrein Dam enabled the monitoring of the inflowing water, which is very important in this study for measuring the total runoff generated from the watershed (Section 4.4.1).

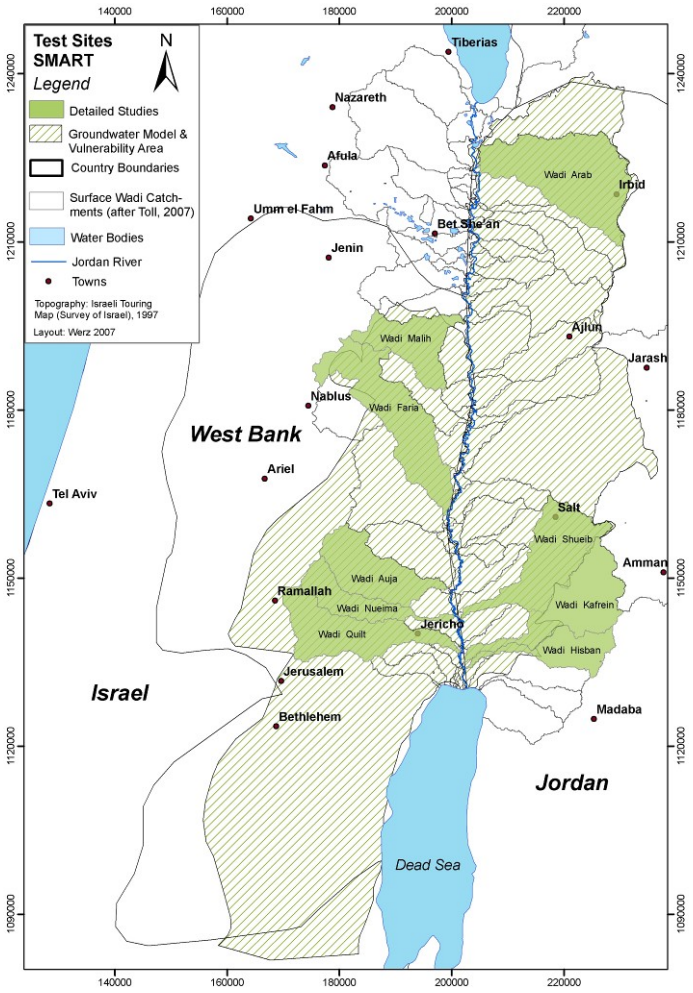

Figure 2.1: Investigation area of SMART project along Lower Jordan River Basin, coordinates are in Palestine grid.

Wadi Kafrein is one of several Wadis along the eastern and western side of the Lower Jordan River Basin which have been chosen as study areas for detailed hydrological investigations within the SMART project.

The investigated area of the project is about 5,000 km^2 including the Jordan Valley and the highlands which border the Valley from both sides (Fig. 2.1). The Jordan Valley suffers from extreme water shortages due to high exploitation rates of groundwater, which exceed the recharge rates and has led to a gradual decrease in groundwater levels over time. The SMART project aims to support further developments for improving water availability while using a multidisciplinary approach toward the management of all water resources available in the area. The present study is mainly concerned with flood water investigations and quantitative modelling of the actual water budget of the Wadi Kafrein catchment.

2.2 Geographic location and geomorphology

The study area is located 15 km northeast of the northern Dead Sea shore. The catchment area drains to the Kafrein Dam and runoff goes from the Highlands of the east to the Jordan Valley in the west (Fig. 2.2a). The geographical borders are taken to be the same as the surface catchment area of Wadi Kafrein. The rectangular border coordinates are 31° 50' 37.7"to 32° 0' 32.2" Northing and 35° 40' 1.8" to 35° 51' 24.7" Easting in World Geodetic System (WGS84). All maps coordinates in this study are given in the WGS84 unless otherwise mentioned. Wadi Kafrein drains an area of 161.4 km^2 and is classified from a hydrological point of view as an upper meso-scale catchment (Becker and Nemec, 1987; Schultz, 1994).

The Wadi has complex topography with relatively large elevation differences over short distances, meaning a steep relief with elevations ranging from 1,079 m asl at the upper east side (east of Fuheis City) down to nearly -139 m asl near the Kafrein Dam. The average elevation is 605 m asl (Section 4.2.1).

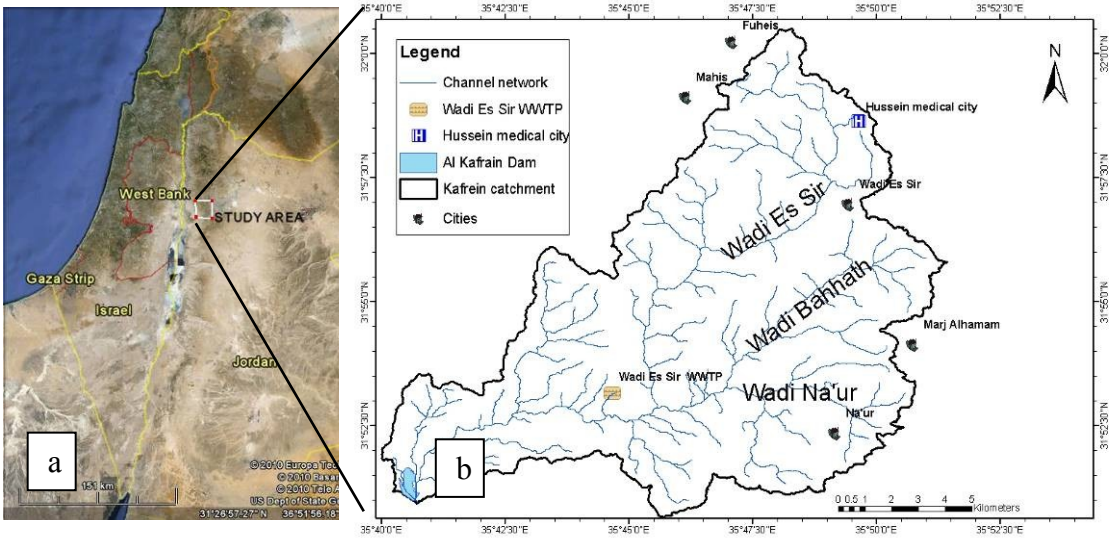

Fig. 2.2 a: Location site of the study area in Jordan (Google earth®). b: Main cites and locations in the study area of Wadi Kafrein.

The highlands in the upper eastern part of the study area are geomorphologically distinct and are characterized by high relief variations, as illustrated above. Some flat plateaus exist in the middle of the study area. Agriculture is present on these plateaus and is sustained by irrigation from the discharge of local springs. The surface features of a drainage basin determine the characteristics of runoff, flooding, and groundwater, and to some extent rainfall occurrences in the arid regions (Sen, 2008). Therefore, all related surface features of the catchment area were analyzed and prepared using the developed Digital Elevation Model (Section 4.2.1). The fluvial morphology of the channels in Wadi Kafrein were classified and used in the hydrological model. The characteristics of the channels play an important role in runoff generation and transmission loss processes. Further discussion is given in Chapter Five.

Wadi Kafrein has three main tributaries with corresponding catchment areas. Wadi As Sir catchment in the North has an areal extent of 59.2 km^2; Wadi Bahhath catchment is 25.6 km^2; and Wadi Na'ur catchment is 22.8 km^2 (Fig. 2.2b). These three main tributaries have springs draining within their respective catchment areas, which are the main sources of baseflow. Tributary catchments located in the west and southwest have smaller areas and are sources of large volumes of sediments due to the erosion of the sparsely vegetated landscape, which is characteristic of this region within the Wadi Kafrein catchment area.

2.3 Land use and vegetation cover

The study area has variable landuse and vegetation cover. Rain-fed agriculture predominates on the high elevations of the east, while along the slopes of valleys agriculture and plant nurseries use springs flows for irrigation (Fig 2.3a). Natural forests occur in the upper part of the catchment area while urbanization and high population density predominates mainly in the eastern part such as at Wadi As Sir and Na'ur cities (Fig. 2.2b). The southern and western parts have lower population densities and almost no vegetation cover; bare rocks dominate with no or very thin

layers of soil, hardly exceeding few centimeters (Fig. 2.3b). Industrial activates are found east of Wadi As Sir. A medical center (Hussein medical city) is located in the eastern part of the study area with a wastewater treatment plant, but since 2006/2007 wastewater from the medical center was diverted to Wadi As Sir WWTP (verbal information from Wadi As Sir WWTP office operators). The wastewater of the two cities, Wadi As Sir and Na'ur, are treated at Wadi As Sir WWTP, the effluent of which is discharged to the Wadi Kafrein stream network and eventually to the Kafrein dam reservoir.

Fig. 2.3a: Agricultural area in the middle of the study area along the Wadi Kafrein channel (31^0 54' 51" N, 35^0 45' 69" E).

Fig. 2.3b: Bare rocks without vegetation dominate the southern and western part of the study area (31^0 51' 53" N, 35^0 42' 56" E).

Due to the wide range of variations in vegetation cover and landuse, vegetation index and landuse maps were prepared using four satellite images and data sets. These maps are discussed in chapter four.

2.4 Geology and structural geology of Wadi Kafrein

The study area of Wadi Kafrein is affected by the regional structure as it is located in the transition zone between the Jordan Valley in the west and the mountain ridge which forms its eastern boarders. It is characterized by a complex tectonic framework and a high density of structural elements. The most distinctive structural feature in the study area is the Amman-Hallabat Structure (Fig. 2.5), which strikes NE-SW and extends from the northeastern part of the Dead Sea to the north of Wadi Na'ur with total length of 80 km and a width of 1-5 km (Shawabkeh, 2001). The fault is mainly composed of dextral strike-slip faults with smaller conjugated antithetic and synthetic faults and sub-parallel anticline and syncline folds (Diabat and Abdelghafoor, 2004).

The following paragraphs are based mainly on Lenz (1999) and verbal discussion with Dr. Till Heinrichs from Göttingen University. Near the Kafrein dam several synclines and anticlines were identified and mapped by Lenz (1999). The predominant strike direction is NNE to NE, almost parallel to Amman-Hallabat monoclinal flexure and most of these features do not exceed one km in length. The reservoir is located on a major N-S oriented syncline, which changes westward to an antiform. The antiform is composed of several synclines and anticlines and forms the plateau ridges of Na'ur Formation (Fig. 2.4a right side). Another distinctive feature is the Kafrein syncline, extending from Kafrein dam toward the northeast. It is formed from the Wadi As Sir Limestone in the left abutment (eastern side) while Na'ur,

Fuheis/Hummer and Shueib Formations form the right abutment (western side), (Fig. 2.4a). The Wadi As Sir Formation layers are folded and dipping toward the reservoir (westward) as shown in Fig. 2.4b.The main fault in the area is a normal fault in the western part of the reservoir dipping toward the center. The down throw of the fault is toward the east with around 90 m near the dam (Macdonald and Partners, 1965) and it increases up to 350 m in the northern part of the dam and the Kurnub sandstone is outcropped against Wadi As Sir Formation. On the right side, the layers are dipping toward the center of the syncline dipping NE to ENE, they are composed mainly of Na'ur Formation but also Fuheis/Hummer and Shueib Formations exists. The central part near the dam is filled with the youngest unconsolidated sediments (Jordan Valley Group) on top of Amman Siliceous Limestone Formation.

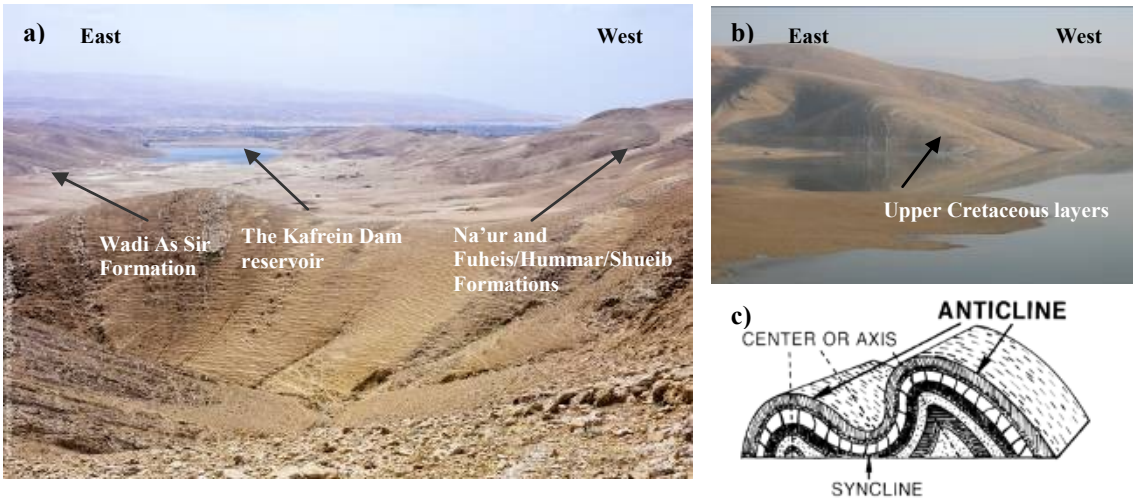

Fig. 2.4a: Kafrein syncline showing the bedded rocks of Ajlun Group (photo taken on March, 2008 by Till Heinrichs-Göttingen University). b: Upper Cretaceous layers on the Eastern limb of the syncline. c: Sketch showing the syncline axis (http://en.wikipedia.org/wiki/Syncline, 08.08.09), (31^0 51' 3.15" N, 35^0 40' 41" E).

The dam is built on top of 40 m of conglomerate, gravel, and sand (Macdonald and Partners, 1965). Plans were in place to cover the upstream section of the base of the dam with a clay layer to control the seepages. Harza and Arabtech (1989) reported doubts that the clay was ever installed. In a separate report prepared by GeohytenCorp (1998), geophysical data shows that the clay layer is not covering the upstream section of the dam base but only the reservoir floor. Due to fractures and joints within the basement rock below the dam, seepage is occurring. Lenz (1999) reveals high fracture densities over a 200 m long section of Na'ur limestone along the right abutment of the reservoir.

2.4.4 Stratigraphy of the study area

2.4.4.1 General overview

The main rock types exposed in the study area are limestone, dolomite, and marlstone from the Late Cretaceous Subperiod (Ajlun and Belqa Groups) and sandstone from the early Cretaceous Subperiod (Kurnub Group). At the south of the study area lie three other formations: the Mukheiris, the Iraq al Amir, and the Um Tina Formations,

all of the Zarqa Ma'in Group. Most large stream channels of the middle and lower Wadi Kafrein watershed have sandstone outcrops.
Limestone, dolomite, and marls dominate the outcrops in the upper highlands, the upper slopes of the wadis, and also in the northern and lower parts of the study area. Figure 2.5 shows the geology in the study area and the main structural features as mapped by Shawabkeh (2001) and Diabat and Abdelghafoor (2004).

The lithostratigraphic description in this study follows the description used by the National Resources Authority (NRA) of Jordan which is based on Masri (1963). Table 2.1 shows the stratigraphic units in Wadi Kafrein area. Further explanations are given below.

Table 2.1: Stratigraphy in Wadi Kafrein catchment area (modified from Powell, 1989).

Period	Epoch	Group	Formation	Hydrological Unit		Brief description	Thickness in the study area
Upper Cretaceous	Campanian Santonian Coniasian	Belqa	Amman Silicified Limestone	Upper Aquifer	B2	Phosphorite, silicified limestone	50 m
			Wadi Um Ghudran	Upper Aquifer	B1	Massive chalk & marlstone. fossiliferous	15-20 m
	Turonian	Ajlun	Wadi As Sir	Upper Aquifer	A7	Thinlayered dolomite or massive grey limestone, fossiliferous. To the top more chertlayers	90-100 m
	Cenomanian		Wadi Shueib	Aquitard	A5/6	White crystalline limestone and ammonities (A6), and thinlayered limestone and marlstone (A5)	50 m
			Hummar	Aquifer	A4	Massive gray, sometimes yellowish limestone, often crystalline and cavernous	60-65 m
			Fuheis	Aquitard	A3	Thinlayered, marlstone, claystone	50 m
			Na'ur	Aquifer/ aquitard	A1/2	Massive hard grey limestone & chertlayers (A2), and gray marlstone (A1)	100-180 m
Lower Cretaceous	Albian Aptian Neocomian	Kurnub	Subeihi	Kurnub Aquifer	K2	Multicoloured sandstone	150-200 m
			Aardo	Kurnub Aquifer	K1	White, yellow massive sandstone	
Jurassic Triassic Permian	Angular unconformity		UmTina Iraq El Amir Mukheiris	Aquifer Aquifer Aquifer		Marine sandstone-carbonate-shale associations	50 m 65 m 70 m
		Zarqa Ma'in					

2.4.4.2 Zarqa Ma'in Group

The term Zarqa Group was first introduced by Wetzel (1947). The Zarqa Group consists of Jurassic and Triassic rocks in Jordan. Parker (1970) subdivided the Zarqa Group into Ma'in and Azab Formations, while Bandel and Khoury (1981) considered these names invalid as they have been subsequently used for individual Jurassic and Triassic Formations. Bandel and Khoury described the Triassic rocks of Jordan and included nine subdivisions. Zarqa Ma'in is the name used by the Natural Resources Authority (NRA) to designate all Triassic rocks the scheme of Bandel and Khoury

(1981) is used by the NRA to describe formations. A description of each Formation visible in the study area as a rocky outcropping is given below.

Mukkayris Sandstone Shale Formation

This group is of Triassic age (late Anisian-Early Landinian) and represents the oldest rocks that crop out in the study area. It has a thickness of about 70 m in Wadi Na'ur (in the south eastern part of the Kafrein watershed).

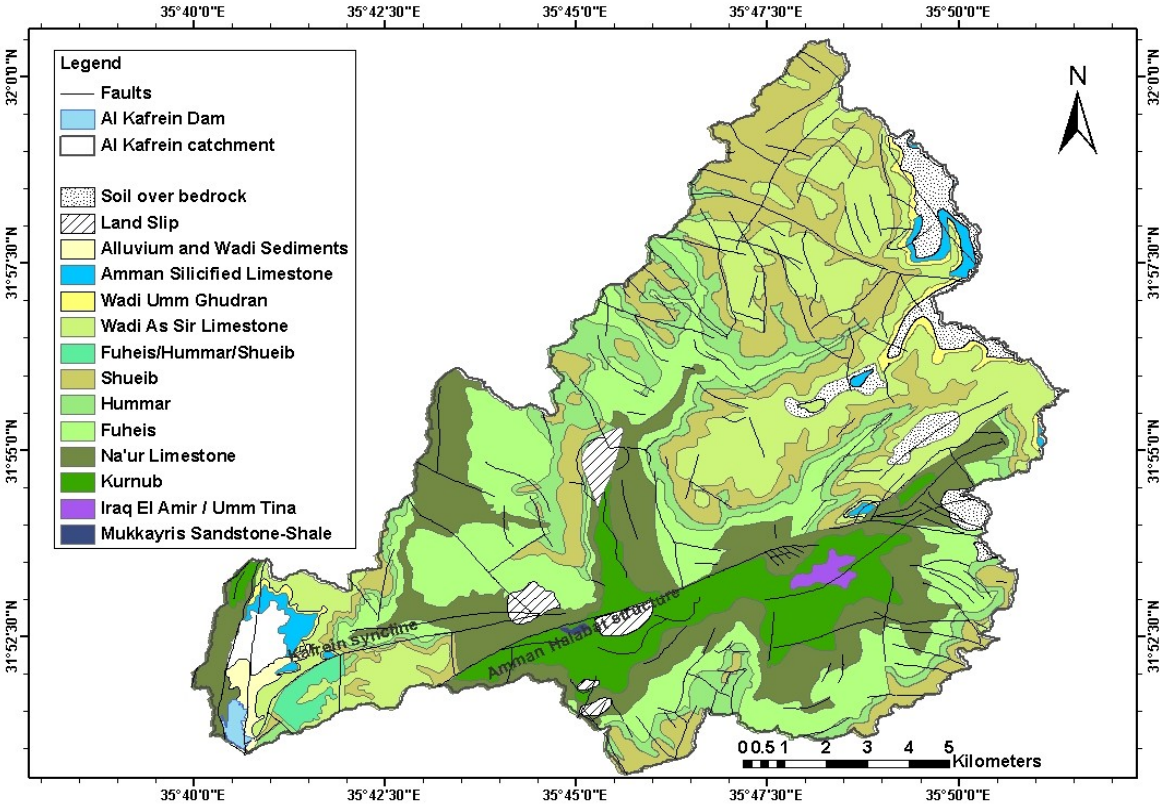

Fig. 2.5: Geological map of the Kafrein catchment (modified from Shawabkeh, 2001; Diabat and Abdelghafoor, 2004).

Bandel and Khoury (1981) divided this group into three members: Lower, Middle, and Upper members. It consists mainly of cross-bedded sandstone, silt, clay, calcareous sandstone, green silty shale, sandstone intercalated with clay stone, siltstone, and cross bedded sandstone. This Formation was deposited in a fluvial to intertidal environment.

Iraq El Amir Formation

This Formation is of Ladinian age and it crops out in Wadi Na'ur and Wadi Es Salit in the southern part of the study area. Total thickness is 65 m and consists mainly of marl and marly limestone. The lithofacies indicate that this Formation was influenced by marine transgression (Diabat and Abdelghafoor, 2004).

Um Tina Formation

The Um Tina Formation crops out in Wadi Na'ur and Wadi Es Salit with a total thickness of 50 m. It consists mainly of thin, medium, and thick bedded limestone and massive bioturbated limestone with coquina intercalated with yellowish grey marl. The presence of oolites and stromatolites, found in several marly limestone packages, indicates that the Formation was deposited in a marine subtidal to intertidal environment (Diabat and Abdelghafoor, 2004).

2.4.4.3 Kurnub Group

The Kurnub Group is widely distributed in Jordan and crops out along the rift margins. It was encountered in many drill holes throughout the subsurface to the east and northeast of Jordan (Andrews, 1992). Based on shelly fauna and plants found in north Jordan, the age ranges from Neoconian to Albian (Edwards, 1929; Wetzel and Morton, 1959; Bender, 1974). The Kurnub sandstone was deposited in a braided river system, grading upwards to become a meandering river environment (Andrews, 1992). Over this time period, the sea occasionally transgressed southwards into the north of Jordan (Bender, 1974; Powell, 1989).

Fig. 2.6: White medium to coarse sandstone outcropping to the north of Adasiyya (31^0 52' 15" N, 35^0 45' 40" E).

Later, the sea became permanent and deposited the marine limestone and shales of the Ajlun Group. The Kurnub group is exposed mainly in the southern part of the study area. The lower part consists of white, medium to coarse-grained, pebbly, cross-bedded sandstone (Fig. 2.6). The upper part is varicolored, medium- grained, cross-bedded sandstone with burrows and plant remains. The Kurnub Group is up to 150 m thick.

2.4.4.4 Ajlun Group

The Ajlun group was firstly termed by Quennell (1951) and was used to describe the carbonate strata of Cenomanian and Turonian age. Burdon (1959) adapted the term while Wetzel and Morton (1959) referred to these rock sequences as "Calcaire de Judea". Then the group was subdivided by Wolfart (1959) into seven lithostratigraphical units (A1-7).

Masri (1963) recognized five Formations and named them in sequence as follows: Na'ur (A1/A2), Fuheis (A3), Hummar (A4), Shueib (A5-6) and Wadi As Sir (A7). Powell (1989) and Teimah and Abu Saad (1993) followed in part the scheme of Masri (Makhlouf et al. 1996). Most of the outcropping rocks in the study area belong to this Group, Fig. 2.5.

Na'ur Limestone Formation

Of the Cenomanian, this Formation represents the stratigraphic bottom of the Ajlun Group. This Formation is well exposed in the northern and central parts of Jordan

(Makhlouf et al., 1996), while in the study area it crops out along the central and western parts as shown in Fig. 2.5. A total thickness of 100-150 m was given to this Formation by Shawabkeh (2001) and 180 m by Diabat and Abdelghafoor (2004), as mapped in the Karama and Amman geological maps respectively. Schultze et al. (2003) reported a thickness of 140 m in the northern part of Jordan and 150 m in central Jordan.

The name of this Formation was derived from Na'ur village, which is located in the south eastern part of the study area (20 km west of Amman). The Formation is equivalent to the A1-A2 units of Wolfart (1959) and the lower part of the Nodular Limestone unit of Bender (1974). The Na'ur Formation is divided into upper and lower members. The lower member consists of fine to medium-grained sandstone, rich in glauconite, and interbedded with siltstone mudstone, marl, with secondary gypsum and horizontal burrows.

Fig. 2.7: Na'ur Formation outcropping in Wadi El Nar (31^0 55' 03" N, 35^0 43' 12" E).

The upper member consists of alternating limestone and marl overlain by yellowish-grey marl interbedded with thin layers of marly limestone in the middle part. The top of the Formation is marked by 10-15 m of light to dark grey and pink dolomitic limestone with chert nodules at the top (Fig. 2.7). Na'ur Formation was deposited in tidal to lagoonal and open-marine environments (Shawabkeh 2001).

Fuheis Formation

This Formation has a Middle Cenomanian age (Schultze et al., 2003) and consists of yellow grey calcareous silt, marl, marly limestone, and nodular and fossilifereous limestone (Shawabkeh, 2001). This Formation is distributed all over the area along the deep wadis. The name is derived from the village of Fuheis 20 km west of Amman and the Formation is equivalent to the A3 unit of Wolfart (1959). The thickness of the Formation is around 50 m as mapped by Shawabkeh (2001) and it was deposited in a subtidal marine environment (Diabat and Abdelghafoor, 2004).

Hummar Formation

The age of this Formation is Middle to Middle-Late Cenomanian (Schulze et al., 2004) and it consists of grey limestone, dolomitic limestone, and dolomite characterized by abundant oysters, rudists, and gastropods (Schulze et al., 2003).

The name of the Formation is derived from the village of Hummar west of Amman and it is equivalent to the A4 unit of Wolfart (1959). It crops out in the northwestern part of the study area and to the north of Wadi Hisban with a thickness of 65 m (Shawabkeh, 2001) while Lenz (1999) measured a thickness of 40-50 m to the east of Wadi Kafrein. The Formation forms an important confined aquifer in the area and was deposited in an intertidal marine environment (Shawabkeh, 2001).

Shueib Formation

The name was first introduced by Masri (1963) to include the marly limestones which are exposed in Wadi Shueib and it is equivalent to the A5-6 unit of Wolfart (1959). The Formation is of Early Turonian age (Shawabkeh, 2001). It crops out in the northeastern part of the study area and occurs as soft weathering package producing broad talus cover above the prominent Hummar Limestone Formation. It is up to 50 m in thickness and consists of alternating limestone, chalky limestone, marly to clayey limestone, and nodular limestone (Fig. 2.8). It was deposited in a moderate to shallow subtidal marine environment (Diabat and Abdelghafoor, 2004).

Fig. 2.8: Shueib Formation outcropping in the north of the study area. (31^0 59' 14" N, 35^0 47' 31" E).

Wadi As Sir Limestone Formation

The name of this Formation was first introduced by Masri (1963) and it is equivalent to the A7 unit of Wolfart (1959). The Formation is of Turonian age and has a thickness of 100 m (Shawabkeh, 2001). It is marked in the base by massive, hard, buff dolomitic limestone (Fig. 2.9) and consists of bedded massive dolomitic limestone and dolomite with chert bands, chalky limestone, and marl. Wadi As Sir Formation covers the northern and central parts of the study area and also crops out in the southwestern part of the study area near Kafrein Dam (Fig. 2.4). The Formation was deposited in a shallow marine environment (Diabat and Abdelghafoor, 2004) and forms a very important aquifer in Jordan.

Fig. 2.9: Wadi As Sir Formation at the north eastern part of the study area (31^0 58' 5" N, 35^0 48' 47" E).

2.4.4.5 Belqa Group

The Belqa Group presents the Upper Cretaceous to Paleogene rocks in the study area (Quennel, 1951; Parker, 1970). It includes the Wadi Umm Ghudran, Amman Al Hisa, Muwaqqar, Umm Rijam and Wadi Shallala Formations (Powell, 1989). Only the first two Formations crop out in the study area.

Wadi Um Ghudran Formation

Of Coniacian-Santonian age, this Formation represents the basal part of the Belqa Group (Diabat and Abdelghafoor, 2004) and is equivalent to the B1 unit of Walfort (1959). White, massive chalk and marl, with fish teeth, bivalves and gastropod fragments and a thickness of 15 m are dominant properties of this Formation. Deposition occurred in a moderately deep-water pelagic environment (Shawabkeh, 2001). Wadi Um Ghudran Formation crops out in the northeastern part of the study area.

Amman Silicified Limestone Formation

Amman Silicified Limestone Formation is of Santonian-Campanian age and has a thickness of 50 m in the study area and covers a broad area of Amman city. It consists of dark brown to grey thick beds, chert, silicified limestone, chalk, marl, siliceous coqina and cherty phosphate, brecciated chert and Tripoli (Diabat and Abdelghafoor, 2004). It crops out in the northeastern part of the study area and was deposited in full marine to subtidal environments (Shawabkeh, 2001). See Fig. 2.10.

Fig. 2.10: Amman silicified limestone with chert layer north to the Kafrein dam. (31^0 52' 40" N, 35^0 41' 23" E)

2.5 Hydrogeology

2.5.1 Aquifer systems

The aquifer systems in Jordan have been divided to three main aquifer complexes according to their spatial distribution, lithology and the age of the geological units (Salameh and Bannayan, 1993; MWI and GTZ, 2004). The following is a brief geological description.

1. Deep Sandstone Aquifer Complex

- Ram and Khreim Group (Paleozoic age: Cambrian-Silurian)
- Zarqa and Kurnub Group (Mesozoic age: Jurassic-Lower Cretaceous)

2. Upper Cretaceous Aquifer Complex

- Lower Ajlun Group (A1/6) which includes the Na'ur aquifer (A1/2), Fuheis aquitard (A3), Hummar aquifer (A4), and Shueib aquitard (A5/6). (Mesozoic age: Upper Cretaceous).
- Amman-Wadi As Sir aquifer (B2/A7), (Mesozoic age: Upper Cretaceous).

3. Shallow Aquifer Complex

- Basalt Aquifer, sedimentary rocks, and alluvial deposits (Cenozoic age: Tertiary-Quaternary).

Also these aquifers can be divided to two main types:

- Bedrock (consolidated) aquifers: this includes the Deep Sandstone Aquifer Complex, the Upper Cretaceous Aquifer Complex and the basalt aquifer of the Shallow Aquifer Complex. These aquifers together compromise the main source of groundwater in Jordan.
- Unconsolidated aquifers: limited to the aquifers in the Jordan Valley. Of minor importance compared with the Bedrock aquifers.

The Deep Sandstone Aquifer Complex

The Ram Group Aquifer of Cambrian age is the oldest aquifer which belongs to this Complex. It is also known as the Disi Aquifer in Jordan and as Saq Aquifer in Saudi Arabia. It does not crop out in the catchment area of Wadi Kafrein and its outcropping is limited to the southern part of the country and to the lower slopes of the escarpment east of the Dead Sea. It extends beneath the whole country forming a large aquifer and the deepest aquifer in north Jordan (Fig. 2.11). It consists mainly of sandstones interbedded with siltstone, mudstone, limestone and dolomite. The thickness of this aquifer is around 1,000 m up to 2,500 m in the east of Jordan while its base is estimated to be more than 2,000 m below sea level (bsl) in the northern and eastern part of the country and around 4000 m (bsl) in the north western part of the country (WAJ and BGR, 1994; Hobler et al., 2001). The aquifer has been recharged during the last humid period before around 5,000 years and is being continuously drained, leading to a gradual depletion of groundwater (Hobler et al., 2001).

The Zarqa Group of Permian to Jurassic age has similar constituents to the underlying Ram Group Aquifer. The Zarqa Group Aquifer is characterized as a multi-layered bedrock aquifer with different permeability and storability, but the aquifer is considered as one hydraulic system because the aquifers are hydraulically connected to each other. The Zarqa Group crops out only in the lower Zarqa River basin and along the escarpment between the Rift and the Highlands to the east. Its thickness increases from the central part of Jordan toward north and east to reach 1800 m (MWI and GTZ, 2004).

The second group of this Complex is the Khreim Group Aquitard of Silurian age. It overlies the Ram Group and it consists of sandstone, siltstone, and shale. It has a low permeability and separates the Ram Group from the overlying aquifer forming a confining layer, leading it to be considered as an aquitard.

The Lower Cretaceous Kurnub Group consists of white, multi-colored, and grey sandstone, mostly medium to coarse grained, with thin beds of grey and brownish siltstone. The thickness of the Kurnub Group decreases gradually from the northwestern to the southeastern part of Jordan with lowest thicknesses in the east which reaches 100-200 m in Azraq and 40-100 m in Hamad (Margane et al., 2002). In addition to its outcropping along the Rift escarpment of Wadi Zarqa River toward the south, it crops out in the catchment area of Wadi Kafrein in the southern and southeastern part; in Wadi Na'ur and Wadi Bahhath (Fig. 2.5). Other out crops of the Kurnub Group is found in the deeply eroded cores of anticlines in Baq'a area, and in Wadi Hisban which is located to the south of Wadi Kafrein.

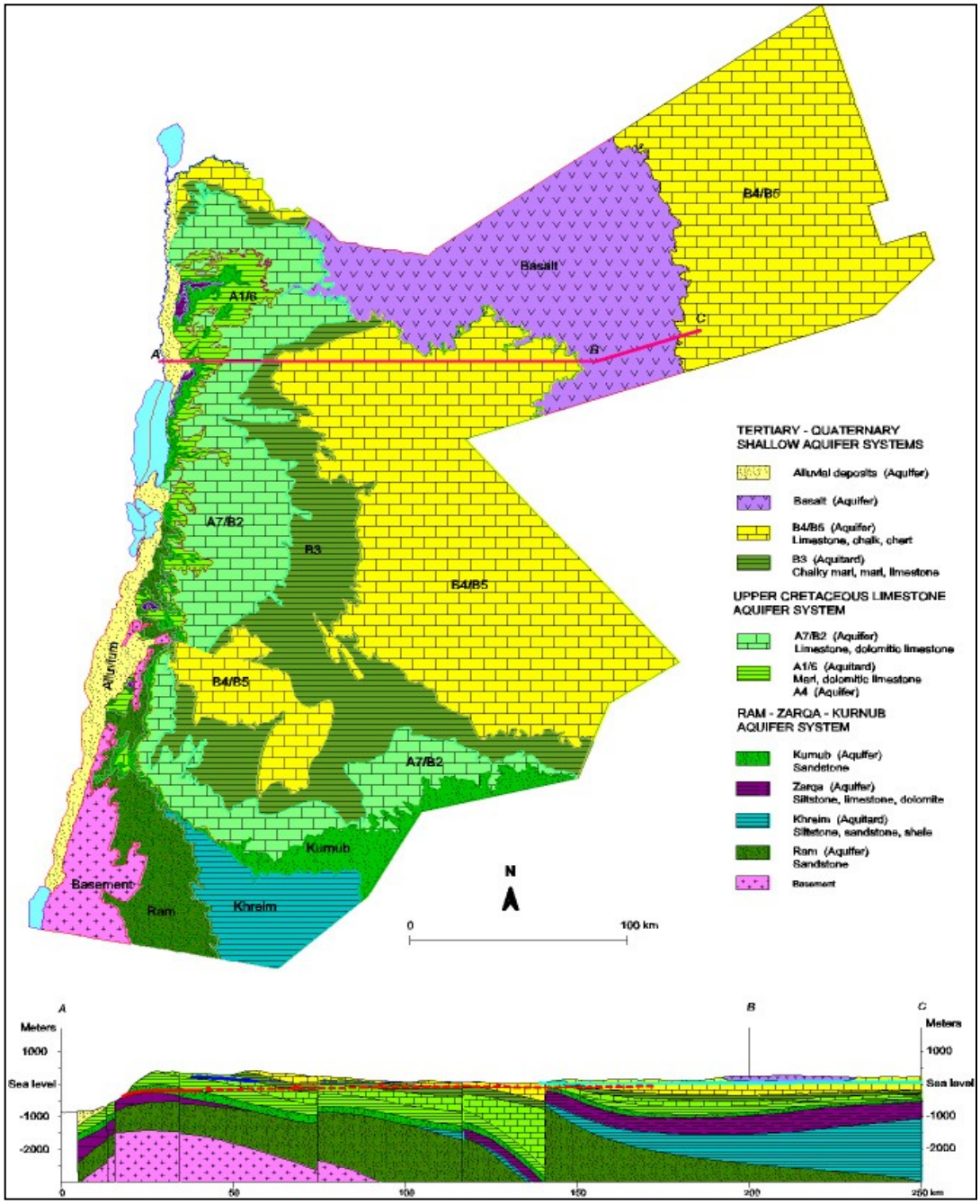

Fig 2.11: Hydrogeological map of the main aquifers and aquitards in Jordan with their spatial distribution (MWI and GTZ, 2004).

Salameh and Udluft (1985) detected three different directions of the groundwater flow in Zarqa and Kurnub aquifers; in the southern part of Jordan it flows towards the northeast, in central Jordan towards west and in the northern Jordan towards the southwest.

Upper Cretaceous Aquifer Complex

This Aquifer Complex includes the Upper Cretaceous Ajlun and Belqa Groups and is divided to several hydrological units (Table 2.1). It consists of alternating sequences

of marl, limestone, dolomite and shale. It is divided to two main aquifer systems; the Lower Ajlun Group aquifers (A1/6) and Amman-Wadi As Sir aquifer (B2/A7).

The Lower Ajlun Group aquifers (A1/6) overlie the Kurnub Group with a disconformity and extend all over Jordan except its southern parts. It is dominated by sequences of marl, limestone, dolomite, and shale and it is divided into the following four hydrological units:

1. The Na'ur aquifer/aquitard (A1/2) forms the lower part of this sequence and consists mainly of marls forming a confining layer which separates the aquifer from the underlying Kurnub Group Aquifer.

2. The Fuheis aquitard (A3) consists of about 80 m of marl and shale, which separates the A1/2 aquifer/aquitard from the overlying A4 aquifer (Salameh, 1996).

3. The Hummar Aquifer (A4) consists of marl and shale and crops out along the highlands. In the study area it crops out in the central and eastern part.

4. Wadi Shueib aquitard (A5/6) which consists of fossiliferous limestone, massive crystalline and thinly bedded porcellaneous limestone with a thickness ranging from 30 to 130 m (MWI and GTZ, 2004).

Amman-Wadi As Sir aquifer (A7/B2) represents the most important aquifer in Jordan because of its wide extent and relatively high permeability. It is the uppermost unit of Ajlun Group (A7) and the lower unit of Belqa Group (B2); together they form one hydrogeological unit consisting of limestone, chert-limestone, sandy limestone, and marly limestone and crop out along the highland where the Formation is being recharged. In Wadi Kafrein it crops out in the northern part and in the middle part along Wadi Bahhath (Fig. 2.5). Another outcropping of this Formation is found in the lower part of the study area near Kafrein Dam and along the Kafrein Syncline. Wadi As Sir Formation is folded and partially overturned in the western limb of the syncline (Fig. 2.4a).

Wadi As Sir Aquifer together with Na'ur and Hummar aquifers are of local importance in the study area. All springs issue from these hydrological units except Wadi Kafrein spring, which issues from the Kurnub Group.

Shallow Aquifer Complex

This aquifer complex can be divided into four systems; the Basalt Aquifer, the Alluvial Deposits of the Jordan Valley, Wadi Araba, and the Eastern Shore of the Dead Sea.

The Basalt Aquifer of Oligocene-Pleistocene age is composed of massive alkali basalt and forms a good aquifer with significant hydrogeological importance. It crops out along the eastern margin of the Dead Sea, at the rims of and on the plateau facing the Yarmouk Valley and in the lower Wadi el Arab, in the subsurface of the Jordan Valley and in Harrat-Ash Shaam basaltic province north and east of Azraq (Hobler et al., 2001; Margane et Al., 2002). The maximum observed thickness of basalt is 479 m

in Harrat-Ash Shaam area with a general increase towards Jebel Druze in Syria where it may reach around 1,500 m (Wolfart, 1966).

The Alluvial Deposits of the Jordan Valley extends from the northern shore of the Dead Sea up to the downstream of the Yarmouk River with total length of 100 km and a width ranging from 4.5 km in Al Karameh area to 13 km in Wadi Hisban (MWI and GTZ, 2004). It is recharged from the eastern and western boundaries of the Dead Sea and the Jordan River. It consists of sand, gravel, conglomerate, marl, travertine, limestone, and evaporates. The thickness of the alluvium ranges from zero in the eastern boundary to 750 m in the deepest part of the basin near the Jordan River.

Wadi Araba Alluvial Aquifer extends from the southern shore of the Dead Sea to the northern shores of the Gulf of Aqaba and presents the main source of groundwater in Wadi Araba basin. The aquifer consists of conglomerates, gravels, sands, silts, and clays.

The Eastern Shore of the Dead Sea consists of the Lisan Formation and Holocene gravel and boulders. It is recharged from stream runoff, lateral flows of adjacent aquifers, or from the underlying basalt aquifer (Salameh and Bannayan, 1993; MWI and GTZ, 2004).

2.5.2 Springs

In Jordan, around 800 springs are monitored by the Ministry of Water and Irrigation-Surface Water Monitoring Division, with oldest spring discharge records dating back to 1937. Several reports and publications are available about spring locations, discharges, and abstraction amounts (NRA, 1966; WAJ, 1986; UNDP, 1994; WAJ and BGR, 1996).

Spring discharge represents an important source of water in the study area; it is used for irrigation by local people and for domestic purposes as well. Twenty-two springs discharge in the catchment area of Wadi Kafrein with an average volume of 12.3 MCM/yr; Fig. 2.12 shows the spring locations and the issuing aquifer of each spring.

The average discharge volumes of the springs range from 0.66 m^3/hr of El Kashabeh spring in Wadi Na'ur up to 397 m^3/hr from Al Bahhath spring in Wadi Al Bahhath, (calculated from monthly measurements records, 1980-2006).

Almost half of the total spring flow volumes issue from Hummar (A4) aquifer (47.6%), with a total annual volume of 5.8 MCM, among which Al Bahhath spring discharges a total amount of 3.5 MCM/yr . The water of Al Bahhath spring used to be collected in water tanks for different purposes without any control (Fig. 2.13a). Recently and in the summer of 2009 a decision was issued which prevents the use of the spring water by these tanks to protect the water resources and to increase the amount of water reaching the Kafrein dam used for irrigation purposes in the Jordan Valley.

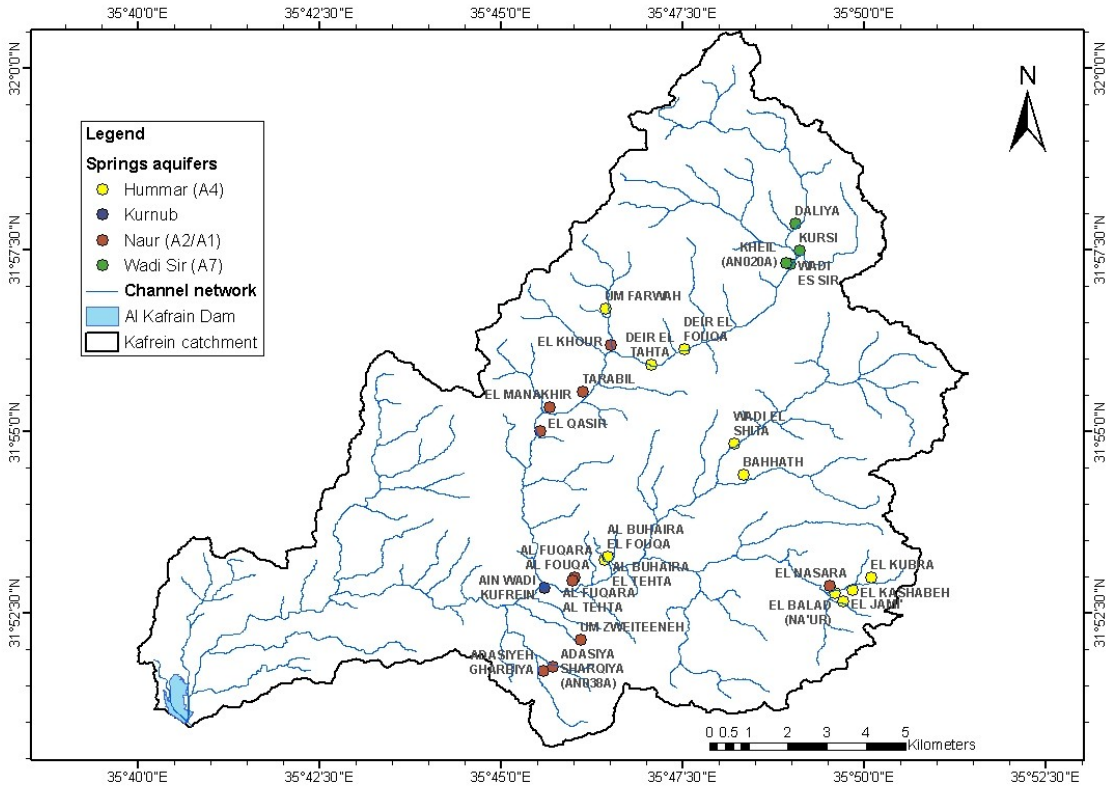

Fig. 2.12: Classification of Kafrein spring discharges according to their aquifers.

The second big and important spring in the catchment area is Wadi As Sir spring (Fig. 2.13b) with average discharge of 380m^3/hr. A water purification plant was established near the spring during the 1950s and in 1999 modern filters were installed to treat around 9,000m^3/day to supply the city of Wadi As Sir with the daily needs of water (Verbal information, Mr. Hani Median /station operator, also records of the station).

Fig. 2.13a: Al Bahhath spring with an annual discharge of 3.5 MCM presents a main source of baseflow in the study area.

Fig. 2.13b: Wadi As Sir spring, the water is pumped to Wadi As Sir Water Purification Plant supplying the city of Wadi As Sir with its water needs.

The springs of Wadi Kafrein emerge from four main hydrological units; Kurnub Group, Na'ur (A2/A1), Hummar (A4) and Wadi As Sir (A7), the volume percentages are given in Fig. 2.14 where it is illustrated that more than 80% of the springs emerge from Wadi As Sir and Hummar aquifers.

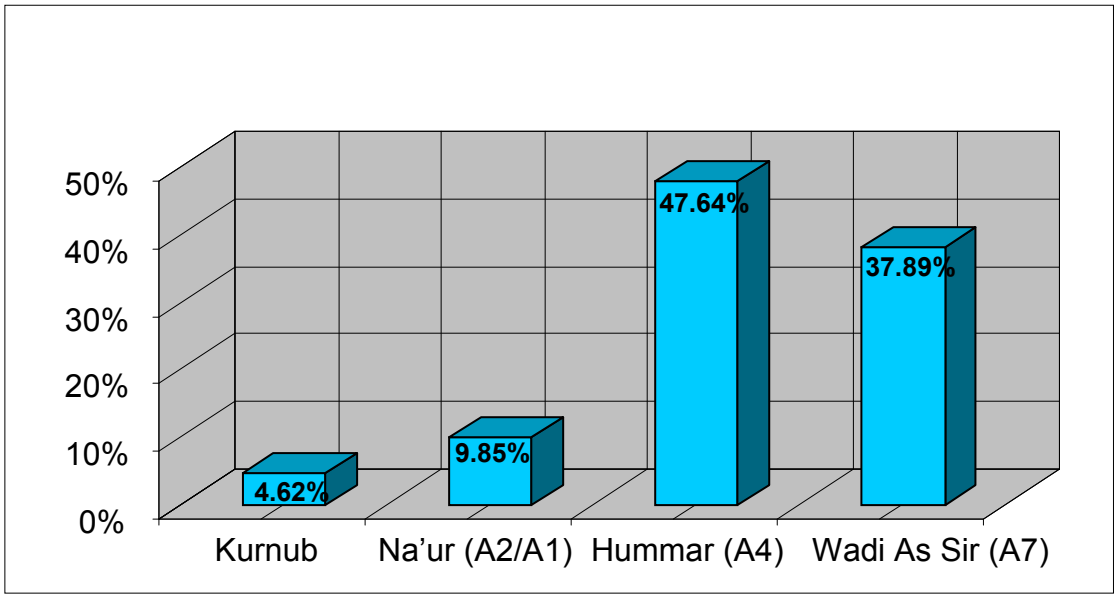

Fig. 2.14: Volume percentages of total spring discharge from the hydrological units.

2.6 Climatology and hydrological processes

Large changes in topographical elevations over relatively short horizontal distances, as referred to in section 2.2, lead to a wide variety in the local climatic conditions of the study area. In the following paragraphs, a description of the climatic situation prevailing in the study area is given with illustration of temperature, rainfall, and evaporation with respect to spatial and temporal variations. Due to the fact that hydrological processes in arid and semi arid regions are different from those in the humid regions, good understanding of these processes in semi arid areas is needed. Special attention will be given to runoff generation mechanisms especially because of its direct importance to the aim of this study.

2.6.1 Climatological characteristics of the study area

The geographical distribution of arid and semi arid regions in the world lie between 10-30° N and S latitude lines (Landsberg and Schloemer, 1967); as Jordan lies between 29-33° N, an arid to semi arid climate prevails by per definition. Due to the diversity of the topography in Jordan within relatively short distances, different climatic conditions affect the country. Jordan has been divided to 12 agro-climatic zones from which the desert accounts for ca. 80% of the total area (MWI and GTZ, 2004). The study area of Wadi Kafrein is classified within the Northern Highlands (Wadi As Sir)-ACZ6 Agro-climatological zone with total area of 1,695 km^2 and mean annual rainfall of 295 mm (MWI and GTZ, 2004).

Though the study area has a total catchment area of 161.4 km^2 and a maximum width at any point of less than 20 km, wide differences in climatic conditions occur.
A small part of the study area, in the uppermost northeastern part where precipitation exceeds the 500 mm, a Mediterranean climate prevails. This climate type dominates the whole highlands in the north of Jordan and extends along the mountain chains east

of the Dead Sea and southward. It is characterized by wet cold winter months from October until April and dry hot summer months from May to September. More to the west and southwest, a semi arid climate prevails where precipitation amounts decreases and temperatures increase. These variations lead to clear vegetation cover changes (Section 2.3 and Fig. 2.3a-b), which in turn leads to differences in hydrological responses.

2.6.2 Hydrological processes

2.6.2.1 Precipitation

Most of the precipitation over the catchment area (as well as over Jordan) takes the form of rainfall; around 28 frontal depressions per year reach the eastern Mediterranean originating from Mediterranean or Polar regions. They center over or near Cyprus then move northeast (10.5 depressions), east-northeast (11 depressions), southeast (2 depressions), and 5 depressions fill up (HMSO, 1962). Figure 2.15 shows the frontal depressions track in the Mediterranean basin.

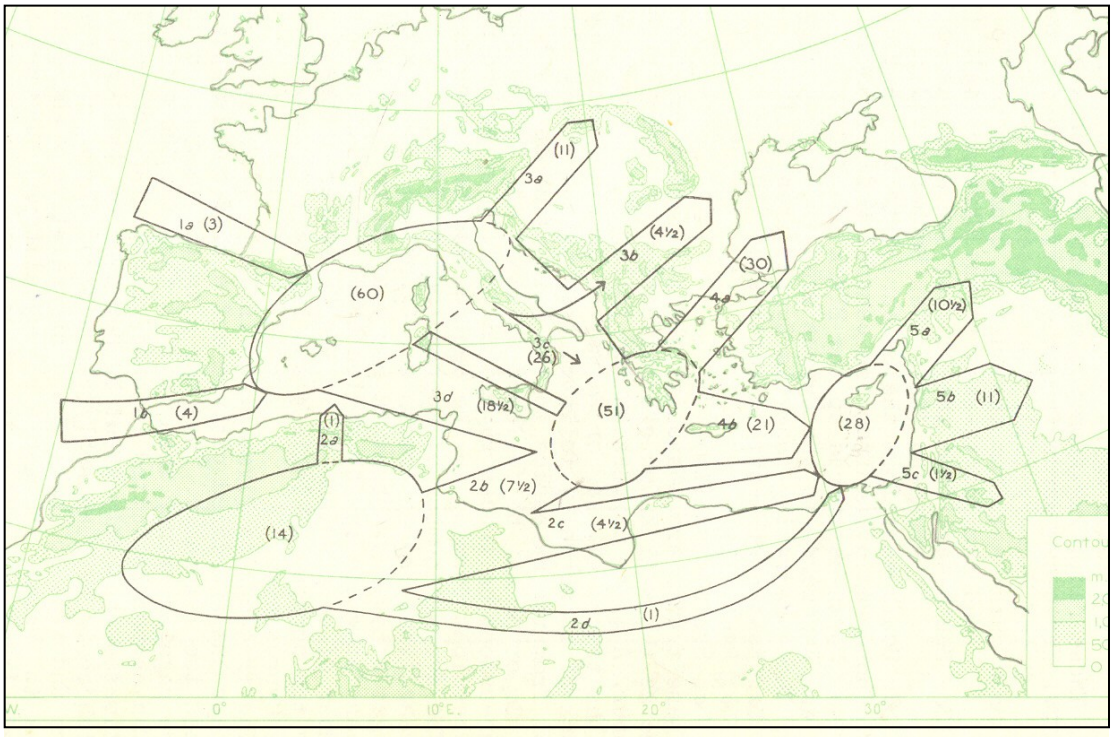

Fig. 2.15: Main winter frontal depressions track in the Mediterranean Basin with annual averages frequencies given between brackets (HMSO, 1962, p.33).

Snow and hail are not common phenomena and are limited exclusively to the highlands. Snow occurs once or twice a year over the eastern highlands of the study area with a mean number of snowy days in Salt station (1991-2000) and Sweileh station (1985-2000) of 3.9 and 4 days, respectively (Jordan Meteorological Department, 2002). Hail occurs even less frequently with long term average of 0.1 and 0.7 days in Salt and Sweileh stations respectively, (calculated from the same period of time as snow).

The Salt station is located around 7 km northwest of the study area (32^0 20' N, 35^0 44' E) while Sweileh station is located around 4 km to the northeast of the study area (32^0 00' N and 35^0 54' E). Both stations are operated by the Jordan Meteorological Department.

The long term annual average precipitation over Wadi Kafrein ranges from 514 mm in the upper eastern part near Wadi As Sir to 179 mm near the Kafrein dam. The average area precipitation of Wadi Kafrein is 387 mm calculated from historical data of 10 stations covering the period from 1980-2008. Figure 2.16 shows the stations network locations and the spatial precipitation distribution over the study area. Data were obtained from Ministry of Water and Irrigation/ Jordan. The interpolation was done using the ordinary Kriging method (Spatial analyst tool, ArcGIS).

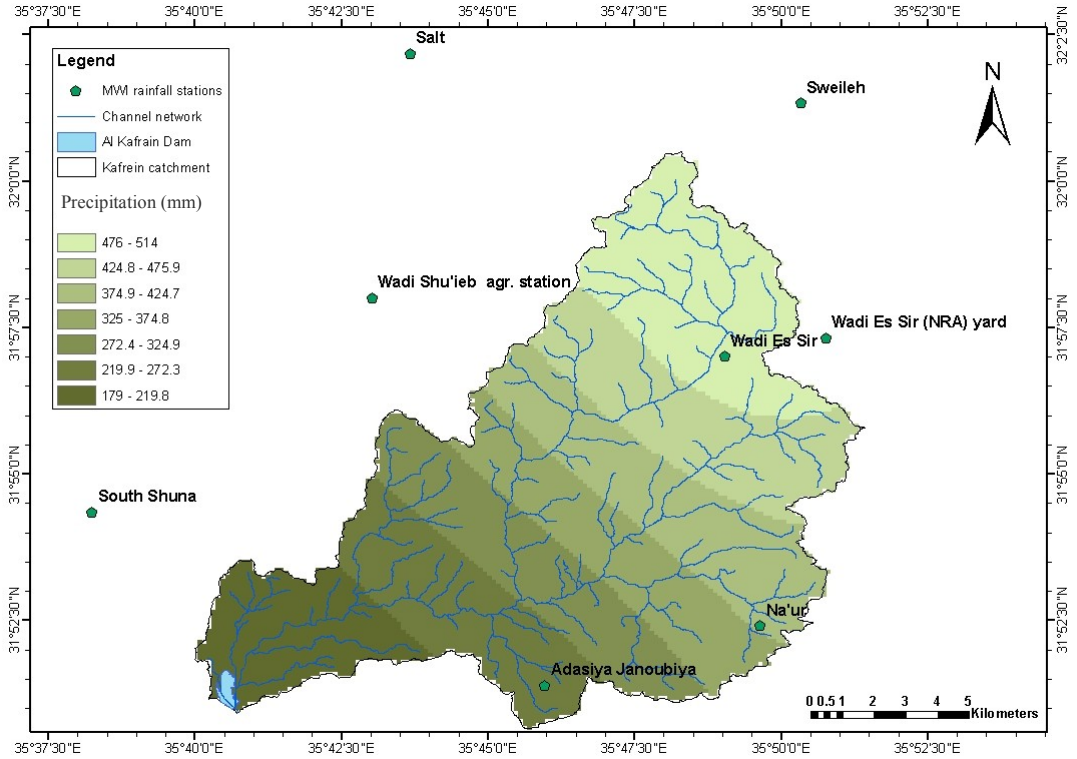

Fig. 2.16: Average annual rainfall over Wadi Kafrein catchment area.

Three rainfall stations where selected to present the spatial distribution of precipitation over Wadi Kafrein; Wadi As Sir station, located in the eastern high lands (720 m asl) of the study area, Adassiya Janoubiya station, located in the southern part (530 m asl), and South Shuna station (-230 m asl), located 5 km northwest of Kafrein Dam and which represents the precipitation pattern in the Jordan Valley (Fig. 2.16). Spatial variation in precipitation amounts is clear with respect to elevation as shown in Figs. 2.16 and 2.17.

The highest precipitation amount in the analyzed period was recorded in Al Salt station with 1,188 mm in the wet year 1991/1992, and also all other stations in the area recorded the highest amounts of precipitation in the same year, while the lowest value of precipitation was recorded in South Shuna station with 58 mm in the dry year 1998/1999. This spatial and temporal variation of precipitation is reflected on the

annual water storages in Kafrein dam and has a direct impact on runoff generation and concentration zones. Also it affects the groundwater recharge which in turn affects positively or negatively the agricultural sector.

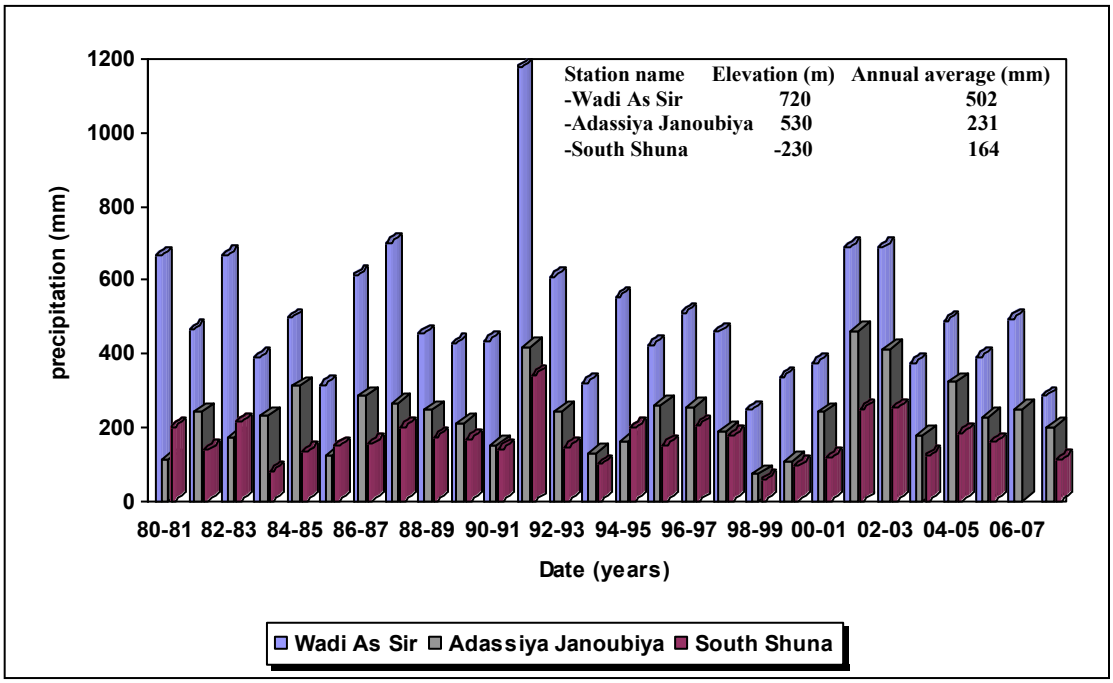

Fig. 2.17: Spatial variations of precipitation over Wadi Kafrein catchment with respect to elevation.

2.6.2.2 Temperature

The topography variations also affect the temperature over the study area but with a reversed effect compared to precipitation; temperature increases with lower elevations. Records are available for the two climatological stations Wadi As Sir AL0057, located in the upper eastern part of the study area, and South Shuna station AM0007, which lies in the Jordan Valley. The highest maximum temperature in Wadi As Sir station was recorded in the summer of 2002 with 39 °C while the lowest minimum temperature was recorded in the winter of 2003 with -11 °C.

The South Shuna station's highest maximum temperature was recorded to be 49 °C in the summer of 2003 and the lowest minimum of 1 °C was recorded in the winter of 2002; the average temperature in the highlands is 17.2 °C and in the Jordan Valley it is 25.4 °C. Figure 2.18 summarizes the spatial and temporal variations of temperature in Wadi Kafrein catchment. It can be noticed from Fig. 2.18 that the maximum temperature ranges of Wadi As Sir station is more or less similar to the minimum temperature range of South Shuna; this indicates an obviously large variation of temperature distribution over the study area. Data was available for Wadi As Sir station from 2002-2006 and for South Shuna from 1997-2006.

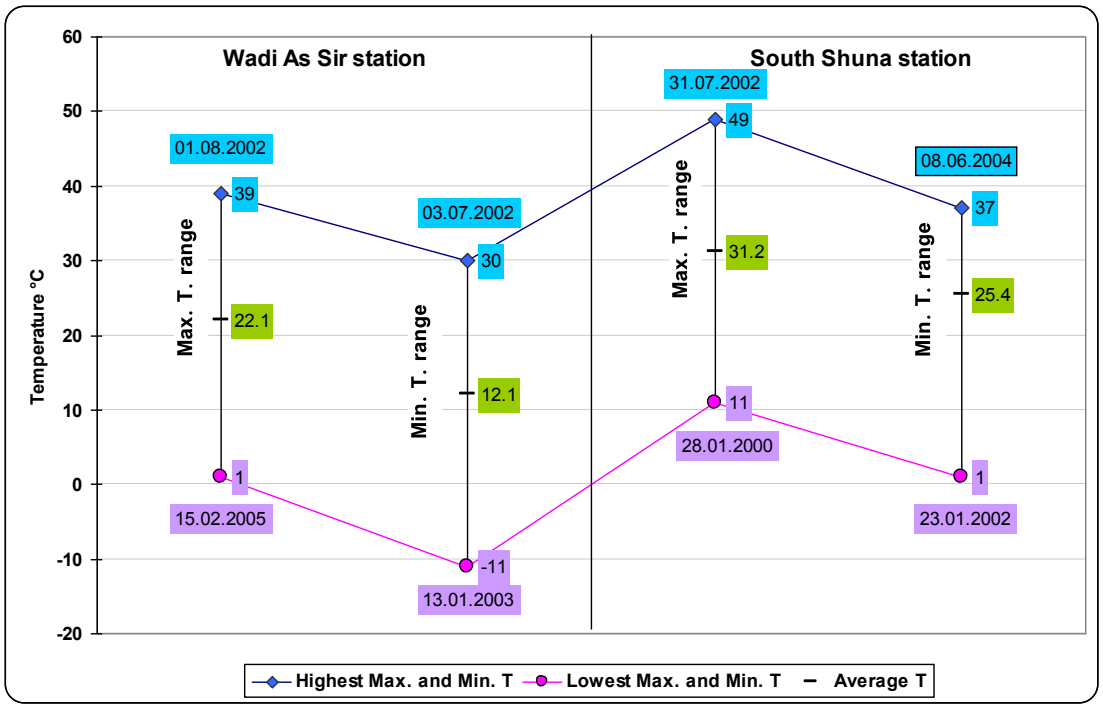

Fig.2.18: Spatial and temporal variations of temperature in Wadi As Sir and South Shuna stations.

2.6.2.3 Evaporation

Evaporation rates depend on several factors like air temperature, water temperature, and absolute humidity of layers of air just above the free-water surface. Also, it is affected by the wind which carries away the vapor from the free water surface and keeps the absolute humidity low. The driving force behind evaporation is solar radiation because it warms both the water and the air (Fetter, 1988). Air temperature and the above mentioned factors vary in space and time (the variations of climatic conditions) and affect directly the potential of evaporation and the evaporation rates. This leads in the Kafrein area to an increase in the potential evaporation rates when moving westward to the Jordan Valley.

The A-pan evaporation values measured in Wadi As Sir and South Shuna stations were used to verify the spatial and temporal variations. Wadi As Sir station represents the prevailing climatic conditions over the highlands while South Shuna station the prevailing climatic conditions in the Jordan Valley. Figure 2.19 shows the spatial effect where higher evaporation rates are measured with lower elevations. The temporal variation is caused by increases in solar radiation during summer months leading to higher values in both stations. The highest monthly evaporation rates over the eastern northeastern part of the catchment area occur during July with an average value of 335 mm with gradual increases toward west-southwest of the catchment to an average of 450 mm. The lowest rates of evaporation occur during January with an average of 65 mm in Wadi As Sir station up to105 mm in South Shuna station. It is worth mentioning that the available data series for Wadi As Sir station is rather short (June 2002-April 2006) and could not be considered as representative for a long term evaluation; though it was presented here to compare these values with those recorded in South Shuna to emphasize the strong effect of the spatial variations caused by elevation differences.

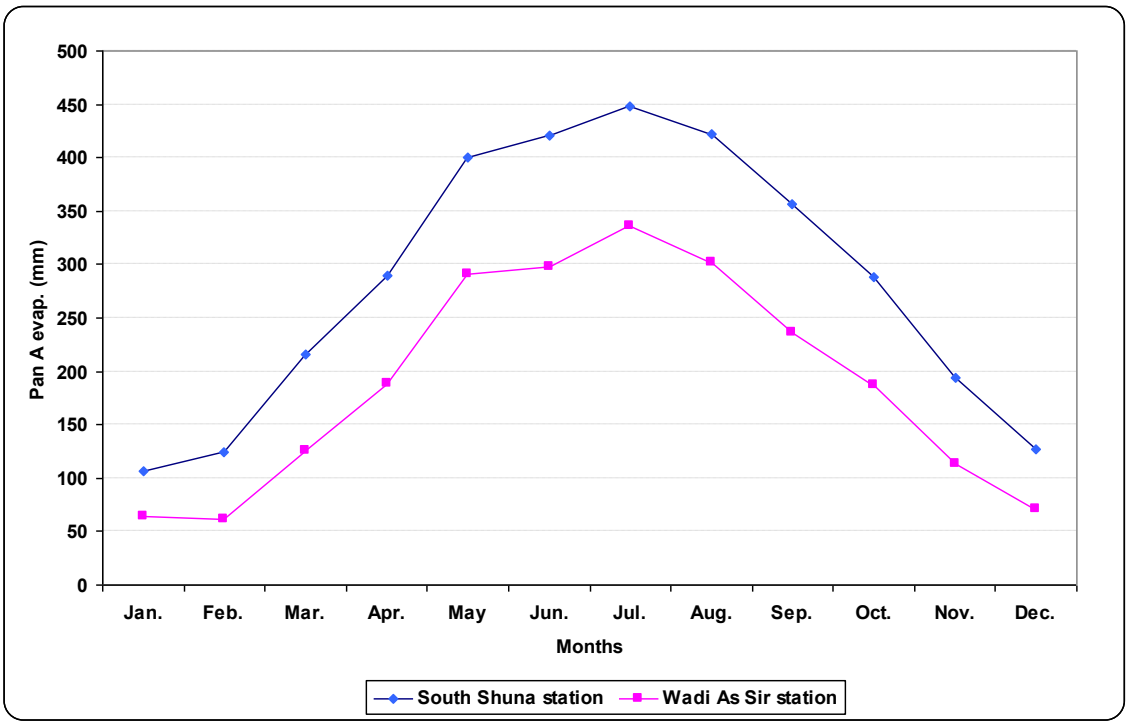

Fig. 2.19: Evaporation rates (class A land pan).

The monthly evaporation rates for Wadi Kafrein catchment were calculated by using the A-pan measured values in Baq'a station (with a coefficient of 0.74) and Penman equation by Salzgitter and JCE (1992). They calculated the annual evaporation in Wadi Kafrein catchment as 1,928 mm with the highest monthly evaporation rates being 240-260 mm during the period June to August and the lowest evaporation rates being 64-66 mm during the period December to January.

2.6.2.4 Runoff generation and concentrations

The vegetation cover in the middle and upper part of the study area intercepts some of the rainfall before it reaches the ground "*Interception*;" a portion of the intercepted rain goes back to the atmosphere via "*Transpiration*" while the other portion falls to the ground via "*Throughfall*". The amount of rain which reaches the ground either evaporates, infiltrates into the soil, forms puddles (*depression storage*), or flows over the surface as thin sheet of water forming what is known as "*Overland flow*" or runoff. All these processes are illustrated in Fig. 2.20, while more details on the runoff processes is given below.

Horton (1933) was the first who discussed the overland flow and defined it as: "Neglecting interception by vegetation, surface runoff is that part of rainfall which is not absorbed by the soil by infiltration. If the soil has an infiltration capacity "f", expressed in inches per hour, then when rainfall intensity "i" is less than "f", the rain is absorbed and there is no surface runoff. It may be said that a first approximation that if "i" is greater than "f", surface runoff will occur at a rate (i-f)".

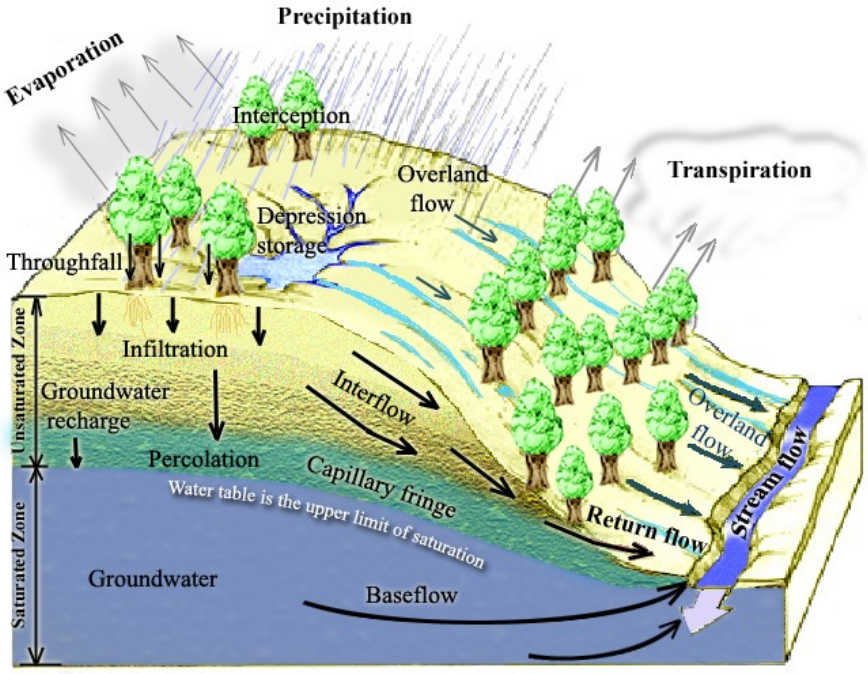

Fig. 2.20: Physical processes involved in runoff generation (Tarboton, 2003).

This mechanism of runoff generation is called Infiltration Excess Overland flow **(IEOF)** or the Hortonian overland flow (Fig. 2.22a). It occurs when the precipitation rate (rainfall intensity) exceeds the infiltration rate of the soil (Horton, 1933; Freeze, 1972; Dunne, 1983; Fetter, 1988). The Hortonian overland flow is considered to be the dominant runoff generation type in semi arid regions where rainfall intensities are high and vegetation cover is sparse (Puigdefabregas et al., 1998; Guentner and Bronstert, 2004).

Several conditions could promote the occurrence of **IEOF** by the reduction of the near surface saturated hydraulic conductivity (Buttle, 1998). Such conditions are related to urbanization activates and the associated sealing of surfaces (Ziegler et al., 2004) or to the crusting of soil surface (Patrick, 2002). This type of overland flow is applicable in zones with low infiltration capacity and the impervious surfaces in urban areas. The prevailing conditions in the lower part of the study area where the Aridic soil moisture regime prevails (see Section 4.2.4) with thin layer of crusted soil surface and no vegetation cover (see Section 2.3) suggest that **IEOF** is most probably the runoff mechanism which dominates these zones.

The spatial variability of soil properties, which affects the infiltration capacity and the spatial variability of surface water inputs, limits the infiltration excess runoff to some parts of the drainage basin during a rainfall event. A new concept was presented by Betson (1964) who pointed out that only a part of the catchment could contribute to Hortonian overland flow. This refinement of the Hortonian overland flow is known today as the partial area concept as illustrated in Fig. 2.22b.

Another mechanism which may produce overland flow in semi arid regions is the Saturation Excess Overland Flow (**SEOF**) see Fig. 2.22c. It occurs when the storage capacity of the soil is completely filled, leading any additional rainfall, regardless of

intensity, to flow over the surface (Kirkby, 1988). In zones where the soil texture is coarse and the soil permeability is high, the **SEOF** is the dominant runoff generation process. In semi arid regions, this mechanism occurs under specific conditions like rainfall in the valley bottom (Ceballos and Schnabel, 1998) or soils where a relatively permeable topsoil layer overlies less permeable material, which was defined by Gerits et al. (1990) as a separate type of overland flow called Topsoil saturation overland flow. This is a typical mechanism in case of plough pans, shallow profiles over bedrock, sand and gravel overlying layers of compact structures, etc. (Bergsma, 1983). In some parts of the study area, cultivation is common where several agricultural activities take place, and it is usually above a shallow soil layer overlying compacted bedrocks with low hydraulic conductivity. Figure 2.21a shows a thin layer of soil overlying massive limestone rocks while Fig. 2.21b shows a thin soil layer not exceeding 20 cm overlying compacted bedrock.

Fig. 2.21a : Thin layers of soil overlaying massive limestone (31^0 59' 13" N, 35^0 49' 06" E).

Fig. 2.21 b: thin layer of soil overlaying compacted Bedrock (31^0 59' 25" N, 35^0 48' 33" E).

In their study, Hewlett and Hibbert (1967) observed high rates of runoff generated in their research catchment without any saturation areas being formed. To explain this, they related the runoff to a subsurface storm flow (Fig. 2.22d). Some of the subsurface water returns to the surface and adds to the overland flow; this is called the return flow and it is illustrated in Fig. 2.22c as (q_r).

It is possible in the same catchment area to have infiltration excess, saturation excess or only subsurface responses at different times or different locations due to different antecedent conditions or soil characteristics or rainfall intensities (Beven, 2000). This might lead to the generation of a perched water table and even to saturation at the surface of a soil that may be unsaturated at depth (Fig. 2.22.e).

Runoff generation types and processes were not studied earlier in Wadi Kafrein; this research is the first to deal with these processes and explains the different mechanisms leading to runoff. The previous hydrological studies carried out on Wadi Kafrein catchment refer to quantitative amounts of runoff calculated using synthesized data and lumped methods (e.g. Soil Conservation Service- Curve Number method "SCS-CN").

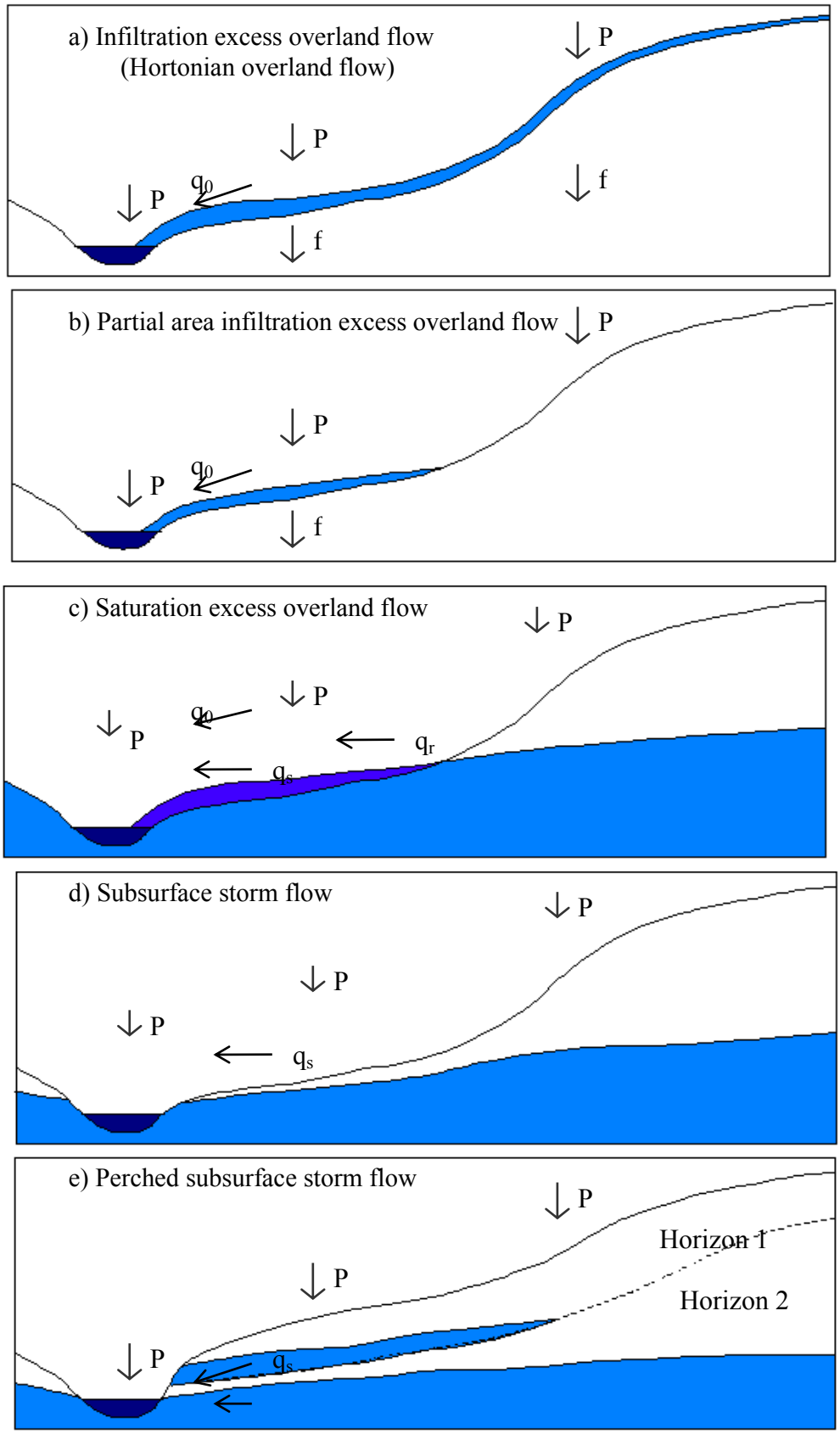

Fig. 2.22: Classification of runoff generation mechanisms (after Beven, 2000).

2.6.2.5 Transmission losses and runoff routing

In arid and semi arid regions the generated overland flow is characterized by a general decrease in volume in the downstream direction. Some of the flash flood water infiltrates into the sediments, which comprise the channel bed; these losses of water are called transmission losses and they can be a significant portion of the total runoff volume (Lane, 1983). These losses are also considered to be an important source of groundwater recharge in arid and semi arid regions (Shentsis and Rosenthal, 2003; Goodrich et al., 2004). The duration of flow at a particular location in the channel network depends on the velocity and size of the flood affected by the hydrodynamics of the flow and the cumulative transmission losses upstream of that location (Mudd, 2006).

Transmission losses were studied by Renard and Keppel (1966) at the Walnut Gulch experimental Watershed located in Arizona, United States, where large flood volume losses were reported as measurements progressed downstream (Table 2.2). Further studies about transmission losses are cited by Pilgrim et al. (1988).

Table 2.2: Effect of transmission losses on a flood at Walnut Gulch, Arizona (Renard and Keppel, 1966; Pilgrim et al., 1988).

Drainage basin area (km^2)	Volume of flood (1000 m^3)	Peak discharge (m^3/s)
95	92.3	41.9
114	79.9	27.2
149	40.1	15.6

By studying the runoff generation process, the amount of water which reaches the stream and flows downstream towards a catchment outlet within a period of time is measured. However, the routing of the runoff from the source areas to the outlet is an important component which must be taken into consideration. The boundary between runoff generation and runoff routing is not a very precise one and it is generally not possible to predict the volume and timing of the inflows, precisely making the routing problems one of the velocities of surface and subsurface flows on the Hillslope as well as in the stream channel (Beven, 2000).

There is no available data or information about the volumes of transmission losses or runoff routing in the catchment area of Wadi Kafrein despite their role and affect on the total runoff volume as discussed above. In this study, the transmission amounts will be calculated for the catchment area due to its importance and influence on runoff and the routing component to taken in consideration in the modelling process.

3 Modelling rainfall-runoff in arid and semi arid regions

3.1 Why model rainfall-runoff

Modelling rainfall-runoff is not an easy mission. From detailed lab and small-scale field studies on the movement of water through soils and rocks, patterns of water movement were shown to be highly complex (Beven, 2000). Nevertheless, many hydrologists have been able to develop effective rainfall-runoff models, which play a vital role in the management of floods, water resources, water quality, and environmental protection in large-scale catchments. Hydrological models are continually getting more efficient and accurate, and are now being used as powerful tools in making decisions by decision makers concerned with increasing demand on water resources. In arid and semi arid regions, these models are of utmost importance.

The problem encountered with hydrological modelling in arid and semi arid regions is that the large amount of data required to support a hydrological model is usually severely lacking (Wheater et al., 2008). Another problem faced in arid and semi arid regions is that hydrological responses are not consistent, but vary spatially within the catchment of interest and occur over irregular intervals of time. Both the problem of lacking initial data and the inherent problem of semi arid to arid catchments being hard to predict were initially valid for the catchment that has been studied here, Wadi Kafrein. With the developed hydrological model on Wadi Kafrein and the extensive amount of data that was collected for this research, these problems were overcome and a further understanding of arid to semi arid catchment hydrology was achieved.

The focus of this chapter is to review the modelling concept, review hydrological model types, and then assess and discuss in detail the problems in modelling rainfall-runoff in arid and semi arid regions. As an initial precaution, one should note that the climatological conditions in arid and semi arid regions are relatively harsh, and that hydrological responses are sensitive to changes in space and time, often causing several problems which need to be taken into consideration when modelling. It is also important to recognize that not all models existing today are capable of simulating hydrological processes of arid and semi arid regions. Many models have been developed for humid regions, which have completely different hydrological systems and responses from arid to semi arid regions. Due to the importance of this fact, a review of current available models is given in order to assess model suitability for arid and semi arid regions. Finally, criteria for model tool selection are identified to choose a suitable model for the study area.

3.2 Classification of hydrological models

A model is defined as any device that represents an approximation of a field situation (Anderson and Woessner, 2002). It consists of a set of simultaneous equations or a logical set of operations contained within a computer program. Models have parameters, which are numerical measures of a property or characteristics that are constant under specified conditions (Wheater, 2008). Different model types or source codes are available and several attempts were made to classify hydrological models

(e.g. Fleming, 1975; Singh, 1995; Refsgaard, 1996; Wheater, 2008). By reviewing the available literature, it was found that most of the models' classifications are based on the hydrological process description, but another classification was found, based on the technological level of the models, as given by Abbott et al. (1991). A summary of model classification is given for both classification types, with more emphasis on model classification with respect to hydrological process description due to its relevance for this research.

3.2.1 Model classification according to hydrological process description

Hydrological models can be classified to be deterministic or stochastic; in the deterministic approach, the models are grouped according to whether they give a lumped or a distributed description of the considered area and whether the description of the hydrological processes is empirical (black box), conceptual (grey box), or physically based (white box). Models based on stochastic approach are derived from a time series analysis of historical records, and then the model can be used to generate a long-term hypothetical sequence of events with the same statistical properties as the historical records. Today, a joint stochastic-deterministic methodology is common, presenting a useful framework for addressing some of the fundamental problems in hydrology such as taking spatial variability into account and assessing uncertainties in modelling. The given classification is schematic and many model codes do not fit exactly into one given class. The following classification is based on Refsgaard (1996) where an excellent and detailed description of all these classes is given.

3.2.1.1 Deterministic models

In deterministic models, a set of input values always gives the same output values. These models are classified into three groups: empirical, lumped-conceptual, and distributed-physically based (Fig. 3.1). The empirical models use mathematical equations, which are based on analysis of concurrent input and output time series not from the physical processes in the catchment area. Examples of empirical models used in hydrological modelling are the Constrained Linear Systems (CLS) models (Todini and Wallis, 1977) and the Antecedent Precipitation Index (API) model (WMO, 1994).

A model is said to be lumped if the parameters, inputs and outputs, are spatially averaged to one value for the whole modeled catchment area; a typical example of lumped-conceptual model group is the Stanford modelling system (Crawford and Linsley, 1966).

In the distributed-physically based model, the parameters, inputs, and outputs vary spatially. Typical examples of models using this approach are the IHDM model (Beven et al., 1987), the THALES model (Grayson et al., 1992) and the MIKE SHE model (Refsgaard and Storm, 1995).

The physically based models are based on the best available understanding of the physics of hydrological processes and on a continuum representation of catchment processes. The equations of motion of the constituent processes are solved numerically using a grid, which is usually discretized relatively crudely in catchment-scale applications (Wheater, 2008). The physically based distributed models are

thought to have an advantage over simpler black box or even lumped physically based models, due to their use of spatially distributed parameters which have a physical significance (Bathurst, 1986). This type of model has been developed from a need to analyze and solve specific hydrological problems often required in multi-objective and multi decision management investigations (Storm and Refsgaard, 1996).

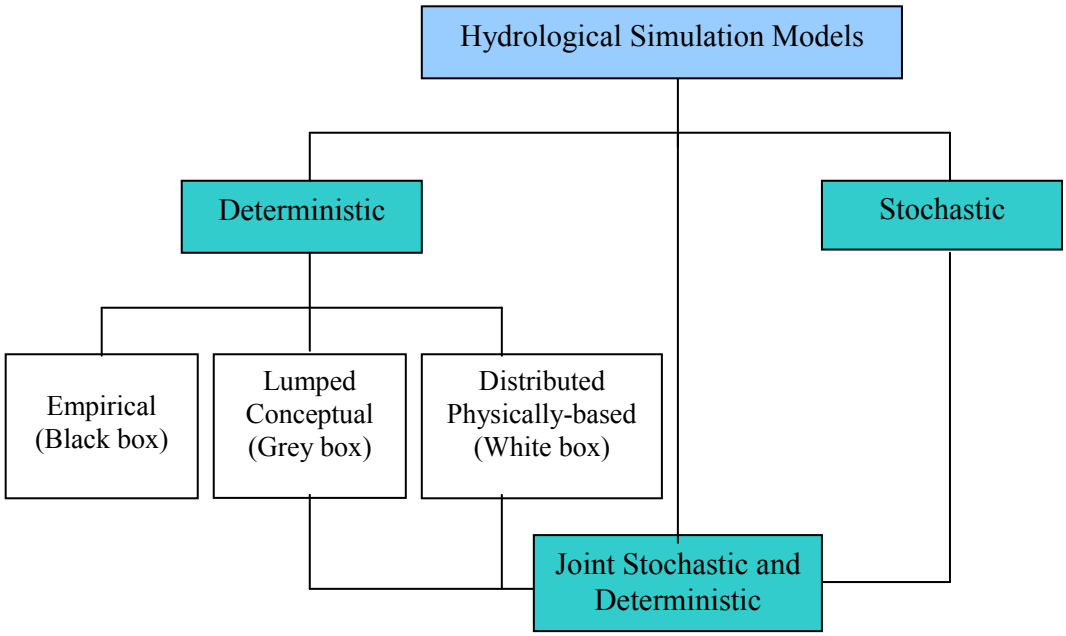

Fig. 3.1: Classification of hydrological models according to process description (modified from Refsgaard, 1996).

3.2.1.2 Stochastic models

A model is classified as stochastic if, due to random components, a set of input values do not necessarily produce the same output values. The stochastic model is based on probability laws which seek to account for random behavior which cannot be explained deterministically. For example, precipitation exhibits highly random behavior when observed as a function of time and space, but for long term predictions the probability theory and probability laws provide an appropriate frame work (O'Connell, 2000). The technique of generating several synthetic series with identical statistical properties based on historical records is called the Monte Carlo technique (Refsgaard, 1996). A description of stochastic time series models is given by Salas (1992). Several rainfall-runoff models are based on the stochastic time series approach (e.g. Freeze, 1980; Storm et al., 1988).

3.2.2 Model classification according to technological level

This type of classification, which has been given by Abbott et al. (1991), is based on the level of technology involved in the models (i.e. the level of sophistication). Models can be seen as falling into one of five generational categories:

- **First generation (Computerized Formula):** appeared in the 1950s, and was characterized by the use of the first computers as calculation devices for analytical expressions.

- **Second generation (One-off Numerical Models):** appeared in the 1960s; models of this generation are characterized as being constructed, developed, and applied by mostly universities or research institutes to usually solve one specific problem. Utilization was restricted to the developers of the code.

- **Third generation (Generalized Numerical Modelling System):** a development of the second generation due to the problem solving versatility of that code. In hydrology, the first distributed physically-based systems were made in the beginning of the 1980s, while the much simpler lumped conceptual systems appeared in the 1960s (Refsgaard, 1996).

- **Fourth generation (The Industrial User-friendly Software Product):** the products of this generation are user friendly software which can be applied by professional engineers and scientists. The models of this generation differ from the third generation by being fully menu-based, with interactive execution and online help menus; also they provide comprehensive error message and automatic checks for obviously erroneous input data. These models have powerful graphics facilities, are much better documented and proven, and they are more easily transferable and installable.

- **Fifth generation (Intelligent Modelling System):** designed for technically-skilled but non-expert users and they merge into hydroinformatics tools, generally, such as diagnostic and real time control systems and management support systems.

The fourth generation systems have no demands on user experience in computer systems or numerical techniques but they require that the user has an experience in modelling. Most of the present models belong to the fourth generation while the fifth generation systems are still in the experimental stage, except for real-time control applications used in urban drainage systems (Refsgaard, 1996).

3.3 Problems of rainfall-runoff modelling in arid and semi arid regions

Today, an increase in global managerial and scientific awareness of hydrological modelling problems in arid and semi arid regions is taking place. Several organizations and agencies like UNESCO, which initiated a Global Network for Water and Development Information for Arid Lands (G-WADI), are working to increase the understanding of the hydrological processes in arid and semi arid regions. This global network is aiming to strengthen the global capacity to manage water resources in arid and semi arid regions and it seeks to provide a global forum for the exchange of experience, information, and tools. Furthermore, several books have been published, dealing with hydrological processes in arid and semi arid regions (e.g. Simmers, 2003), and other books are dedicated to address the importance of

hydrological modelling in arid and semi arid regions with some recent examples of modelling in arid regions like India and South Africa (e.g. Wheater et al., 2008). Nevertheless, most of the developed modelling tools were developed primarily for humid area applications while less attention was given for arid and semi arid regions. Several problems are involved in modelling rainfall-runoff in arid and semi arid regions; a good example of such problems or challenges is given by Hughes (2008), from his southern African experience, where he addressed several factors, which had hampered the development and the successful application of hydrological models and which are summarized as follows:

- A high degree of spatial and temporal variation in hydrometeorological variables and resulting streamflow

- A lack of adequately long or continuous records of rainfall (and other hydrometeorological variables) and streamflow

- A lack of quantitative understanding of the mechanisms of some critical hydrological process (notably channel transmission losses and surface-ground water interactions)

These limitations are common in several arid and semi arid regions other than South Africa; the data scarcity, low quality, and the discontinuity of records in arid and semi arid regions have been addressed by several authors world wide (e.g. McMahon, 1979; Pilgrim et al., 1988; Sen, 2008).

In the case of Wadi Kafrein, the high variability of precipitation and meteorological parameters, addressed and discussed earlier in Section 2.6.2 of this thesis, give an example of the first limiting factor of hydrological modelling in arid to semi arid regions, according to Hughes (2008). To address the third limiting factor by Hughes (2008), as stated above, distinctive features of arid zone hydrology, addressed by Pilgrim et al. (1988), are summarized below. These distinctive features, which affect, to a large degree, runoff generation and runoff routing, are the basis for likely differences between models for humid zones and models for arid to semi arid zones, due to the influences they have on the dynamics of the catchment.

- There is a different mix of hydrological processes with some humid zone processes (e.g. Baseflow) essentially absent, while channel transmission losses are of critical importance.

- Arid and semi arid zones are often in delicate hydrological balance; the whole nature of the hydrology and values of model parameters may be changed by a prolonged wet or dry sequence.

- Rainfall tends to be more variable in space and time compared to humid regions.

- Plant cover is sparse and consists mainly of xerophytes, ephemeral grass, and small leafy plants. These plants have water retention mechanisms and rooting characteristics adapted for survival, which vary with xerophytes species found in different regions. Also, vegetation cover density may vary

drastically from the time after a wet period to that after a prolonged dry period. Such variations have potential effects on the demand of soil water. In addition, typically a wide variation in the soil water balance exists for differences in spacing of vegetation on the individual plant to plant scale.

- There is a relative absence of organic matter and litter on ground surface, which probably has a significant effect on many hydrological processes like interception, infiltration, evapotransipiration, and runoff.

- In many arid regions, phreatophytes located along stream channels have a significant effect on groundwater recharge and presumably on channel transmission losses.

From the above descriptions of distinctive hydrology related features in arid to semi arid regions, one can conclude how sensitive arid and semi arid regions are with respect to their response to hydrological processes. Modelling these processes could be a great challenge and due to the inclusion of what are sometimes key processes such as transmission losses and runoff generation mechanisms, complications in establishing accurate models are common. With these complications in mind, which arise out of the features just described by Pilgrim et al. (1988), the next task is to evaluate selected hydrological models and to find out suitable criteria for selection of the right model code for simulating the hydrological processes in Wadi Kafrein. In this selection process, consideration for the aims and the objectives of this research as stated in Section 1.3 is integral, and overcoming spatial and temporal variations, which is one of the most distinctive features of arid and semi arid region hydrology, will be required.

3.4 Evaluation of potential rainfall-runoff models for Wadi Kafrein

Almost all modelling tools which have been used for different purposes have been primarily developed for humid area applications (Wheater, 2008). This indicates the difficulties involved in finding a suitable model for arid and semi arid regions; additionally the different hydrological systems possibly found within an arid or semi arid region need different modelling approaches. Pilgrim et al. (1988) distinguished between three broad classes of hydrological systems in arid regions for which every class needs its own approach. These hydrological systems are:

- Sloping regions with an integrated stream network
- Plain lands with a primitive or no stream network
- Regions with major inputs of surface water or groundwater from more humid regions, frequently with extensive irrigated agriculture

Most of the applications of rainfall-runoff models are in the sloping regions which happen to only be a minor part of the arid and semi arid regions in the world (Pilgrim et al., 1988) but this criterion matches the steep relief of Wadi Kafrein, as discussed in Section 2.2 of this thesis. To simulate the hydrological processes in Wadi Kafrein, a close look on the available model codes is needed first, from which the most

appropriate code will be selected which should fulfill the model selection tool criteria described in the coming Section 3.5.

Several hydrological model source codes were evaluated to be used in this study, with examples including all three types of deterministic models mentioned earlier in this chapter. A brief description of every potential model is given, summarizing the aim of developing the model, the needed input files, the resulting output files, cases studies where the model was applied, model documentation, and the model code availability.

3.4.1 Potential empirical models

- Constrained Linear Systems : CLS

CLS is a deterministic empirical model, and a multiple input with single output linear system model. The model was developed in the Department of Earth and Geo-Environmental Sciences, University of Bologna, Italy. It has been developed with the aim of simulating non-linear rainfall runoff and flood routing processes. The model needs rainfall, an antecedent moisture condition, and watershed maps as input files. It generates a discharge hydrograph as an output. The model has been extensively tested and verified with several applications and case studies, for example: the Arno River, Italy; Nile River, eastern Africa; and the Niger River, western Africa. The model code and documentation are not available in the public domain but they can be obtained from the Department of Earth and Geo-Environmental Sciences, University of Bologna, Italy. Some useful references related to the CLS model are: Natale and Todini (1977); Todini and Wallis (1977).

3.4.2 Potential lumped models

- Hydrologic Engineering Center-Hydrologic Modelling System: HEC-HMS

HEC-HMS is a surface water model designed to simulate the rainfall-runoff processes of dendritic watershed systems with an application in a wide range of geographic areas. The model was developed by the US Army Corps of Engineers USACE-HEC. It is a lumped parameter surface water model. The model requires three types of input files: time series data (e.g. precipitation, discharge, and temperature gages…etc.), paired data (e.g. storage discharge, elevation-storage, and elevation-area functions…etc), and gridded data (e.g. precipitation, temperature, crop coefficient, percolation rate, elevation grids…etc.). The main output of the model is a tabular and graphical discharge. The model was applied intensively by the USACE and others. Some applications are the Chicken Ranch Slough and Strong Ranch Slough (CRS/SRS) watershed/USA (Ford et al., 2008), the Bonanza catchment/USA (Ford et al., 2002). The latest model manual user is available online (Scharffenberg and Fleming, 2009). The model source code and further documentation are available for the public domain in the model main webpage under:
<http://www.hec.usace.army.mil/software/hec-hms/>.

- Hydrologic Simulation Program-FORTRAN: HSPF

HSBF is a surface water model developed by the United States Environmental Protection Agency (USEPA). It belongs to the lumped parameter surface water models which can run in either single event or continuous simulation mode. The model aims to quantify runoff and address water quality impairments associated with combined point and nonpoint sources. The model requires as input files meteorological and hydrologic data, soils and topographic information, land use, as well as drainage and system (physical and man made) charectarestics. The initial result from this program is a time history of the quantity and quality of water transported over land surface and through various soil zones down to groundwater aquifers. Also, the model can predict runoff flow rate, sediment loads, nutrients, pesticides, toxic chemicals, and other quality constituent concentrations. The model was applied hundreds of times all over the world. The model is open for the public domain and a bibliography, which includes useful references related to model development and applications, is available under the following link: <http://www.aquaterra.com/hspfbib.html>. The model manual user and further information about the model is available for public domain by Bicknell et al. (2005).

- Identification of unit Hydrographs And Component flows from Rainfall, Evaporation and Streamflow IHACRES

IHACRES is a catchment-scale rainfall-streamflow model with spatially lumped approach. The model was developed in the integrated Catchment Assessment and Management (iCAM) centre of The Australian National University and the Cooperative Research Centre (CRC) for Catchment Hydrology. The model aims to assist in characterizing the dynamic relationship between basin rainfall and streamflow. The model has six parameters and it requires rainfall, temperature, and streamflow as input files while it provides a streamflow simulation as output. It has been used in several catchments, e.g. the Salmon Brook (Western Australia), the Teifi catchment (Wales, UK), the Murrindindi River (southeast of Australia) among others. The model is available in the public domain and further application description and further information about the model is available in the following articles: Littlewood et al. (1997), Ye et al. (1997), Croke et al. (2005).

3.4.3 Potential physically based models

- Distributed Hydrology Soil Vegetation Model: DHSVM

DHSVM is a distributed physically based model. It was developed in the Pacific Northwest National Laboratory, Richard, Washington, USA, and aims to provide a dynamic representation of watershed processes (evapotranspiration, snow cover, soil moisture, and runoff) at the spatial scale described by digital elevation model data. The model has twenty-two parameters with physical meaning estimated from physical measurements. It needs hydrometeorological data, rainfall, soil texture, hydraulic information, a Digital Elevation Model, vegetation information, and land use maps. It produces a runoff hydrograph as an output. The model has been used in several studies to evaluate the mass and energy fluxes under snow free conditions, for evaluation of canopy snow interaction and ground snowpack, interaction between

climate and hydrology…etc. One recent application of the model is the coupled version of DHSVM with WRF (Weather Research and Forecasting) which was used to forecast snowmelt runoff in the Juntanghu watershed of the northern slope of Tianshan Mountains in Central Asia by Zhao et al. (2009). The model is available for public domain. Publications on model features together with model development and applications can be found under the following link: <http://www.hydro.washington.edu/Lettenmaier/Models/DHSVM/publications.shtml >. Recent publications on the model development and description and on model application are: Lanini et al. (2009) for the former and Cuo et al. (2009) for the later.

- MIKE-Systeme Hydrologique Europeen: MIKE SHE

MIKE-SHE is a physically based distributed model. It has been developed by a joint cooperation between the Danish Hydraulic Institute, the British Institute of Hydrology, and SOGREAH (France). MIKE SHE is an advanced integrated hydrological modelling system. It simulates the water flows in the land base phase of the hydrological cycle from rainfall to river flow. This includes the overland flow, infiltration to soil, evapotranspiration, and groundwater flow. The model requires meteorological, soil, land use, and DEM data for inputs while it provides a wide range of fully distributed gridded form of output files of all hydrological cycle components. The model was used in many studies; e.g. the Gyeongancheon catchment (Korea/ Im et al., 2008), the Neuenkirchen catchment (Germany/ Xevi et al., 1997), and the Rizana spring catchment (Slovenia/ Janza, 2009). The model is not available in the public domain; it is a proprietary code model, meaning the full functional license is rather expensive to purchase. The model is well documented and extensively used. It has a world wide user group, which meets annually to share model results and model applications. A comprehensive introduction to the model history, philosophy, and structure is given by Abbott et al. (1986a, b).

- SHE-TRANsport origin is in the SHE model: SHETRAN

The SHE-TRANsport origin is in the SHE model (Systeme Hydrologique Europeen). It is a physically based distributed river basin model. It has been developed within the Water Resource Systems Research Laboratory, School of Civil Engineering and Geosciences, University of New Castle, New Castle upon Tyne, UK. The model objective is to simulate transient three dimensional flows and transport in basins up to 5,000 km^2. The model requires hydrometeorologic data, rainfall, soils, basins geomorphology, and land use; also other data is needed for particular applications. The outputs are discharge, sediments, and solute graphs. The model has several applications; e.g. the Agri basin (Italy), the Slapton Wood, Devon (England), the Murg basin (Switzerland), the La Reine catchment (Chile)…etc. The software is not open for the public domain but model documentation is available at the SHETRAN web site: <http://www.ceg.ncl.ac.uk/shetran/index.htm>. More than a hundred publications are available while the recent ones are: Birkinshaw et al. (2010a, b) and Bovolo et al. (2009).

- TRAIN-ZIN

TRAIN-ZIN is a coupled physically based distributed model. TRAIN has been developed in the Federal Institute of Technology ETH, Department of Geography, Zürich, Switzerland by Menzel (1997). It was designed to simulate the spatial pattern of the individual water budget components at different spatial and temporal scales. The model can be applied at the point and the regional scale with one hour or one day as a temporal resolution. The ZIN model has been developed in the Institute of Hydrology, University of Freiburg, Germany by Lange (1999). It was designed to simulate short term runoff generation processes in arid environments and uses rainfall temporal resolution of five minutes; also, radar data can possibly be used. The TRAIN-ZIN model requires as input files hydrometorological data, rainfall, soil, land use, DEM and geomorphological data of the catchment. The output is a daily water balance, a five minutes runoff discharge, and several maps of the hydrological cycle components (rainfall, snow, runoff, evapotranspiration, soil moisture, and deep infiltration). The model has several applications; e.g. the Faria catchment (West Bank, Palestine / Shadeed, 2008), the Harod catchment (Israel/ Fischer, 2007; Ritter, 2009). The model is not available in the public domain but it can be acquired in addition to a user's manual from Institute of Hydrology, University of Freiburg, Germany.

3.5 Model selection criteria

Problems with model selection arise not from problems with model availability, but with model suitability. By searching the literature and the libraries of different universities and research agencies one can find hundreds, if not literally, thousands, of models which have been designed to simulate hydrological processes and which help to better understand various problems related to water and land use management. In the end, the right selection will provide an invaluable tool for decision makers in finding out the optimum solutions to catchment management problems. To increase the usefulness of a hydrological model, it is important to choose the right model which will be able to fulfill the demands of the modelling application. This can be achieved by developing model selection criteria.

In Chapter Two, the different runoff mechanisms were discussed and the conclusions indicated that the infiltration excess overland flow is the dominant mechanism in the arid and semi arid regions. Nevertheless, saturation excess overland flow is also responsible for some runoff which is generated in the formerly mentioned areas. For simulating and quantifying these two very important processes, together with transmission losses and runoff routing, the physically based distributed models provides a good tool to achieve this task. So for Wadi Kafrein, the physically based distributed models showed an advantage compared with the conventional rainfall-runoff models, in order to understand hydrological processes and to analyze the runoff generation mechanisms and amounts.

Although the traditional hydrological models of lumped conceptual type are well suited to deal with the main part of current water resources assessment and flood and drought forecasting, more advanced tools are required for the remaining problems including prediction capabilities. Distributed models are able to predict, therefore making them highly effective management tools (Refsgaard and Abbott, 1996).

The physically based distributed models present a better possibility in solving several hydrological problems, especially the ones from human impacts on land use change. Such problems can be solved using the physical basis which takes into consideration the spatial and temporal distribution of physical parameters over the catchment. The data to be used in a physically based model needs to be prepared in a special way in which considerations of the physical properties of the catchment are included, meaning the spatial distribution of the data within the catchment need to be sufficient and representative. One of the strong qualities of using physically based distributed models is from the philosophy of the model use by estimating the necessary data and parameter values which are not available with only an approximate accuracy. Furthermore, the physical basis of the model does not require a long hydrological and meteorological data series for calibration because the calibrated set of parameters should be applied outside the range of the conditions used in the calibration stage of the model (Abbott et al., 1986a).

The physically based distributed models can be, in principle, applied to solve all types of hydrological problems; they are based on our understanding of the physics of the hydrological processes and it uses within its source code physically based equations for processes description.

Based on the above discussion and by considering the objectives of this research, it has been recognized that a rainfall-runoff model with physically based distributed approach represents the best choice. Model selection tool criteria have been identified to choose the best model from the discussed models list in Section 3.4.

For the model code to be used in this study, the following minimum capabilities are required:

- **The ability of the model to simulate the hydrological processes:** accurate partitioning of precipitation, evapotranspiration, runoff, and infiltration components is required. The simulation of the runoff component and related factors such as the runoff mechanism, transmission losses, and the routing processes are of special importance.

- **The ability of the model to deal with the prevailing climatic conditions and the hydrologic processes in arid and semi arid regions:** represented by the high variations of precipitation and runoff distributions in space and time.

- **The physically based distributed structure of the model:** flexibility in model application and capability for simulating hydrological processes efficiently and accurately.

- **The availability of the model for public use:** availability in the public domain as an open source will be given a preference over the commercial models. The availability of documentation and support is desirable.

- **The availability of resources to meet the model input requirements:** the required data should have the format, type, and time step, obtained by having first defined the available resources for this study.

- **The model should be able to fulfill the objectives of this study which have been mentioned in the first chapter.**

- **A priority will be given for models which will be able to simulate the human effect on hydrological processes**: the effect of urbanization on hydrological processes and the dynamic of water flow in the study area.

One cannot say that one model is better than another. Simply put, the development of the world's existing hydrological models has been borne out of the desire to fulfill many purposes: some models were developed with the aim of solving a particular hydrological problem, while others were developed for commercial purposes; while even some other models, which have been the topic of scientific papers, simply aim to simulate hypothetical scenarios in order to enhance our knowledge and understanding of our environment.

The models discussed in section 3.4 are only a few examples of models which have been developed and which are available. The empirical and lumped parameter models have been excluded in the consideration as a potential main model tool due to their structure which does not take into consideration the spatial distribution of the parameters. As discussed in Chapter 2, Wadi Kafrein has highly spatially variable soil properties, topography, slopes, vegetation, and precipitation, and therefore a model that does not take this into consideration simply does not meet the criteria for model selection. Therefore, the physically based models are the best available models for use in this study. The potential physically based models listed in section 3.4.3 will be discussed in more detail to select the suitable modelling tool to be applied in Wadi Kafrein.

DHSVM is a distributed hydrologic model that explicitly represents the effects of topography and vegetation on water fluxes through the landscape. The model has been applied predominantly to mountainous watersheds in the Pacific Northwest in the United States. During the literature review assessment of the DHSVM model, it has been found that most of the model applications can be arranged in three main categories as follow:

- In hydrological forest managements; (i.e. Storck et al., 1998; Alila et al., 2001; Thyer et al., 2003).
- In land use and land cover changes; (i.e. Burges et al., 1998; VanShaar et al., 2002).
- In climatic changes impacts (i.e. Leung and Wigmosta, 1999; Wigmosta and Leung, 2001).

As stated earlier the model was applied predominantly to mountainous watersheds in the Pacific Northwest in the United States; these watersheds receive rain year-around and receives very heavy snowfall, which is known to be one of the snowiest places in the world. Therefore the hydrological responses of these watersheds are different compared with the arid and semi arid regions similar to Wadi Kafrein. Also no publications or reports were found which refers to model application or evaluation in arid or semi arid regions. Therefore the DHSVM was excluded as a main modelling tool for Wadi Kafrein watershed.

The MIKE SHE model and the developed model based on it; the SHETRAN, are both powerful models with several extensions and modules making them among the best available and long term developed physically based hydrological models. MIKE SHE covers the major processes in the hydrological cycle and includes process models for evapotranspiration, overland flow, unsaturated flow, groundwater flow and channel flow and their interactions. Each of these processes can be represented at different levels of spatial distribution and complexity, according to the goals of the modelling study, the availability of field data and the modeler's choices, (Butts et al., 2004). MIKE SHE uses MIKE 11 to simulate channel flow. MIKE 11 includes comprehensive facilities for modelling complex channel networks, lakes and reservoirs, and river structures, such as gates, sluices, and weirs. Also the detailed model description and documentation with plenty of successful applications puts MIKE SHE on the top of potential models list. Nevertheless, the cost of the model is rather expensive.

For the aim of this study the TRAIN-ZIN model was chosen for the following reasons:

- The availability of the model in the public domain
- It is the only model among the potential models list which was developed and further enhanced to simulate the hydrological processes in arid and semi arid regions
- The model simulates the runoff components in much detail with high spatial and temporal resolution
- The model has several successful applications in arid and semi arid regions
- The model can fulfill the objectives of this study and has the required capabilities mentioned earlier in this chapter

Further description of the TRAIN-ZIN model will be given in Chapter 5 which emphasize on the model application, parameterization, calibration and validation processes.

4 Methodology of data acquisition and analysis

4.1 Data acquisition and database

Water plays a critical role in the development of arid and semi arid areas. In order to maximize water usage sustainably, one needs to understand hydrological processes and mechanisms. Hydrological models are highly suitable tools for solving this task and can also help to increase our understanding of natural as well as anthropogenic environments. However, without consistent, reliable, and up-to-date databases, hydrological studies are hard to perform. The quality of hydrological models is, therefore, strongly dependent on the quality of the input data.

The main limitation to the development of hydrological studies in arid and semi arid regions is the lack of high quality data. What is available from quantitative observations, already simulated models, or other previous studies done in Wadi Kafrein is highly insufficient for building a proper and accurate hydrological model. For this research project, scarce data has propelled the scientific desire and need to develop a suitable methodology, using innovative techniques to produce a high quality input data which can be used in the hydrological model of Wadi Kafrein. The poor quality of the available spatial and temporal data, in addition to the unavailability of some essential data such as land use map, soil map, and runoff measurements, were the main motivation to build up a comprehensive database for Wadi Kafrein watershed before starting the modelling process.

Without high quality inputs, high quality outputs cannot be expected. For rainfall-runoff models, the inputs are watershed characteristics like drainage area, channel network geometry, topography, soil and land use characteristics, and time series of surface water inputs. The output, a time series of streamflow at an outlet location, has a quality which is dependent on the quality of all the given inputs (Tarboton, 2003).

In order to implement any hydrological model, a set of basic data is needed. Basic data sets can be classified to be of any of the following groups:

- **Structural data**: includes surface catchment, stream network, sub catchments, and/or basin delineation.

- **Time-series input data**: includes precipitation measurements from point sources, evapo-transpiration calculated from measured climatological parameters.

- **Physical properties data**: includes channel roughness coefficients, channel widths, alluvium depths, soil properties, etc.

- **Observed data (*for surface modelling*):** includes runoff measurements for calibration and validation purposes.

A detailed hydrological database has been prepared to be used as input for the rainfall-runoff model of Wadi Kafrein. Climatological parameters and rainfall

amounts were measured with high resolution. Runoff and stage heights of several small-scale subwadis in addition to the total water storages of the Kafrein dam reservoir were measured with high temporal resolution. Land use maps and soil maps, which are needed for the model, were prepared using non-traditional techniques. These were previously not available in the required spatial or temporal resolution. Satellite images, remote sensing techniques, and GIS applications were the techniques employed. A detailed soil map and four land use/cover maps were thus prepared to fulfill the aims of this study. The description of the methodology of data acquisition and data analysis is given in the coming sections.

4.2 Remote sensing and GIS in hydrological modelling

Remote sensing provides a solid visual effect, and provides a basis for gathering spatial information on things such as urban areas, vegetation, and water. Satellite images, which are used in remote sensing, can provide important information, concerning topography. Also, satellite images facilitate the preparation of some needed catchment properties like watershed properties, stream network properties and a *Digital Elevation Model* (DEM). Remote sensing data is finding more and more use in hydrological studies and models. Early on, Schultz (1994) expected an increase in the role of remote sensing in hydrology and he had addressed several reasons as to why:

- Time series from remote sensing are relatively long and are readily available
- A new type of remote sensing information can now be provided
- The recent tendency in hydrology toward macro-scale hydrological modelling requires data quantities with spatial and temporal resolution which cannot be provided by conventional observation techniques

Most remote sensing images are recorded in digital form and then processed by computers to produce images for interpreters to study. The image consists of small and equal areas or picture elements arranged in regular rows and columns called raster arrays. The position of any picture or pixel is determined on an x-y coordinate system. Each pixel also has a numerical value called a *Digital Number* (DN), that records the intensity of electromagnetic energy measured for the ground resolution cell represented by that pixel (Sabins, 1997).

Practical applications of remote sensing usually require links to other types of information. Among others, the *Geographic Information System* (GIS) is widely used in parallel with remote sensing applications. GISs are designed to analyze spatially distributed data and more specifically to analyze interrelationships between different types of data which are matched to each other within a specific geographic region. In spite of the differences between remote sensing and GISs, it is only partially incorrect to state that remote sensing is primarily a means of collecting data, and that GISs are primarily a means of analyzing and storing data (Campbell, 1996). The concept of GIS is the ideal which permits a full utilization of the goals of remote sensing. One can say that remote sensing achieves its maximum usefulness when images from one date, or formed from one part of the spectrum, can be integrated with those acquired

at a different date or a different portion of the spectrum. GIS provides the maximum flexibility in both display and analysis (Campbell, 1996).

Different types of hydrological models are available with different needs for input files; but from earlier review in Chapter Three, the physically based distributed models were found to be the best choice for this research. The physically-based distributed models are data demanding; the parameters' values must be provided with a spatial distribution. In this context, the availability of high quality remote sensing data (satellite images) together with the GIS application presents a very useful and powerful combination for data input preparation of physically based models. Remote sensing data and GIS applications provide great facilities for hydrologists to deal with a wide range of hydrological problems. These hydrological problems are usually highly complex and distributed over large areas which may have a large area or may be complex and spatially distributed hydrological processes.

In hydrological modelling, several thematic maps are needed as input files; a thematic map is a map which shows a particular theme (one attribute) for a specific geographic place. It is possible to construct a GIS by having a series of thematic maps (e.g. soil map, topographic map, and land use cover map) with a common geographic reference. GIS enables one to produce an accessible archive of useful information; also to store, to classify, and to visualize spatial data for a specific case study. GIS is a standard technology in many fields and it is widely used in hydrological studies. For the aim of this study, a GIS database has been prepared using ArcGIS 9-ArcMap 9.2 (GIS software developed by ESRI) to support the modelling approach and provide the model with the needed thematic maps with respect to similar resolution and boundary extension. The World Geodetic System (WGS84) was used as a geographic referencing system to all GIS layers and the produced maps in this study.

The *Global Positioning System* (GPS) is a surveying technique which was often used during the field campaigns of this study. Locational information can be acquired with high accuracy using the GPS. These systems are well integrated with GISs and it is easy to read and transfer data from GPS to GIS. One of the most important applications is to assist in the identification of *Ground Control Points* (GCP), which allows resampling of image data to provide accurate planimetric location and to correctly match image detail to maps and other images (Campbell, 1996). The GCPs are discussed in more details in Section 4.2.1.

Concerning the satellite images, recent Cartosat-1 and ASTER images were acquired to enhance the data quality and to support the modelling approach of this research. A high resolution digital elevation model (DEM) has been prepared using the Cartosat-1 satellite images which serves as a base map for many other analyses and model maps' inputs. Detailed land use/cover maps were prepared for the study area for four different months in order to study the vegetation cover changes along the year and to serve as input maps for the hydrological model. Sections 4.2.1 and 4.2.2 describe the methodology used in developing and extracting the needed model maps and in defining the hydrological characteristics of the study area using this type of data. In this study, GIS data were visualized and analyzed using ArcGIS 9-ArcMap 9.2, while the satellite images were analyzed using the remote sensing software RSI Envi 4.3.

4.2.1 Digital elevation model from Cartosat-1 stereo image data

Cartosat-1 is a remote sensing satellite, which was launched in May 2005 by the Indian Space Research Organization (ISRO). It has fore (F) and aft (A) panchromatic cameras which are capable of acquiring stereoscopic data along the orbital track, with a tilt in flight direction of +26° and -5°, respectively. The cameras are mounted on the satellite in such a way that near simultaneous imaging of the same area from two different angles is possible; this facilitates the generation of accurate three-dimensional maps. Figure 4.1a illustrates the along-track viewing geometry, which enables Cartosat-1 to acquire a stereo pair in about 54 seconds. High-quality DEMs are possible to be produced using these data. The produced data has a horizontal spatial resolution of 2.5 meters and cover a 30-km swath. A detailed description of Cartosat-1 technical features and data products is given by Cartosat-1 Data User's Handbook (2006) and Krishnaswamy and Kalyanaraman (2009).

4.2.1.1 Cartosat-1 data accuracy

A study of accuracy assessment for DEMs prepared by the Cartosat-1 stereo image data has been done by Evans et al. (2008), who compared the vertical accuracy amongst the National Elevation Dataset (NED), Shuttle Radar Topography Mission (SRTM) DEM, and the Advanced Spaceborne Thermal Emission and Reflection Radiometer (ASTER) DEM. They concluded that Cartosat-1 DEMs compare quite well with the most accurate reference DEMs. In another study of the Cartosat-1 Scientific Assessment Programme (C-SAP), Titarov (2008) evaluated the Cartosat-1 Geometric potential and found that the derived DEM accuracy has a 2 m Root Mean Square Error (RMSE) for flat areas and 7 m RMSE for mountainous areas (as compared to reference DEMs). In general, Cartosat-1 has a good potential for generating DEMs with a grid spacing of about 10 m and accuracy (RMSE) of about 3 m, but it has been reported that this can be achieved by only using GCPs (Kocaman et al., 2008). The DEM generated from Cartosat-1 has been also evaluated by Kumar (2006) in Dehradum, India. The study concluded that the generated DEM from Cartosat-1 data are very useful for topographic analysis in the field of water resources, agriculture, etc. All the above mentioned studies and references refer to the potential of Cartosat-1 stereo images in producing a high quality and reliable DEM. Therefore, Cartosat-1 images were chosen among other satellite images to be used in this study, taking in consideration the accuracy and the high resolution.

4.2.1.2 Data acquisition and correction

The Cartosat-1 imagery data used in this study consist of a single stereo pair acquired on April 12, 2007 with geographic extents of 3519442.5-3549592.5 Northing and 737292.5-771587.5 Easting and spatial reference WGS_1984_UTM_ZONE_36N. Figure 4.1b shows the acquired image with some distinctive features (i.e. dams or rivers).

To gather useful information from satellite images in a way that they can be used in mapping and GISs, these images must be prepared with the aim of removing distortion. This process is called orthorectification. Additionally, for 2.5 m ground sampling distance (GSD), the data are not accurate enough and they require a

correction which can be made by GCPs - the so called bias correction (Jacobsen et al., 2008).

Within the evaluation program of Cartosat-1 images, Kocaman et al. (2008) found that the GCP distribution seems to have an influence on the accuracy of the generated DEM and recommended the use of about 6 GCPs as minimum. Same minimum number of GCPs was also recommended by PCI Geomatics (2006).

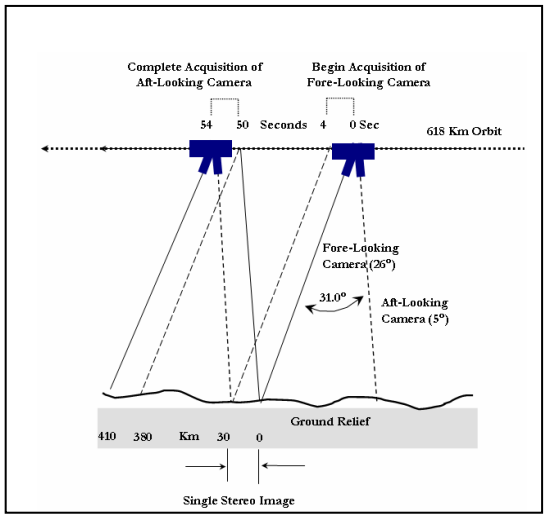

Fig. 4.1a: Along track imaging geometry of the Cartosat-1 fore- and aft-viewing cameras (Evans et. al 2008).

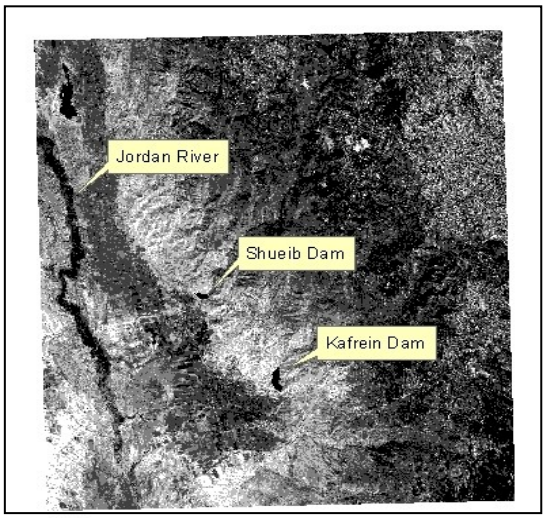

Fig. 4.1b: The acquired Cartosat-1 stereo image data for Lower Jordan Valley.

During a field campaign in October, 2007, a GCP set including 47 points was taken using Differential Corrected GPS measurements covering the study area. These GCPs were taken from easily identifiable points on the satellite image and on grounds such as road intersections, farm boarders, and tunnels/bridges (Fig. 4.2a). The taken GCP set covers the catchment area of Wadi Kafrein in a detailed way as shown in Fig. 4.2b.

Fig. 4.2a: Taking a GCP measurement in Jordan Valley using Differential Corrected GPS measurements.

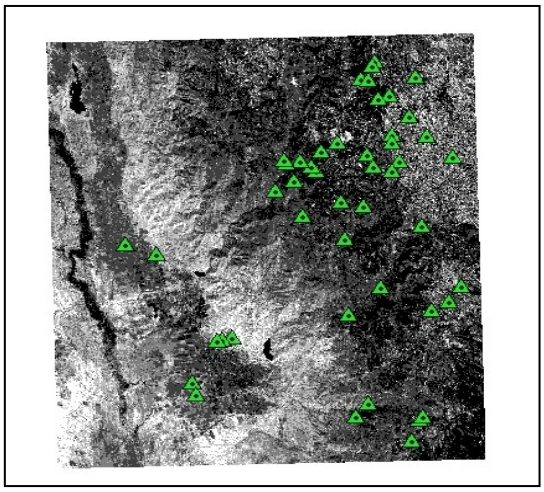

Fig. 4.2b: The GCP set taken to correct the acquired Cartosat-1 stereo image data.

4.2.1.3 Methodology and results

For the aim of this study, a high accuracy DEM has been extracted from Cartosat-1 satellite images with a final cell size of 5m x 5m. Data correction and DEM extraction procedures are described in detail by PCI Geomatics (2006) and are available online under: http://www.pcigeomatics.com/support/tutorials/pdf/cartosat_tutorial.pdf.

Using the prepared DEM within GIS environment, the elevation characteristics have been calculated. The maximum elevation in the study area is 1,079 m on the upper northeastern side of the study area. Elevation then decreases westward to a 139 m bsl (below sea level) minimum near the Kafrein dam reservoir, with an average elevation for the whole catchment area of 605 m. The catchment has a width of around 15 km and a length of 17 km, while the greatest variations in elevation occur in the first 5 km moving from northeast toward south west. In the southern boundaries near Na'ur and Aldassiya cities, the slope is steeper and more than half of the drop in elevation occurs in the first 2-3 km (Fig. 4.3).

The high resolution DEM has been used as a main input for the modelling process and was used to calculate the needed hydrological charectarestics of the study area. Using the prepared DEM the catchment watershed was calculated; stream network and steepness map were prepared.

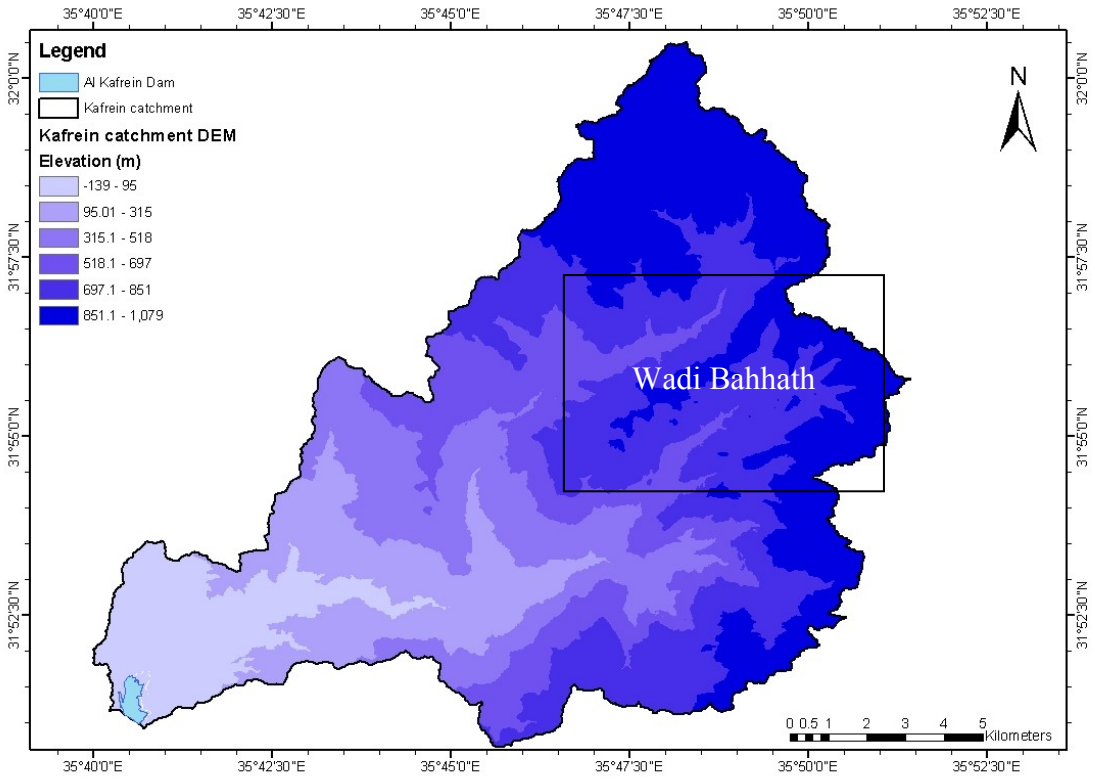

Fig. 4.3: High accuracy DEM extracted from Cartosat-1 imagery data with final cell size of 5m x 5m.

The accuracy of the derived DEM has been evaluated by comparing the produced DEM with ground truthing GPS measured points. Several previous elevation models are available for the Wadi Kafrein catchment with resolutions which are not suitable for detailed rainfall-runoff investigations. Figure 4.4 shows 3 different DEM for Wadi Bahhath where big variations in resolution can be noticed. The width of all maps in Fig. 4.4 is 7 km.

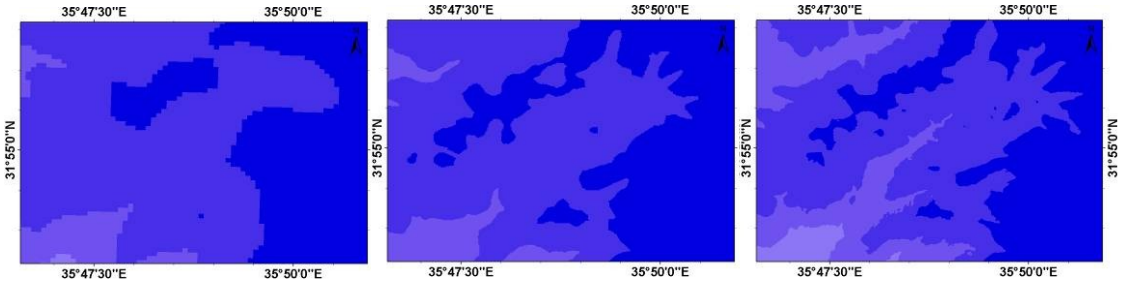

Fig. 4.4a: 100 m cell size **b: 20m cell size** **c: DEM with 5m cell size**

4.2.2 Land use and land cover maps from ASTER satellite images

The Advanced Spaceborne Thermal Emission and Reflection Radiometer (ASTER) is an imaging instrument launched in 1999 by NASA and Japan's Ministry of International Trade and Industry and Japan's Earth Remote Sensing Data Analysis Center (ERSDAC). It is a multispectral (14 band) high-resolution sensor with three different instruments operating in the visible spectrum, five operating in the Near Infrared (VNIR) spectrum, six in the Short wave Infrared (SWIR) and Thermal Infrared (TIR) regions of the electromagnetic energy spectrum (Yamaguchi et al., 1998; Mather, 2004).

4.2.2.1 ASTER satellite images accuracy

ASTER has 3 bands of 15 m spatial resolution in the visible and near-infrared wavelength regions. These three bands have the same spectral zones as Landsat7 ETM+ multispectral bands. Jinlong et al. (2003) compared the performance of the ASTER image with that of the ETM fusion image from four key aspects in order to accelerate its application for agricultural monitoring. These four key aspects are geometric correction, typical surface features identification, land target area measurement, image classification, and interpretation. They found that the ASTER image:

- can be geometrically corrected with high accuracy
- is better than the ETM+ fusion image for typical surface features identification
- records small land targets in detail
- can be more suitable for recognition by eye
- can be used for measuring land target area with high accuracy
- has the same high quality performance as the ETM image for image classification and interpretation.

They concluded that ASTER shows great potential for the applications of agricultural monitoring. In another study done by Montzka et al. (2006) ASTER satellite imagery

was used to extract detailed information on agricultural crops and impervious surfaces, which in turn was used in water balance modelling. Their results indicated that the model can produce more detailed local water balances using remote sensing data. Zhu and Blumberg (2002) concluded that classification using ASTER data for urban studies is reliable with high classification precision up to 88.6% average overall accuracy.

In another study to assess the applicability of the VNIR bands of the ASTER imagery in mapping land cover in the dry lands of northern Ethiopia, the results showed that ASTER imagery can have an over all accuracy of about 80% in mapping land cover in the dry lands (Aynekulu et al., 2008). The ASTER imagery have been widely used in land use and land cover classification and several studies proved the reliability of these data for land cover classification and the high accuracy which is acquired. As it has been stated earlier in this chapter, the land cover maps are an important component which is needed in order to apply a physically based hydrological model.

Several ASTER images were acquired in this study to classify the land cover in the Wadi Kafrein catchment also to study the effect of temporal variations of vegetation on hydrological modelling as vegetation percentages vary according to the different seasons.

4.2.2.2 Data acquisition and correction

The multi-temporal ASTER satellite images of the dates November 30, 2006; January 17, 2007; March 22, 2007; and May 25, 2007 have been acquired for land cover classification in the Wadi Kafrein catchment. The images have a resolution cell size of 15m x 15m. All images were first projected to WGS 1984 coordinate system and then they were clipped off for the study area of Wadi Kafrein.

A total of 47 GCPs were identified covering the whole catchment area of Wadi Kafrein (see more 4.2.1.2 and Fig. 4.2). These steps are usually done before starting the classification in a preparation stage known as preprocessing. Figure 4.5 and 4.6 are two ASTER satellite images taken on November, 2006 and March, 2007, respectively. In both images the urban areas can be easily distinguished in the upper eastern and lower eastern side of the image while the bare rock region in the lower western side is recognized by the white reflecting surface. Another distinctive feature which can be recognized in the image is the Kafrein dam lake. An increase in the size of the lake in March can be seen as an effect of the precipitation during the winter season.

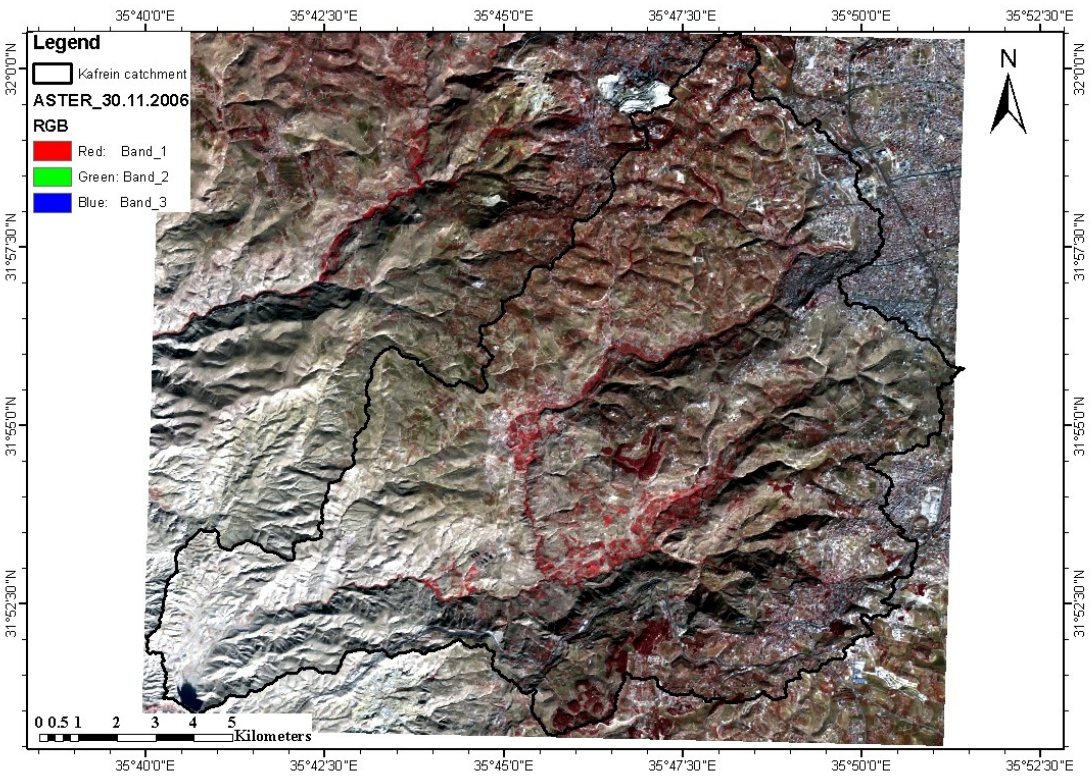

Fig. 4.5: ASTER 15m x 15m color composite of Wadi Kafrein obtained on November 30, 2006 (RGB-bands of 3, 2, 1).

In the satellite image of March, 2007, more red color is present (Fig. 4.6) compared to the image of November, 2006 (Fig. 4.5). This reflects the increase in the vegetation cover in the flat areas in the both catchments of Wadi Kafrein and the adjacent catchment of Wadi Shueib.

For a better visualization and a more detailed overview, a land cover classification is needed. In the next section the methodology of the land cover classification is explained and the results are shown. The vegetation cover was studied and analyzed in detail using the vegetation indices. All acquired ASTER satellite images are given in Appendix B.

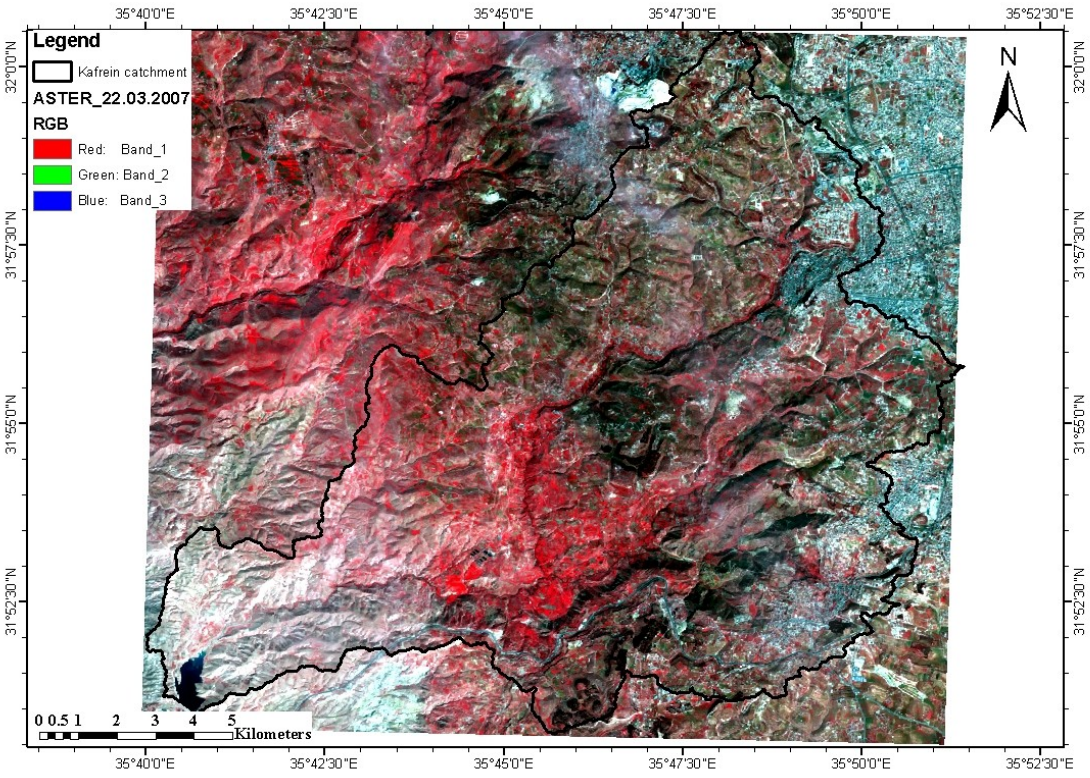

Fig. 4.6: ASTER 15m x 15m color composite of Wadi Kafrein obtained on March 22, 2007 (RGB- bands of 3, 2, 1).

4.2.2.3 Methodology and results of land use/ land cover classification

Remote sensing has become a main source of information for characterizing land use and land cover classes and changes in a regional and global scale. The term *land cover* refers to the type of material which exists on the landscape; for example a forest, water body, or anthropogenic materials like asphalt. On the other hand, the term *land use* refers to what people do on the land surface; for example agriculture, commerce, settlement (Jensen, 2005). Usually the term land use has an emphasis on the functional role of land in economic activities, while land cover often designates only the vegetation, either natural or cultivated, on the earth's surface. Land cover lacks the emphasis on economic function that is essential to the concept of land use. Hydrologists can focus solely on land cover because of their concern with only the physical components of the landscape that pertain to the movement of moisture (Campbell, 1996). Visible to near infrared ASTER data of the bands 1,2,3 were used for the land cover classification. Theses bands were chosen because they have the highest spatial resolution (15m/pixel).The land cover map is considered as one of the main input files in surface water studies as it represents the interaction layer between the rainfall and the catchment surface.

Image classification is the process of assigning pixels to classes. Each pixel is treated as an individual unit composed of values in several spectral bands. If the pixels are compared to one another and to pixels of known identity then it is possible to assemble groups of similar pixels into classes which match the informational categories of interest (Campbell, 1996).

The two most common methods for identifying and classifying land covers in satellite images are the *unsupervised* and the *supervised* classifications. In the unsupervised classification, multiband spectral response patterns are grouped into clusters that are statistically separable, so that a small range of DNs, (for instance 3 bands), can establish one cluster that is set apart from a specified range combination for another cluster. The unsupervised classification is too generalized and the clusters only roughly match some of the actual classes (Short, 2010). In a supervised classification, the identity and location of some of the land cover classes/types are known a priori through a combination of field work, an interpretation of the satellite images, map analysis, and personal experience (Hodgson et al., 2003). These identified locations or sites are commonly referred to as *training sites* because the spectral characteristics of these known areas are used to train the classification algorithm for eventual land-cover mapping of the reminder of the image. The multivariate statistical parameters (means, standard deviations, covariance matrices, correlation matrices, etc.) are calculated for each training site, then every pixel within and out of the training sites is evaluated and assigned to the class of which it has the highest likelihood of being a member (Jensen, 2005). The supervised classification is much more accurate for mapping classes (Short, 2010) but it depends heavily on the skills of the image analyst.

The land cover classes of Wadi Kafrein were identified by a supervised classification of the four acquired ASTER satellite images data. In the supervised classification, various algorithms can be used to assign an unknown pixel to one of the identified classes. The *Maximum Likelihood Classification algorithm* is one of the most widely used supervised classification algorithms (Mclver and Friedl, 2002; Wu and Shao, 2002). It is based on probability of each given pixel belonging to any of each class. The pixel is then assigned to the class for which the probability is the highest (Jensen, 2005). The four acquired ASTER images were classified using an algorithm based on the maximum likelihood.

Nine classes of interest where selected based on intensive field observations and previous knowledge of the available land cover taking place in the catchment area of Wadi Kafrein. The training areas were first assigned to representative sites which were known a priori from field observations and the interpretation of the satellite images. Following is a brief description of the classes with spatial distribution maps of every class shown in the upper right side of the class image.

- **Urban areas**

The urban areas are comprised of houses, buildings, or anthropogenic materials of roads and impervious surfaces. As shown in the distribution map, the urbanization is located in the eastern side of the catchment area which is in fact the western extent of the Amman city. The lower eastern part is the Na'ur city. The total area of the urbanization is 6.60%.

- **Water**

In Wadi Kafrein catchment area, the dam reservoir presents the biggest water surface body ranging from a few thousand square meters during dry periods up to 800,000 m^2 when the dam is full. Other surfaces are found in the Wadi Es Sir WWTP but with limited size. Water surfaces present less than 0.40% of the total area of Wadi Kafrein.

- **Bare rock**

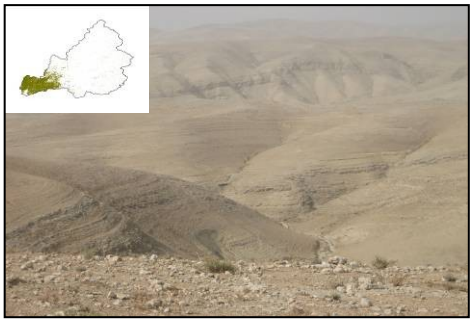

This class is the area which extends west of the longitude 35° 43' 30". It is composed of limestone with mostly no vegetation cover as can be seen in the photo. Annual average precipitation over this area is less than 200 mm. The area covered with bare rock is 13.2%. The area is not populated except few Bedouins who move there during the winter season.

- **Forest**

The forest cover is limited to a small part in the middle of the catchment over a hill called Abu El-Sous. Another small area of dense forest is located in the southern part of the study area along the left side of Al-Adassiya Street towards the Dead Sea as can be seen in the distribution map. The forest cover doesn't exceed 5.3% of the area. It consists mainly of oak and pine trees.

- **Olive trees**

Olive trees are common in the study area; most local people prefer to plant olives as no irrigation is needed. Several fields around the urban areas are planted with olives and these fields are mostly in the upper and the eastern part of the study area in elevations which are usually higher than 500 m. The total area covered by olive trees is 14.8% of the total catchment area.

- **Agriculture**

Agricultural areas are mainly located on the flat surfaces and on both sides of the main Wadi where a baseflow is used for irrigation. Agriculture consists mainly of field crops, but some orchards are also available which can not be easily separated by remote sensing. The area of agricultural cover varies between summer and winter with an average of 13.6% based on the 4 analyzed satellite images.

- **Bare soil**

This class presents the areas where a soil layer is available but no vegetation cover. In specific time of the year these fields are planted with seasonal crops; therefore their percentages varies. In average bare soil covers about 15.2% of the area while this areas decrease during the winter season as some grass and small bushes will grow there.

- **Sparse vegetation**

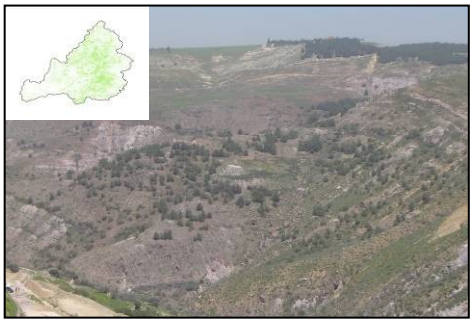

This land cover is a combination of several classes; that is the bare soil, forest trees, and some sparsely scattered bushes. In contrary to the bare soil, the area covered by this class increases during the winter season which become covered with some bushes and vegetation. On average, sparse vegetation covers 27.4% which represents the highest land cover in Wadi Kafrein.

- **Shrubs**

This class includes all small trees and small bushes which are mainly distributed along the main tributaries of Wadi Kafrein where most of the springs are flowing. Surfaces covered by shrubs do not exceed on average 3.5%, but this value varies around the year as they depend mainly on the surface water in the main stream.

The accuracy of the classification of different classes has been evaluated by comparing the land cover maps with the images of Wadi Kafrein area obtained by Google Earth® and by field investigations. Figure 4.7 shows part of four classes overlying the Google Earth® map with a 40% transparency. Abu El-Sous (forest) can be seen in Fig. 4.7a, and this fits very well with the underlying Google Earth® map. Also, Fig. 4.7b, where the small and individual houses are, is also well classified. The Kafrein Dam boundaries also fit the Google Earth® image while the bigger area covered in Fig. 4.7c is related to the increase in the Kafrein Dam storages as the classified map belongs to March. The bare rocks shown in Fig. 4.7d present very well the real land cover in the study area. Overall, the classification accuracy is very good and acceptable.

(a) **Forest (Abu Es Sous)**

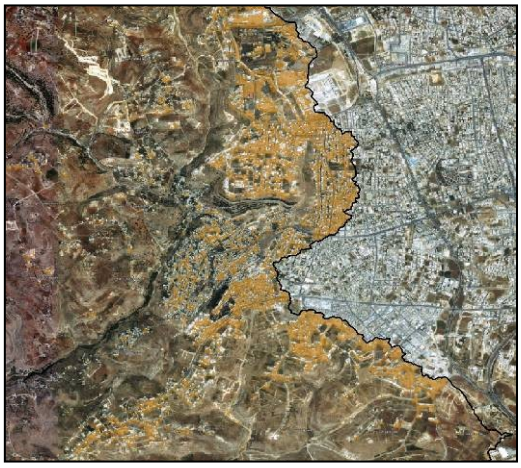

(b) Urban areas (West of Amman)

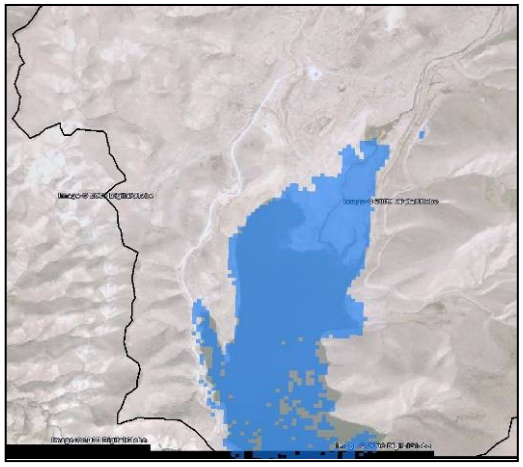

(c) Water (Kafrein Dam)

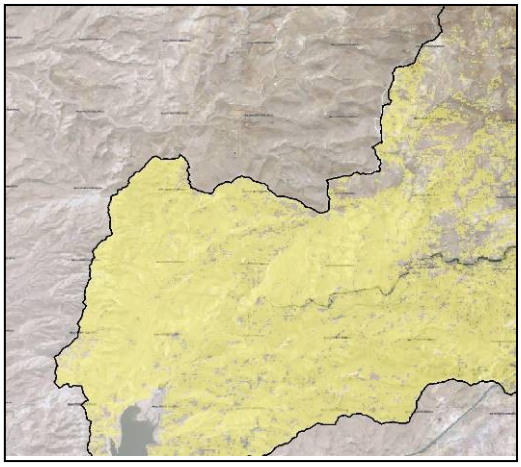

(d) Bare rock (Near the dam)

Fig. 4.7: Land covers validation sites using Google Earth® image and field investigation.

The land covers shown in Fig. 4.7 are parts of the whole ASTER image which was classified for the month March and shown in Fig. 4.8. The prepared Google Earth® image after being corrected and projected to the WGS 1984 system is shown in Fig. 4.9 and includes the sites of Fig.4.7a-d. All four acquired and analyzed land cover maps are given in Appendix C.

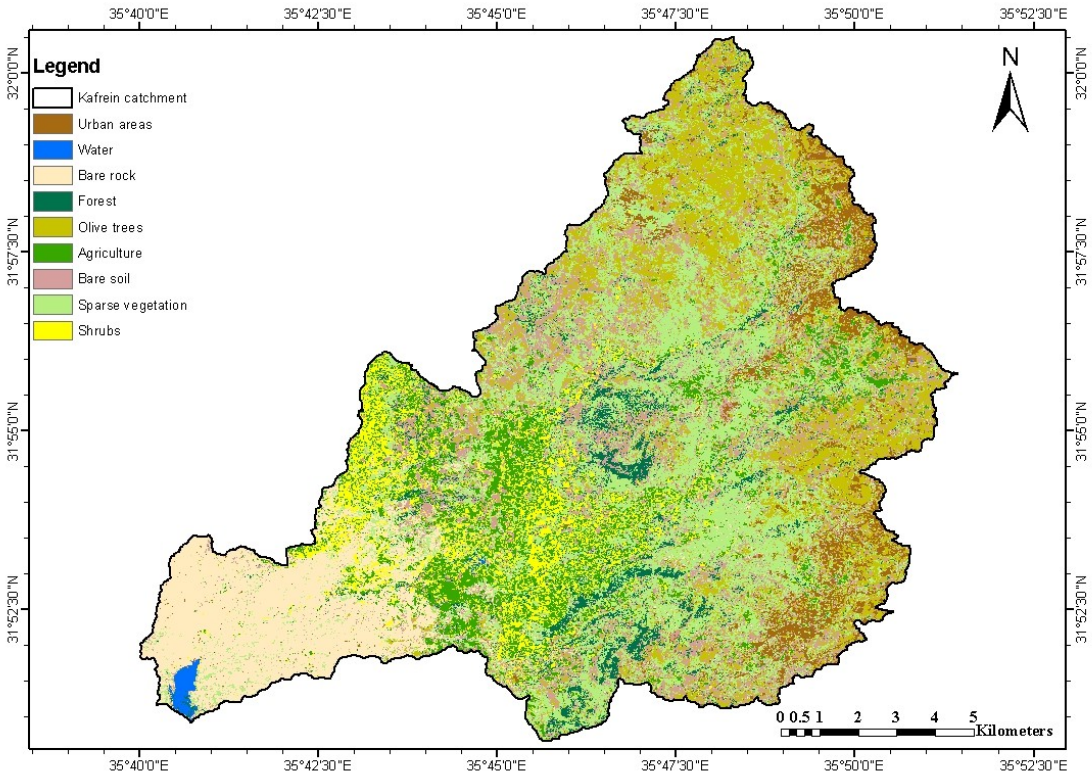

Fig. 4.8: March 2007 land cover classes using a supervised classification algorithm - Maximum Likelihood Classifier.

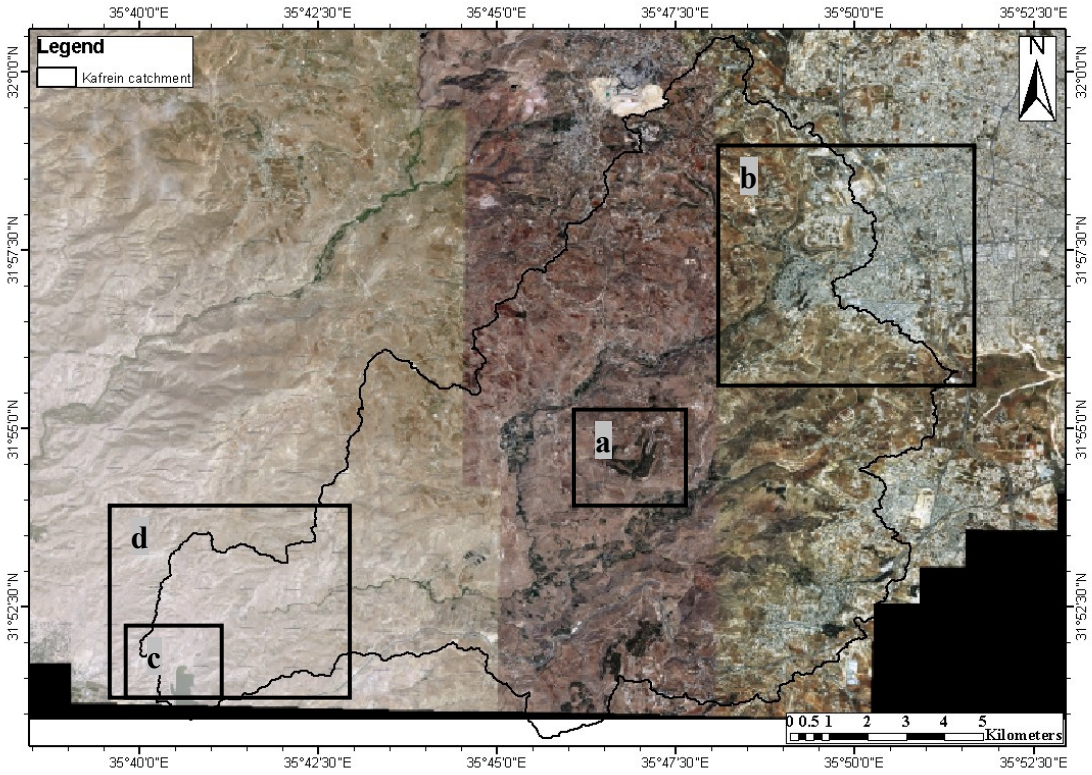

Fig. 4.9: Google Earth® image of Wadi Kafrein catchment after correction and projection to the WGS 1984 system.

4.2.3 Spatial and temporal assessment of vegetation

A wide spatial variation in land cover is present within Wadi Kafrein as shown in Fig. 4.8, but to get a closer look on these variations, the vegetation cover has to be assessed further. Vegetation assessment can be done, using a vegetation index. A vegetation index is a parameter which quantifies the relative abundance and activity of green vegetation. *Leaf-area-index* (LAI), percentage green cover, chlorophyll content, green biomass, and absorbed photosynthetically active radiation (APAR) are included in the vegetation index (Jensen, 2007). The vegetation index can be produced by dividing the data in the infrared band by the DNs in the red band (Gibson et al., 2000).

Vegetation index has been developed as a method of enhancing the visibility of healthy vegetation on satellite images and is now a key tool for environmental monitoring. Many vegetation indices are available; detailed summaries of vegetation indices can be found in Running et al. (1994) and Lyon et al. (1998). In this study, the *Normalized Differenced Vegetation Index* (NDVI) has been used. The NDVI is known as being simple and accurate. *Density Slicing* (DS), which will be discussed in the following paragraphs, was also used in conjunction with NDVI with the intention of NDVI enhancement.

4.2.3.1 NDVI and DS analysis

Vegetation indices are generally spectral transformations of two or more bands designed to enhance the contribution of vegetation properties and allow reliable spatial and temporal inter-comparisons of terrestrial photosynthetic activity and canopy structural variations (Heute et al., 2002). One of the most used vegetation indices, and the one used in this study, is the NDVI. The NDVI is defined as the difference between the visible red and near-infrared bands over their sum. For ASTER data, the bands 2 and 3 of the Visible and Near Infrared (VNIR) sensor are relevant to calculate the $NDVI_{ASTER}$ (Botkin et al., 1984; Montzka et al., 2006) as follows:

$$NDVI_{ASTER} = \frac{Band3 - Band2}{Band3 + Band2}$$

The index returns pixel values ranging from -1 (no vegetation, low reflectance in both bands 2 and 3) to +1 (pixel dominated by actively photosynthesizing vegetation) (Stefanov and Netzband, 2005). The strength of the NDVI is in its ratioing concept, which reduces many forms of multiplicative noise (illumination differences, cloud shadows, atmospheric attenuation, and certain topographic variations) present in multiple bands (Huete et al., 2002). Also, NDVI is successful as a vegetation cover because it is sufficiently stable enough to allow meaningful comparisons of seasonal and inter-annual changes in vegetation growth and activity. However, NDVI has the disadvantage that the ratio index can be influenced by additive noise effects such as atmospheric path radiance. Another disadvantage is that the usual strong correlation between NDVI with the LAI may not be as strong during the periods of maximum LAI because of NDVI saturation when LAI is very high (Wang et al., 2005).

To enhance the results of the NDVI, several techniques may be followed. In this study, *Density Slicing* (DS) has been implemented. DS is a process of image enhancement in which the continuous grey tone of an image is converted into a series of density intervals, or slices, each corresponding to a specified range in *density number* (DN) (Sabins, 1997).

4.2.3.2 Methodology and results of calculation

For the assessment of the spatial and temporal vegetation cover variations in Wadi Kafrein, the pre-processed multi-temporal ASTER images were used to calculate NDVI. The results were later enhanced using DS.

Density Slicing (DS), also known as "level slicing" was done by dividing the DNs distributed along the x-axis of the image histogram into five intervals or slices, as shown in Fig. 4.10 and 4.11. The main aim of DS is to increase the amount of information which can be visually interpreted from the data.

Results from the NDVI and DS indicate that the time of least vegetation cover within the study area is from summer until the beginning of winter, which may be as late as November. In November, the vegetation did not start to grow yet, as can be seen in Fig. 4.10. Maximum spread of fresh vegetation (Grasslands) has been observed during spring months, as can be seen from the NDVI-DS maps of Wadi Kafrein for the month of March (Fig. 4.11). Figure 4.11 is a good representation of the beginning of spring, where the land receives rainfall, the temperature is not too high, and the humidity is moderate. All images analyzed for vegetation assessment are given in Appendix D.

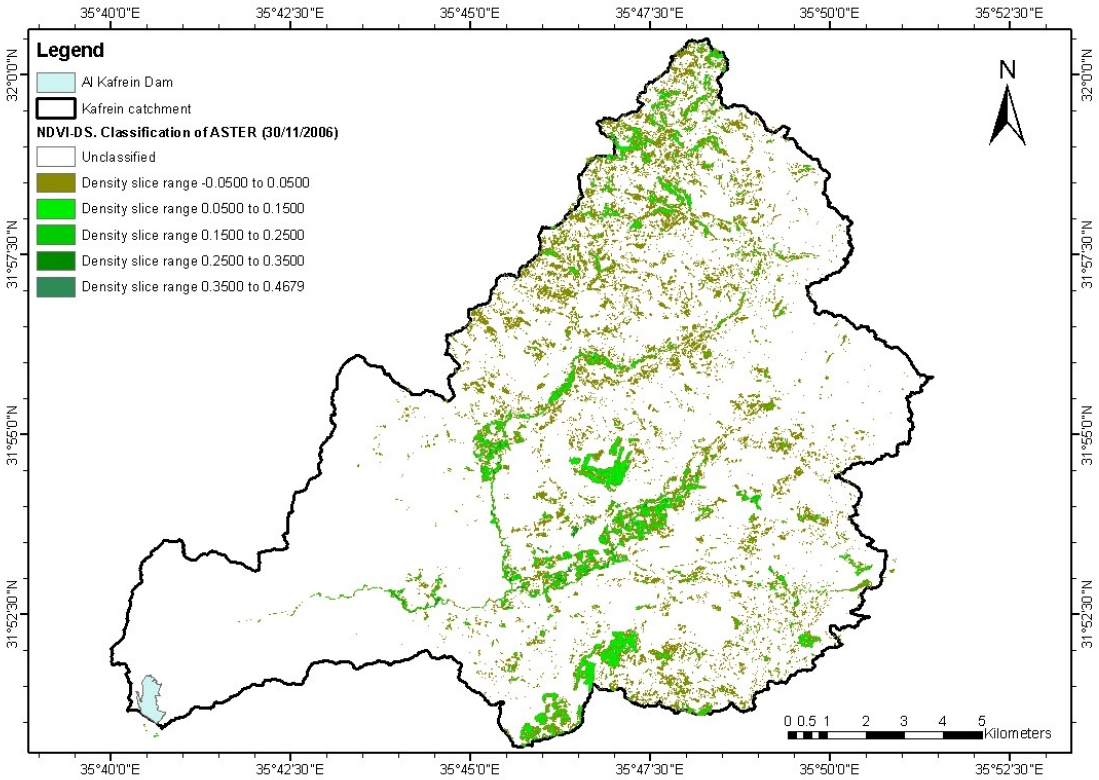

Fig. 4.10: NDVI-DS map of Wadi Kafrein during November 2006

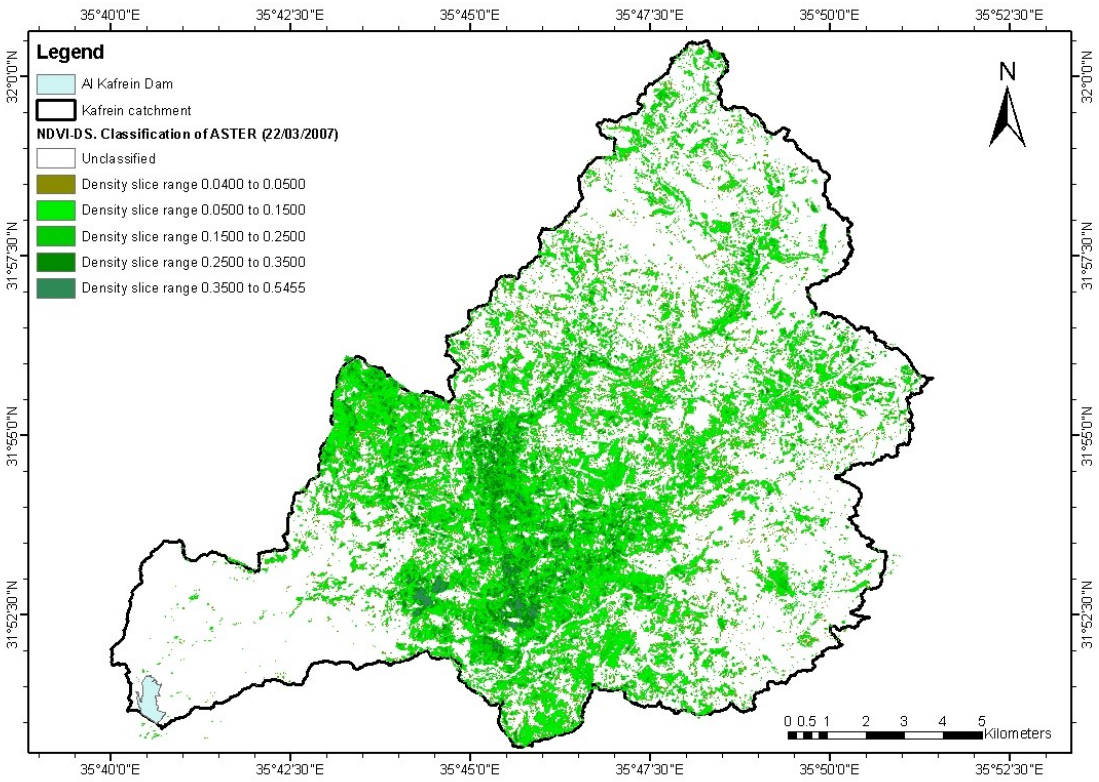

Fig. 4.11: NDVI-DS map of Wadi Kafrein during March 2007

4.2.4 Developing of soil map using remote sensing and GIS

Several input components and data are needed to build up a detailed hydrological model, of which the soil map may be one of the most important as an interface to vegetation (transpiration) and atmosphere. Soil properties determine, to a large extent, whether rain is either diverted as runoff or percolated and allowed to infiltrate into the ground. No known soil map has previously been created for the Wadi Kafrein watershed. Yet, a soil map is a necessary component for the construction of the comprehensive hydrological model of Wadi Kafrein.

Soil mapping in Jordan started in the 1950s at a scale of 1:1,000,000 using the US soil classification system of 1938, but most of the studies and soil surveys were limited to separate and localized parts of the country (Al Qudah, 2001). Soil types were studied in detail in some locations in Jordan by the "National Soil Map and Land Use Project of Jordan," and the resulting soil maps were published in the Jordan Soil Atlas (JSA), but the catchment area of Wadi Kafrein was not included. Instead, the project surveyed a wide range of the adjacent catchment area, the Wadi Shueib. The soil of this catchment has also been studied in greater detail by several other research teams.

In order to present a spatial distribution of the soils, intensive soil mapping can be carried out in the catchment area, but this implies a tremendous effort and time in addition to cost. Therefore, a more typical approach is to make a few observations at designated representative sites within the catchment area, especially for the parameters which have the largest influence on the modelling results (Bathurst, 1986).

In some cases, where some areas are not accessible or are too remote to be measured, remote sensing techniques may be applied in order to provide a spatial distribution of the catchment area (e.g. Schmuge, 1983; Rango, 1985).

Several options are available for developing a soil map for modelling purposes; this includes the use of results of previous studies and/or data from satellite images using remote sensing techniques. As the soil map is a main input component to the hydrological study of Wadi Kafrein, a remote sensing approach has been developed and the soil units from the well studied adjacent catchment of Wadi Shueib have subsequently been extrapolated to Wadi Kafrein. In this approach, satellite images were corrected and later a supervised classification was performed after selecting appropriate training areas. Ground truthing and comparisons to the JSA were used to evaluate the results.

4.2.4.1 National Soil Map of Jordan

The study of the National Soil Map and Land Use of Jordan was identified by a staff from the Ministry of Agriculture; Soil Survey Section in 1986, later the study was carried out by a combined team of expatriate consultants and Jordanian staff and commenced on the 2nd of July 1989. The project was divided to three levels as follows (Ministry of Agriculture, 1993; 1994):

- **Level one:** a broad reconnaissance of the soils of the whole kingdom with mapping at 1:250,000 scale
- **Level two:** a semi detailed soil survey and the production of soil, land use, and land suitability maps of 9,000 km^2 at 1:50,000 scale
- **Level three:** soil and land suitability maps at 1:10,000 scale of about 800 km^2 based on a detailed soil survey

The soils of Jordan were classified according to the criteria and definitions of the USDA's Soil Taxonomy (1975) and the (1990) keys to Soil Taxonomy. In Level Two of the project, five separated areas were selected for a semi detailed soil survey, starting from the Northwestern Area (Salt-Irbid-Mafraq) down to the Southern Highlands (Shoubak-Tafila). The semi detailed soil survey of level two of the North-western Area did not cover the study area of Wadi Kafrein but it covered a wide part of the adjacent catchment Wadi Shueib which occurs under the same climatic conditions and shares a lot of its physical characteristics with the Wadi Kafrein catchment. Al Salt City which is located in the upper part of the Wadi Shueib catchment is around 7 km north of Wadi Kafrein (Fig. 4.13).

A more detailed study on the soil types and properties of Wadi Shueib has been carried out by Kuntz (2003) based on the results of the "National Soil Map and Land Use Project" (Level Two) presented in the JSA (1:50,000 scale) and the results were used in a wider study on the vulnerability of groundwater aquifers in Wadi Shueib by Werz (2006). The idea of developing a soil map with high resolution using the available data from the Jordan Soil Atlas and the previous studies has been applied. The methodology of data extrapolation and results are given in the following paragraphs.

4.2.4.2 Methodology of extrapolation

Satellite images using remote sensing techniques in combination with the developed DEM and GIS applications were used to develop a detailed soil map with 15m x 15m cell size resolution. As a first step of extrapolation, all acquired satellite images of ASTER and Cartosat-1 were preprocessed, i.e. the images were converted to WGS 1984 coordinates and clipped and sorted to include those pertinent for the study area of Wadi Kafrein. Also, a total set of 47 GCPs were identified covering the whole catchment area of Wadi Kafrein (see 4.2.1.2), this being especially necessary to correct the Cartosat-1 data from which the high accuracy DEM was developed.

The multispectral ASTER images were subjected to radiometric and parametric corrections; later the urban areas and the water surfaces were masked and a master image was selected. Then all images and DEM were referenced to this master image.
Based on differing soil moisture regimes within Wadi Kafrein, the watershed was divided into two main areas: The Ustic-Aridic transition soil moisture regime, and the Xeric soil moisture regime (Table 4.1).

In order to find the areal distribution of the different soil units, the DEM was spatially analyzed; i.e.: single raster layers of elevation, slope, aspect, and horizontal and vertical curvature were generated. Also, the satellite images were analyzed and band ratios were calculated to highlight iron oxides, carbonates, and clay minerals. All layers were later combined in one synthetic multi-band file with a spatial resolution of 15 m.

Finally, to extrapolate the various soil units from Wadi Shueib to Wadi Kafrein, training areas were selected based on distinctive soil units of the Wadi Shueib soil map of the scale 1:50,000. The supervised classification method was used, which is known for its accuracy for mapping classes compared to the unsupervised classification (Short, 2010), and was applied on both catchments so that the results of Wadi Shueib soil classification can be used for accuracy evaluation by comparing them to the previously available 1:50,000 soil map of Wadi Shueib (Alkhoury et al., 2010b).

4.2.4.3 Results

In the "National Soil Map and Land Use Project" published by Ministry of Agriculture (1994), the soil of North Western Area was divided to 81 units, out of which 9 soil units were identified in the Wadi Kafrein catchment (soil units 2 to 81 in Fig. 4.12) and 3 additional units were introduced which represents the soils in the lower part of the study area (soil units 82 to 84) which were not identified by the project.

The resulted soil units of Wadi Kafrein were divided to two main groups based on the soil moisture regime, namely Xeric and the transition regime Ustic-Aridic as defined in the USDA Soil Taxonomy (USDA, 1975 and 1999).

- The **Xeric** soil moisture regime is defined as: Moisture control section is moist in some part more than half the time that the soil temperature is higher than

5°C, or is moist in some part for at least 90 consecutive days in 6 years out of ten when soil temperature is higher than 8°C. The mean annual temperature is less than 22°C.

- The **Ustic** is defined as: a moisture control section is moist in some part for more than 180 cumulative days or is continuously moist in some part for 90 consecutive days when soil temperature is greater than 22°C.

- The **Aridic** is defined as: Moisture control section is dry in all parts more than half the time that the soil temperature is above 5°C at 50 cm depth and the section is never moist in some or all parts for 90 consecutive days when soil temperature at 50 cm depth exceeds 8°C.

- **Ustic-Aridic**: Moisture regime intermediate between the Ustic and Aridic moisture regimes.

The Ustic-Aridic transition soil moisture regime which is found in the lower part of the study area, extending from 35° 43' 30" E west ward until it reaches the Kafrein dam and further to the Lower Jordan Valley. Under this type five soil units were identified; units from 80-84 as shown in Fig. 4.12. The mean annual precipitation over these soil units' areas is less than 250 mm and generally no vegetation cover is present. The rest of the catchment area is covered with soil units belonging to Xeric moisture regime. They are dominant in areas with rainfall of more than 200 mm / year (Table 4.1) and have different land covers as described earlier in section 4.2.2.

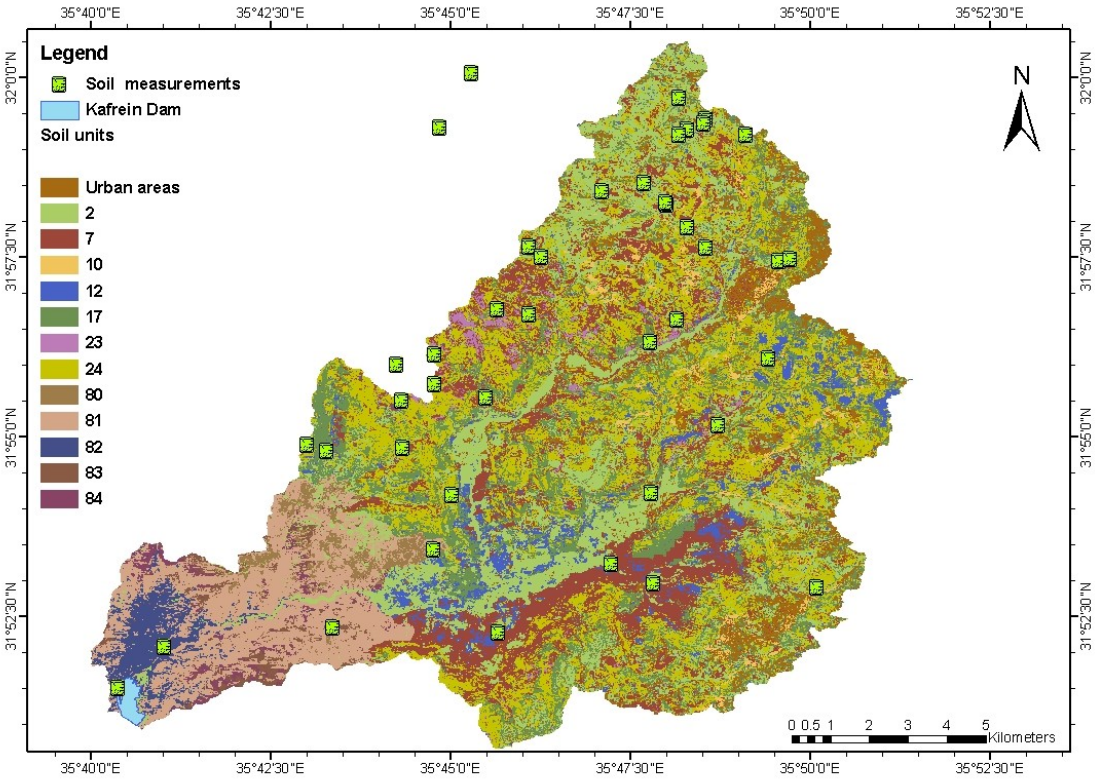

Fig. 4.12: The developed soil map of Wadi Kafrein with final resolution of 15m x 15m cell size.

Soil units with Ustic-Aridic transition soil moisture regime (80-84) belong to Ardisols soil order with mainly Ustochreptic as subgroup. While the rest of the catchment area of Wadi Kafrein (soil units with Xeric soil moisture regime 2-24) is dominated by Inceptisols soil order with Xerochrepts as Great Group, but also Mollisols and Entisols orders exist with Haploxeroll and Xerothents as Great Group respectively (Table 4.1). The dominant subgroups are Typic Xerochrepts, Lithic Xerochrepts, and Calcixerollic Xerochrepts.

Table 4.1: Description of the soil map units of Wadi Kafrein.

Unit ID		M. annual ppt. (mm)	Elevation (m)	Area %	Km^2	USDA Subgroup Classification*	WRB Classification**
2	Xeric	225-500	150-950	16	26	1-Calcixerollic Xerochrepts-50% 2-Typic Xerochrepts-20% 3-Lithic Haploxeroll-10%	1-Calcaric Cambisol-65% 2-Chromic Cambisol-35%
7		300-500	350-1030	15	24	1-Typic Xerochrepts-50% 2-Vertic Xerochrepts-15% 3-Lithic Xerochrept-10%	1-Chromic Cambisol-60% 2-Vertic Cambisol-20%
10		250-500	600-900	2	3	1-Typic Xerochrepts-60% 2-Vertic Xerochrepts-10% 3-Lithic Xerochrepts-10% 4- Lithic Xerorthents-10%	1-Chromic Cambisol-70% 2- Leptosols-10%
12		200-500	100-950	13	21	1- Typic Xerochrepts-45% 2-Lithic Xerochrepts-15% 3-Calcixerollic Xerochrepts-10%	1-Chromic Cambisol-50% 2-Calcaric Cambisol-30%
17		250-500	300-950	21	33	1-Typic Xerochrepts-30% 2- Lithic Haploxeroll-15% 3- Lithic Xerochrepts-15% 4- Lithic Xerorthents-10%	1-Mollic Leptosol-305 2-Dystric Leptosol-30% 3-Lithic leptosol-20%
23		300-450	500-900	2	3	1- Lithic Xerochrepts-30% 2- Typic Xerochrepts-20% 3- Lithic Xerorthents-20% 4- Lithic Haploxeroll-10%	1-Dystric Leptosol-35% 2-Rendzic Leptosol-35%
24		350-500	450-1000	17	27	1- Lithic Xerochrepts-40% 2- Typic Xerochrepts-30% 3- Lithic Xerorthents-10% 4- Lithic Haploxeroll-10%	1-Lithic Leptosols-50% 2-Mollic Leptosols-30%
80	Ustic-Aridic	200-250	150-300	1	1	1-UstochrepticCamborthids-30% 2-Ustochreptic Calolorthide-40%	1-Aridic Cambisols-40% 2-Lithic Leptosols-60%
81		150-250	-140-250	2	3	1-UstochrepticCamborthids-30% 2-UstochrepticCalcoirothids-30%	1-Aridic Cambisols-50% 2-Lithic Leptosols-50%
82		150-200	-140-50	1	1	--------	1-Lithic Leptosol-30% 2-Yermic Cambisol-40%
83		200-250	50-300	2	2	--------	1-Yermic Cambisol-60% 2-Lithic Leptosols-30%
84		200-250	50-150	1	2	--------	1-Takyric Calcisol-30% 2-Aridic Calcisol-40%

*** Ministry of Agriculture 1994**
**** Kuntz 2003, Werz 2006 (World Reference Base)**

The soil units have different vegetation covers and geomorphology but all the area is formed on limestone geology. Description of every soil unit land cover and their morphology will be given while the slopes of the surfaces were determined using the developed slope map and the acquired Google Earth® image.

Soil unit 2

Distributed over low slopes, along main Wadi channel at the valley floor (7-18°) on deep to moderately deep colluviums; usually used for agriculture and olive trees.

Soil unit 7	Distributed across high plateaus, over terrace remnants with moderate colluvial cover; lies over Kurnub sandstone and on moderate slopes (5-25°); covered by rainfed crops and tree crops.
Soil unit 10	Covers a very small percentage of the study area; limited to concave colluvial foot slopes (5-15°); used for irrigated agriculture.
Soil unit 12	Distributed over high plateaus and terrace remnants; often over moderate colluvium (0-15°); mainly used for olive trees and irrigated agriculture.
Soil unit 17	Found over steep to very steep slopes (20-75°); mainly grassland; olive trees; 21% of the catchment area.
Soil unit 23	Covers the high convex ridge and upper slopes over shallow colluvium (5-15°); used for agricultural crops and olive trees.
Soil unit 24	On high convex ridges; upper slopes; similar to Soil unit 23; develops on top of high fractured and stony colluviums; forest trees and rainfed tree crops; covers 17% of the study area.
Soil unit 80	Aridic soil unit; covers low to moderate slopes (5-30°); in lower part of the study area over moderately deep to deep colluvium; grasslands.
Soil unit 81	Very steep escarpments of lower elevations (35-90°); lacks vegetation; low grass cover has been reported in other catchments.
Soil unit 82	Found over deep colluviums, just north of Kafrein dam; small area; covers gentle slopes and the Wadi floor (0-18°); no vegetation.
Soil unit 83	Covers flat areas or convex hill slopes (0-18°); only 2% of Wadi Kafrein area; low grass, otherwise no vegetation.
Soil unit 84	Aridic soil unit; valley floors and depressions of elevations less than 200 m (asl); 1% of study area; no vegetation cover.

Soil units with Xeric soil moisture regimes cover 86% of Wadi Kafrein's total area, while the Ustic-Aridic soil moisture regime exists in only 7% of the study area. 7% of the surface is urban.

The results of the extrapolated soil map were validated by comparing the produced map with the soil map of Kuntz (2003) and the Jordan Soil Atlas maps published by Ministry of Agriculture (1994). Soil unit characteristics were also compared to make sure that they were consistent among all studies, past and present. The geomorphology of the soil units and their spatial distribution is in good agreement with what is given in the references of the Jordan Soil Map Project and the detailed soil map study of Wadi Shueib. Another evaluation was considered here by the good agreement between the distributions of these soil units regarding the slopes with the slope map of Wadi Kafrein.

4.3 Precipitation and climatological data

4.3.1 Precipitation and raingauges network

Rainfall is the primary hydrological input for every surface modelling study. The results are highly dependent on rainfall measurement accuracy and the representation of the spatial distribution of rainfall in the studied watershed.

Rainfall in arid and semi arid regions is characterized by high spatial and temporal variability. In terms of temporal variability, rainfall is limited to a few months in winter; a few events can produce rainfall volumes which exceed the volume of precipitation for the entire rest of the year. The spatial variability of rainfall has been studied in some arid areas and the negative impact of sparse rainfall gauging networks on rainfall-runoff modelling has been reported.

In order to get high resolution rainfall data and overcome the spatial and temporal variability limitations, fully automated rain gauges were installed in addition to the available network within the study area (Fig. 4.13). Also, manually built supportive rain gauges were installed along with these rain gauges as secondary sources of data accuracy control (Fig. 4.14 a, b). The available precipitation data measured by the MWI is on a daily basis, which is not sufficient for detailed hydrological modelling. Therefore, these additional fully automated rain gauges were installed in the catchment area.

The installed Data Logging Rain Gauges have two main components: the Tipping Bucket Rainfall Collector and a HOBO Event/Temperature Data Logger. The tipping bucket mechanism is designed to measure 0.2 mm of rainfall for every tip.

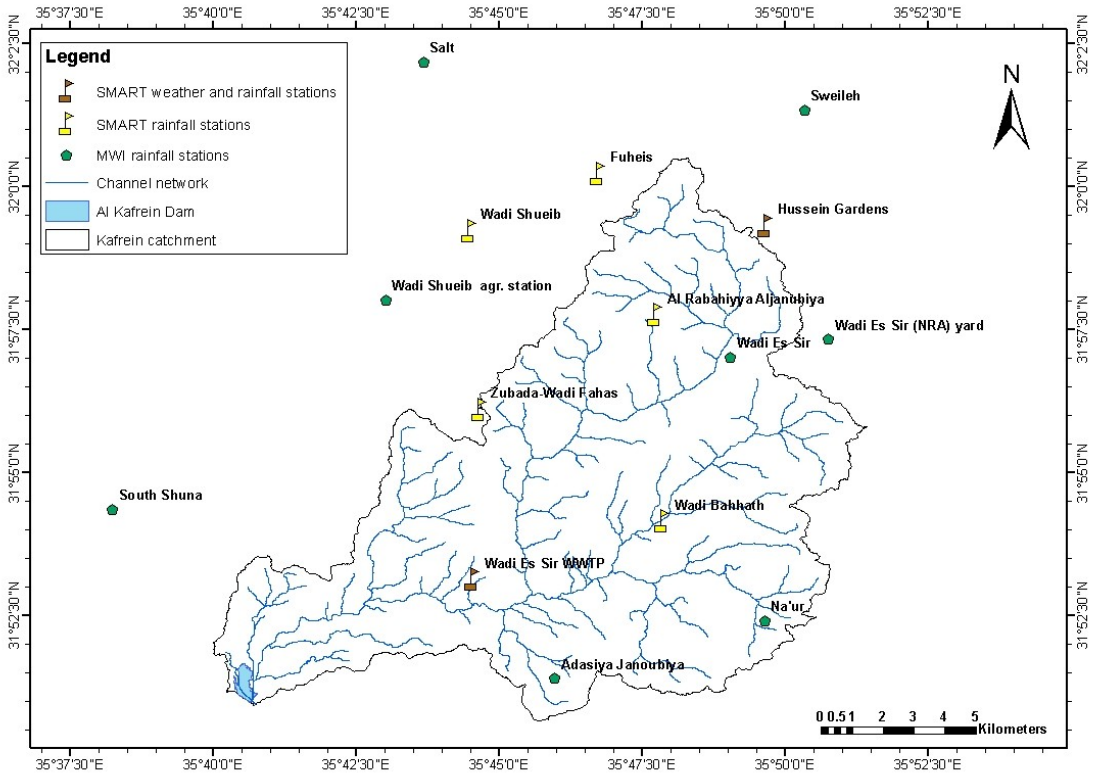

Fig. 4.13: Site map of the used rain gauges and weather stations in this study.

The maximum rainfall rate which can be measured accurately is up to 127 cm/hour which is much beyond the long term annual precipitation of Wadi Kafrein watershed. Prior to installation, all rain gauges where calibrated in the Laboratory of Water Research of Jordan University, Department of Geology. The calibration has been done following the calibration procedures described in the User manual (Onset Computer Corporation, 2005).

The final installation sites where chosen by taking into consideration the spatial distribution of the rain gauges network, the suitability of the site for installation also to be in close proximity to the monitored subwadis for runoff measurements.

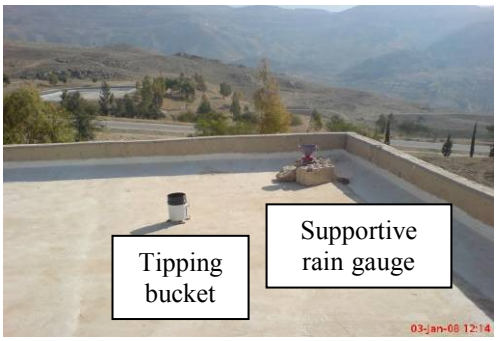

Fig. 4.14a: Tipping bucket rain gauge in the measurement site of Wadi Es Sir WWTP.

Fig. 4.14b: Manual built supportive rain gauges for data accuracy.

In order to get accurate measurements, the following steps have been followed during and after the installation:

- The rain gauge housing was fixed in a level position using the built-in water bubble balance.
- A clear and unobstructed location has been selected. A distance of at least three times the height of any close obstructions was taken to avoid any interference to measurement accuracy.
- All rain gauges and the supportive rain gauges were fixed properly against any possible vibration which could significantly affect the tipping mechanism in very windy locations.
- The additional supportive rain gauges were installed together with the automated rain gauges in order to overcome any missed data which might be a result of technical failure.
- The rain gauges were checked periodically: calibration, battery change; cleaning the filter screen, the funnel, and the tipping-bucket mechanism.

4.3.2 Climatological parameters acquisition

Within Wadi Kafrein catchment area, one climatological station is available, which takes daily measurements. The station is located in the upper part of the study area (Highlands), which has a different climate from the lower-western part (Jordan Valley). These differences in climate within the Wadi have already been discussed in Section 2.6. Also, the temporal resolution offered by this station is not sufficient for evapotranspiration simulation.

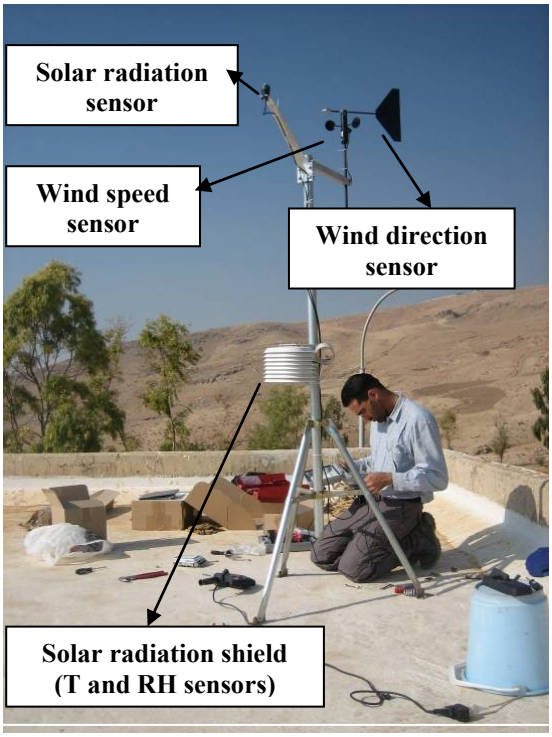

Fig. 4.15: Two meter weather station Configuration. Installation site at Wadi Es Sir WWTP (31^0 53' 05" N, 35^0 44' 33" E).

To overcome the spatial and temporal variations of the climatological parameters, two automated weather stations were installed in the catchment area to measure the climatological parameters needed for the model. The site locations of the stations were chosen based on two main criteria; firstly: the suitability and the safety of the site for installation, secondly: the coverage of the Highlands and the Jordan Valley climatological variations within the catchment area.

The first station was installed in the upper northeastern part of the study area in King Hussein Gardens (KHG). The site elevation is 987 m asl with long term annual rainfall average of 500 mm. A Mediterranean climate is present here (Fig. 4.13). The second station was installed in the lower southwestern part of the study area in Wadi Es Sir WWTP (Fig. 4.15). The elevation of the second station is 232 m asl with long

term annual average rainfall of 250 mm, and has a semi arid climate. More to the west, close to the Kafrein dam, the long term rainfall amount is less than 200 mm where an arid climate prevails. The distance between the two stations is around 14 km, a noticeable difference in the measured climatological values has been measured which indicates the importance of the data quality for hydrological modelling and its influence in such arid and semi arid regions where variations take place within short distances.

The weather stations measure the main climatological parameters which are needed for the aim of this study. Wind speed is measured in m/s; wind direction in degrees from North; temperature is measured in °C, relative humidity is measured in percent; and solar radiation is in W/m^2 (Fig. 4.15). Close to every weather station is an automatic rain gauge (tipping bucket), and the manual built supportive rain gauge has been installed as well. The HOBO weather stations have a data logger, which is designed to take the measurements through the connected climatic sensors without any need for calibration. A reading of the climatological parameters was taken every 5 minutes.

All of the sensors' functionalities were configured prior the shipment to Jordan. They were tested at "Stegemühle" experimental site in Göttingen, Germany. The installation procedures described by the Onset-HOBO Weather Station User's Guide (Onset Computer Corporation, 2004) has been followed. Installation and site selection of the weather stations was based on the following criteria:

- The locations were away from any obstacles like trees or buildings for at least three times the height of the nearest obstruction.
- The tripods of the stations were fixed tightly to the ground.
- The light sensor, the raingauge, and the wind speed sensors were balanced using a water bubble level.
- The wind direction arm was directed to North using GPS GARMIN instrument.
- The Temperature and Relative Humidity sensors were installed inside the solar radiation shield.

4.4 Runoff measurements at different scales

Runoff was measured in several sites, using different approaches and catchment scales. The water shed of Wadi Kafrein has a total area of 161.4 km^2, and is controlled by a dam at the outlet to the Jordan Valley. This dam has been surveyed and modeled in order to measure the runoff with a temporally high resolution. Also, in order to study the effect of land cover and topography and to analyze the driving forces of runoff generation and mechanisms, small scale subwadis with areas ranging from 0.26 to 6.97 km^2 were monitored, and the runoff was measured continuously in high resolution.

4.4.1 Calculating Kafrein dam storage capacity for runoff measurements

A dam was constructed in 1967 at the point where Wadi Kafrein enters into the Jordan Valley. The initial capacity of the dam was 3.8 MCM. Due to sedimentation, a high

percentage of seepage, and an increase in water demand, the Jordan Valley Authority (JVA) decided to increase the dam capacity (Ministry of Public Works and Housing, 1993). In 1996/1997 the dam wall was raised by seven meters, which increased the dam capacity up to 8 MCM.

Water which is stored in the reservoir lake behind the dam comes from three sources: spring discharge, Wadi Es Sir WWTP effluent, and water from storm runoff during the winter season. The storm runoff is usually very short, and typically lasts for few minutes up to several hours. Overland flow occurs only when the rate of precipitation exceeds the infiltration capacity; this process is more common in arid and semi arid regions. For surface modelling purposes, continuous runoff measurements are needed because runoff volumes change rapidly during storms events. Typical storm events are capable of destroying gauging stations and changing the geometry of the wadis due to their severity.

The streamflow entering the dam and the reservoir storage volumes are monitored on a daily basis by the JVA-Kafrein dam operation office. The storage is measured by gauge reading of the reservoir staff gauges. The staff gauges of the Kafrein dam were installed in steps (Fig. 4.16). The staff gauges consist of two concrete gauge posts with graduated measuring plates (gauge plates). The latest evaluation of reservoir capacity has been made in 1996; however, the geometry of the reservoir had changed due to sediments which were carried by flood flows or by the suspended load of the baseflow. This has caused a change in the reservoir capacity since the engineering of the present staff gauges. Furthermore, a time step resolution of one measurement per day is not sufficient for the aim of this study since a storm event will most likely start and end within a time span of a few hours.

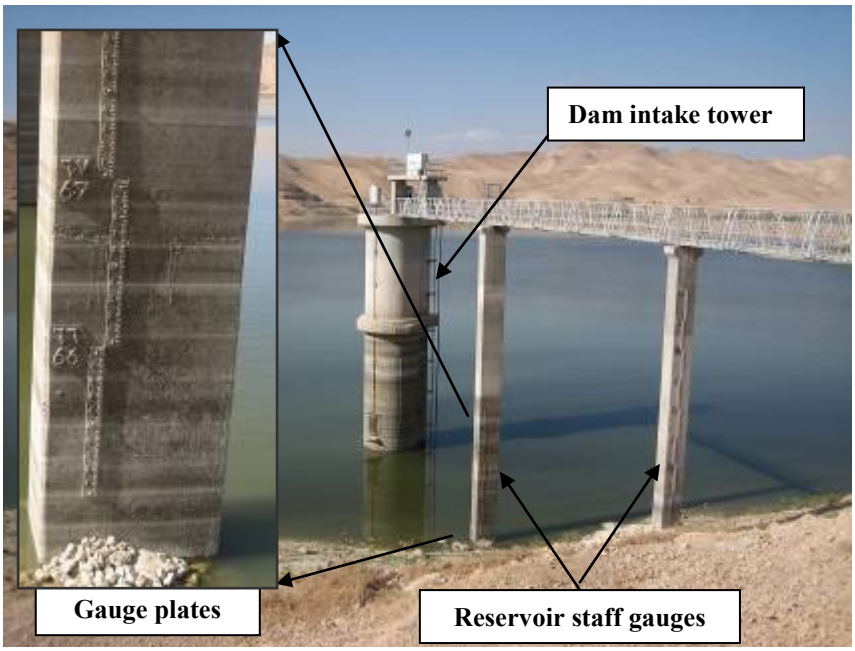

Fig. 4.16: Kafrein dam intake tower and staff gauges (photo taken 9/11/2007).

Alternative approaches to measure the total runoff entering the reservoir were needed due to the absence of existing monitoring gauging station as well as the high magnitudes of runoff and the difficulty in their measurement. In order to get accurate

measurements with better resolution, the storage capacity of the Kafrein dam has been re-evaluated by using the differential GPS measurements to survey the dam geometry and to obtain an up-to-date digital elevation model of the reservoir with high accuracy (Fig. 4.17). The measurements were taken when the Kafrein reservoir was almost empty. To achieve higher accuracy and shorter time step measurements of the water storage, an automatic pressure transducer was installed in the intake tower of the Kafrein reservoir with one hour time step and 0.2 cm accuracy error. Together, the high accuracy DEM of the reservoir and the measurements of elevation changes allow a continuous calculation of the storm runoff volumes with high resolution and accuracy. The results of the measurements and runoff calculations are discussed in Section (5.4.3.1).

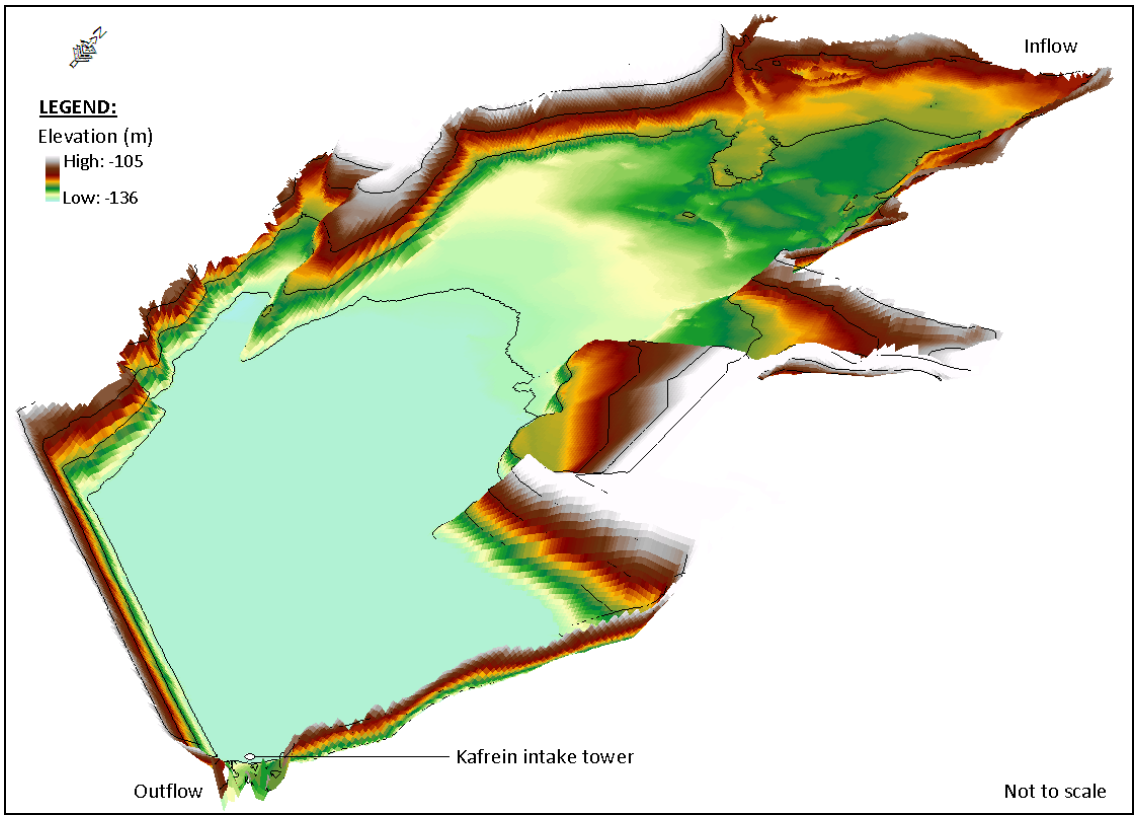

Fig. 4.17: High accuracy digital elevation model of the Kafrein surface water reservoir (Intake tower is not to scale).

4.4.2 Subwadis selection and instrumentation

The aim of the re-evaluation of Kafrein dam storage by preparing the high accuracy DEM is to measure the runoff generated from the whole catchment area. This is important to calibrate and validate the results of the hydrological model of Wadi Kafrein, but it is not practical to investigate the driving factors causing runoff using the scale of the entire catchment. Therefore, four small subwadis in Wadi Kafrein catchment in addition to a fifth subwadi in Wadi Shueib catchment, the neighboring catchment of Kafrein, were selected in order to monitor and measure runoff volumes. In this system, the environment of measurement is more controlled and has less risk compared with measurements during huge runoff events generated from the total catchment area of Wadi Kafrein (161.4 Km^2). The subwadi monitored in Wadi Shueib

was selected because no subwadi with similar characteristics of geological formation and land cover was found suitable for measurement and instrumentation in Wadi Kafrein. Each of the five subwadis has different characteristics. These wadis differ in altitude, slope, catchment size, geological formations, and land use/cover, (Table 4.2). Each of these subwadis consists mainly of one representative geological formation which was earlier discussed in Section 2.4.4. The subwadis were selected based on their physical characteristics; also, the possibility of instrument installation and runoff measurement has been taken in consideration. The ease of access and time needed to reach the subwadis after the beginning of a rainfall event were considered too.

These different characteristics and variations between the subwadis give the opportunity to investigate the effect of these characteristics on runoff generation in a more precise way.

Table 4.2: Characteristics of the monitored subwadis in Wadi Kafrein and Wadi Shueib (Modified from Alkhoury et al., 2009).

Wadi Name	ID	Monitoring point [m asl]	Slope	Area %	Area [km^2]	Geology	Land Use/cover
Wadi Kuraysh	S1	760	0°-20° 20°<x<40° ≥40	81.4% 17.1% 01.5%	6.97	Shueib Formation	Natural forest Olive trees Urban
Wadi Naqib	S2	630	0°-20° 20°<x<40° ≥40	77.9% 20.1% 02.0%	2.76	Shueib Formation	Olive trees Urban
Wadi Fahas	S3	500	0°-20° 20°<x<40° ≥40	90.8% 09.0% 0.2%	3.16	Fuheis Formation	Olive trees Bare soils
Wadi An Nar	S4	290	0°-20° 20°<x<40° ≥40	90.3% 09.6% 0.1%	3.30	Na'ur Formation	Bare rocks Olive trees
Wadi Kurnub	S5	515	0°-20° 20°<x<40° ≥40	62.7% 33.1% 04.2%	0.26	Kurnub Group	Sand stones

The selected subwadis are shown in Fig. 4.18; a rain gauge close to every subwadi was installed. Five rain gauges were installed in Wadi Kafrein while two rain gauges were installed in Wadi Shueib.

Runoff events were recorded in special locations with automatic pressure transducers, which measure the pressure (water level) above the transducer. The automatic pressure transducers have an accuracy of 0.1 cm and were programmed for continuous monitoring with one measurement every 2 minutes. The special locations are areas with a defined cross section (e.g. concrete structures, circular culverts). Before installation, the already existing constructions had to be cleaned and small structures were built to drive the runoff directly to the measurement location (Fig. 4.19a, b). The automatic pressure transducers were installed and protected in a metal box and then were fixed in the circular culvert or concrete structure (Fig. 4.19c, d).

The physical characteristics of the selected subwadis were studied through field work and presented here as thematic maps which have been prepared for every subwadi. These maps show the DEM, slope, and soil units for every subwadi. Also, a map with a Google Earth® image shows the land cover, the stream network, and the location of the closest rainfall gauging station.

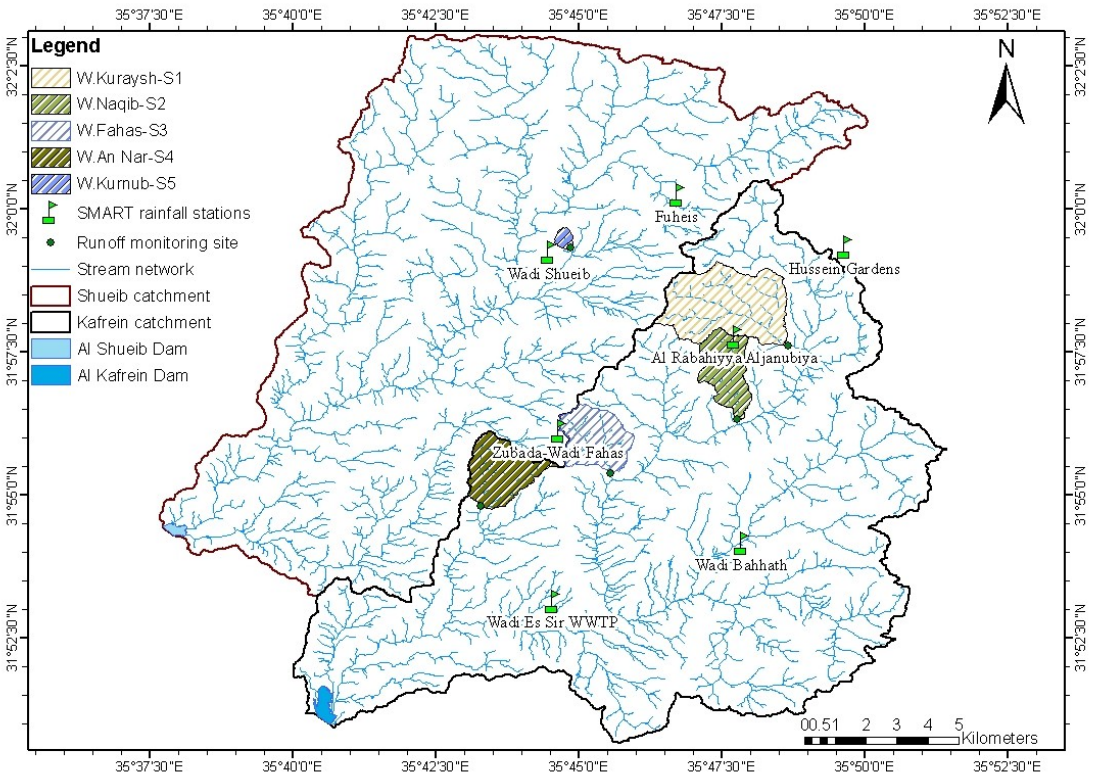

Fig. 4.18: Subwadis selected for detailed runoff measurements in Wadi Kafrein and Wadi Shueib.

Fig. 4.19: a. Construction work in Wadi An Nar S4
b. Water diversion to the circular culvert in Wadi Kurnub S5
c. The automatic pressure transducers (divers) were installed inside a metal box and fixed in the bottom of the circular culvert
d. Diver installation in Wadi Kuraysh S1

Wadi Kuraysh-S1

Wadi Kuraysh is the biggest subwadi with a total watershed of almost 7 km^2, receiving the highest amount of precipitation with a long term annual average of 500 mm. The catchment area of S1 consists of the Wadi Shueib Formation (nodular limestone, marl, marly limestone, dolomitic limestone, coquina, fossiliferous limestone and nodular marly limestone). The catchment area is covered with natural forest trees, mainly on the lower (steep) slopes, as can be seen in the middle of map 4.20a. The catchment is cultivated and urbanized in most of the upper (flat) slopes, the cultivated areas consisting mainly of olive trees. Urbanization is taking place on the flat areas in the western side of the catchment where slopes are less than 20 degrees (Fig. 4.20a and c). The highest points are located in the western side of the catchment area where urbanization is taking place with maximum elevation of 1030 m asl decreasing to 759 m asl as shown in Fig. 4.20b The average elevation of Wadi Kuraysh is 926 m asl. The steepest slopes are along the main stream and at the downstream side with a maximum slope of 72 degrees, while the average slope of the total catchment area is 13 degrees (Fig. 4.20c). As can be seen from the soil map (Fig.4.20d), soil unit 2 is dominant along the main Wadi channel and over low slopes while soil unit 7 is covering the high plateaus and the terrace remnants with moderate to low slopes.

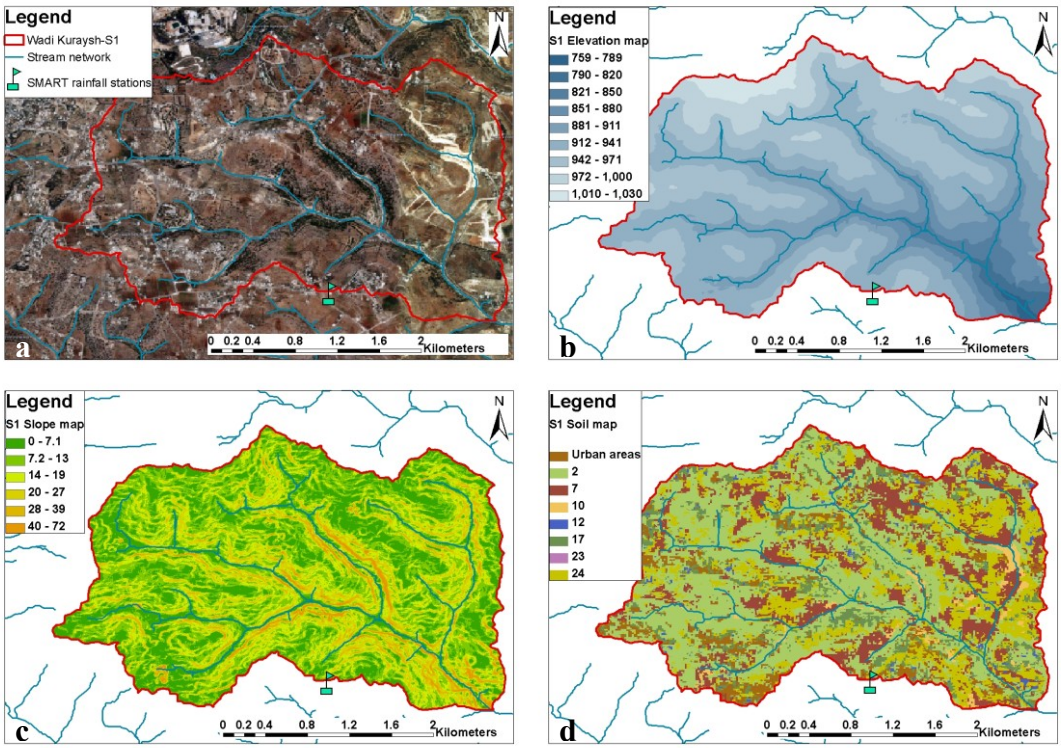

Fig. 4.20: Wadi Kuraysh thematic maps.

Wadi Naqib-S2

Wadi Naqib-S2 has a total area of 2.8 km^2 and a long term annual average precipitation of 450 mm. The catchment area of S2 consists of Wadi Shueib Formation similar to S1. Most of the catchment is cultivated and rainfall is collected for irrigating the planted trees and fields of olive trees. Urbanization is limited to the northern boundaries (Fig.4.21a), which is the extension of Alrabahiyya Aljanubiya

living area with slopes less than 20 degrees. The catchment area has steep slopes (Fig. 4.21c) and a large variation in elevation (Fig. 4.21b) ranging from 967 m asl at the northern boundary down to 631 m asl. The total catchment area elevation average is 853 m asl. Most of the slopes are cultivated for agricultural purposes and terraces are very common. The maximum slope is 70 degrees (Fig. 4.21c) with an average area slope of 15 degrees. The lower part of the catchment is easily reachable where the runoff monitoring point is installed at an elevation of 630 m asl. The dominant soil units are soil unit 7, which is distributed over the high plateaus, and unit 24 which lies over the upper slopes (Fig.4.21d). Also, soil units 2, 10, 17, and 23 are found but with limited distribution.

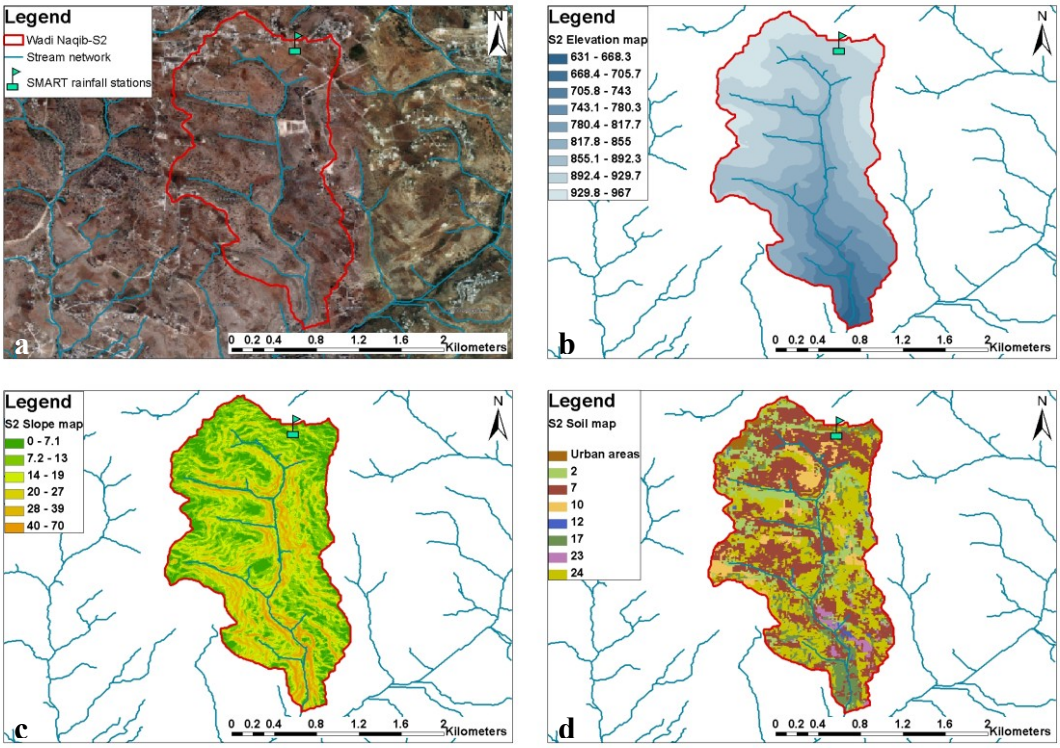

Fig. 4.21: Wadi Naqib thematic maps.

Wadi Fahas-S3

Wadi Fahas has a catchment area of 3.2 km^2 and a long term annual average precipitation of 350 mm. The catchment area of S3 consists of Fuheis Formation (grey-green marl, calcareous siltstone, thinly bedded nodular limestone and secondary gypsum). This subwadi got its name from the village of Fahas with most urbanization taking place close to its lower boundaries (Fig.4.22a). The area is highly cultivated and olive trees are the dominant land cover. Most of the surfaces are flat (Fig. 4.22c) with maximum steepness of 63 degrees and a total catchment slope average of 11 degrees. The elevation in S3 ranges from 500 m asl to 769 m asl with an average elevation of 641 m asl, Fig (4.22b). The S3 runoff monitoring point is located at an elevation of 500 m asl and the point is accessible by a paved street just above the monitoring point. The rainfall gauge station was installed in its upper northeastern part in the area of Zabada. Soil unit 2 is dominating the catchment area and covers the high convex ridges and upper slopes. Soil units 7, 17, and 23, are found in Wadi Fahas (Fig. 4.22d).

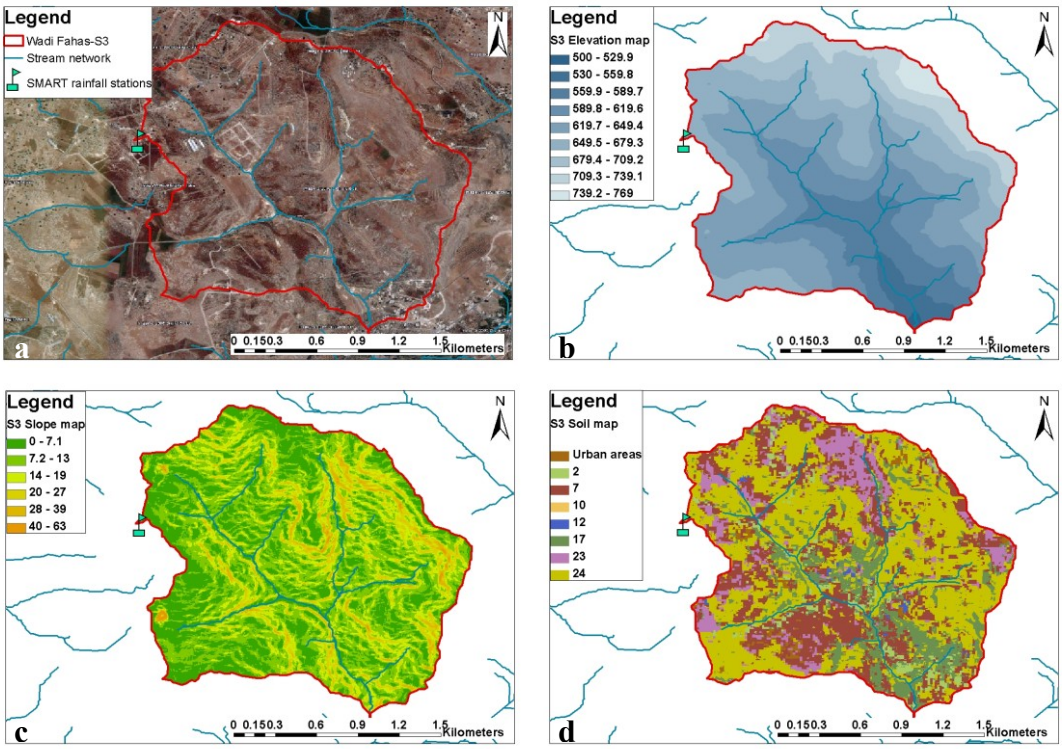

Fig. 4.22: Wadi Fahas thematic maps.

Wadi An Nar-S4

Wadi An Nar has a catchment area of 3.3 km^2 and a long term annual average precipitation of 300 mm. The catchment area of S4 subwadi consists of Na'ur Formation (fine-to- medium grained sandstone interbedded with siltstone, mudstone, and marl in its basal parts, while the upper part of the Formation consists of shelly limestone, marl, dolomitic limestone, and dolomite with chert nodules at the top). Wadi An Nar is located in the transition boundary where bare rocks dominate the western side of the catchment area until it reaches the Kafrein dam. S4 has no vegetation cover except small fields of olive trees on the eastern side of the catchment (Fig. 4.23a). The dominating land cover is bare rocks on the steep slopes of the main tributary, which extends north-west. No urbanization is taking place there. The elevation of Wadi An Nar catchment varies from 289 m asl up to 648 m asl on its eastern boundaries with an average area elevation of 447 m (Fig. 4.23b). The Wadi has two tributaries where the north-west tributary has the steepest slopes (Fig. 4.23c). The maximum slope is 66 degrees with an average slope of the catchment of 12 degrees. Soil unit 17 dominates the western side of the catchment over the steep slopes. This soil unit is found over the steep to very steep slopes and is covered by grass during the spring months. Soil unit 24 dominates most of the catchment area of the eastern side where the slopes are more gentle (less than 20 degrees) and rain fed trees are common (Fig. 4.23d). Other soil units are found in the catchment area with limited coverage (soil units 2,7,12, and 23).

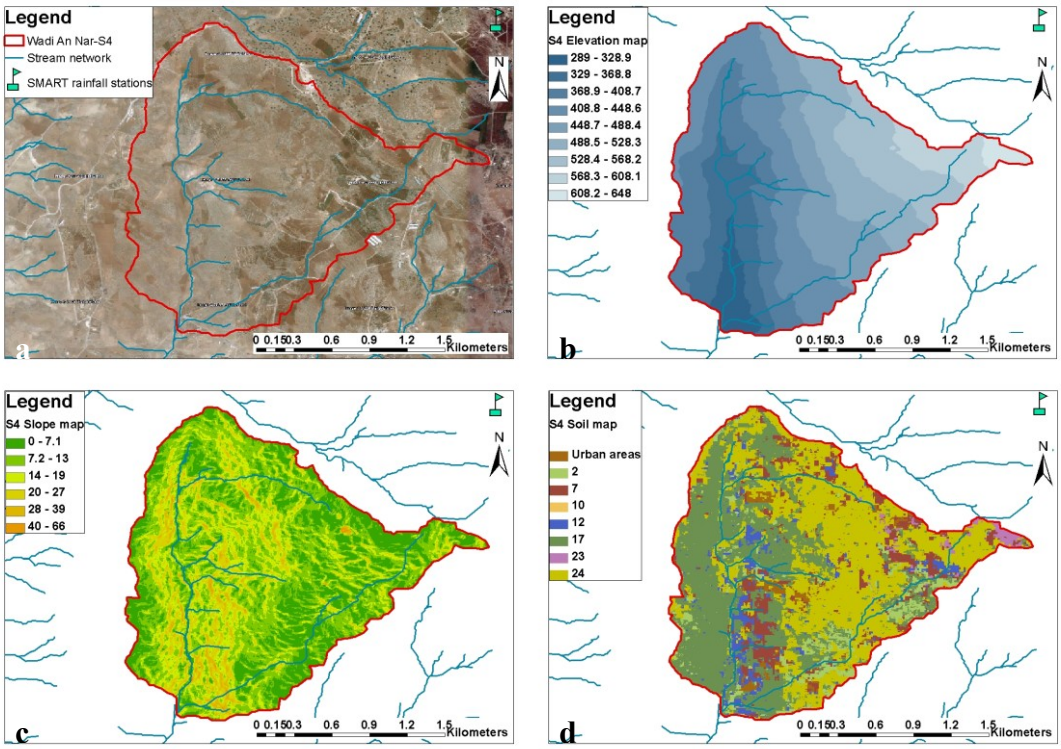

Fig. 4.23: Wadi An Nar thematic maps.

All runoff measuring points of the subwadis of Wadi Kafrein are connected to streets. These streets make the time needed to reach the measuring points acceptable. Reaching the subwadis during storm events or shortly after is important so as to be able to conduct the field work and measure the runoff to calibrate the stage height stations.

Wadi Kurnub-S5

Wadi Kurnub is by far the smallest monitored subwadi with a surface catchment area of 0.3 km^2. This subwadi is located in Wadi Shueib catchment, the adjacent catchment area to Wadi Kafrein (Fig. 4.18). The catchment area of Wadi Kurnub receives a total long term annual precipitation of 450 mm. The S5 subwadi consists of varicoloured, medium-grained, cross-bedded sandstone (Kurnub Group). Neither vegetation nor urban activity exists in this subwadi (Fig. 4.23a). The elevation of Wadi Kurnub ranges from 516 m asl up to 692 m asl with an average of 608 m asl (Fig. 4.23b). Wadi Kurnub has the steepest slopes among all monitored subwadis with maximum slope of 67 degrees and an average area slope of 19 degrees (Fig. 4.23c). The slopes which are greater than 40 degrees account for 4.2% of the total catchment, which is the highest among all subwadis (Table 4.2). The dominant soil unit is soil unit 7 which has a typical distribution over the high plateaus and on top of the Kurnub sandstone. Soil unit 17 is also found, and is present over steep to very steep slopes. Soil units 12 and 24 are also found with limited cover (Fig. 4.23d). The catchment area of Wadi Kurnub can be reached through the main street, which connects the city of Mahis to Wadi Shueib; also the subwadi is reachable through a minor street close to Fuheis and Mahis WWTP.

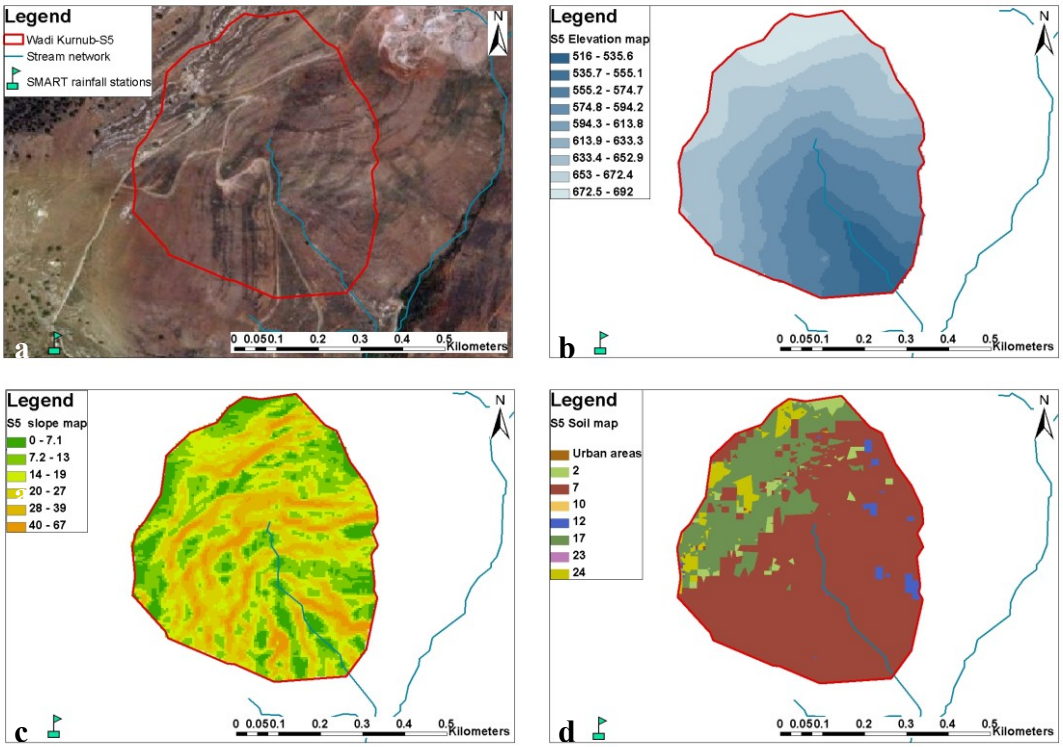

Fig. 4.24: Wadi Kurnub thematic maps.

The outlets of all subwadis are controlled by a circular culvert except S1 which has a rectangular structure (Fig. 4.19d), while in S2 and S3 the water is diverted through the circular culverts to rectangular structures just under the streets which are crossing the main subwadi channels. The automatic pressure transducers were installed in these already constructed concrete structures and runoff measurements were taken there (Fig. 4.19b).

5 Development of a hydrological model for Wadi Kafrein catchment

5.1 Introduction

The classification of rainfall-runoff models in addition to the associated problems, their applications and suitability for arid and semi arid regions, and other related topics have been discussed in chapter three. Also, the need of a numerical model for Wadi Kafrein has already been justified in earlier chapters with specific explanations as to why the numerical model has a meaningful purpose. What is needed now is to build up a hydrological model for Wadi Kafrein catchment in order to simulate the hydrological processes. Although there are slight differences in the steps toward development of every hydrological model, the basic steps are similar. A description of the basic steps toward hydrological model development has been outlined by many authors (i.e. Refsgaard, 1996; Parkin, 2000b; Anderson and Woessner, 2002). Figure 5.1 shows the model development outline for the Wadi Kafrein hydrological model, which was purposefully created for this study.

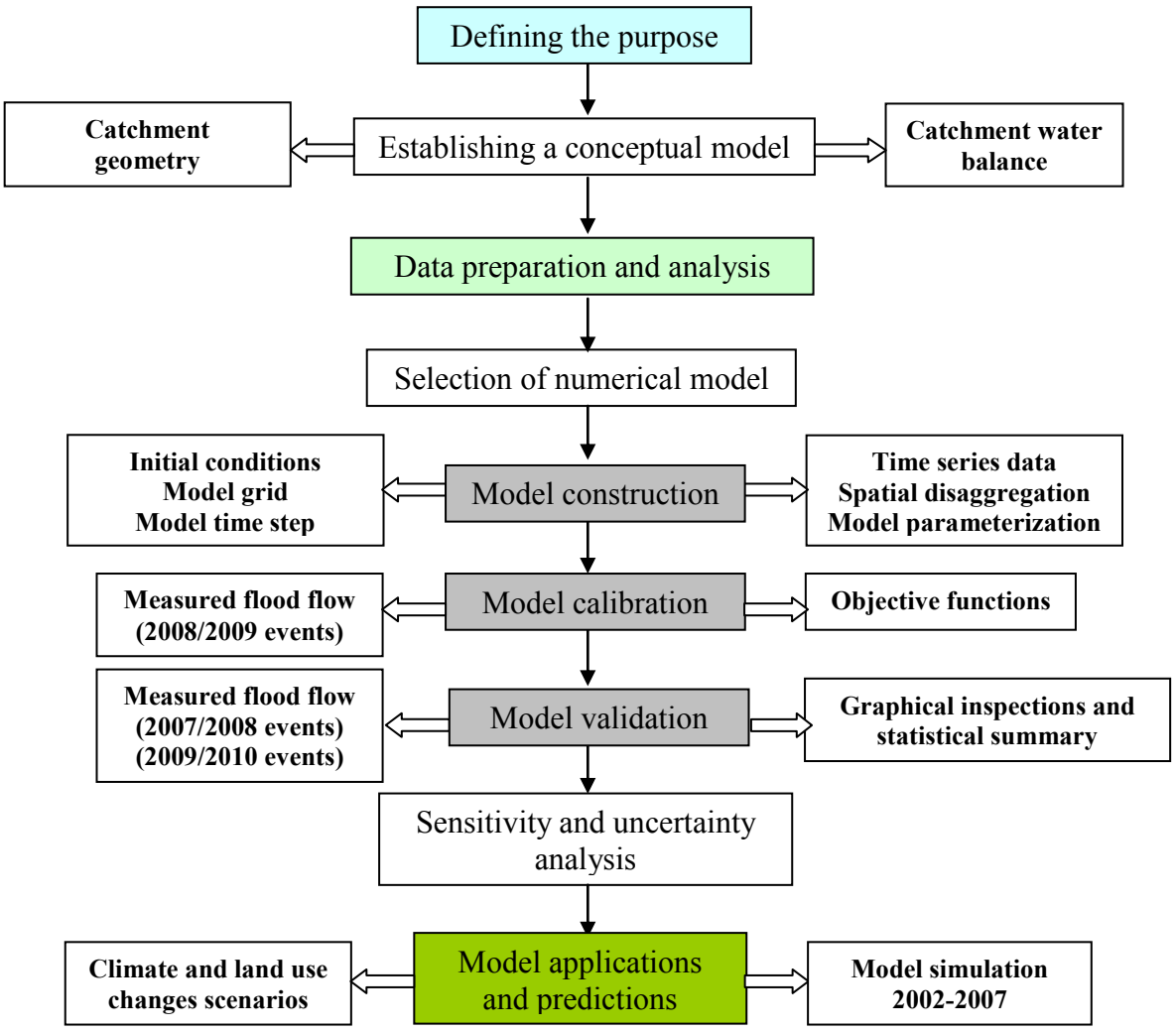

Fig. 5.1: A schematic diagram illustrating the steps of the hydrological model development of Wadi Kafrein (Modified from Anderson and Woessner, 2002).

5.2 Definition of purposes

The first step in preparing the modelling protocol is to define the aim for applying the model. In this research, simulation of the rainfall-runoff processes for a gauged catchment of Wadi Kafrein is one of the main purposes. Another important purpose for modelling the Wadi Kafrein catchment is to identify the driving forces behind runoff generation and the main controlling factors for a semi arid region similar to Wadi Kafrein. The water budget components will be quantified; climatic and land-use scenario changes are to be depicted. Upon achieving a successful application of the model to Wadi Kafrein, an optimal outcome would be to successfully quantify the hydrological components of other catchments in the lower Jordan Valley, which are deemed as having similar characteristics in terms of climate, topography, land use, and land cover.

5.3 Development of Conceptual Model

The first step in developing the conceptual model is to define the catchment area boundary. The bounded area should include the surface area from which the modeled area receives recharge or other hydrological input. The boundary of this study has been identified by using the high resolution DEM extracted from the Cartosat-1 stereo image data with the final cell size resolution of 5m x 5m. The DEM was used as basic map in ArcGIS and the catchment boundaries were defined using the "Hydrology Modelling" extension. The watersheds were defined; also, the stream network was identified which plays an important role in runoff flow. It is known that the dominant runoff process in arid and semi arid regions is overland flow, which is commonly referred as Hortonian flow. Evapotranspiration is expected to be the main component to which most of the rainfall will be transferred; nevertheless, evapotranspiration was never modeled in the study area and due to the unavailability of climatic data, evapotranspiration was estimated using lumped approaches and climatic data outside the catchment area. Groundwater presents the main source of water in Jordan, and Wadi Kafrein catchment area is one of several wadis along the Jordan Rift, forming together the "Jordan Rift Side Wadis Groundwater Basin." Recharge from these wadis is of great importance and quantifying the amount of recharge in Wadi Kafrein, using a physically based model is also of great importance.

5.4 Data preparation and analysis

For successful hydrological modelling, climatic data and rainfall-runoff data need to be prepared and analyzed appropriately so as to be successfully incorporated into the modelling process. The measured rainfall, climatic parameters, and runoff data will be discussed here. Also, the acquired rainfall and climatic data from MWI and Jordan Meteorological Department (JMD), in addition to Kafrein dam water budget data acquired from JVA-Kafrein dam operation office, will be discussed.

Field work started in March, 2007, while instrumentation started in November, 2007, and ended at the end of December, 2009. Rainfall data is from 1980 until 2009 and was measured at available rainfall stations, which are shown in Fig. 4.13. Daily time steps for this rainfall data were kindly provided by the MWI of Jordan. The Kafrein

dam water budgets, which were available from 2002 until 2009, were kindly provided by JVA- Kafrein dam operation office. Climatic data have been available from 2002-2007 for the two weather stations, Wadi Es Sir and South Shuna, which are operated by MWI. The acquired data of rainfall and climatic parameters from MWI and JMD were used in climatic change scenarios and in model validation using historical data of stream flow for the entire Wadi Kafrein catchment. The acquired water budget of the Kafrein dam data were used in the calibrating and validating of the hydrological model. These issues are discussed in Chapter Six under "Model applications and predictions." Here, a hydrological year (water year) is considered; it is a twelve month period from October through September of the next year. In this study, two hydrological years are covered; namely 2007/2008 and 2008/2009.

5.4.1 Rainfall events during the study period

The measured rainfall data of this research covers the consecutive hydrological years 2007/2008 and 2008/2009, while the hydrological year 2009/2010 data were analyzed until December 2009 and used for the model validation process. Several tipping buckets were installed (Fig. 4.13), which is by far the most commonly used type of automatic rain gauge today. The hydrological year 2007/2008 was a dry year with total aerial rainfall of 167 mm compared to a long term annual average of 387 mm.

The Wadi Es Sir Rain station (4 km southwest of King Hussein Gardens rain gauge, Fig. 4.13) recorded a total rainfall of 283.7 mm in 2007/2008. Wadi Es Sir rain gauge operated by MWI of Jordan has a long term annual average of 524 mm/yr (Agrar and Hydrotechnik GMBH, 1977). Only 292 mm was measured in King Hussein Gardens rain gauge (R1) in 2007/2008. Several rainfall events took place with relatively low rainfall intensities and a rather long lag time between the events. One snow storm took place during the entire monitoring period, which occurred on January 30, 2008 and lasted for 2 days.

Rain gauges for this research were installed in November, 2007. The records of MWI show that rainfall of the hydrological year 2007/2008 started on October, 18 with only 1 mm as measured in Wadi Es Sir rain station and 2.5 mm in Wadi Es Sir (NRA) station, followed by a month of no rainfall. Therefore, the rainfall measurements of this research are considered to be representative for the entirety of this hydrological year. The monthly sums of the measured rainfall in 2007/2008 are given in Table 5.1. Most rain occurred in January and February. Rainfall started late and ended early. In March, very few mm of rain were measured at all rain gauges. The rainfall amounts range from 5.6 mm at R1 to 0.2 mm at R4. Rainfall was distributed over 132 days, extending from 20.11.2007 to 30.03.2008.

Table 5.1: Monthly rainfall amounts as measured in the rain gauges in the hydrological year 2007/2008

Month/ Station ID	King Hussein Gardens-R1	Rabahiyya Janubiya-R2	Zabada /Fahas-R3	Wadi Es Sir WWTP-R4	Wadi Bahhath-R5	Wadi Shueib-R6	Fuheis R7
Nov.2007	61	No data	No data	23	No data	No data	No data
Dec.2007	26.8	22.2	18.8	16.2	No data	28.4	23
Jan.2008	88.2	61	68	45.6	75.6	74	69.4
Feb.2008	110.4	57.4	38.6	27.6	27	63.6	52.6
Mar.2008	5.6	1.2	1	0.2	1.8	1.6	3.2

The rain gauge, R1, was installed in the recharge area in the high lands where the highest rainfall over Wadi Kafrein naturally occurs. The R1 station is close to Wadi Es Sir and Wadi Es Sir (NRA yard) stations, which are both operated by MWI. The historical data indicates the highest amount of rainfall over the Kafrein catchment occurring at these stations.

Figure 5.2 shows the daily rainfall amounts as measured in R1 for the hydrological year 2007/2008, with a total rainfall amount of 292 mm. The maximum daily rainfall amount was recorded on 21.11.2007, with a total height of 41.8 mm. This record was followed by several low intensity rainfall events, with almost every event not exceeding 15 mm. For lower elevations where an arid to semi arid climate prevails, a rain gauge has been installed at the Wadi Es Sir WWTP (Fig. 4.13).

The lowest rainfall amounts were recorded at this station, with total rainfall amount of 113 mm in 2007/2008 as shown in Fig. 5.3. The maximum daily rainfall at R4 was also measured on 21.11.2007 with a total amount of 14.8 mm. The spatial variation of rainfall over the catchment area of Wadi Kafrein is clear with a large decrease in rainfall, moving from the eastern high lands (R1) westward (R4), as is shown in Figs. 5.2, 5.3 and Table 5.1.

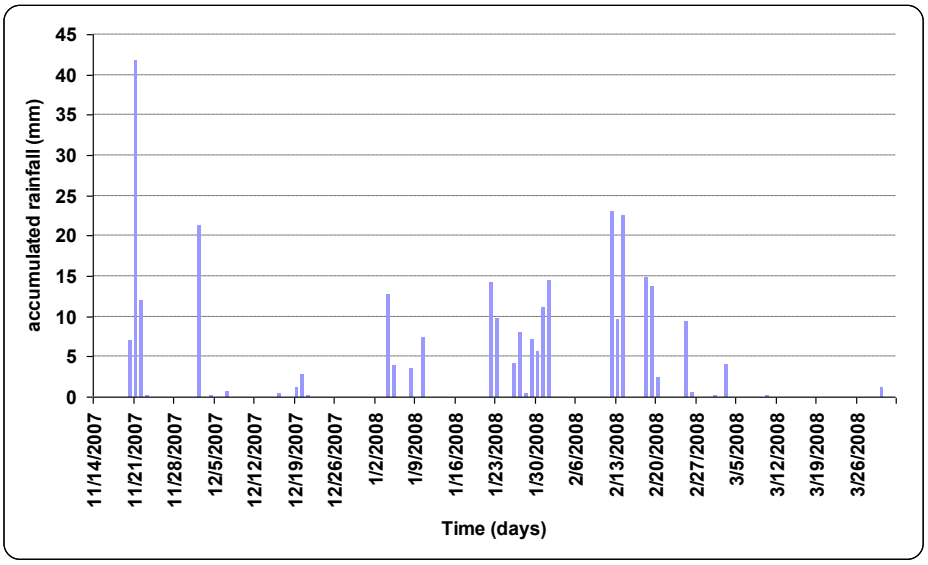

Fig. 5.2: Daily rainfall amount as measured in King Hussein Gardens rain gauge 2007/2008.

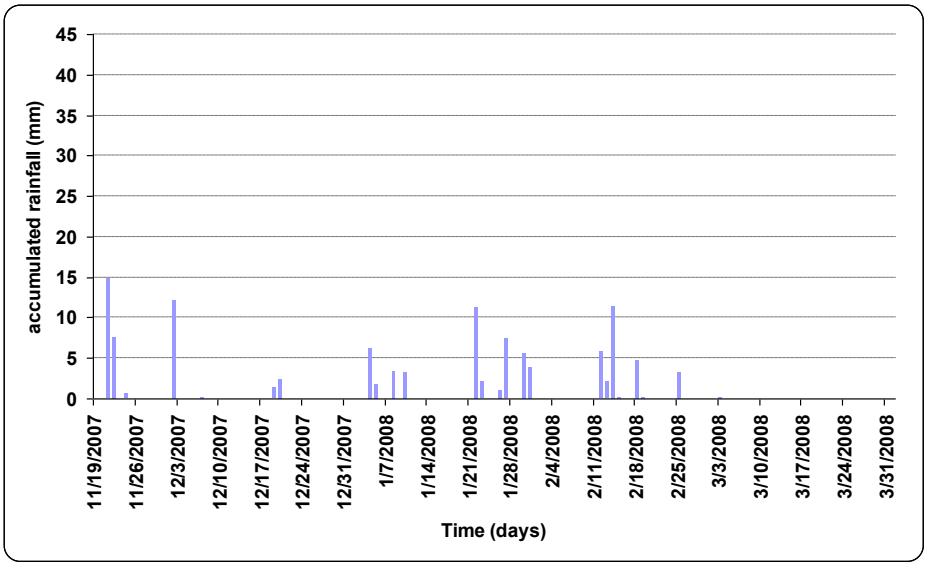

Fig. 5.3: Daily rainfall amount as measured in Wadi Es Sir WWTP rain gauge 2007/2008.

The hydrological year 2008/2009 witnessed higher rainfall and a greater intensity of rainfall. The aerial rainfall was calculated to be 250 mm, which is also less than the long term annual average (387 mm). Monthly sums of the measured rainfall are given in Table 5.2. Rainfall was highest in February and second highest rainfall was in March. This hydrological year was unique because the lowest rainfall was recorded in January, which is known to be (together with February) the wettest month in the winter season. The rainfall amounts in January 2009 ranged from 5 mm in R1 to only 0.8 mm in R4. February was wet and the highest rainfall amounts are shown in Table 5.2. Rainfall was distributed over 184 days between the periods of 25.10.2008 until 26.04.2009

Table 5.2: Monthly rainfall amounts as measured in the rain gauges in the hydrological year 2008/2009.

Month/ Station ID	King Hussein Gardens-R1	Rabahiyya Janubiya-R2	Zabada/Fahas R3	Wadi Es Sir WWTP-R4	Wadi Bahhath R5	Wadi Shueib-R6
Oct.2008	18.2	9.2	13.4	12.8	13.8	No data
Nov.2008	7.2	3.2	0.4	4.2	1.6	No data
Dec.2008	55.4	26.8	31.2	19.8	31.4	31.6
Jan.2009	5	2.8	1.4	0.8	3.4	4.6
Feb.2009	228.6	106.8	121.8	84.8	132.8	159.2
Mar.2009	89.8	60.6	69	63.8	83.2	76
Apr.2009	7.6	1.8	2	1.2	No data	No data

Figure 5.4 shows the daily rainfall amounts as measured at R1, with a total sum of 411.8 mm, which is the highest total rainfall measurement among all stations (Table 5.2). The maximum daily rainfall amount was measured on 28.02.2009 with total height of 70.8 mm. The lowest rainfall amounts were measured at R4, with a total sum of 187 mm for the whole season.

The daily rainfall at R4 is shown in Fig. 5.5, with maximum daily accumulated rainfall of 23.8 mm, measured on 21.02.2009. Again, the spatial variations are clear as can be seen in Fig. 5.4, 5.5, and in Table 5.2.

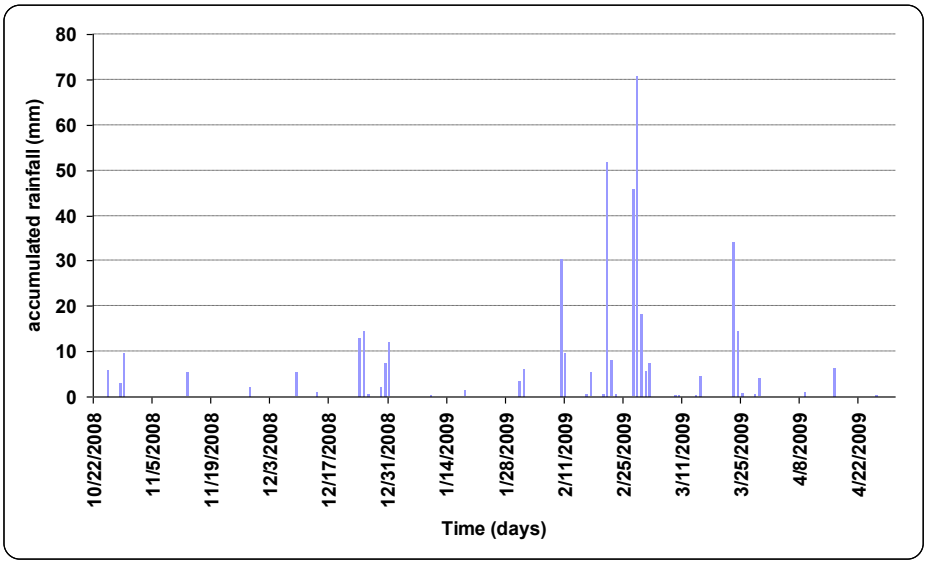

Fig. 5.4: Daily rainfall amount as measured in King Hussein Gardens rain gauge in 2008/2009.

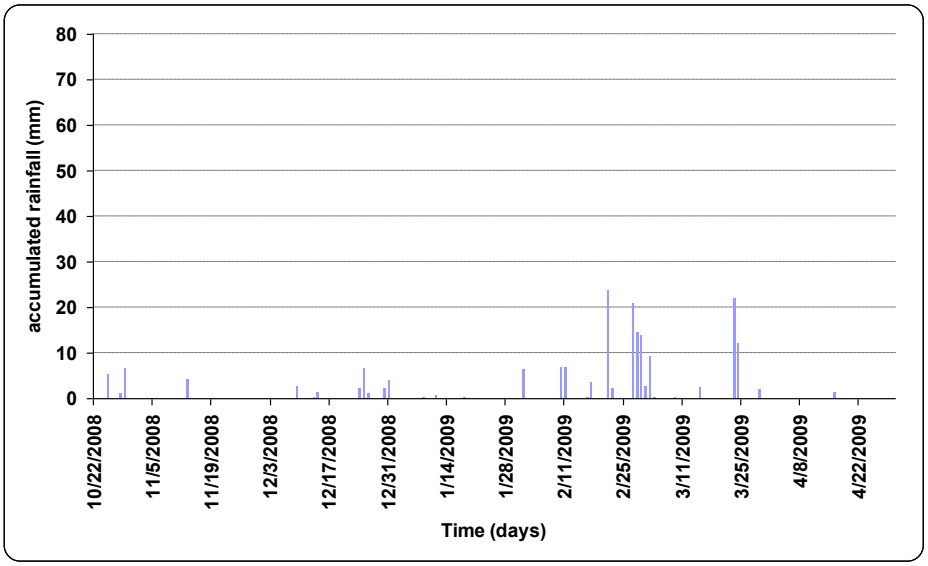

Fig. 5.5: Daily rainfall amount as measured in Wadi Es Sir WWTP rain gauge in 2008/2009.

During the monitored months of 2009/2010, several rainfall events were also measured and the generated runoff was measured and used to validate the results of the hydrological model which is described later.

5.4.2 Climatological parameter measurement and analysis

The climatic parameters were measured in Wadi Kafrein using two automatic weather stations. The first weather station was representative of the high lands on the eastern side (KHG weather station) and the other station was close to the Jordan valley on the western side (Wadi Es Sir WWTP weather station). The geographic locations of both stations are depicted in Fig. 4.13.

The monitoring period of the climatic parameters extends from November, 2007 until December, 2009. The climatic parameters were measured with the aim in mind that evapotransipiration should be precisely calculated with the measured parameters. As explained in Section 4.3.2, the available weather station in Wadi Es Sir (operated by the MWI) is not spatially representative nor is the temporal resolution sufficient for ultimately simulating evapotransipiration with high accuracy.

In order to acquire an overview on the measured climatic parameters, the maximum, minimum, and average of the 5 minutes data have been calculated for every parameter. These are shown in Table 5.3 for KHG weather station and Table 5.4 for Wadi Es Sir WWTP weather station. A noticeable variation in temperature can be seen between both stations with an almost 7 degrees higher average for Wadi Es Sir WWTP. In the hydrological year 2007/2008, the hottest month was August, 2008 at both stations, while for the hydrological year 2008/2009, the hottest month was June, 2009. This fact indicates that spatially, climatic conditions are relatively consistent, and trends, although with different magnitudes of values, are similar for both stations at a given time. For example, the maximum temperature at Wadi Es Sir WWTP weather station was 5 °C more than the maximum temperature at KHG weather station during this period.

Table 5.3: Maximum, Minimum and Average of climatic parameters of KHG weather station.

Year/Parameter		Temp. (°C)	RH (%)	Wind speed (m/s)	Solar radiation (W/m^2)
2007/2008	Max.	35.7	100	9.5	1277
	Min.	-2.4	3.3	0	0
	Av.	**15.6**	**56.9**	**2**	**231**
2008/2009	Max.	35.7	100	8.2	1277
	Min.	-0.2	0	0	0
	Av.	**16.3**	**48.1**	**2**	**224**

In general, no large variations in climatic parameter values between both hydrological years are noticed. Table 5.3 and table 5.4 show slight differences among averages, maximum, and minimum.

Table 5.4: Maximum, Minimum and Average of climatic parameters of Wadi Es Sir WWTP weather station.

Year/Parameter		Temp. (°C)	RH (%)	Wind speed (m/s)	Solar radiation (W/m^2)
2007/2008	Max.	40.6	100	15.2	1277
	Min.	2.5	2.8	0	0
	Av.	**22.5**	**43.3**	**2.2**	**230**
2008/2009	Max.	41.1	100	15.2	1277
	Min.	5.4	1.3	0.6	0
	Av.	**22.4**	**48.4**	**2.4**	**239**

5.4.3 Runoff hydrographs of Kafrein catchment and the subwadis

Runoff was continuously monitored in the subwadis as well as in the whole catchment area, while runoff measurements were taken during several rain events in order to calibrate the stage heights of the subwadis. During the hydrological year 2007/2008, the rainfall intensity was low with a long lag time between events. This combination

of low rainfall intensities and long lag time between events resulted in no runoff events in any of the monitored subwadis, while few events were recorded with low magnitude for the whole catchment area. In the second monitoring year, 2008/2009, the rainfall events had relatively high rainfall intensities and had short lag times between events, which caused several runoff events. These runoff events were monitored and measured in the subwadis as well in the entire catchment area using the staff gauges and the monitoring approach as explained in the coming section.

5.4.3.1 Runoff calculations of the Kafrein dam reservoir

In this research, the mass balance equation has been considered, accounting for all hydrological parameters influencing the Kafrein dam reservoir storage. The dam receives water from different sources and loses water due to evaporation, irrigation, and seepage. Therefore, including these inputs and outputs in runoff calculations is essential.

The daily measurements of the Kafrein dam water budget, operated by the JVA-Kafrein dam operation office, and the hourly measurements of the stage height, and DEM of the Kafrein reservoir, prepared in this research, were all integrated to calculate the generated runoff from Kafrein catchment area on an hourly basis. The difference in water storage in the reservoir after a storm event should indicate the amount of generated runoff; nevertheless, the inflow includes baseflow from spring discharges, effluent discharging from Wadi Es Sir WWTP, and direct rainfall over the reservoir. The outflows consist of the water amounts taken for irrigation, direct infiltration to the groundwater and seepages from the dam floor, in addition to the direct evaporation from the reservoir surface (Fig. 5.6).

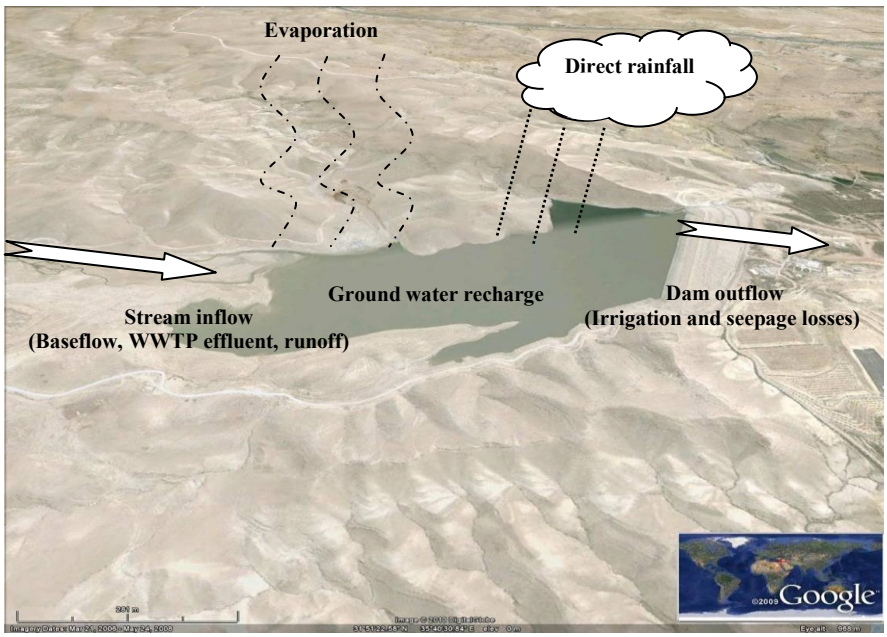

Fig. 5.6: Kafrein dam reservoir mass balance components (background image from Google Earth®).

The storage of the Kafrein Dam reservoir can be calculated using a mass balance, which accounts for all terms controlling its storage as follows:

$$S_{t+1} = S_t + I_t + R_t - E_t - O_t - L_t \quad (5.1)$$

Where:
S_{t+1} : Storage of the reservoir at the beginning of time period t+1
S_t : Storage of the reservoir at the beginning of time period t
I_t : Inflow to the reservoir during the time interval t to t+1; ($I_t = Q_t + B_t + W_t$)
R_t : Rainfall on the surface of the reservoir
E_t : Evaporation from the reservoir surface
O_t : Outflow from reservoir (irrigation)
L_t : Losses due to spillways and seepages to groundwater

And;
Q_t : Runoff during the time interval t to t+1
B_t : Baseflow during the time interval t to t+1
W_t : WWTP effluent during the time interval t to t+1

The difference in water storage of the reservoir was calculated using the rating curve (Fig. 5.7), which was prepared for the Kafrein dam by using the high accuracy DEM of the reservoir (section 4.4.1), which uses the differential GPS measurements and hourly measurements of the stage height differences of the water surface.

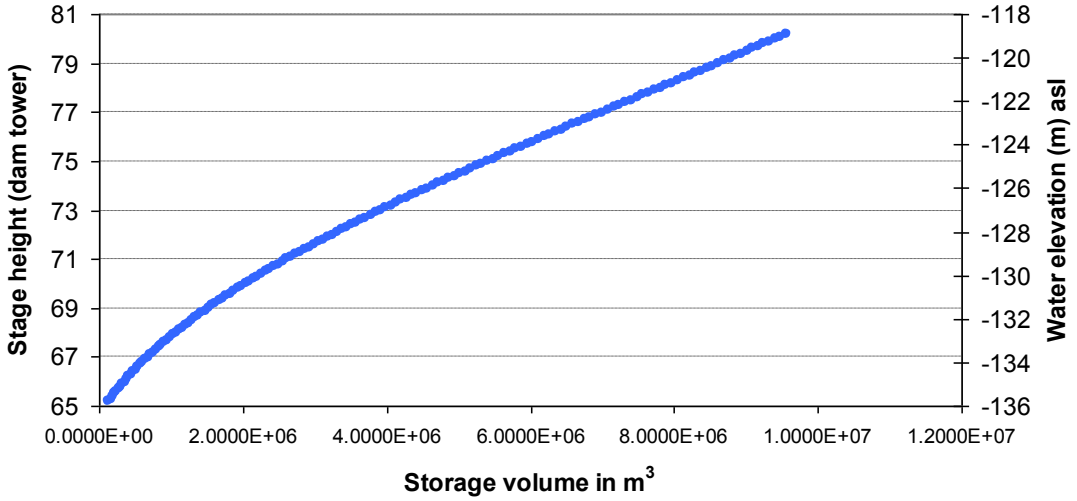

Fig. 5.7: Kafrein reservoir rating curve calculated by differential GPS measurements and high accuracy automatic pressure transducer.

To calculate the inflow to the reservoir, the spring discharge was calculated from the data acquired from MWI while the Wadi Es Sir WWTP effluent was calculated from the hourly acquired data from Wadi Es Sir WWTP office. Outflow, evaporation from reservoir surface, and the loss values were acquired from JVA-Kafrein dam operation office. The aim is to calculate the unknown in this equation, i.e. the runoff amounts. By rearranging equation (5.1), the runoff amounts can be calculated as follows:

$$Q_t = \Delta S - (B_t + W_t + R_t) + (O_t + E_t + L_t) \quad (5.2)$$

ΔS is the difference in dam storage as measured on an hourly basis, using the above mentioned approach. Evaporation of surface water from the reservoir is an important component to the water balance equation. It is possible to compute the quantity of

evaporated water from the reservoir once all inflows (rainfall over the reservoir, surface and groundwater inflow, wastewater discharge), outflows (seepage to groundwater, irrigation, spillway discharges), and changes to water storage are known. Fetter (1988) says that error values of ± 10% from measurements of inflow and outflow are possible, except for the ground water flux. The difference between the total measured inflow and total measured outflow on a daily basis represents the total flux of groundwater.

In this research, evaporation was calculated using the well known "Class-A land pan." A Class-A land pan has been installed near the dam operation office few meters below the level of the reservoir. The pan is 122 cm in diameter and 25.4 cm deep; the pan is placed over a wood support allowing the air to circulate all around as shown in (Fig. 5.8). This land pan, in addition to a nearby rain gauge, is operated by the Kafrein dam operation office and the data were kindly provided to support this research.

Evaporated water volumes were calculated from water depth changes in the pan. These changes were measured early every morning and subsequently the pan was refilled up to achieve the required 20 cm depth. On rainy days, the quantity of rainfall measured at the nearby rain gauge is subtracted from the measured value in the land pan. The difference in stage height of the water stored in the dam was also measured early every morning.

Fig. 5.8: Class A land pan used to calculate the evaporation from the reservoir.

Evaporation-calculations equation is available in the dam office where the area of the reservoir water surface is calculated for every stage height, allowing the calculation of the total volume of the evaporated water from the reservoir. To evaluate the accuracy of the measured evaporation values, an automatic pressure transducer was installed in the Class-A land pan with 0.1 cm accuracy. Measurements were taken hourly and these were in good agreement with the daily measurements.

Daily rainfall and evaporation amounts were downscaled to an hourly basis using temporally high resolution rainfall and solar radiation measurements from the Wadi Es Sir WWTP weather station (section 5.3.2). Evaporation at hour "i" of the day "x" from the reservoir surface equals:

$$E_{ix} = \left(SR_{ix} / SR_{dx}\right) E_{dx} \qquad (5.3)$$

Where:

E_{ix} : Evaporation from reservoir surface at hour i of day x
SR_{ix} : Solar radiation as measured at Wadi Es Sir WWTP at hour i of day x
SR_{dx} : Daily solar radiation as measured at Wadi Es Sir WWTP at day x
E_{dx} : Daily evaporation amount as measured at Kafrein dam site at day x

Similarly, the daily rainfall amounts measured at the Kafrein dam site were downscaled to an hourly time step using the time index of the measured rainfall amount from Wadi Es Sir WWTP rain gauge which represents the closest rain gauge to the dam site.

$$R_{ix} = \left(Rrg_{ix} / Rrg_{dx}\right) R_{dx} \tag{5.4}$$

Where:
R_{ix} : Rainfall amount over the reservoir surface at hour i of day x
Rrg_{ix} : Rainfall amount at Wadi Es Sir WWTP rain gauge at hour i of day x
Rrg_{dx} : Daily rainfall amount as measured at Wadi Es Sir WWTP rain gauge at day x
R_{dx} : Daily rainfall amount as measured at Kafrein dam site at day x

Regarding irrigation and seepage volumes, which were measured on-site at a daily time step, values were downscaled to an hourly time step by distributing the irrigation amount over the irrigation hours of that day while the seepage values were distributed over the day hours. The spillways or seepages from the dam are measured using a V-noch (Fig. 5.9) and all the water is collected in a pool a few kilometers downstream of the dam.

Fig. 5.9: Seepage from Kafrein dam reservoir measured using a V-noch and a stage height (Photo taken on 16th of April, 2007).

5.4.3.2 Runoff measurements in the subwadis

After proper rehabilitation of the subwadi monitoring stations, automatic pressure transducers were installed and fixed as explained earlier (Section 4.4.2). Water height was recorded continuously with a temporal resolution of two minutes. To calculate the runoff, several measurements were done using the salt dilution method, the current meter, or the dipping bar, depending on the circumstances of the runoff event and its magnitude.

As the winter season of 2007/2008 was dry, no single runoff event took place in any of the 5 subwadis; it's even still possible to see the mortar powder spilled during the installation process, at the end of the rainy season as shown in Fig. 5.10 from the subwadi S3.

Fig. 5.10: The mortar powder spilled during installation can still be seen at the end of the water year 2007/2008 (in one of the monitored subwadies).

In the next hydrological year, the first runoff event which took place in the subwadis was on the October 29th, 2008. This event was only observed in **Wadi Kurnub-S5**; it was the 3rd rainy day and there was low rainfall intensity. Therefore the rainfall event on this date generated a weak runoff flow which was only observed in the subwadi S5 in the Wadi Shueib catchment area. The runoff was observed in the field as it wetted the circular culvert floor which is not possible to be measured using the pressure transducer neither by current meter or the salt dilution method.

In the end of December 2009, two runoff events took place; on the 25th and 30th of December with relatively low amounts yielding few cubic meters of runoff with few centimeters height in the culvert. The stage height of S5 in the 25th of December is shown in Figures 5.11 while Table 5.5 illustrates the characteristics of the rain storms occurred in S5.

Table 5.5: Rain storms characteristics for S5 runoff events (modified from Alkhoury et al. 2009).

Rain storms	Rainfall [mm]	Duration [h]	Rain Station	Runoff
25.10.08	10.8	5	Fuheis	Not generated
28-29.10.08	9.4	24	Fuheis	Generated
24-25.12.08	14.2	16	Shueib	Generated
30-31.12.08	12.4	23	Shueib	Generated
31.01.09	5.6	3.5	Shueib	Not generated
10-11.02.09	24.6	24	Shueib	Generated
21-22.02.09	48.4	38	Shueib	Generated
27-28.02.09	77.2	40	Shueib	Generated

During January 2009 rainfall was very low; the rain gauge in Wadi Shueib recorded only 4.6 mm in the whole month, consequently no single runoff event was recorded in any of the subwadis. The fourth runoff event in S5 occurred on the 10th of February, 2009. The rainfall intensity during the 10th of February storm was 6.6 mm in its first hour, causing direct runoff which was measured as being 29.5 l/s at peak discharge, as measured with a current meter (Fig. 5.12).

The generated runoff during the 10th of February rain storm was measured over 5 minute time step intervals, using a current meter. Figure 5.12 shows the hydrograph of the storm from the 10th of February, 2009 and the generated runoff during its peak (Fig. 5.13).

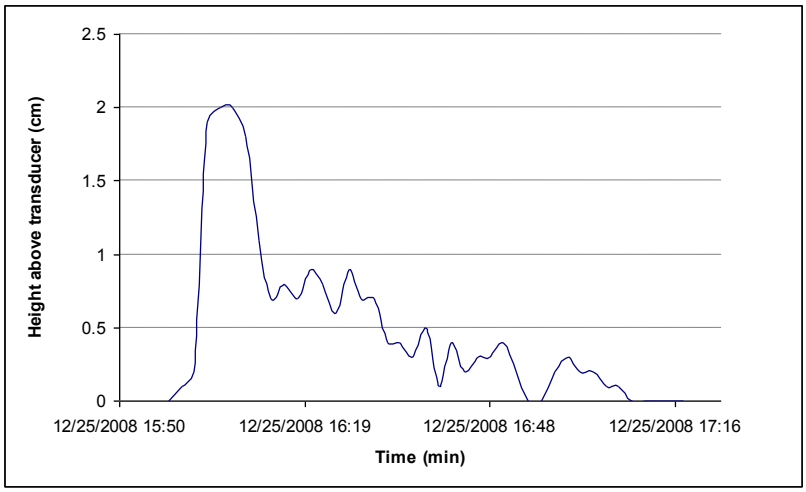

Fig. 5.11: Stage height in S5 due to runoff event on 25th December 2008.

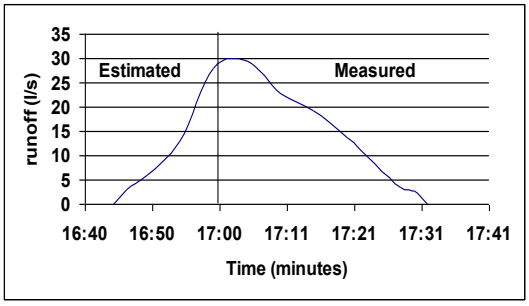

Fig. 5.12: Storm hydrograph in subwadi S5 during the rain storm of 10.02.2009.

Fig. 5.13: The generated runoff in S5 during the rain storm of 10.02.2009.

In the other sub-wadis, no runoff was generated from the beginning of the winter season until the 10th of February, where runoff was observed for the first time in **Wadi El Nar-S4**. The generated runoff amounts were very low and did not exceed the 3 cm in heights in the circular culvert which was not possible to be monitored neither measured using the current meter or the salt dilution method. Figure 5.14 shows the wetted floor of the circular culvert in S4 due to runoff event on the 10th February, 2009.

Fig. 5.14: First runoff event at S4 during the 10th of February, 2009 rainfall event.

Due to the high intensity of rainfall with relatively short lag times between rain storms in February 2009, runoff was generated in most of the subwadis shortly after or during the rainstorms. Runoff was first recorded and measured in S4 during the 21st of February, 2009. Stage heights were continuously recording all runoff events. The second runoff event started on the 27th of February and lasted until the 3rd of March, 2009 in which six hydrographs were measured and the peak discharge ranged from 10 l/s to more than 250 l/s (Figs. 5.19-5.24). The recorded heights varied from few cm in the circular culvert to more than 40 cm as can be seen for the 27th of February, 2009 (Fig. 5.15). The third runoff event took place on the 23rd of March, 2009 (Fig. 5.26).

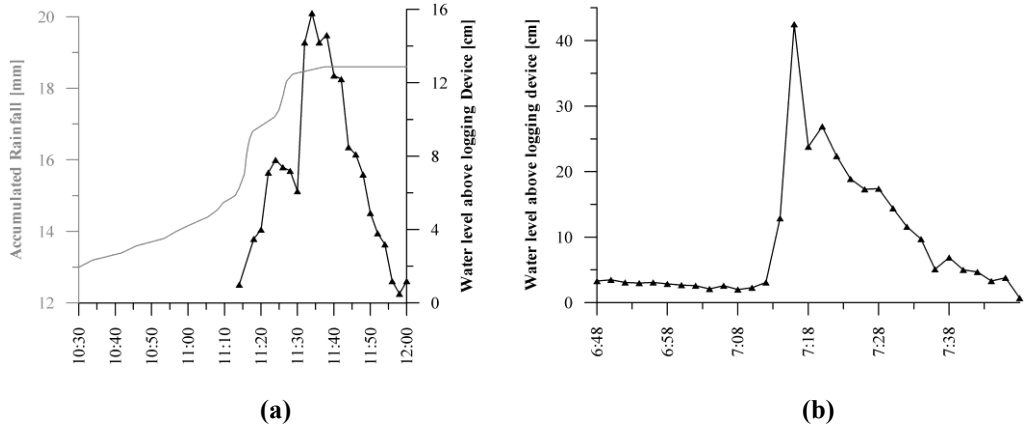

Fig. 5.15: (a) Runoff event recorded in S4 subwadi on the 21.02.2009. Accumulated rainfall of the nearby rainfall station can also be seen (R3). (b) Runoff event recorded in the S4 subwadi on the 27.02.2009 (Alkhoury et al., 2009).

The hydrological modelling process requires data on runoff to calibrate and validate the model; stage height measurements alone are not sufficient for this task. Continuous measurements of runoff are costly, time consuming, and in cases of runoff events with big magnitudes, not practical. A possible worthy solution may be to evaluate the *stage-discharge relationship* or *stage discharge rating curve.* The *stage-discharge relationship* or *stage discharge rating curve* is a unique parameter, which considers the relationship between the stage height of a stream and the corresponding discharge at a stream section. Rating curves for the subwadis may be constructed with comparative ease and economy by conducting several concurrent runoff and stage height measurements.

Several methods, with varying definitions, for applying stage-discharge rating curves are described in the United States Geological Survey (USGS) publications of Dawdy (1961), Rantz (1963), Bailey and Ray (1966) , Rantz et al. (1982a, 1982b). Further publications are found by the Regulation of the International Organization for Standardization (ISO), n. 1100-2 1998 (ISO, 1998) and the World Meteorological Organization (WMO) Publications of report n. 519 (1980) and report n. 650 (1986).

The most commonly used stage-discharge ratings treat discharge as a unique function of the stage. These ratings follow a power curve of the form given in the following equation (Herschy, 1995; ISO, 1998; Braca, 2008):

$$Q = C(h - a)^{\alpha} \tag{5.5}$$

Where:

Q : Discharge
h : observed stage height (water level time series)
C,a,α : calibration parameters

The "**C**" parameter is the discharge when the effective depth of flow (**h-a**) is equal to 1, while "**a**" is the gauge height of zero flow and "**α**" is the slope of the rating curve (on logarithmic paper). The (**h-a**) is the effective depth of water on the control.

Equation (5.5) is based on the Manning equation which is frequently used as the governing equation for steady uniform flow problems:

$$Q=\left(\frac{1}{n}S_o^{1/2}\right)\left(AR^{2/3}\right) \quad (5.6)$$

= function of (roughness and slope) & (depth and geometry)

Where:
n : Manning's roughness coefficient
S_0 : bottom slope
A : area
R : hydraulic radius

The relationship between rating curve parameters and physical conditions is also evident if the power equation (equation 5.5) is compared with Manning's equation (equation 5.6) for determining discharges in steady flow situations. The exponent in equation (5.5) will be affected due to changes in the channel resistance and slope with stage. Values of the exponent "**α**" vary from 1.3 to 1.8 for wide streams, and for deep narrow streams exponent values are greater than 2 and may exceed the value of 3 (DHV, 1999).

For most stations, equation (5.5) is an over-simplification. In general, the rating will be a compound curve consisting of different segments for different flow ranges. Each of these segments may follow the form of equation (5.5) but have unique values for C, a, and α (Braca, 2008). The segments are typically connected by short transition curves. Statistical methods have been developed to fit the curves in the form of equation (5.5) or polynomial curves to measured stages and discharges (Herschy, 1995). However, for most natural streams, the graphical fitting of a curve to the measured data is the preferred method (ISO, 1998).

Due to the absence of any runoff events in the first monitoring year 2007/2008 and the few runoff events, which occurred in the hydrological year 2008/2009, it was not possible to make sufficient runoff measurements in all subwadis for establishing rating curves for each subwadi. Runoff events usually occur simultaneously in all subwadis; also, runoff events occur over short time intervals. Several runoff measurements were made in S4 and concurrent stage height was recorded in S4 during the two runoff storms in February, 2009 while no runoff measurements were possible during the third event on the 23rd of March, 2009 as it occurred overnight.

Several measurements were used to prepare a rating curve for the subwadi S4 and the parameters "**C,**" "**a,**" and "**α**" were defined by a trial and error method using a special

calculation table prepared based on the measured runoff values in the field. Due to the relatively large difference between the lower and upper runoff values, three segments were used to fit the curve. Nevertheless, measurements to cover the upper and lower ends of the rating curve are lacking, therefore the ratings are often extrapolated to estimate flows outside the range of the measured values. Several methods are available to extrapolate the rating (Rantz et al., 1982a, 1982b). A rating curve for Wadi An Nar-S4 has been prepared using the above mentioned equations and the results are presented graphically (Fig. 5.16) where the Q (discharge) is given in cm^3/s and the stage height in centimeters.

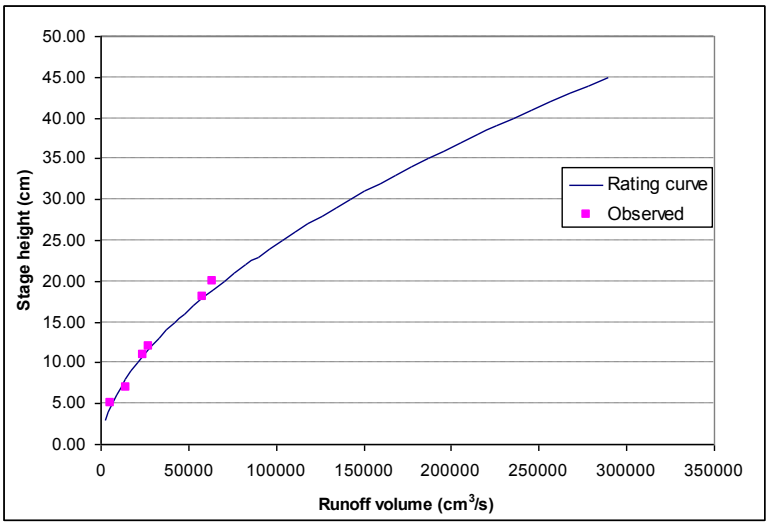

Fig.5.16: Rating curve of Wadi An Nar-S4

Using the prepared rating curve of Wadi An Nar-S4, all measured stage heights were converted to hydrographs and the results are shown in figures 5.17-5.26. During the rainstorm event on the *21st of February, 2009*, runoff was generated twice, in which a total runoff of 41.2 m^3 was generated in the first event (Fig. 5.17) while only 4.7 m^3 was generated during the second runoff event (Fig. 5.18). In total, all runoff generated on the 21st of February rainstorm is 45.9 m^3. The areal rainfall during the 21st of February was calculated to be 30.4 mm using the inverse distance weighting method (5.6.6.1).

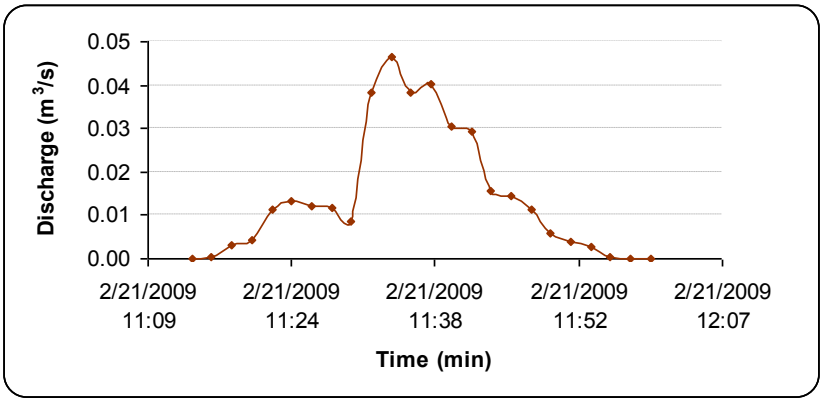

Fig. 5.17: First runoff hydrograph at S4 during the 21st of February, 2009 rainfall event.

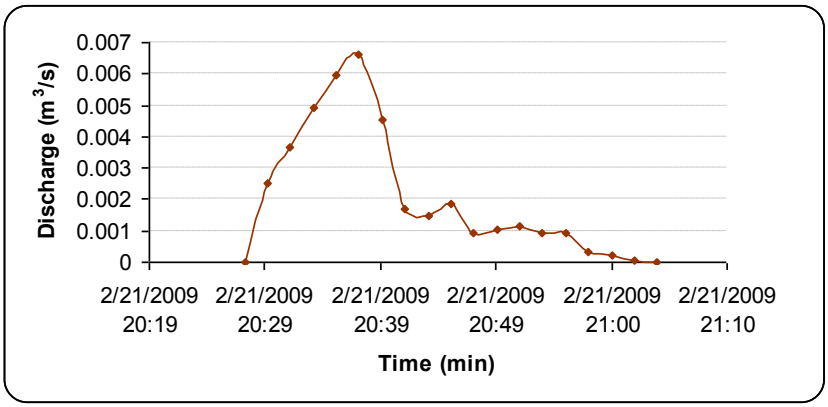

Fig. 5.18: Second runoff hydrograph at S4 during the 21st of February, 2009 rainfall event.

The next rainfall event started on *February 27th, 2009* and lasted until the *3rd of March, 2009*. As the lag time between the two events is relatively short, the antecedent soil moisture was high. The area rainfall on the 27th of February was 29.6 mm (close to rainfall amount on February 21st). Total runoff generated on this date was 104.8 m^3 with peak flow of 262 l/s, generated in the early morning (Fig. 5.19). A second runoff event occurred in the afternoon with a peak discharge of 37.5 l/s and a total runoff generation of 213.9 m^3 (Fig. 5.20). Figure 5.19 indicates a sharp rising limb, which lasts for a short time. Figure 5.20 shows a rising limb, which is smoother and which has a lower peak flow but is lasting for a longer time. The difference between the two hydrographs reflects the saturation situation of the soil. Saturation Excess Overland Flow (**SEOF**) is responsible for this. On the following day, February 28th, a total area rainfall of 25.7 mm was calculated and the generated runoff events are presented in Fig. 5.21 and 5.22. Runoff amounts recorded on the 28th of February are 285 m^3 and 24.3 m^3 respectively. During the 1st and 3rd of March, 2009 a total area rainfall of 14.7 mm and 8.6 mm were calculated, causing runoff amounts of 218 m^3 and 97.9 m^3 respectively (Fig. 5.23 and 5.24).

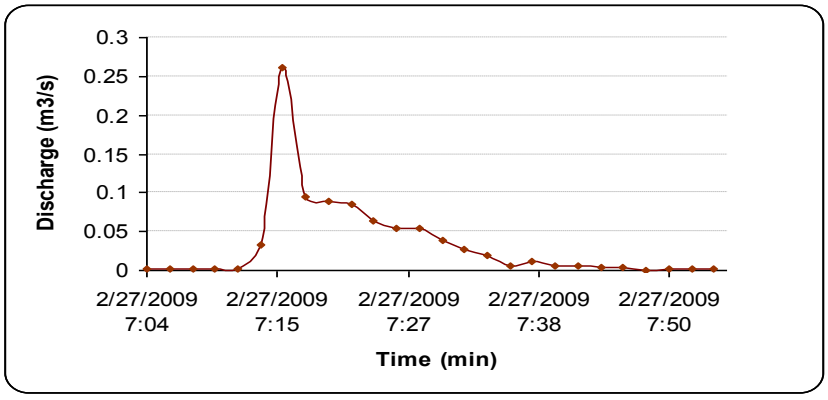

Fig. 5.19: First runoff hydrograph at S4 during the 27th of February, 2009 rainfall event.

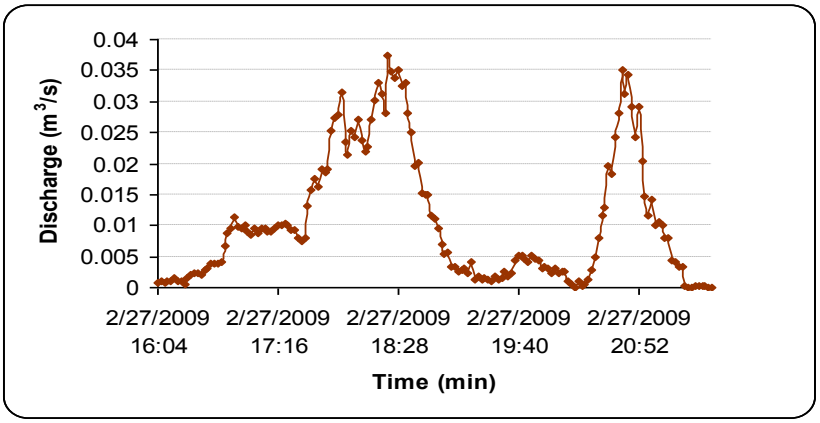

Fig. 5.20: Second runoff hydrograph at S4 during the 27th of February, 2009 rainfall event.

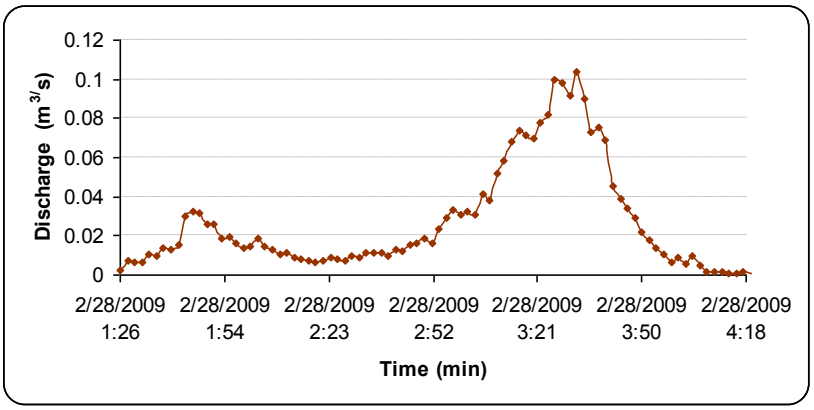

Fig. 5.21: First runoff hydrograph at S4 during the 28th of February, 2009 rainfall event.

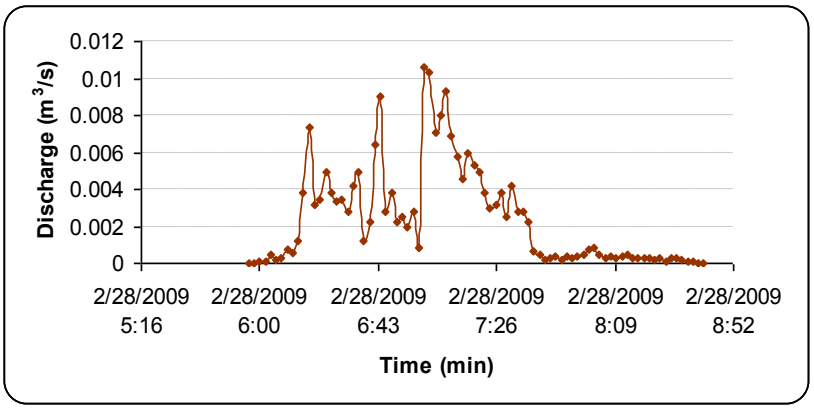

Fig. 5.22: Second runoff hydrograph at S4 during the 28th of February, 2009 rainfall event.

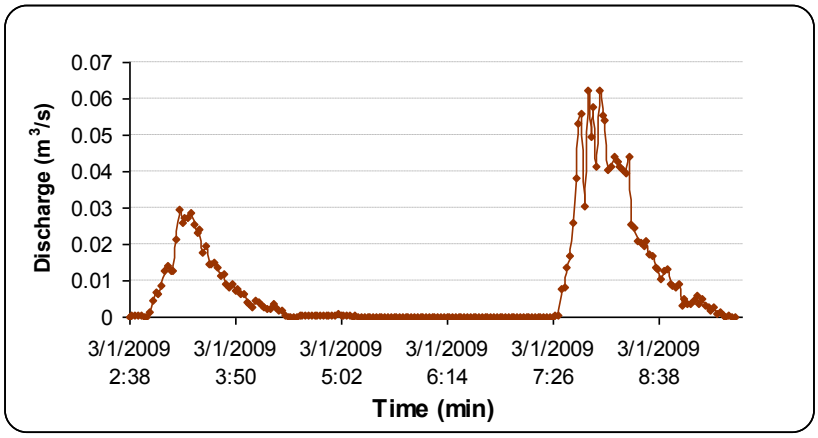

Fig. 5.23: Runoff hydrograph at S4 during the 1st of March, 2009 rainfall event.

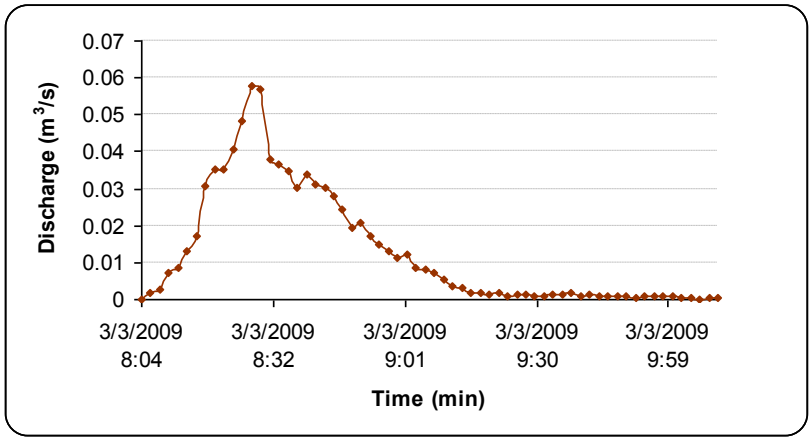

Fig. 5.24: Runoff hydrograph at S4 during the 3rd of March, 2009 rainfall event.

All runoff events generated from the rainfall from 27th of February until the 3rd of March are shown in Fig. 5.25 in which the variations in peak flows, lag times, and hydrograph width of every runoff event can be seen and compared together easily.

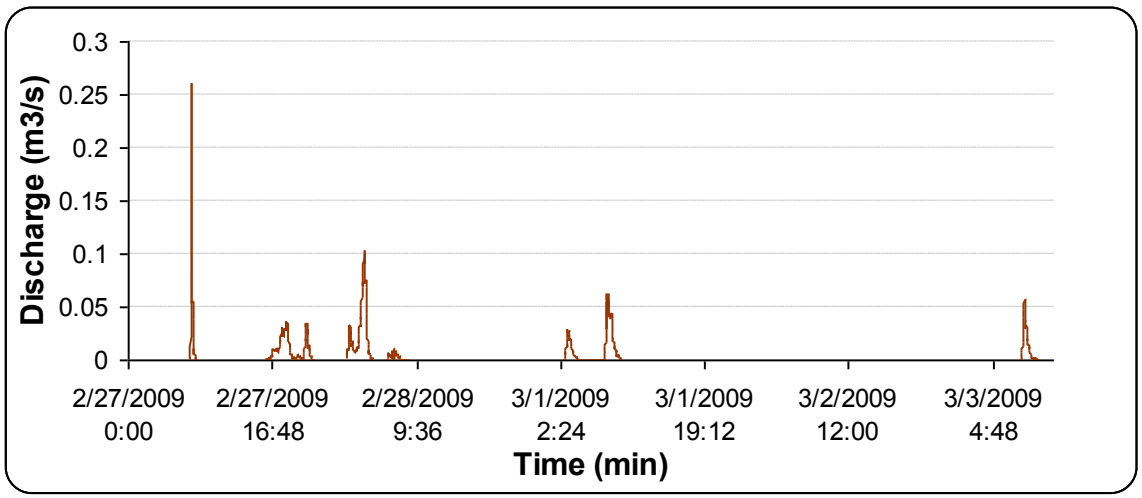

Fig. 5.25: All runoff events monitored in S4 during the rainstorm 27.02-03.03.2009.

The total runoff volumes measured in S4 during the second rainstorm (27th February-3rd of March 2009) is 943.9 m^3. The third and biggest runoff event occurred on the *23rd of March, 2009* in which a total volume of 399.8 m^3 was measured in S4. Figure 5.26 shows the hydrograph of this event, which lasted for over three hours during the night.

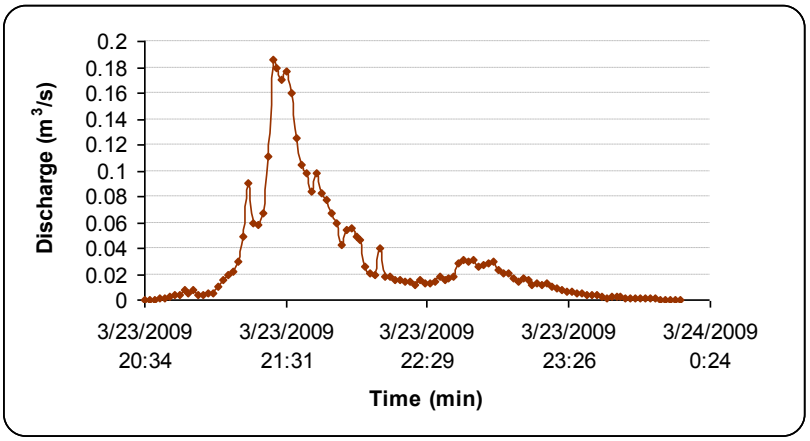

Fig. 5.26: Runoff event monitored in S4 during the big rainfall event in 23rd March 2009

After calculating runoff in both the entire catchment and subwadis, applying the numerical model, which was selected based on the model tool selection criteria explained in chapter three, is now possible. The model is needed in order to simulate the hydrological processes in Wadi Kafrein and to achieve the objectives of this research, which were discussed in chapter one.

Following is a description of the numerical model which has been used in this research. The runoff routines of the model will be discussed in more details due to their relevance to the aims of this research.

5.5 TRAIN-ZIN model description

TRAIN-ZIN is a hydrological model which consists of two models programmed and developed separately with different focuses and different temporal resolutions. The TRAIN model focuses on the vertical exchanges of water, with evapotranspiration as one of the principle mechanisms. The ZIN model is mainly focused on horizontal water fluxes and interactions, with emphasis on runoff generation mechanisms and the related transmission losses and routing processes.

5.5.1 TRAIN model

The **TRAIN** model is a physically-based, spatially distributed hydrological model. The model was initially developed by Menzel (1999) at the Federal Institute of Technology (ETH), Department of Geography, Zürich, Switzerland and further developments took place at The Potsdam Institute for Climate Impact Research (PIK), Germany. The model requires measurements which comprise quantitative and complete water and energy balances as well as information from comprehensive field studies, including information on natural vegetation and agricultural land (Menzel, 1997; Menzel et al., 2009).

The model has been designed to simulate the spatial pattern of the individual water budget components at different spatial and temporal resolution. Typical applications at the point and the regional scale are possible with temporal resolutions of one hour or one day. For an aerial simulation of the water budget, the investigated spatial unit is subdivided into regular grid with cell sizes depending on the spatial resolution of the input data. The model includes several routines (modules) and is focused on the processes involved in the Soil-Vegetation-Atmosphere interface with evapotranspiration being identified as one of the principal mechanisms. For the regionalization of the water balance components, specific local elements (topography, land-use, soils) and varying meteorological conditions are included in the calculation process (Menzel, 2007). Figure 5.27 illustrates the model input requirements in addition to the simulated processes and the related output data.

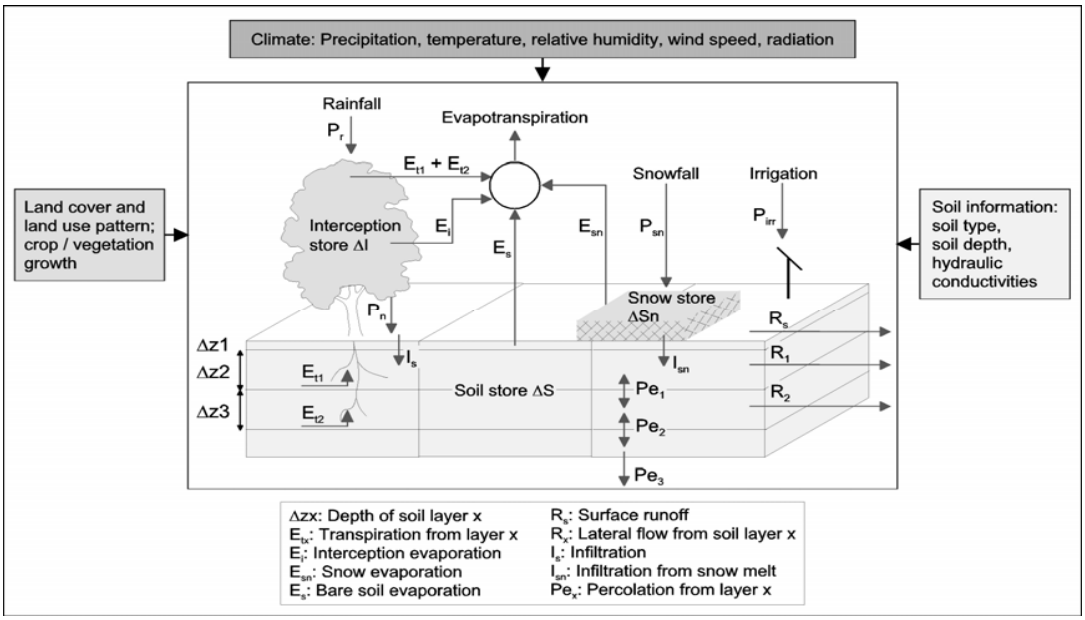

Fig. 5.27: Schematic diagram illustrating the TRAIN model input requirements, the simulated processes and the related output data (Menzel et al., 2007).

The transpiration process is simulated based on the Penman-Monteith equation (Monteith, 1965), which depends on the calculation of canopy resistances. Canopy resistances are modified by the state of growth of the vegetation, soil moisture status, as well as weather conditions (Menzel, 1996). The interception and interception-evaporation are simulated according to Menzel (1997). Interception-evaporation is modeled so as to occur with varying intensities, which are dependent on the actual amount of water accumulated in the canopy as well as the present weather conditions. The calculations of the soil water status and percolation follow a modified version of the conceptual approach from the HBV-model (Bergstreom, 1995). The simulated amounts of deep percolation and of infiltration excess (which leads to runoff) are aggregated for each pixel and termed "water availability," i.e., the amount of water theoretically disposable for certain uses (Menzel, 2009). The snow accumulation and snow melt schemes are based on simple, conceptual approaches, such as the degree-day equation. Melted snow is treated in the same way as rainfall for further calculation of infiltration/percolation.

5.5.2 ZIN model

The **ZIN** model is a physically based rainfall-runoff distributed model, which was initially developed to simulate high magnitude runoff events in arid regions. The initial version of ZIN was developed by Lange (1999) and subsequently applied, without any calibration with measured runoff values, to the arid region of Nahal Zin in the Negev desert. Model parameterization is based on the physical characteristics of the catchment area and on field measurements. Therefore, the parameters are required to be in high spatial resolution. To increase the efficiency of the model parameterization, the catchment area is divided into spatially homogenous sub-units in which the geomorphological characteristics of every sub-unit can be determined using satellite images, topographic maps, and field measurements.

The rainfall-runoff model of ZIN consists of three main routines and the spatially distributed model parameters are grouped according to spatial sub-unit based similarities. Rainfall is considered to be an input as it varies in space and time and depends on the characteristics of the storm event. A grid map of rainfall intensities is used in the model which can be acquired using radar data or measurements from rain gauge networks. The model and the related parameters are categorized spatially for every sub-unit as follow:

- **Runoff generation**: characterized by terrain types of the spatial sub-units.
- **Runoff concentration**: characterized by sub-tributaries.
- **Channel routing and transmission losses**: characterized by channel types.

The catchment area is sub-classified into several terrain types with different infiltration characteristics, which are defined as model parameters. These terrain types and their parameters determine the spatial sub-units for the **runoff generation** component. To simulate the **runoff concentration,** the stream (drainage) network of the catchment area is sub-aggregated into several channel segments. Every segment has an adjacent basin, and these basins and segments together are equal to the spatial sub-units of the entire catchment area. The channel segments used in the runoff concentration routine define the spatial sub-unit parameters for the **channel routing and transmission losses** routine.

The ZIN model aggregates the spatially homogenous sub-units independently to every sub-routine, which provides high accuracy and requires minimum spatial resolution. Figure 5.28 summarizes the sub-routine of the ZIN model, which includes different types of spatial subdivision.

Since this research emphasizes runoff generation and process mechanisms, the sub-routine of the ZIN model will be explained including the development of the model code which took place to enhance the model performance in simulating runoff in arid and semi arid regions. Later, the coupling process will be discussed with explanation of the changes on both coupled models.

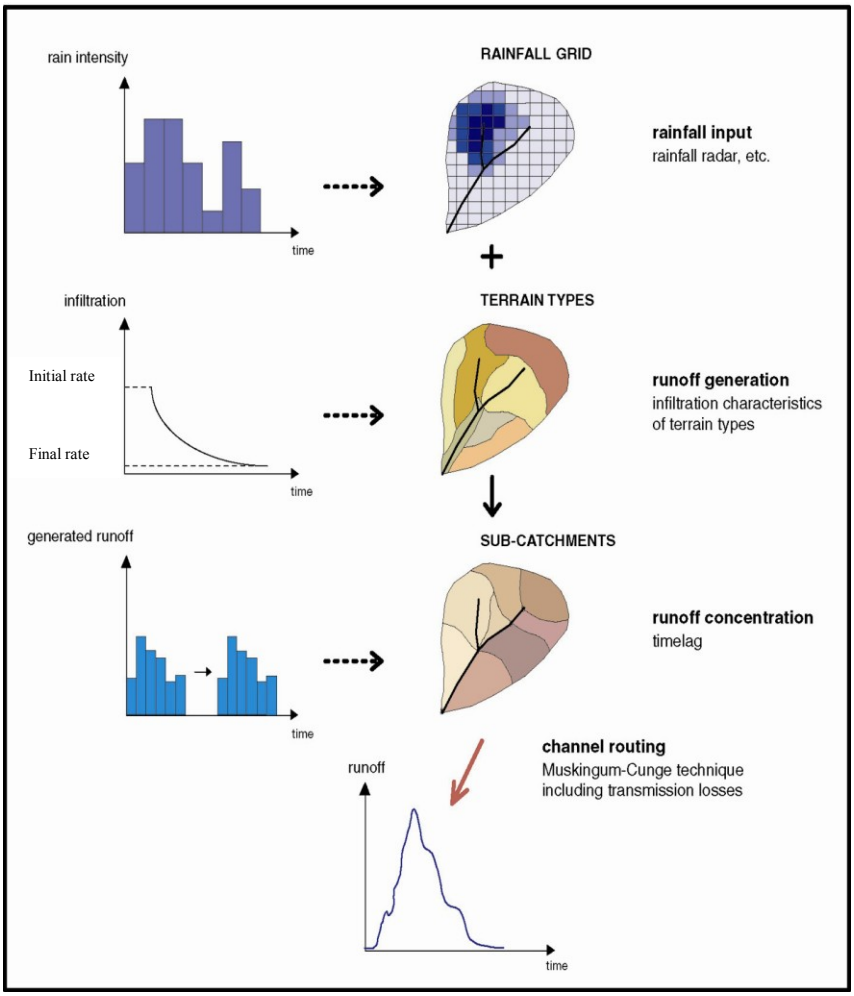

Fig. 5.28: Flowchart of the ZIN Model (Thormählen, 2003; modified from Lange, 1999).

5.5.2.1 Runoff generation

The runoff generation routine determines the amount of rainfall which is diverted to runoff. Considering Hortonian overland flow as the dominant runoff generation process in arid and semi arid regions; runoff will generate when the rainfall intensity exceeds the infiltration rate of the soil. The ZIN model calculates the generated runoff based on Horton (1933). Part of the rainfall will reach the surface as rain through and part of the rainfall will be lost due to interception by the vegetation cover; therefore initial losses are defined for every terrain (5.6.5.1) taking into consideration the soil type and the land cover. These losses present the difference between the initial infiltration rate and the final infiltration rate as shown in Fig. 5.28.

The temporal decay of the soil infiltration rate will determine the runoff generation. Rainfall amounts which are stored in the soil will either evaporate or percolate. The initial version of ZIN calculated the percolation as a constant value, later; the model code was modified by Scheutz (2006) who integrated the Van Genuchten (1980) equation to calculate the water amounts which percolate using a dynamic function.

5.5.2.2 Runoff concentration

Runoff concentration routine describes the transformation of the generated runoff at each model element to lateral flow into the adjacent channel. This can be done after dividing the channel network to segments which are adjoined by small sub-catchments (model elements) delineated based on catchment topography. The runoff amounts which are calculated from the runoff generation routine are summed up for each sub-catchment and each time step. The runoff concentration routine follows a conceptualization which is usually based on the unit hydrograph concept (Sherman, 1932). The ZIN model uses a mean response function of model elements consisting of a hydrologic time-lag and a standardized shape. The hydrograph shape does not change during the runoff concentration process but the lateral inflow to the channel is delayed.

5.5.2.3 Channel routing and transmission losses

When flood runoff hydrographs from an upstream catchment area enter the stream channel, they are propagated downstream as flood waves. The resulting unsteady flow means that flow characteristics like discharge, water level, velocity and the cross sectional area of flow at any point change with time. The non-uniform nature of the flow means that flow characteristics vary between different points along the stream channel.

In this routine of the ZIN model, the subdivision of the drainage network into channel segments delimited by channel nodes is predefined by the sub-catchments used to parameterize the runoff concentration. The *flow routing* is the procedure to determine the magnitude and timing of the flow at some point based on known or assumed values upstream. The flow is routed from node to node accounting for lateral inflow and transmission losses.

Flow routing in open channels is, in general, unsteady, gradually varied turbulent flow but may also involve rapidly varied flow at certain locations. It is governed by the laws of conservation of mass, momentum and energy which are expressed as continuity, momentum, and energy equations. The momentum and energy equations have the same form, except for correction factors and therefore only the momentum equation will be expressed here. Strictly speaking, flow routing is 3-dimensional in nature, primarily because of spatial heterogeneities and no uniformities in the horizontal and vertical planes. Therefore; the governing equations are also 3-dimensional. However, because of the lack of data on the spatial variability of roughness, sources and sinks, and initial and boundary conditions and the difficulties encountered in solving them, a one-dimensional form is often employed (Singh, 2004). The description of one-dimensional unsteady flow with a free surface is given by the de Saint Venant equations. The de Saint Venant equations consist of two equations: the Continuity and the Momentum equation.
The Continuity equation is given as (Kutija and O'Connel, 2000):

$$\frac{\partial \mathrm{Q}}{\partial \mathrm{x}} + b_s \frac{\partial h}{\partial t} = q_L \tag{5.7}$$

While the Momentum equation is given as:

$$\frac{\partial \mathrm{Q}}{\partial \mathrm{t}} + \frac{\partial}{\partial x}\left(\frac{\beta Q^2}{A}\right) + gA\frac{\partial h}{\partial x} - gAS_0 + gA\frac{Q|Q|}{K^2} = 0 \qquad (5.8)$$

Where:

x : space variable (m)
t : time variable (s)
h : water depth (m)
Q: discharge (m^3/s)
b_s: storage width (m)
Q : $K\sqrt{S_0}$
q_L : lateral flow ($m^3/s/m$)
A : cross-sectional area (m^2)
g : gravity acceleration (m/s^2)
S_0 : bottom slope
K : conveyance (m^3/s)
β : Boussinesq coefficient

These equations do not have analytical solutions; therefore, they are solved by a variety of numerical methods (Sleigh and Goodwill, 2000), of which the method of *finite differences* is the most commonly used. But due to their complexity, different types of approximations in the type of *Kinematic wave* and *Diffusive wave* approximations are used. The term *Dynamic wave* is used to refer for the full de Saint Venant Equations. These approximations use the continuity equation, while each of the approximations uses just a part of the momentum equation as follows:

$$\frac{\partial \mathrm{Q}}{\partial \mathrm{t}} + \frac{\partial}{\partial x}\left(\frac{\beta Q^2}{A}\right) + gA\frac{\partial h}{\partial x} - gAS_0 + gA\frac{Q|Q|}{K^2} = 0$$

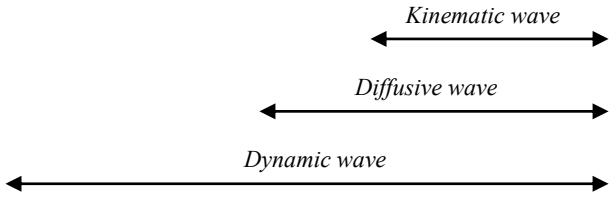

The Kinematic wave can only reproduce the effects of gravitational and frictional forces. Therefore, it is applicable to streams with significant bottom slope (>0.1%) and for the calculation of overland flow. The diffusive wave includes the effects of the pressure force so it is capable of including some deceleration effects. However, the lack of inertial forces means that it cannot completely capture backwater effects or reverse flows (Kutija and O'Connel, 2000).

The flow routing methods can be divided into two different types: the *hydraulic methods,* in which it is based on the de Saint Venant equations or its approximations, and the model solutions are provided in terms of space (distance x along the channel) as well as time (t). Such models are known as the *distributed* models. The second type is the *hydrological methods*. They are based on conservation of mass, the model solutions are provided in terms of time (t) only. Because the space is treated in a lumped manner, such methods are termed as *lumped.*

The full scale dynamic wave model (Saint Venant equations) is an example of the most sophisticated flood routing models, while the simplest is presented by the Muskingum model. It is the most frequently used model due to its simplicity and it has the following form (Tung and Asce, 1985; Brunner and Gorbrecht, 1991):

$$S_t = K\left[XI_t + (1-X)O_t\right] \tag{5.9}$$

Where:
S_t: absolute channel storage at time t
I_t and O_t: rates of inflow and outflow at time t, respectively
K: storage time constant for the river reach
X: weighting factor varying between 0 and 0.5

The finite difference formulation of equation (5.9) results in the Muskingum equation (Cunge, 1969; Weinmann and Laurenson, 1979):

$$Q_{j+1}^{n+1} = C_1 Q_j^n + C_2 Q_j^{n+1} + C_3 Q_{j+1}^n \tag{5.10}$$

With

$$C_1 = \frac{\frac{\Delta t}{K} + 2X}{F} \tag{5.11}$$

$$C_2 = \frac{\frac{\Delta t}{K} - 2X}{F} \tag{5.12}$$

$$C_3 = \frac{2(1-X) - \frac{\Delta t}{K}}{F} \tag{5.13}$$

$$F = \frac{\Delta t}{K} + 2(1-X) \tag{5.14}$$

Where:
n : time superscript
j : space subscript
Q : discharge
Δt : routing time increment of the difference cell

In the original Muskigum equation (5.9), the value of the storage coefficient "**K**" and the weighting factor "**X**" are determined by trial and error or by calibration with observed hydrographs (Miller and Cunge, 1975). In the approach of Muskigum-Cunge, the coefficients "**K**" and "**X**" are expressed in terms of flow, channel, and finite difference cell parameters (Cunge, 1969; Koussis, 1978; Weinmann and Lawrenson, 1979; Ponce and Theurer, 1982) as:

$$K = \frac{\Delta x}{c} \tag{5.15}$$

$$X = \frac{1}{2}\left(1 - \frac{q}{S_0 c \Delta x}\right) \tag{5.16}$$

Where:

Δx: space increment of the finite difference cell
c : representative flood flow celerity
q : representative unit width discharge
S_0 : channel bed slope

In the case of a wide channel, where the hydraulic radius approaches the flow depth, an approximation is given as follows:

$$c \approx 5/3v \tag{5.17}$$

Where:
v: flow velocity which can be obtained using a uniform flow formula like the Manning equation (equation 5.6).

To determine "**q**" in equation (5.16), different modes of the Muskingum-Cunge exist based on the selected "**q**" value. In the linear mode, a constant value with time of "**q**" is used; this means a constant routing parameter of "**K**" and "**X**" with time. The linear mode is not capable of predicting wave steeping. The non-linear mode calculates the unknown flow in each time step by extrapolating the available "**q**" values from previously computed time and distance steps. The non-liner mode is more accurate than the linear mode because the routing parameters are calculated in each time step taking into consideration the different discharges at different celerities. The ZIN model uses the non-linear MVPMC3 method given by Ponce and Chaganti (1994) as:

$$q = \frac{Q_j^n + Q_j^{n+1} + Q_{j+1}^n}{3} \tag{5.18}$$

In the original version of the ZIN model, a constant infiltration rate was assigned to each channel segment in order to estimate the transmission losses. It was considered that only the inner channels out of all channel widths are active during flood events. Because the geometry of a channel is complicated, as it composed of inner channels as well as bars and banks, the model simplified the channel geometry by linear interpolation between the width covered by inner channels and the width at bankfull stage (Fig. 5.29). Only at bankfull stage is the complete cross section (including the inner channels and all bars) inundated (Lange, 1999). The simplified approach of losses due to infiltration to inner channels has been replaced by Leistert (2005) by integrating the Green-Ampt infiltration model (Green and Ampt, 1911). The Green-Ampt infiltration scheme gained considerable attention partially due to the ever growing trend of the physically-based hydrological modelling (Philipp, 1983). For a better spatial resolution, the channel cross-section profile (flood plain) was divided to two sections presenting two individual storages. One section comprises the bars and the banks that form the transition from inner channel to the second section, the flood plains. The Green-Ampt approach is applied to the inner channel section while an empirical approach based on single linear storage is used to calculate the infiltration into the floodplains. For inner channels, the infiltration depends on the variable flooded area of each segment and on the time of the beginning of the event. The flooded area for each time step is calculated as a result of constant segment length and the variable segment width. For each time step, the transmission losses are computed by multiplying the area by the infiltration rate as follows:

$$TL = \Delta t A(k_b - k_f)\exp\left(\frac{-t}{k_b + bv}\right) \quad (5.19)$$

Where:
TL: transmission loss
Δt : time step
A : area
k_b : initial infiltration rate (bars, banks and floodplain)
k_f : hydraulic conductivity (underlying strata)
bv : flooded width

The linear approximation of the flooded area in the ZIN model has been also replaced by Leistert (2005) with two composite power functions. The expansion of the flooded area has been approximated with a slow growing function, but this does not reflect the real cross-sectional geometry. The floodplains are often huge and smooth, and a small rise in the water level can cause a flooding of large areas; therefore a fast growing function in addition to the slow growing function are used to simulate the flooded area.

The entire channel width was divided into three sections as shown in Fig. (5.30), in which the first section, '**A,**' represents the inner channel. This section is assumed to become flooded immediately and completely. The second section, '**B,**' represents the bars and the banks with steep incline; and the third section, '**C,**' represents the entire floodplain area. Transmission losses into over-bank areas are simulated using equation (5.19) with the difference that from bank and bar infiltration has time starting when the water depth exceeds a certain height. Consequently, infiltration takes place when the over-bank areas are flooded.

The flooded area of the inner section '**A**' is simulated as:

$$bv = bc.v \quad (5.20)$$

Where:
bv: flooded area
bc: maximum channel width
v : percentage of inner channel maximum width

While in the bars and banks section, '**B**,' the flooded area is simulated as:

$$bv_1 = bc.v\left(1 + H^x\right) \quad (5.21)$$

Where:
bv_1: variable channel for section B
H : water depth
x : constant which determines the inclination of bars and banks function (bv_1)

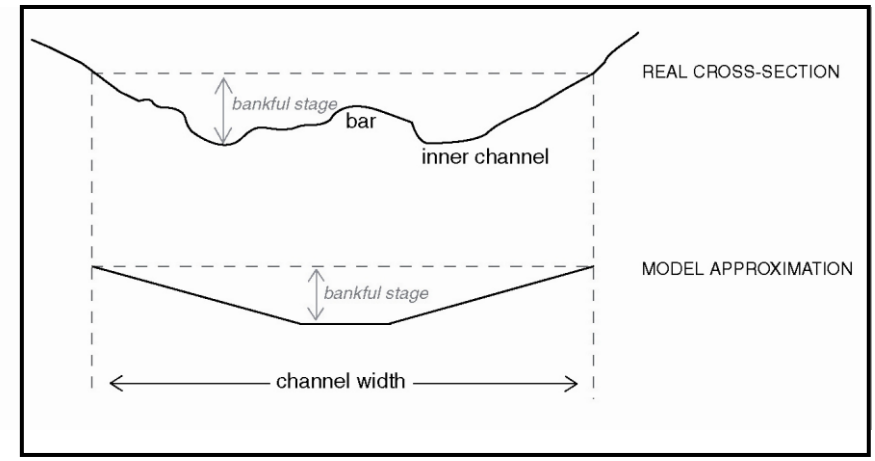

Fig. 5.29: Simplified representation of cross-sectional channel geometry (Lange, 1999).

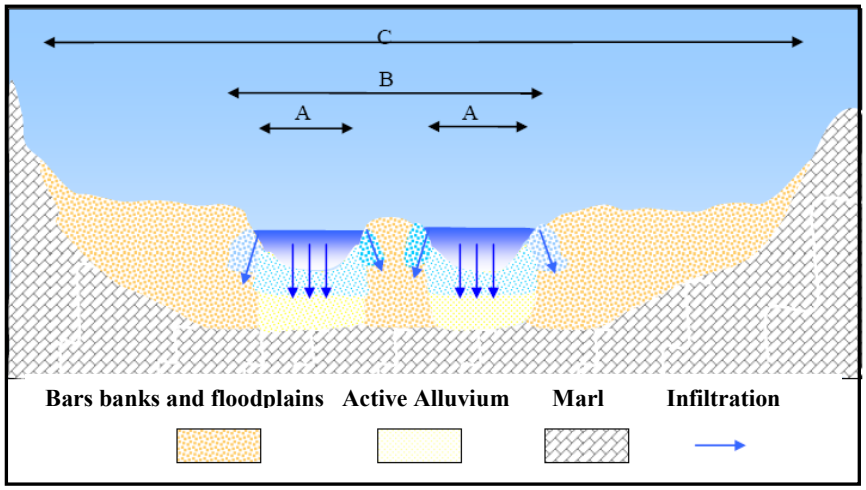

Fig. 5.30: Schematic representation of cross sectional channel geometry after modification (modified from Leistert, 2005).

For the third section '**C**' the growth of the flooded area is simulated as:

$$bv_2 = \sqrt[d]{\left(\frac{H - f_a}{f_b}\right)} \tag{5.22}$$

Where:
bv_2: variable water width for section C
d: a constant which determines the inclination of the floodplain function (bv_2)
f_a and f_b: functions to fulfill the criterion of continuity (equations 5.21 and 5.22)
With:

$$f_a = Hf - f_b.bc^d \tag{5.23}$$

And;

$$f_b = \frac{Hf - \sqrt[x]{y}}{bc^d\left(1 - \left((1+y)v\right)^d\right)} \tag{5.24}$$

Where:
Hf: water depth where maximum segment width is over-flooded
y : relative fraction of bars and banks of total inner channel width

5.5.3 TRAIN-ZIN

One may notice from the earlier discussion of both models that the TRAIN model simulates long term fluxes of the individual water budget components with special focus on the vertical exchange of water at the soil-vegetation-atmosphere interface (Menzel et al., 2009). The ZIN model, on the other hand, simulates short term horizontal water flux and losses. The TRAIN model is considered to be an ideal supplement to the ZIN model which together can provide a powerful physically based hydrological model, which is able to simulate the hydrological processes in arid and semi arid areas with high accuracy and different spatial and temporal scales.

The idea of coupling the two models was initiated within the GLOWA Jordan River project and a coupled model was first released by Gunkel (2006) as the TRAIN-ZIN model. Both models, in their initial versions, include a soil storage routine which was used for dynamic coupling with a flexible time step. This flexible time step is adapted to periods of rain and no-rain (Fig. 5.31). During times of rain, the runoff generation routine of the ZIN model is active, describing the filling of the soil storage and the overland flow generation (IEOF and SEOF). Also, the runoff concentration and runoff routing routine are also activated and are conducted using a relatively high time step on the order of minutes. Meanwhile, concerning the activation of the ZIN routines during rain, certain modules of the TRAIN model are deactivated such as the evapotranspiration routine, which is negligible during the rainfall. During the time of no rain, the soil routine of TRAIN is active and the evapotranspiration process is simulated. Considering the soil storage emptying by evaporation and percolation during the no-rain period is very important to simulate the next rainfall event because this constitutes the antecedent soil storage (GLOWA, 2006).

The evapotranspiration process is simulated by TRAIN using a one hour time step, which is very sufficient when referring to the temporal resolution. This is contrary to the runoff generation processes, which are required in a high temporal resolution and are simulated by the ZIN model. The fact that TRAIN provides the missing long term soil moisture reduction terms to ZIN makes it possible to simulate the runoff generation processes in a continuous mode; similarly the runoff generation, concentration, and routing routine of ZIN provide additional hydrological components to TRAIN. The final result of this coupling process is a two-dimensional model which accounts for lateral fluxes and spatial concentration of water resources.

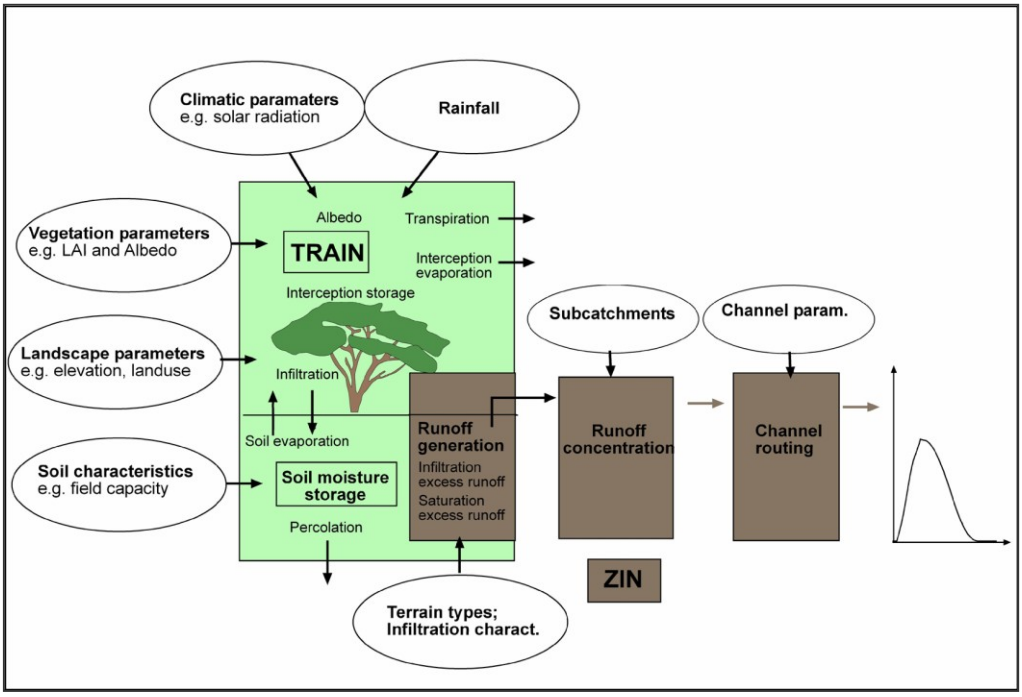

Fig. 5.31: The TRAIN-ZIN Coupling (Gunkel, 2006).

A tight coupling of both models was achieved without a direct link through an iterative solution. In fact, the models do not run in parallel rather successively. The process can be summarized as follows: the rainfall is first simulated by TRAIN and the values are passed to ZIN which in its turn starts its own calculations using shorter time steps. The daily evaporation calculations are converted to values for ZIN time steps considering the hourly radiation and rainfall, while the simulated soil moisture contents by TRAIN is passed-on to ZIN as initial soil moisture to be used in ZIN calculations. This process ensures a feedback and exchange between the two models in a real time (Fisher, 2007).

Since the coupled model was released, several successful applications were documented. These applications included hydrological modelling of a micro-scale (1.1 km^2) Mediterranean catchment by Scheutz (2006), a meso-scale (170 km^2) semi arid catchment by Fischer (2007) and another meso-scale (320 km^2) semi arid catchment by Shadeed (2008). The model is continuously enhanced and upgraded in the Institute of Hydrology of Freiburg University in Germany, to simulate the hydrological processes in arid and semi arid regions with high spatial and temporal resolutions.

5.6 Model construction

It has been justified in chapter three why a physically based model is the best in simulating hydrological processes in Wadi Kafrein. The needed data for hydrological modelling has been acquired and discussed in chapter four. In the previous section of this chapter, the physical basis for the selected TRAIN-ZIN model had been explained. Therefore, the next step is to construct the hydrological model of Wadi Kafrein, using the acquired data to fit the selected model. *Model construction* is the

process of data preparation in the right format and entering these data as a set of input files which can be recognized by the model code. Model construction process consists of several steps: it includes the definition of *model grid*, *modelling time steps,* and the *initial conditions* of the model. Model construction also includes the preparation of *model time series* data: model parameter values *(Parameterization)* and model spatial data are also known as *spatial discretization* of the catchment. Model construction is a preparatory step for model calibration. Therefore, an explanation of these steps is given below.

5.6.1 Initial condition and modelling boundary

To setup the *initial condition* of the model, the water year was simulated by starting from the first rainfall day and considering no antecedent soil moisture before the rainy season and ending at the beginning of the next water year. In catchment areas like Wadi Kafrein, rainfall is limited to winter months that are from October until April of the following year. During the summer months, high temperatures are observed in Wadi Kafrein. Therefore, the stored water in soil after the rainfall season is removed by evaporation or is percolated, leading to a dry soil layer by the end of the water year and the start of the next water year. The *modelling boundary* is identified as the surface catchment area of Wadi Kafrein over which flow occurs and which ultimately arrives at the reservoir behind the Kafrein dam.

5.6.2 Defining the model grid

As a spatially distributed model, TRAIN-ZIN requires the specification of an appropriate grid or mesh, which subdivides the model space into a finite number of regions. For a *finite-difference model*, these regions take usually the form of grid squares or rectangles. The TRAIN-ZIN model requires the following grid maps to simulate the different hydrological processes:

1. **Terrain types** grid map (runoff generation routine), see section 5.6.5.1
2. **Sub-catchments** grid map (runoff concentration routine), see section 5.6.5.2
3. **DEM** grid map (evapotranspiration routine), see section 4.2.1.3
4. **Land use** grid map (evapotranspiration routine), see section 4.2.2.3
5. **Climatic parameters** grid maps (humidity, radiation, temperature, and wind speed), see section 5.6.6.1

All grids given in the model input files must have a specific scale. This scale is determined by the user and it usually depends on the model type and the aim of the modelling process. By defining a very fine scale, the time required to run the model will increase because computing time depends on the total number of grid cells within every grid map. Possibly, one may discretize the fine DEM prepared in this research to 5m x 5m cell grid but this will produce around 6.5 million cells which require tremendous computing power from the computer due to lengthy calculations for each

consecutive run as well as requiring much electrical power for the computer. For a macro scale catchment like Wadi Kafrein, suitable is to have a grid cell size of 50m x 50m, which maintains the spatial distribution of the model physical structure, saves a lot of time, and reduces the required power recourses.

5.6.3 Modelling time step

The TRAIN-ZIN model has built-in time step calculations, which limit the size of the time step by taking stability and accuracy criteria into consideration. The TRAIN routines require the climatic data on a daily basis level and for accuracy criteria, radiation data on an hourly basis level is required. On the other hand, ZIN requires a higher temporal resolution. Two time steps are required to be specified in the ZIN model:

- **ZIN Step**: the ZIN-Model time step, in minutes, which was set to 5 minutes.
- **Route step**: the length of the routing time step, in minutes, which was set to one minute.

5.6.4 Time series data

For hydrological modelling, four types of data are required, as explained in chapter 4 (section 4.1); data can be: structural, time series, physical properties, and observed data. To run the model, two time series data are required:

- **Rainfall data** time series: prepared as a five minutes time step
- **Radiation data** time series: prepared as an hourly time step

Both data time series are prepared in a tabulated format and provided to the model. These time series are necessary to run the model and present a *forcing data* for the model. Other time series data are required to calibrate and validate the results of the model; these *calibration/validation data* were prepared as explained in section 5.4.3 of this chapter.

5.6.5 Spatial disaggregation

It has been explained in section 5.5.3 that TRAIN-ZIN does not run in parallel but in a successive way which means that every model makes its own calculations and through the coupling approach a real time data exchange takes place. Based on this approach, TRAIN requires land cover and soil grid maps to set the evapotranspiration routine parameters in addition to the climatic parameters measured from the two weather stations (section 4.3.2). No further disaggregation is required by the TRAIN model to simulate the evapotranspiration processes. For ZIN, the model space of the catchment is required to be discretized to sub-units to parameterize the three model routines explained in section 5.5.2. The spatial disaggregation for every routine is given in the following paragraphs.

5.6.5.1 Spatial disaggregation for runoff generation

In this step of the model construction, the entire catchment area of Wadi Kafrein was divided to several sub-units (what is defined for this routine as *terrain types*) based on soil and land cover characteristics of the catchment. The developed soil map and land cover described in chapter four were used here to define the sub-units of the runoff generation routine. This yielded eight different terrain types as shown in Fig. (5.32).

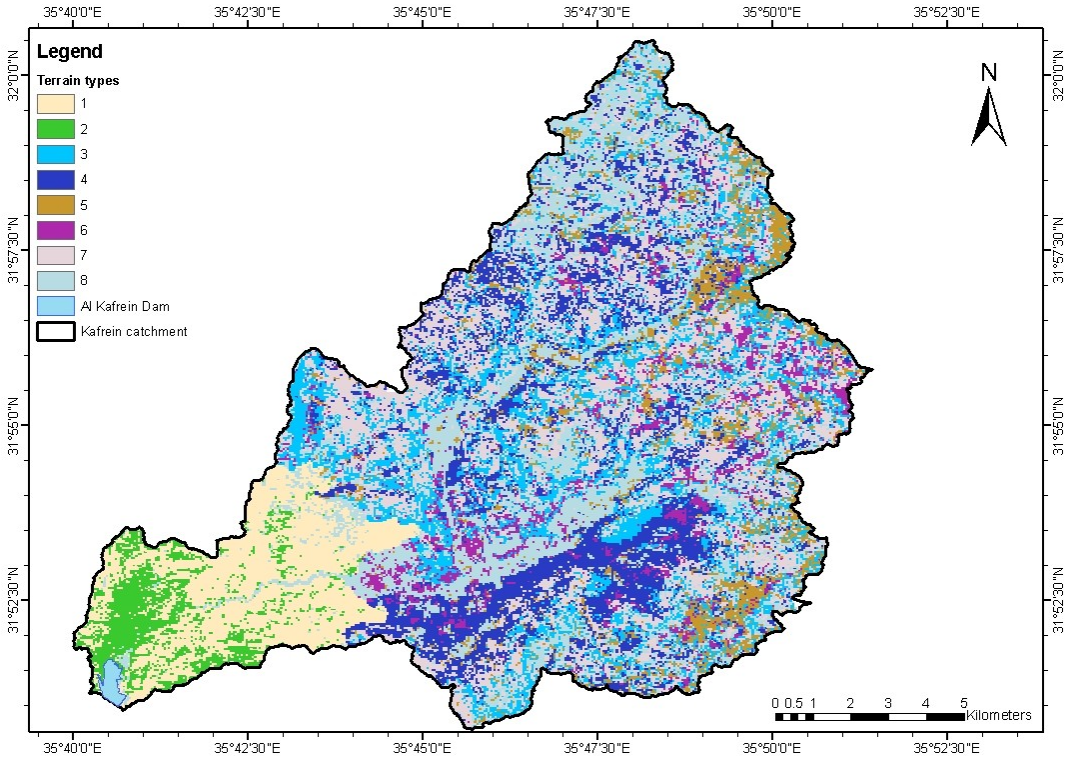

Fig.5.32: Sub-units (terrain types) for runoff generation parameterization.

The aim of dividing the catchment area to several terrain types is to prepare a runoff generation map. This map is discretized spatially to grids with similar spatial distribution defined in the model grid. Every grid cell is assigned a special number based on the terrain type which is similar to every sub-unit. The properties of every grid represented by its soil characteristics is given in a tabular way in which the model code is able to read and so runoff generation routine calculations can be performed.

Every terrain type has specific surface characteristics:
Terrains 1 and 2 represent the sub-units which are characterized as having no vegetation and as having clear outcropping of the bare rock of Ajlun group geological formations. They differ from each other by the soil characteristics of the thin soil layer covering them, when present, and by the steepness of the terrain, which plays an important role in the runoff generation process. These two terrains have the potential for generating runoff over their surfaces.

Terrain 3 is characterized by its sharp steepness; it covers a wide part of subwadi S4 and other parts in the middle and south of the study area. Terrain 3 also includes some areas without any vegetation (mainly subwadi S4). It is covered by grass and olive trees, but the grass cover is limited temporally to a short period during the winter

months. This terrain can also be a potential source for generating runoff due to sharp slopes and low vegetation cover.

Terrain 4 is represented by the outcrops of the Kurnub sandstone group and has low slopes. When vegetation is available, terrain 4 may also have either rain fed agriculture or tree crops.

Terrain 5 represents the urbanized area in Wadi Kafrein and is approximately 7% of the total area. This terrain is mainly impervious surfaces, which are buildings and road network; nevertheless, a part of this terrain can be pervious, e.g., unpaved parking places and the gardens within urban areas. This terrain is considered as a potential surface for runoff generation.

Terrain 6 is represented by areas of high plateaus and terrace remnants and it has low to moderate slopes. Its surface is used mainly for agricultural activities and olive trees plantations. The characteristics of this terrain make this terrain a poor source for runoff generation.

Terrain 7 is represented by a highly fractured and stony colluvium and covers the high convex ridges. The cultivated land cover surface includes mostly agriculture and olive trees, which are on areas where terraces are constructed; therefore this terrain is not a promising terrain for runoff generation.

Terrain 8 is found in the valley floor. This terrain has moderate to deep colluvium and is not expected to generate much runoff. Rather, this terrain is of considerable importance concerning transmission losses. The main featured characteristics of the different terrain types are summarized in Table 5.6.

Table 5.6: Terrain types of Wadi Kafrein.

Terrain ID	Associated soil units	Slope in degree /steepness	Elevation	Land cover	rainfall amounts
1	80-81	5-90 / medium to very steep	-140 to 300	Bare rocks /alluvium and Wadi sediments	150-250
2	82-83-84	0-20 / low	-140 to 300	Bare rocks /Wadi Es Sir L.S and F-H-S	150-250
3	17	20-75 / steep to very steep	300-950	Grass land and olive trees	250-500
4	7	0-20/ low	350-1030	Rain fed, tree crops and sparse vegetation	300-500
5	1	0-14/ low	750-1000	Urban areas	400-550
6	10-12	0-15 / low	100-950	Irrigated agriculture and olive trees	200-500
7	23-24	5-15 / low	450-1000	Forest, agriculture and olive trees	300-500
8	2	7-18/ low	150-950	Irrigated field crops-shrubs /natural forests	225-500

5.6.5.2 Spatial disaggregation for runoff concentration

The spatial concentration of runoff is controlled by the morphological characteristics of the catchment area. The highly accurate stream network, which was prepared using the 5m x 5m DEM, was used to disaggregate the catchment area into sub-catchments. The channel network was disaggregated into several segments, taking into

consideration the major junctions where the channel nodes were placed. The acquired Google Earth® image and the developed high accuracy DEM were used in the background of the main channel network for placing the channel nodes.

Every segment which was defined by an upper and lower node has an adjacent basin (defined for this routine as *sub-catchments)*. All these sub-catchments present the spatial sub-units of the runoff concentration routine (Fig. 5.33). To calculate the distance between the segment nodes, the *Cournant Condition* for explicit numerical solution schemes of the Saint-Venant equations for open channel flow was used (Cournat and Friedrichs, 1948):

$$\Delta t \leq \Delta x / v_k \qquad (5.25)$$

Where:
Δt : time step (routing time step)
Δx: distance step (presents the length of the channel segment)
v_k : kinematic wave celerity (denoted as "c" in equation 5.16)

If the *Cournat Condition* is not satisfied, this will result in a water accumulation (Chow et al., 1988). The time step, "**Δt,**" has been defined as one minute as given in routing time step in section 5.6.3. A measured value of maximum flood velocity, "**v_k,**" for Wadi Kafrein is not available; therefore, a value must be given based on measured values of similar catchments from earlier studies.

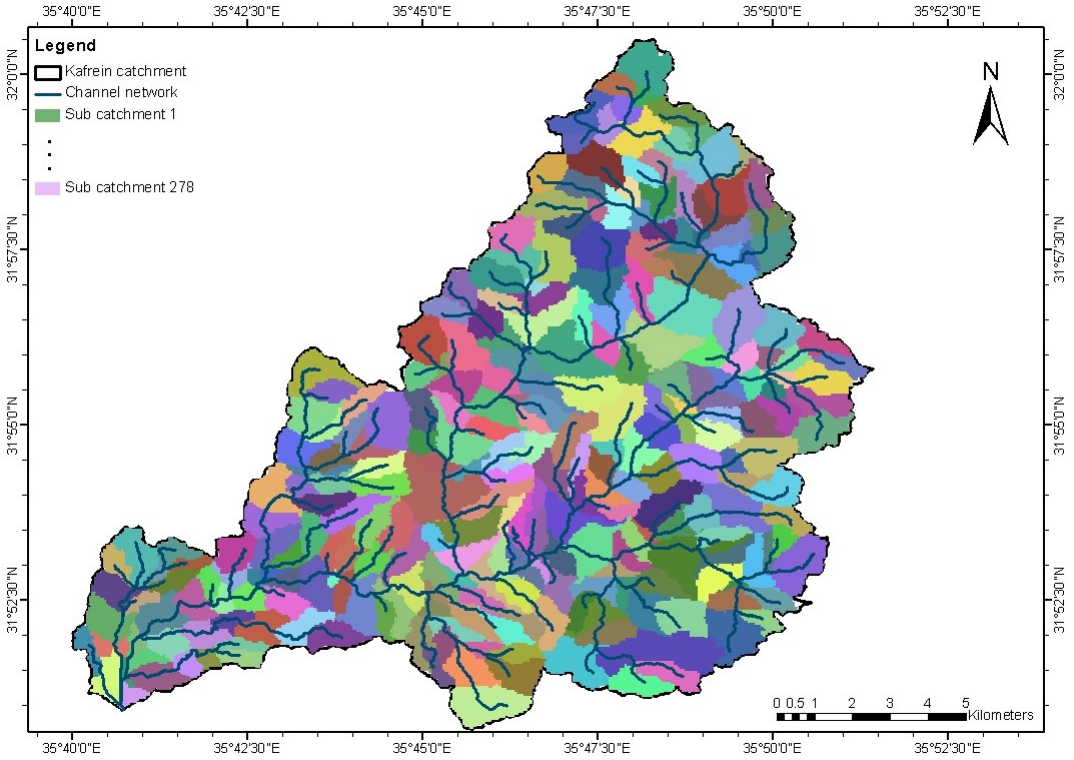

Fig.5.33: Sub units (sub-catchments/tributaries) for runoff concentration parameterization.

It was reported by the Central Water Authority of Jordan (1966) that a surface flow velocity of 5 m/s in Wadi Yutum occurred during the big flood event of November 1966. Similar velocities were observed during the November 1972 flood in Wadi Watir, southeastern Sinai, Egypt (Baker et al., 1988). The resulting peak flows of

November 1966 flood ranged from 325 to 540 m^3/s in several catchments ranging in area between 170 and 500 km^2 (Schick, 1971).

In the absence of a measured value in Wadi Kafrein for the kinematic wave celerity, the value measured by the Central Water Authority of Jordan was used here. Based on equations (5.17 and 5.25), a lower boundary of channel segment length, "**Δx**," was assigned as being 500 m. An ArcGIS environment (which includes the Google Earth® images and the DEM as explained earlier) was used to delineate the channel network of Wadi Kafrein, considering the Cournat boundary to calculate the distance steps between the single channel nodes. This resulted in 278 channel segments with 839 m as an average length. As explained earlier, every channel segment has a sub-catchment (sub-tributaries) contributing to the channel segment from both sides. The average area of these sub-catchments is 0.58 km^2.

5.6.5.3 Spatial disaggregation for channel flow and transmission losses

The generated 278 segments from channel network delineation for runoff concentration are used here as the sub-units (defined for this routine as *channel types*) for channel flow and transmission losses routine. This routine is controlled by twelve different parameters, which are required to be given for every single segment. Consequently, a total of 3,336 different parameter values are to be determined.

A practical solution to parameterize this routine is to classify the segmented channels to several channel types, which will reduce the required number of parameter values. Nevertheless, there are several classification systems, which are based on macrophytes (Holmes, 1989), invertebrates and fish (Furse et al., 1984), recreational potential (Zachman, 1984), stability characteristics for engineering works (Simons, 1978), or a combination of disciplines (Otto and Braukman, 1984). These differently based classification systems may produce entirely different groupings. Furthermore, the geomorphic characteristics of fluvial systems in the study area influence the resultant classification (Kondolf and Piegay, 2003). Even in the same study area, the channel network undergoes profound changes along the channel length; therefore, the classification system must either limit itself to homogenous sections of the channel (Rosgen, 1994; Montgomery and Buffington, 1997; Montgomery et al., 1998) or to a system which addresses the nature of longitudinal change as a basis for classifying different regions (Frissel et al., 1986; Montgomery, 1999).

To simulate the channel flow and transmission losses using the routing routine explained earlier, most convenient is to use a channel classification based on similarities in morphological characteristics. Montgomery and Buffington (1997, 1998) proposed a hierarchical valley segment and reach level classification of mountain channel networks based on morphologic attributes related to relative sediment supply and the ratio of sediment supply to transport capacity.

In the catchment area of Wadi Kafrein, observations have clearly indicated that a variation in channel morphological characteristics exists with channel length. The classification system used in this research is based on the following criteria: channel width, gradient, and sub-catchment land cover. The developed DEM, slope map, and the acquired Google Earth® images were all integrated within GIS and the channels were classified accordingly. As some channel segment characteristics are not easy to

be determined, effective field observations were highly valued. Following this approach the 278 channel segments were grouped to four channel types. Their spatial distribution is given in Fig. 5.34 while channel type characteristics are given in Table 5.7.

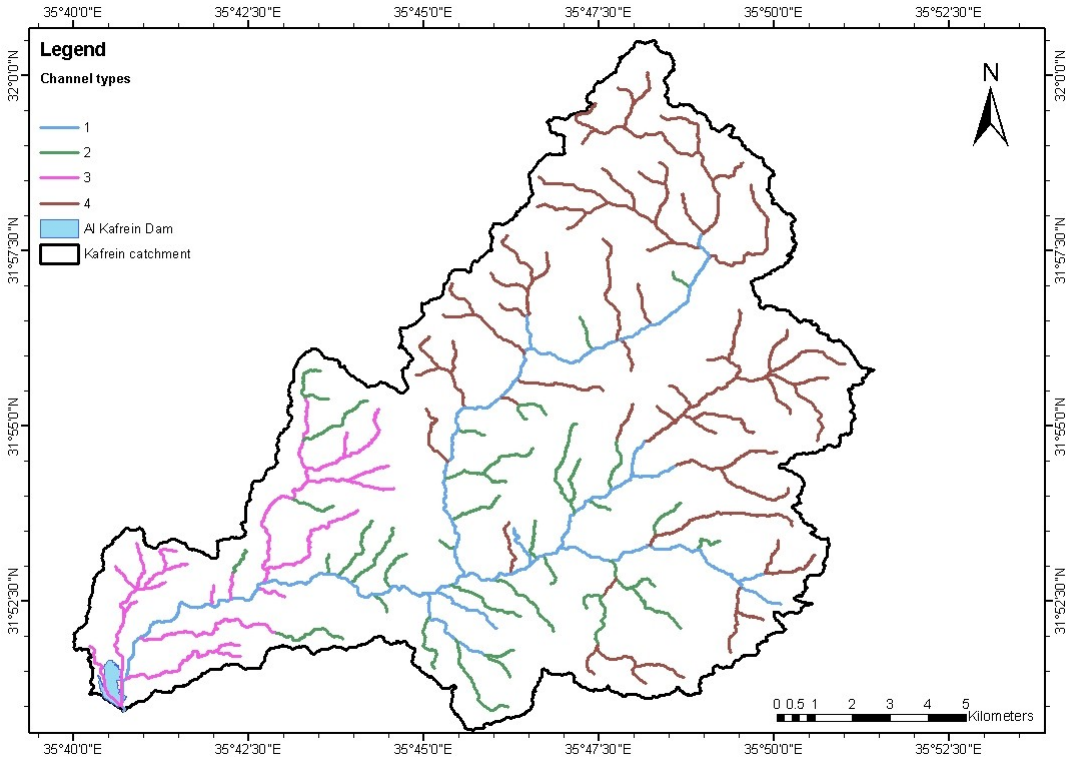

Fig.5.34: Sub-units (channel types) for channel flow and transmission losses parameterization.

Segments of channel type 4 are distributed in the upper part of the area and run through agricultural fields, which are considered as a source of fine sediments. Segments of channel type 3 are distributed over areas where no vegetation and a thin soil layer are found; due to its sub-catchment cover, the channels are able to transport coarse and rubble sediments during flood events.

Table 5.7: Channel types characterizes.

Channel ID	Width (m)	Gradient (%)	Sub-catchment cover	Occurrence
1	5-43	2-25	Dense vegetation on channel sides, field crops and agriculture in upper part of channel network	Represent the main channel network and the spring flow channels
2	1.5-12	20-46	Mainly through bare rocks and soil slopes, sparse to no vegetation cover	Middle and lower part
3	1.6-12	0.5-16	Limestone and thin layers of soil with low rainfall amounts and no vegetation cover	Lower western part
4	1.1-14	2-18	Agriculture and urban areas	Northern and eastern part of the catchment

Channel type 1: channels of this type are characterized as being wide with braided channels and having eroding banks; they have an average width of 17.7 m. These channels are optimal for transporting sediment textures ranging from coarse gravel to cobbles. Sediments are bed loaded with side and middle bars. Islands form central bars during flood flows. Channels of this type have a gentle slope ranging from 2-25% with an average of 7%.

Channel type 2: characterized by steep slopes (V notched) and high energy and debris transport. Average slope of these channels was found to be 21%. They have a narrow width ranging from 1.5-12 m and an average of 5 m. They are not braided rather having only one defined main channel.

Channel type 3: these channels have low gradients. The sub-catchments of these channels lack any vegetation cover and have pronounced rocky outcroppings. They have one main channel with low width to depth ratio. Channels of this type are capable of transporting coarse sediments during flood events.

Channel type 4: these channels have narrow to medium width with stable banks and no vegetation within their floodplain; they are optimal for transporting relatively fine suspended sediments coming from their sub-catchments, which are mostly used for agricultural activities.

5.6.6 Model parameterization

After the spatial disaggregation of TRAIN-ZIN model grids, it is required now to give values for the parameters of every routine grid (sub-units in case of ZIN routines). This is explained in more detail in the next four sections. In a distributed model like TRAIN-ZIN, the spatial variations in catchment characteristics and input data are described in a network of grid cells. Every grid cell of the mesh or grid maps described in section 5.6.2 is characterized by one or more parameters. This process of defining the spatial pattern of parameter values is known as *parameterization*. These parameters can be classified to two groups as follows:

- **Physically based parameters:** parameters of this group have physical properties which can be measured in the field. Examples of these parameters are: the soil depth, soil infiltration rate, and channel lengths and widths.

- **Empirical parameters:** parameter values of this group are estimated by the calibration process of the model. Examples of parameters belonging to this group are: parameters of Fisher-Tippet distribution (see section 5.6.6.3) and the Manning coefficient.

5.6.6.1 Parameterization of evapotranspiration

Evapotranspiration is simulated by TRAIN and requires as an input rainfall and climatic data together with soil and land cover maps, which are provided in a grid format (section 5.6.2). All rainfall data measured during the study period were prepared in five minutes time step; actually, this high temporal resolution is important and realistic to simulate the infiltration excess runoff in the ZIN model with high accuracy. The rainfall time step determines the ZIN time step, which determines the

longest possible routing time step. The point measurements acquired from rain gauge network discussed in section 4.3 are required to be presented in a spatial way. Several methods are available for this purpose; among others, the TRAIN-ZIN gives the possibility to generate the spatial distribution of rainfall using one of the following well known methods: the *Thiessen Polygons* and the *Inverse Distance Weighting*.
The Thiessen Polygons method is based on the assumption that the station best represents the area which is closest to it. In mountainous areas, orographic effects can create vastly different microclimates over small distances. Significant precipitation can fall on one side of a ridge but little on the other. In such regions the Thiessen method can yield erroneous results and the earlier mentioned assumption is not valid (Linsley and Franzini, 1979; Fetter, 2001).

The other method of weighting rain gauge measurements is the inverse distance method, in which the influence of the rainfall at a gauged point on the computation of rainfall at an ungauged point is inversely proportional to the distance between the two points (Wei and McGuiness, 1973). In the TRAIN-ZIN model, the weighted rainfall value for every grid cell can be calculated using the inverse distance weighting method:

$$P(x,y) = a.\sum_i \frac{P_i}{d^2} \tag{5.26}$$

With:

$$a = \frac{1}{\sum_i \frac{1}{d^2}} \tag{5.27}$$

Where:
P (x,y): I precipitation value at grid cell (x,y)
P_i: precipitation value at gauge station i
d: distance between grid cell (x,y) and the gauging station i

In this research, the rainfall data has been provided in 5 minutes time interval and was interpolated for every grid cell using the Inverse Distance Weighting (IDW) method. For better interpolation results, an elevation correction factor has been introduced by Hagenlocher and Gunkel (2008) and used in the interpolation. The high resolution Digital Elevation Model prepared in this research was used in the interpolation approach. This has been done because stations are on different elevations and there is a precipitation gradient with elevation change. The station on the lowest elevation has been taken as a reference station. The measured precipitation values at P_{Stat} (at elevation h_{Stat}) of all stations are reduced to precipitation P_{ref} at a reference level h_{ref}:

$$P_{ref} = \frac{P_{stat}}{1 - grad.(h_{stat} - h_{ref})} \tag{5.28}$$

After the application of the IDW, the same gradient is being used to calculate the precipitation value P_j at the elevation of the DEM at each cell:

$$P_j = P_{ref}.(1 + grad.(h_j - h_{ref})) \tag{5.29}$$

The density of the rain gauge network, in addition to the geographic location and elevation of the stations, has a direct impact on the interpolated area rainfall amount, which in turn affects the results of a hydrological model. By using all available rain gauges for this research (section 4.3.1), an area rainfall amount of 167 mm for the hydrological year 2007/2008 was obtained while using two distant stations (R1 and R4); an increase in the interpolated value of 12.3% was obtained. For the next hydrological year 2008/2009 the variations of the interpolated values were up to 16% (Alkhoury et al., 2010a). Such an increase in the interpolated values will cause an overestimation of the precipitated rainfall amount, which consequently will affect the value of ground water recharge and evapotranspiration leading to wrong results.

Regarding the climatic grids, they were prepared by interpolating the measured climatic parameters between the two weather stations; this gives a high accuracy and a physically sound basis for the modelling process, as this takes into consideration the effect of spatial variations over the catchment area. The simulation period of this research extended from November 15th, 2007 until December 23rd, 2009 with a total number of 770 simulated days. For every simulated day, four climatic grid maps were prepared (humidity, radiation, temperature, and wind speed) yielding a total number of 3070 grid maps. In case there is only one weather station or if a user wants to save the time of calculations, TRAIN-ZIN can also simulate the different hydrological processes by having the climatic parameters in a tabular format; i.e., one value of every variable for every day. Nevertheless, considering an interpolated value between the two stations by assigning one value for every grid cell is more accurate than considering one value for the whole catchment area. One last file is required that is the radiation data, they were prepared in hourly basis in a tabular format.

5.6.6.2 Parameterization of runoff generation

The spatial disaggregation of runoff generation routine resulted in eight different terrain types as explained earlier. For each terrain, the parameter values are the same. Nine parameters are required to be given for each terrain type, resulting in 72 values. The parameters of this routine depends on the soil properties. A detailed soil map has been prepared for Wadi Kafrein within the content of this research (section 4.2.4). Prior to this work, Wadi Kafrein catchment lacked any detailed soil class map, while a detailed study on soils had been already conducted in the adjacent catchment, Wadi Shueib. The results of the detailed study prepared by Kuntz (2003) on the soils of Wadi Shueib were based on intensive field work and laboratory analysis. Wadi Shueib catchment falls under the same climatic conditions and morphological properties as Wadi Kafrein, making data extrapolation based on scientific processes very realistic and meaningful. The extrapolated soil map of Wadi Kafrein has been prepared based on comprehensive remote sensing approach in which a single pair of Cartosat-1 and multi-temporal ASTER satellite images in addition to DEM, slope map, and Google Earth® images were used. The results were evaluated by ground truthing and were found to be satisfactory (Alkhoury et al. 2010b); also, the resulting map has good agreement with what was given in the references of the Jordan Soil Map project (Ministry of Agriculture, 1994) and the detailed soil map study of Wadi Shueib (Kuntz, 2003).

The prepared soil map of Wadi Kafrein divided the soil types into 12 soil units (see section 4.2.4) according to the USDA Soil Taxonomy (USDA 1975, 1999) and the

Keys to Soil Taxonomy of the USDA (1990). Each soil unit is defined by its own moisture properties and soil textures which have been studied in detail on a national scale by Ministry of Agriculture (1993, 1994) and catchment scale by Kuntz (2003) and Werz (2006). Based on the measured soil texture of every soil unit of Wadi Kafrein, it is possible to assign all required parameters of this routine.

As a distributed model, TRAIN-ZIN requires the assignment of different parameter values for every single grid cell. This will result in a large number of values for the entire catchment, and if the temporal variations are taken into consideration, the number will become even bigger. This requires an immense number of measurements and efforts. Therefore, it is required to reduce the expenses of parameter estimation. The physical basis of those parameter values allows a degree of hope that this may be possible; in that it should be possible to transfer parameters measured in one location to be representative of similar areas elsewhere. Thus not only may it be possible to define parameters on the basis of vegetation or soil type within the catchment area but it should also be possible to transfer information from studies outside the catchment of interest (Beven and O'Connell, 1982). Table 5.8 summarizes the parameters of runoff generation routine and their calibrated values (see section 5.7).

Table 5.8: Parameters for runoff generation routine.

ID	I_f	L_i	S_d	φ	PWP	K_s	λ	θ_{fc}	ρ
1	2	1	0.10	0.327	0.01	0.085	0.1	0.02	1.32
2	3	1	0.15	0.356	0.046	0.081	0.252	0.138	1.41
3	20	4	0.15	0.35	0.037	0.287	0.234	0.185	1.42
4	30	5	0.45	0.309	0.076	0.228	0.378	0.195	1.44
5	7	6	0.40	0.36	0.124	0.087	0.107	0.18	1.00
6	35	7	0.45	0.432	0.062	0.368	0.234	0.283	1.39
7	25	5	0.20	0.386	0.11	0.258	0.234	0.306	1.38
8	40	9	0.25	0.4	0.131	0.438	0.252	0.282	1.42

Where:
I_f: final infiltration rate, (mm/h)
L_i: initial loss storage, (mm)
S_d: soil depth, (m)
φ: effective porosity, (0-1 fraction of sample volume)
PWP: Permanent Welting Point, (0-1 fraction of sample volume)
K_s: saturated hydraulic conductivity, (cm/h)
λ: van Genuchtens lamda
θ_{fc}: field capacity, (0-1 fraction of sample volume)
ρ: bulk density, (g/cm^3)

All nine parameters can be determined from the soil textures of the 12 soil units. Soil grain size analyses were conducted and the *infiltration rates* of different soil units were measured in several representative sites for every soil unit by Kuntz (2003) and the values ranged from 12 to 252 mm/hr using the double ring infiltrometer, but these values seems to be very high compared to the standard infiltration rates of soil textures given in the literature. Werz (2006) related the increased infiltration rates to either the effect of macropores and the high skeleton content in the soils or to the fact that the required penetration depth of the infiltrometer of 5-10 cm following the DIN 19682-7 (Deutsches Institut für Normung, 1997) was not reached at most locations.

Hillel (2004) gave values of infiltration rates ranging from less than 1 mm/h for sodic clayey soils up to more than 20 mm/hr for sands soil, while the FAO (1988) referred to values from 1-5 mm/hr for clay to less than 30 mm/hr for sand. Lavee et al. (1998) studied the variations in infiltration rates from Mediterranean through semi arid to arid climate and the values ranged from 10-35 mm/hr in the arid and semi arid regions. Lange et al. (1999) referred to infiltration rates of different terrain types in arid catchments with ranges from 5 mm/hr to 50 mm/hr. Based on the above argument, the infiltration rates were assigned for every soil unit and later they were calibrated within the accepted range of infiltration rate of every soil texture.

Initial loss is a parameter reflecting the rainfall portion which is lost mainly due to detention losses, which take place before the generation of Hortonian overland flow. This parameter value depends highly on the soil type and is directly affected by the vegetation land cover; therefore, the values were assigned for every soil unit in which low values are given for areas with bare rock surfaces and sealed soil surface while higher values are given for soil units which have higher infiltration rates.

Soil depths were measured at several sites, covering all soil units in the entire catchment area as shown in Fig. (4.12). The *effective porosity* was estimated from soil textures as given by Rawls et al. (1982). The *Permanent Wilting Point, Saturated hydraulic conductivity, field capacity* and the *bulk density* were calculated based on the measured grain sizes of every soil unit using the SPAW Hydrologic model (Saxton and Willey, 2006). The *van Genuchtens lamda* of every soil unit was assigned based on soil texture as given by Van Genuchten (1978), Carsel and Parrish (1988), and Hendrickx (2003).

5.6.6.3 Parameterization of runoff concentration

The runoff concentration is calculated in TRAIN-ZIN using a Unit Hydrograph approach. In the present research, a synthetic unit hydrograph was used for every sub-catchment. The synthetic unit hydrograph uses the *Fischer-Tippet distribution* which has two parameters: parameter "**a**," which is used to calibrate the concentration time given in minutes; and parameter "**b**," which is used to shape the hydrograph. Parameter "**a**" is influenced by the average steepness of the sub-catchment while parameter "**b**' is influenced by the area of the sub-catchment. Both values were given for every sub-catchment in a tabular format.

5.6.6.4 Parameterization of channel flow and transmission losses

Parameters of this routine are based on the morphological and hydrological characteristics of the channel types mentioned in section 5.6.5.3. For every channel type, a total number of twelve parameters are required to be given. Most of the parameters of this routine are physically based and they are required to be assigned based on field measurements or by analyzing their physical properties using DEM.
For every channel segment, the length and slope is required to be given. This has been done using the high accuracy DEM from which the channel network was prepared and after segmentation the lengths were measured. The slope of every channel segment was calculated by determining the height difference of the two nodes of the segment. The width of the channel segments were calculated by digitizing the area of active channel alluvium between the two nodes of the segment and then this

value was divided by the respective channel length as shown in (Fig. 5.35). Channel segments length, slope, and widths were determined within GIS. Table 5.9 summarizes the parameters required for this routine and their calibrated values (see section 5.7).

Table 5.9: Parameters for channel flow and transmission losses.

ID	A_d	n	c%	F_d	φ	k_i	k_b	k_f	S	vk	I	AMI
1	1.5	0.033	0.3	1	0.5	0	10	4	0.1	0.01	0.1	0.85
2	0.3	0.04	0.8	0.4	0.35	60	80	5	0.1	0.03	0.1	0.7
3	0.5	0.035	0.6	0.7	0.4	75	93	7	0.1	0.02	0.1	0.8
4	0.6	0.028	0.65	0.75	0.4	80	100	10	0.1	0.025	0.1	0.8

Where:
A_d: depth of the active alluvium, (m)
n: Manning coefficient for different channels
c%: percentage covered by inner channel
F_d: depth to bankfull stage, (m)
φ: effective porosity, (0-1 fraction of sample volume)
k_i: hydraulic conductivity of the inner channel, (mm/h)
k_b: initial infiltration rate of bars, banks and the flood plains, (mm/h)
k_f: hydraulic conductivity of the underlying strata, (mm/h)
S: effective suction head, (mm)
vk: critical flow velocity/shear stress
I: infiltration reduction factor
AMI: antecedent moisture index

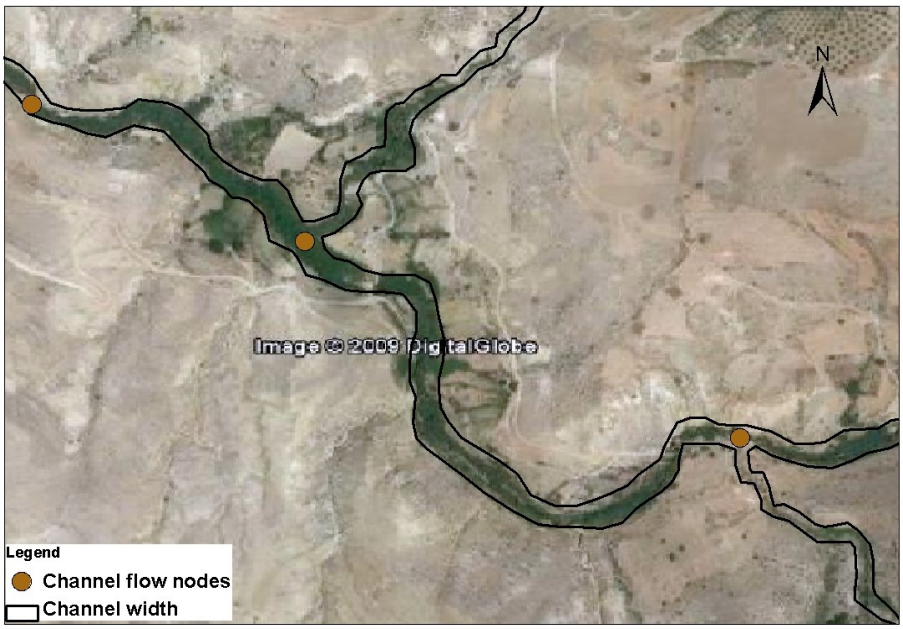

Fig. 5.35: Calculation of the spatially averaged channel width (background image from Google Earth®).

The *depth of the active alluvium, percentage covered by inner channel,* and *the depth to bankfull stage* for every channel type was determined based on field measurements and analysis. The *Manning coefficient* was given based on the roughness of every channel type; the values were estimated from USGS guidelines publications

(Arcement and Schneider, 1989; Phillips and Ingersoll; 1998 Phillips and Tadayon, 2006). The rest of parameters were assigned based on values given in previous studies in arid and semi arid regions (Leistert, 2005; Shadeed, 2008).

5.7 Model calibration and validation

In principle, parameter values should not need to be calibrated since they are based on physical measurements. However, in practice a certain amount of calibration is likely to be required. One reason for this is that measured values are often obtained at the point scale and may not be representative of the grid scale to which the model parameters are applied (Abbot et al., 1986b; Refsgaard and Storm, 1996). The model calibration and validation stage comes directly after the model construction phase, in which the initial model values given during the parameterization phase will be calibrated in this phase.

Model calibration can be defined as the selective improvement of the initial parameter estimates by the comparison of observed and simulated hydrological variables. *Model validation* implies the acceptance of a model as an accurate simulator of the real world system. This will also depend on the comparison of observed and simulated behavior (Beven and O'Connell, 1982). Following is an explanation of the calibration approach, method, and criteria for calibration termination. Finally, a graphical inspection is given.

5.7.1 Calibration approach

In this research, the following approach has been followed: 1) Execution of simulation with initial parameter values from the parameterization phase. 2) Separate adjustment of selected parameters. 3) After every parameter adjustment, comparison between the measured and simulated values. 4) Repetition of steps 1-3 until a convenient fit between the measured and simulated values is reached.

Calibration is conducted with the aim of reducing the differences between the measured parameter values and simulated model output parameter values. These differences in values are related to different sources of uncertainties while the calibration process can deal with only one source and minimize the differences. Ewen et al. (2006) assigned errors in physically based rainfall-runoff models to three groups:

- **Model structure error:** associated with the model's equations
- **Parameter errors:** associated with the parameter values used in the equations
- **Runtime error:** associated with rainfall and other forcing data

The errors or uncertainties from the third group were divided into two parts by Refsgaard and Storm (1996): random or systematic *errors in the input data* and random or systematic *errors in the recorded data*. The former includes precipitation,

temperature, and evapotranspiration or such data used to represent the input conditions in time and space over the catchment. The latter includes river water level, groundwater heads, discharge data or other data used for comparison with the simulated output. By calibration, only errors or uncertainties from the non-optimal parameter values can be minimized while the runtime error depends on the data quality. To achieve a successful calibration process, several points should be determined and be taken into consideration. These are explained in the following sections.

5.7.1.1 Model output variable

The model output variable is a simulated output of the model which can be used to evaluate the model results. Choosing a model output variable depends on the available measured data and the purpose of the modelling work. In this research, the generated runoff values at the catchment outlet were chosen as the model output variable because these values serve the aim of the modelling work and the measured runoff was made available by rigorous calculation procedures as discussed earlier in section 5.4.3.1.

5.7.1.2 Calibration parameters

Refsgaard et al. (1994) suggested during the parameterization phase to evaluate which parameters can be assessed from field data alone and which need some kind of calibration. For the parameters subject to calibration, physically acceptable intervals for the parameter values should be estimated. Furthermore, the number of real calibration parameters should be kept low, both for practical and methodological points of view.

To calibrate the amount of the generated runoff, only three parameters of the runoff generation routine parameters were adjusted. These are the *final infiltration rate*, the *initial loss storage*, and *soil depths* of the eight terrain types. To enhance the shape and time to concentration of the hydrographs, the two parameters, "*a*" and "*b*," of the Fisher Tippet distribution were calibrated for the runoff concentration routine. Parameters affecting the channel flow and the amount of transmission losses were left unchanged because they were assigned based on their physical properties and field data, except slight adjustments were conducted for the roughness coefficients "*Manning n*" of the different channel types.

5.7.1.3 Objective functions

The objective functions are functions which give a quantitative measure of the difference between the measured and the simulated data. The objective functions or accuracy criteria are used during the calibration phase to compare the measured and simulated data to define an objective measure of the goodness of fit associated with each set of the model parameters and estimate the parameter values which provide the best overall agreement between model output and measured data. However, the choice of an objective function is complicated and depends on several factors. The purpose to which the modelling is prepared, the available measured data and the assumptions in the distributed errors in the measured data are factors which must be taken into consideration (Refsgaard and Storm, 1996; Parkin, 2000a). No single objective

function is entirely suitable for all variables and even for a single variable it is not always easy to establish a satisfactory criterion. A large number of different objective functions have been developed (e.g. Green and Stephenson, 1986; Yapo et al., 1998) and choosing the suitable function depends on the early mentioned factors which must be evaluated and taken into consideration by the modeler. Green and Stephenson (1986) listed 21 approaches to be used for single event simulations depending on the simulation objectives, the range of simulation conditions, and other factors. Their study concluded that no single criterion is sufficient to assess adequately the overall measure of fit between measured and simulated hydrographs, particularly in view the many objectives behind the hydrological modelling.

In this research, three steps were followed to evaluate the overall goodness of fit. The first step followed was that, after every parameter value's change, a graphical inspection had to be performed in order to compare measured and simulated values at the outlet of the catchment area. The graphical comparisons provide a good overall indication of the model's capabilities and are more easily assimilated and may impart more practical information than statistical functions alone (Refsgaard and Storm, 1996). This first step was important in helping to evaluate the time of concentration of the generated runoff and the overall shape of the simulated hydrograph compared with the measured one. The second step followed was a comparison between the measured and simulated runoff volumes with a 10% discrepancy between both values allowed. Considering the approach followed in this research in quantifying the runoff amounts in the Kafrein reservoir with several additional input and output sources to the system, a 5% discrepancy between actual and simulated values is a hardly realistic goal. The third step followed was that two objective functions had to be used to statistically evaluate the goodness of fit. The two objective functions are the *Mean of Residuals* and the *Root Mean Square Error.*

The Mean of Residuals is calculated as:

$$x = \frac{1}{n}\sum\left(Q' - Q\right) \tag{5.30}$$

And the Root Mean Square Error:

$$RMS = \frac{1}{n}\sqrt{\sum\left(Q' - Q\right)^2} \tag{5.31}$$

Where:
n: number of data appoints
Q': simulated flow, (m^3/s)
Q: measured flow, (m^3/s)

The *mean of residuals* can indicate the bias in the predictions while the *Root Mean Square error* is a very commonly used function, which does not depend on the amount of data, and thus can be used for inter-comparison between time-series or sites. The optimal value for both functions is the zero value and has the same unit as the flow.

5.7.2 Calibration method

It has been explained earlier that some parameter values cannot be assessed directly from the field and they are estimated during the calibration process (*Empirical parameters*). For these parameter values, three methods are available for application (Refsgaard and Storm, 1996):

- **Manual calibration**: the parameter values are adjusted manually by Trial-and-error approach through a number of simulation runs.

- **Automatic calibration**: the parameter values are fitted by numerical optimization, in which a numerical algorithm finds the extremes of a given numerical objective function.

- **Manual and Automatic calibration:** this is done by adjusting an initial parameter values by trial and error followed by a fine adjustment using automatic optimization within the delineated range of physically realistic values.

The manual calibration method is by far the most widely used and is the most recommended method, especially for the more complicated models (Refsgaard and Storm, 1996). A good graphical representation of the simulation results is a prerequisite for the trial-and-error method.

In this research, a manual calibration method was conducted for few parameters as explained in section 5.7.1.2, which has had the largest impact on model results. The parameter values were adjusted one by one and after every simulation run, the results were compared graphically and quantitatively. The parameter values were ensured to be meaningful and are physically realistic. For example, the infiltration rate values were calibrated within the range of values measured independently in the field and were compared to the standard infiltration rates of soil textures given in literature as discussed in section 5.6.6.2.

5.7.3 Calibration termination

The termination was dependant on the graphical inspection and on the numerical differences between the measured and simulated values of runoff. The parameter values were considered calibrated when the accuracy criteria (three steps) mentioned in section 5.7.1.3 was fulfilled.

5.7.4 Results inspection and model validation

In this research, the objective functions were applied to evaluate the simulation results and evaluation was also supplemented by a graphical inspection of both measured and simulated values, using the most commonly used display by *time series plots*. After calibrating the model, assessment of whether the model is valid for subsequent use is done. Assessment is done by validating the model using time series data different from the data used in the calibration. This step is officially known as *model validation* (Stephenson and Freeze, 1974). For this purpose, the monitored period was divided in

a way that one part was used to calibrate the model parameter, and with the rest of the available data, the model was validated without changing the model parameters; i.e. the catchment conditions remain unchanged (stationary) while different time series are used from those used in the calibration period. Klemes (1986) presented a systematic hierarchy of methods for model calibration and validation. These methods distinguish among cases where catchment conditions are stationary and cases where they are not. Also, distinctions are made among simulations conducted for the same catchment as was used for calibration and validation and simulations conducted for ungauged catchments.

In the present research, the *Differential split sample test* was used to calibrate and validate the hydrological model of Wadi Kafrein. By comparing figures 5.2 to 5.5, it can be noticed that two different conditions are present, In the water year 2007/2008, the rainfall events have lower intensities and short lag times while in the following year, 2008/2009, the rainfall intensities were higher with much dryer and longer lag times between storm events followed by very wet months with short lag times between rainfall events. This can be recognized by the long dry period prior to February and March, 2009 in which no single runoff event was recorded while 80% of the total rainfall amount of the water year 2008/2009 was recorded in only February and March, 2009.

The Differential split sample test is used to test the model's ability to represent changed conditions. Therefore, non-stationary conditions (i.e. changing conditions over time) were used, and the validation period was chosen to be different from the calibration period. The water year 2008/2009 was used for calibration while events from 2007/2008 and 2009/2010 were used for validation purposes. Despite the different conditions of the rain storm characteristics between the periods used for calibration and those used in validation, the overall monitored period is considered as dry (5.4.1), which consequently resulted in few runoff events. Nevertheless, these events were used either for calibration or validation. Figure 5.36 shows the measured and simulated runoff hydrographs for the entire monitored period. Time is given in hours and the vertical solid lines between the hydrographs were used to separate the runoff events from each other (i.e. the periods of no events were skipped).

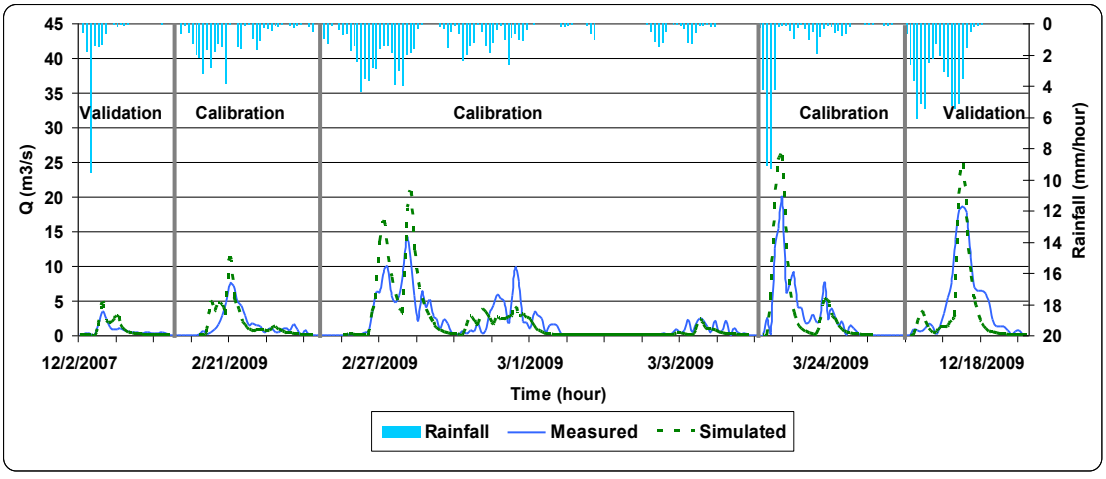

Fig. 5.36: Graphical inspection using time series plots for the calibration and validation periods.

Table 5.10 gives a statistical summary of the results of the calibration and validation runoff events. The measured and simulated runoff events are given in m^3 and the simulated values are compared with the measured ones as percentages. The mean of residuals and the mean square error functions have the same unit of the flow that is (m^3/s). The final results of model calibration and all model output are discussed in detail in section 5.9. The calibrated model has been further validated by a continuous simulation for the period 2002-2007 and the results are discussed in the next chapter of Model Applications and Predictions. In the water year 2009/2010, only three rain gauges were in order and the underestimation of the simulated runoff generation could be attributed to the insufficient number of rain gauges with limited spatial representation (R1-R3).

Table 5.10: Statistical summary of the measured and simulated runoff events.

Events ID	Measured runoff (m^3)	Simulated to measured (%)	Mean of residuals (m^3/s)	Mean Square error (m^3/s)
02. Dec. 2007	6.02E+04	109	0.11	0.11
21.-22. Feb. 2009	1.90E+05	103	-0.03	0.03
27. Feb-03. Mar. 2009	7.73E+05	94	-0.2	0.2
23.-24. Mar. 2009	4.20E+05	105	0.04	0.04
17.-18. Dec. 2009	5.16E+05	71	-1.2	1.2

5.8 Sensitivity and uncertainty analysis

After calibrating the initial parameter values and the acceptance of the model as a simulation tool for the real world, a good exercise is to evaluate how sensitive the model is to changes to every isolated parameter. Also, evaluating which sources are responsible for uncertainty in the model results is important as well (section 5.7.1). The following is an explanation of the conducted sensitivity and uncertainty analysis and their effect on the model results.

5.8.1 Sensitivity analysis

A *sensitivity analysis* is a systematic evaluation of the effect of varying each model's parameters on the model output. One model output is considered, and a base line simulation is chosen (e.g. using calibrated values). A number of simulations are then run by repeatedly increasing then decreasing each parameter value by a fixed percentage (Parkin, 2000a).

In this research, all parameters were subjected to sensitivity analyses including the un-calibrated parameters of *runoff generation*, *runoff concentration*, and *channel flow and transmission losses* routines discussed in sections 5.6.6.2, 5.6.6.3 and 5.6.6.4 respectively.

The *generated runoff* value of the model output was considered to conduct the sensitivity analysis for each parameter. Stated clearly, the *generated runoff* is the sum of two components: *runoff* (as either IEOF or SEOF) and *transmission losses* (portion of the generated runoff which is lost to the ground). Therefore, for those parameters, which affect the transmission losses like active alluvium depth and alluvium infiltration rate, the *transmission losses* value as output was considered to evaluate the model sensitivity.

5.8.1.1 Runoff generation parameters

A set of four simulations were run for 13 parameters of different model routine; by a decrease of 25% and 50% of the calibrated value, then by an increase in the calibrated value of 25% and 50%. For runoff generation parameters, the simulations were done for infiltration rate, initial losses and the soil depths (Fig. 5.37). The soil depth is the most sensitive parameter to any changes because it directly determines the amount of rainfall required to saturate the soil before a runoff is generated. By decreasing the soil depths to 50% of all terrain, discussed in (5.6.5.1), the runoff amount almost doubles (190%). On the other hand, with higher soil depths more rain is required to saturate the soil and consequently less runoff is generated. An increase in 50% in the soil depths will reduce the amount of the generated runoff to 62% of the calibrated value. The thickness of the soil has a more substantial role in *Saturation Excess overland Flow* (SEOF) mechanisms. Therefore, with deeper soil, more rain is required to saturate the soil. If *Infiltration Excess overland Flow* (IEOF) is the dominating process, the infiltration rate has a greater role in determining the amount of generated runoff.

The infiltration rate is also a sensitive parameter, and the generated runoff amounts are more influenced by a decrease in infiltration rate rather than an increase. A decrease of 50% of the calibrated infiltration rate value of all soil units will increase the generated runoff amount by 44% while a 50% increase will reduce the runoff amounts by 11%. Similar to soil depth and infiltration rate, the initial loss parameter also has an inverse relation with the generated runoff, and with a decrease of 50% of the initial loss, an increase of 21% in the generated runoff amount occurs. An increase of 50% will reduce the runoff amount by 14%.

These variations in increase or decrease in the runoff amounts are controlled by the runoff mechanism which is specific for every runoff event and it is possible to have in the same rain storm one or more runoff mechanisms. The initial loss parameter is dependent on soil type and the vegetation cover. Generally, their values for the different terrain are low. Therefore, the increase in value will not reduce the runoff amounts very much when compared with the influence of soil depth.

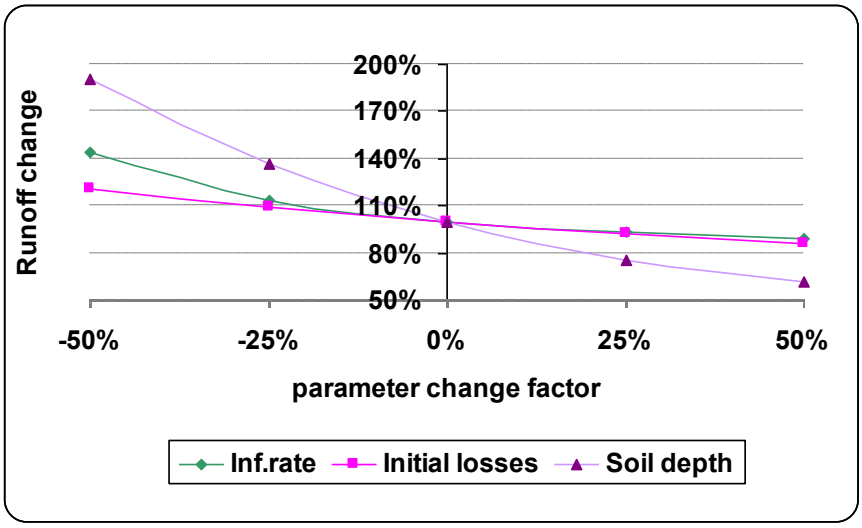

Fig. 5.37: Sensitivity analysis for runoff generation parameters.

5.8.1.2 Runoff concentration parameters

Sensitivity analyses were conducted to Fisher-Tippet distribution parameters "**a**" and "**b**." The first parameter describes the required time for the generated runoff to be transformed from each sub-catchment to a lateral flow of the adjacent channel while the second parameter determines the shape of the synthetic unit hydrograph of every sub-catchment. Variations in the values of these parameters will effect the time to concentration and the width of the curve and do not influence the runoff volume.

5.8.1.3 Routing parameters

To evaluate the effect of parameter changes on transmission losses, six parameters were subjected to sensitivity analysis. These parameters are: *channel length*, *channel slope*, *channel width*, channel roughness coefficient *Manning n*, *percentage covered by the inner channel*, and *depth to bankfull stage.* Channel slope and the depth to bankfull stage have no significant influence on the generated runoff amount rather; they do influence the time arrival of the flood. Channel length and width influence the volume of the transmission losses (Fig. 5.38). In case of shorter and narrower channels, less runoff is lost along and within the channels. An increase of channel lengths and widths by 50% leads to more loss of runoff to the channel beds as transmission losses with 30-40% more losses compared with the calibrated value.

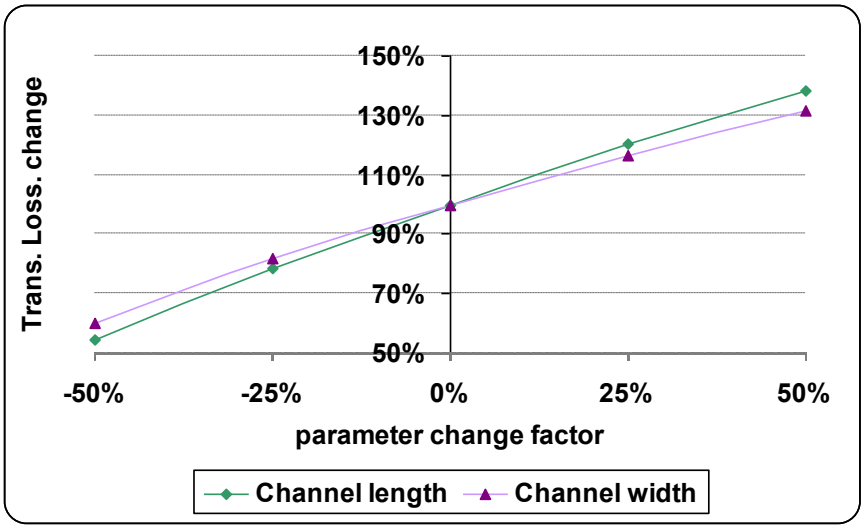

Fig. 5.38: Sensitivity analysis for routing parameters (physical).

Other parameters which influence the amount of transmission losses are the channel roughness coefficient and the percentage of the inner channel to the total width of the channel. A roughness coefficient was assigned for every channel type based on field observations and surface characteristics of the channels; therefore Manning n, in addition to its influence on the flood peak and flood arrival, does influence the amount of transmission loss (Fig. 5.39). By having higher friction between the flood wave and the channel surface, larger volumes of runoff, which have came from the adjacent sub-catchments of every channel segment, will be lost to the channel beds as transmission losses. A decrease of the roughness coefficient by 50% will yield an 8% reduction in transmission loss while an increase of 50% in the roughness coefficient will cause a 7% increase in transmission losses compared with the calibrated value.

The c% parameter is the percentage of the inner channel relative to the total width of the channel, and is acquired through field measurements. When the total channel is wide and the inner channel is narrow, relatively low transmission losses occur. When the total channel is narrow (similar to channel type 4), the percentage of the inner channel is usually higher and transmission losses will also be low due to the inner channel being the part of the channel which will be flooded first (Fig. 5.39).
A decrease of 50% in the inner channel percentage will increase the transmission losses by 8%, while an increase of 50% of the inner channel percentage will cause a reduction of 16.5% in the transmission losses.

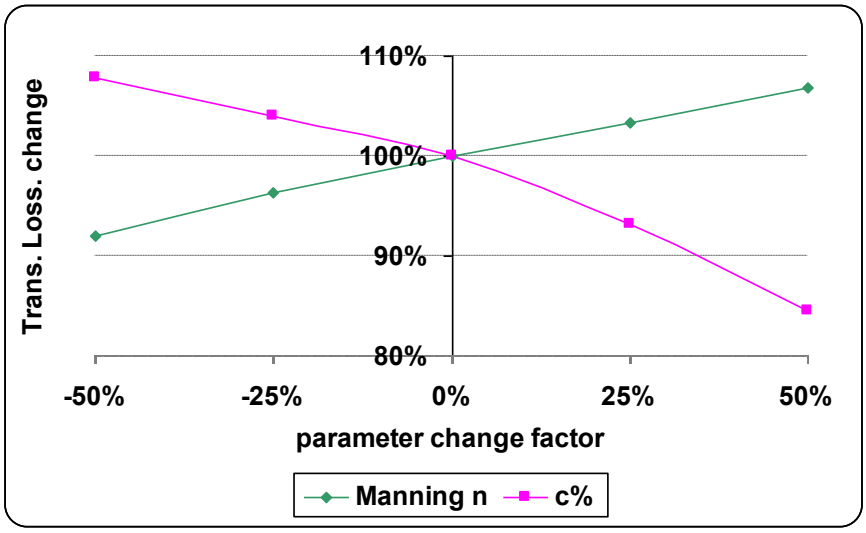

Fig. 5.39: Sensitivity analysis for routing parameters (empirical).

5.8.1.4 Transmission losses parameters

The depth of active alluvium (A_d) and the infiltration rate of the alluvium (k_f) have a direct influence on transmission losses. Deep alluvia along channels means a greater proportion of the flood water will infiltrate into the channel bed, effectively increasing transmission losses. Over the same time with a higher infiltration rate into the alluvium, more transmission losses occur (Fig. 3.40). The increase or decrease in the alluvium depth by 50% will cause an increase and decrease of 5% and 4% respectively, while the infiltration rate of the alluvia has a greater influence on the transmission losses in which 50% reduction will cause 30% reduction in transmission losses and 50% of increase will cause 25% more transmission losses.

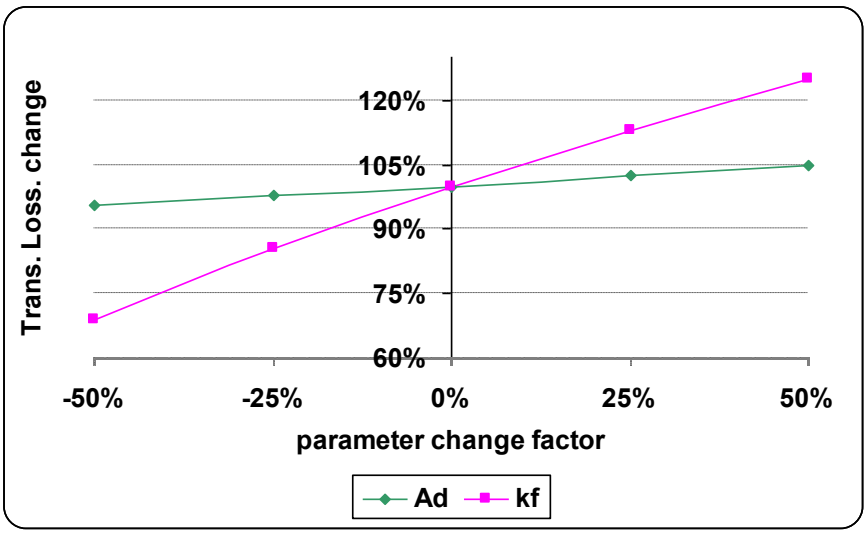

Fig. 5.40: Sensitivity analysis for transmission losses parameters.

5.8.2 Uncertainty analysis

As mentioned earlier, some error or uncertainty in the model is attributed to the input data or the *forcing data* used in the model. The criteria which have been followed to reduce the uncertainty of the measured rainfall using the automatic tipping bucket rain gauges were mentioned in section 4.3.1, and for the climatological data, they were mentioned in section 4.3.2. Still, for the climatic stations an important criterion of their final locations was considered to secure them during the monitoring period; therefore, both weather stations were installed on the roofs of governmental buildings which violate the 2 m height rule required to calculate the evapotranspiration. Therefore, a correction should be considered to adjust wind speed data to standard height to reduce the uncertainty of wind effect.

Wind speed is measured with anemometers. Anemometers are composed of cups or propellers in a weather station, which are turned by the force of the wind (Fig. 4.15). By counting the number of revolutions over a given period of time, the average wind speed over the measuring period is computed and this value is important to calculate the evapotranspiration process in hydrological modelling. Wind speed is affected by the height above the soil surface which is slowest at the surface and increases with height. Therefore; the anemometers are placed at a chosen standard height which is 2 meters above the surface for the calculation of evapotranspiration and they are required to be adjusted in case of higher elevations as recommended by Allen et al. (1998) using the following equation:

$$u_2 = u_z \frac{4.87}{\ln(67.8z - 5.42)} \tag{5.32}$$

Where:
u_2: wind speed at 2 m above ground surface, (m/s)
u_z: measured wind speed at z m above ground surface, (m/s)
z: height of measurement above ground surface, (m)

The two weather stations of King Hussein Gardens and Wadi Es Sir WWTP were installed 6 m and 6.5 m from the surface, respectively. Therefore, the wind speed effect was corrected for both stations, using the above mentioned equation in order to reduce the uncertainty value in the measured wind speed. After correcting the raw data of both stations for wind speed, the grids were interpolated and prepared in the proper format to run the model.

The uncertainties resulting from model parameters are given in Table 5.11. All values are within the range of ± 50%, which are included in the sensitivity analysis discussed earlier. The uncertainty values were estimated based on the experience acquired during the parameter assessment and on previous studies conducted in arid and semi arid regions (e.g. Lange, 1999; Shadeed, 2008).

Table 5.11: Range of the uncertainties for those parameters used in sensitivity analysis.

Model routine	Parameter	Uncertainty range	Notes
Runoff generation	I_f	± 20%	Estimated
	L_i	± 2.5 mm	Estimated, 0-2.5 mm for terrain 1 and 2
	S_d	± 5 cm	Estimated
Runoff concentration	Parameter a	± 15 min	Based on the calibrated events (only hourly values were available).
	Parameter b	± 5%	Sub-catchments areas were calculated using the high resolution DEM (5mx5m cell size).
Routing parameters	Channel length	± 50 m	It was determined by using the acquired Google Earth® images and the DEM.
	Channel slope	± 10%	Using the DEM, differences between nodes elevations
	Channel width	± 10%	It was determined using the acquired Google Earth® images
	n	± 0.01	Estimated, (Chow et al. 1988)
	c%	± 20%	Estimated
	F_d	± 0.5 m	Estimated
Transmission losses	A_d	± 0.5 m	Estimated
	k_f	± 50 mm	Estimated

5.9 Results and discussion

One of the main aims of developing a hydrological model is to quantify the water components of the water cycle. This requires a reliable model which must be ready to quantify and predict the hydrological processes in the real world. Another important use of a calibrated and validated model is to predict the effect of land use changes due to urbanization or the effect of climatic changes on the water components and recharge amounts. The last two topics will be discussed in more detail in the coming chapter, which emphasizes the usage and application of the hydrological model for the catchment area of Wadi Kafrein.

In this research, every component of the water cycle has been simulated and quantified in detail. In the coming sections, all components and their spatial distribution will be discussed with emphasis on storm events, which were used in the calibration phase of the water year 2008/2009. The water balance for the whole monitored period will be discussed in the last section of this chapter. The maps presented in the coming sections are a daily grid of every component in millimeters as a mean value for the catchment area.

5.9.1 Precipitation

Precipitation was spatially interpolated using the IDW method with elevation correction in which the prepared DEM was used as described in section 5.6.6.1. The rainfall is interpolated in daily bases as mean average over the whole catchment area of Wadi Kafrein in millimeters. Precipitation is highest in the northeastern part of the catchment area and decreases westward. Using the IDW interpolation method with the introduced elevation correction factor enhanced the interpolation results by taking into consideration the specific topographic conditions of Wadi Kafrein, which are

characterized by wide variations in elevation over short horizontal distances. These elevation variations affect the spatial distribution of precipitation, as can be noticed in Figs.5.41-5.43.

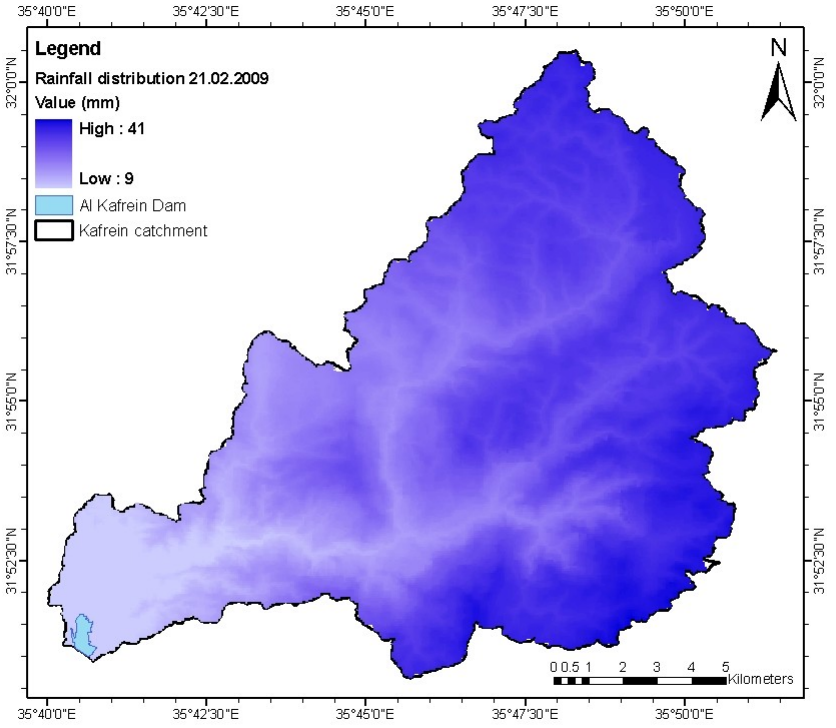

Fig. 5.41: Rainfall spatial distribution for the rainstorm of Feb. 21st, 2009.

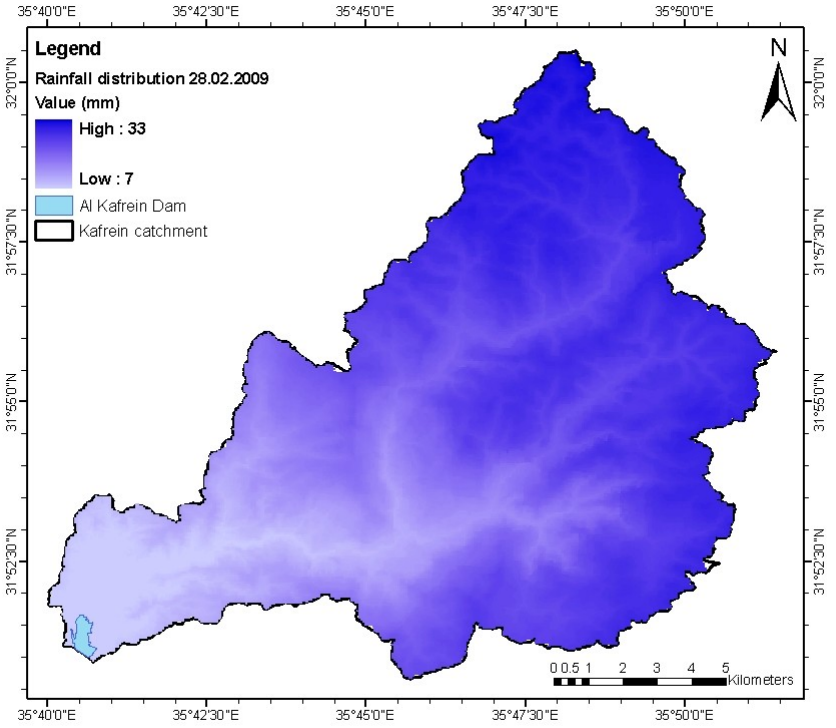

Fig. 5.42: Rainfall spatial distribution for the rainstorm of Feb. 28th, 2009.

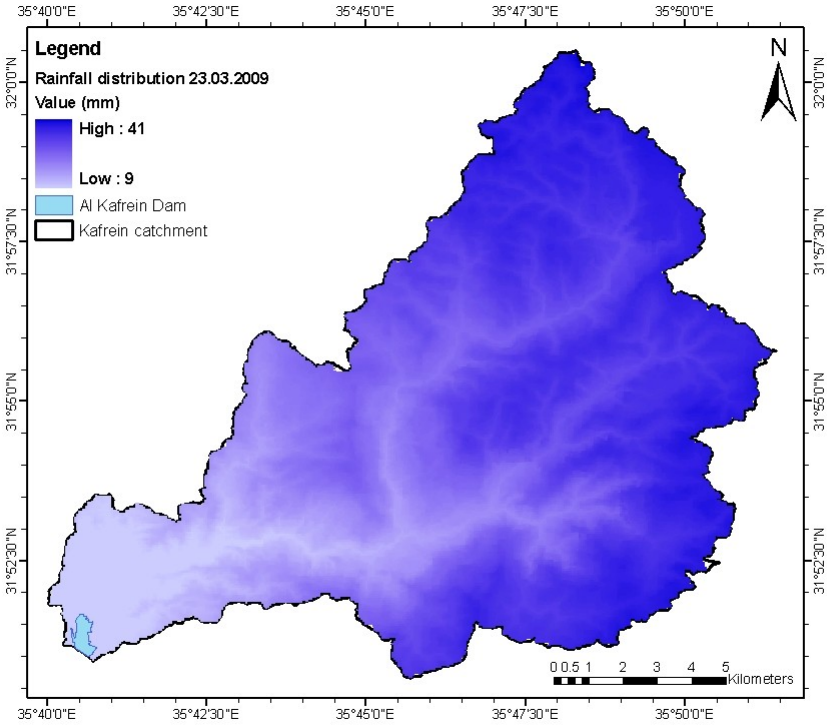

Fig. 5.43: Rainfall spatial distribution for the rainstorm of Mar. 23rd, 2009.

During the modelling period, only one snowfall event took place, which was at the end of January, 2008, in which the snow covered several parts of the eastern highlands of the catchment. The eastern and northeastern parts of the catchment area had the highest snow fall with a maximum snow depth of 21 mm near Marj Alhamam city (Fig. 2.2) on the 31st of January, 2008.

The lowest temperature which was recorded at King Hussein weather station was -2.43 °C during the night hours of January 31st, 2008 while in the other weather station of Wadi Es Sir WWTP the lowest recorded temperature on that day was 2.46 °C. These measurements were taken over time intervals of 5 minutes and the data of both weather stations were used in the interpolation approach. The use of two weather stations was of great importance to consider these variations in temperature and elevation, and has lead to a realistic interpolation of the spatial distribution of snow over the catchment area of Wadi Kafrein (Fig. 5.44-5.46).

During the days where snow occurred, ground truthing with respect to elevation was done and all subwadis were checked. The snow was observed in Wadi Kuraysh (Fig. 5.44) and on the areas around Wadi Naqib (Fig. 5.45), while no snow was observed in the other three subwadis. The simulated snow maps show a snow distribution over elevations higher than 790 m, which is in a good agreement with field observations.

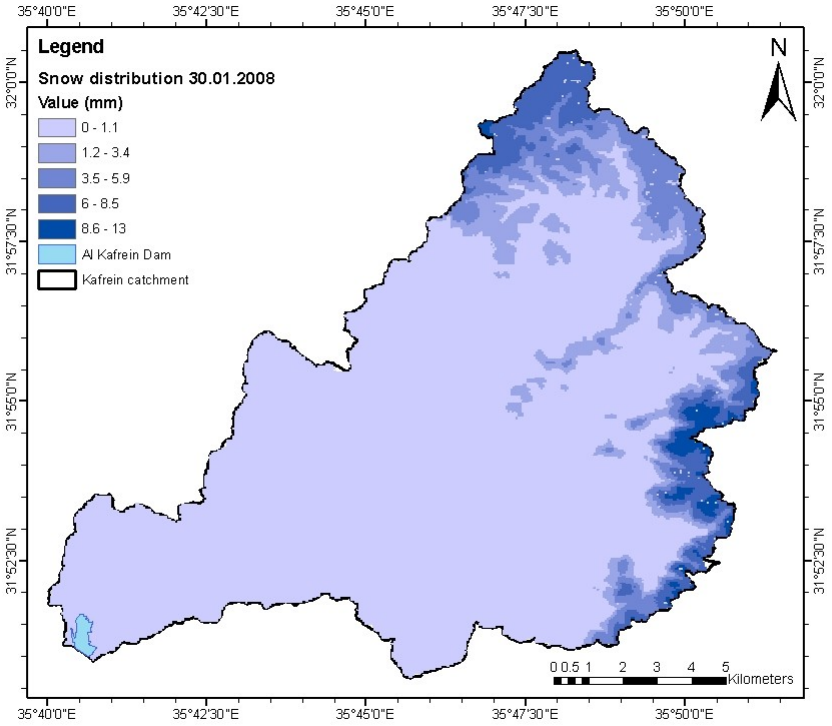

Fig. 5.44: Snow spatial distribution for snow storm of Jan. 30th, 2008.

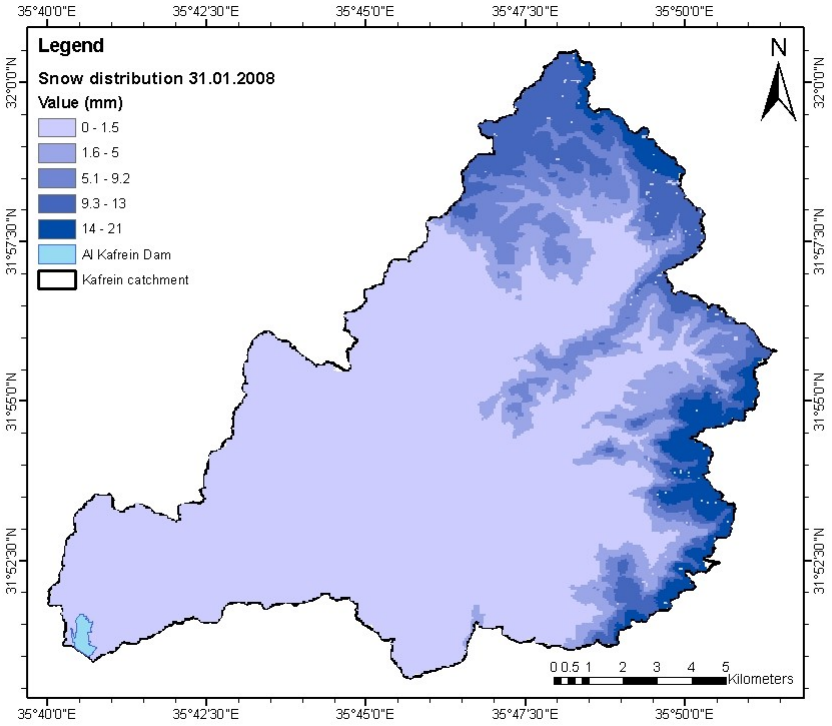

Fig. 5.45: Snow spatial distribution for snow storm of Jan. 31st, 2008.

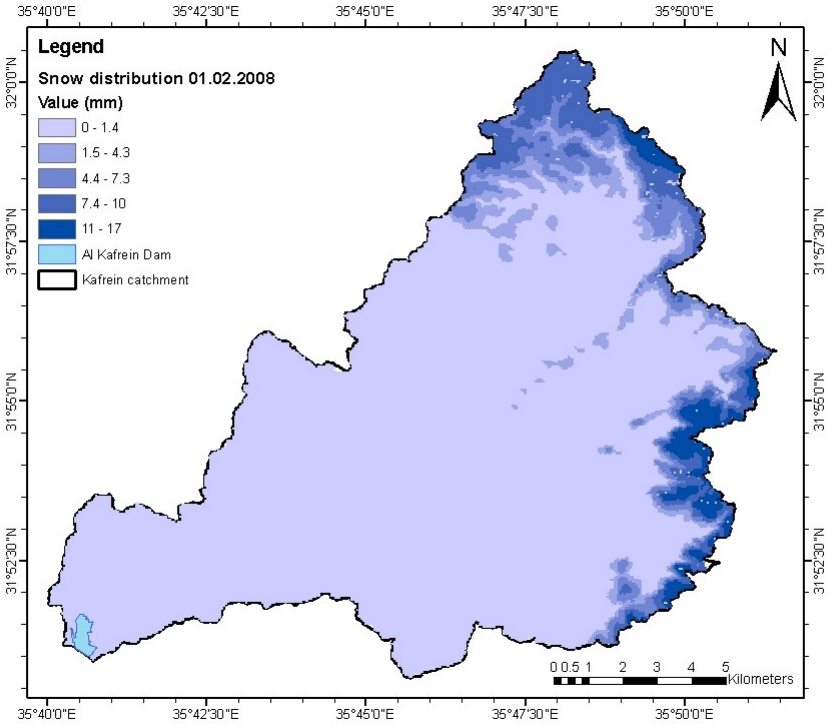

Fig. 5.46: Snow spatial distribution for snow storm of Feb. 1st, 2008.

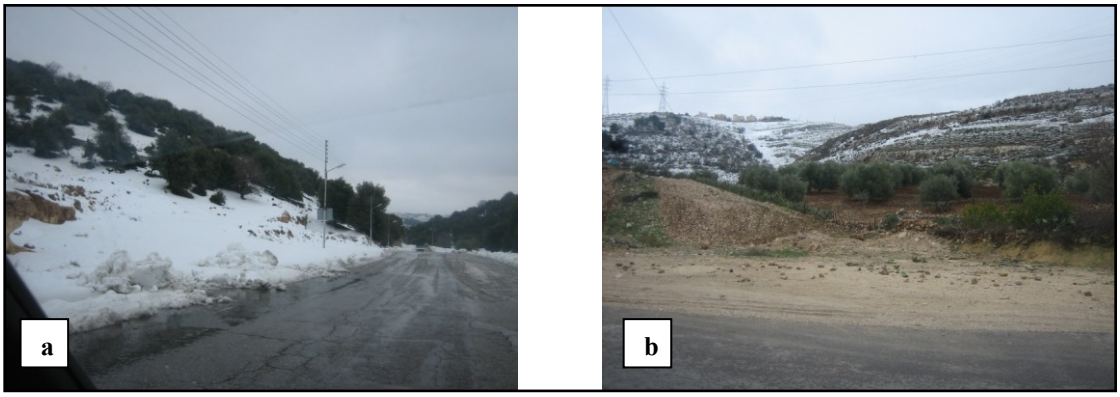

Fig. 5.47: a. Snow over Wadi Kuraysh catchment (S1)

b. Snow distribution on the foothills close to Wadi Naqib (S2)

5.9.2 Evapotranspiration

In a catchment area with a semi arid climate, evapotranspiration is the most substantial component of the water balance. The evapotranspiration is the sum of: evaporation from interception, evaporation from initial losses, transpiration from the canopy, and evaporation from soil. These components are calculated and given on a daily basis as part of the water balance results which will be discussed in section 5.9.5.

The spatial distribution maps of evapotranspiration are presented by daily grids as evaporation due to interception and the evaporation from initial losses.

The evapotranspiration spatial distribution maps of the storm event of February 21st, 2009 are given in Fig 5.48 and 5.49.

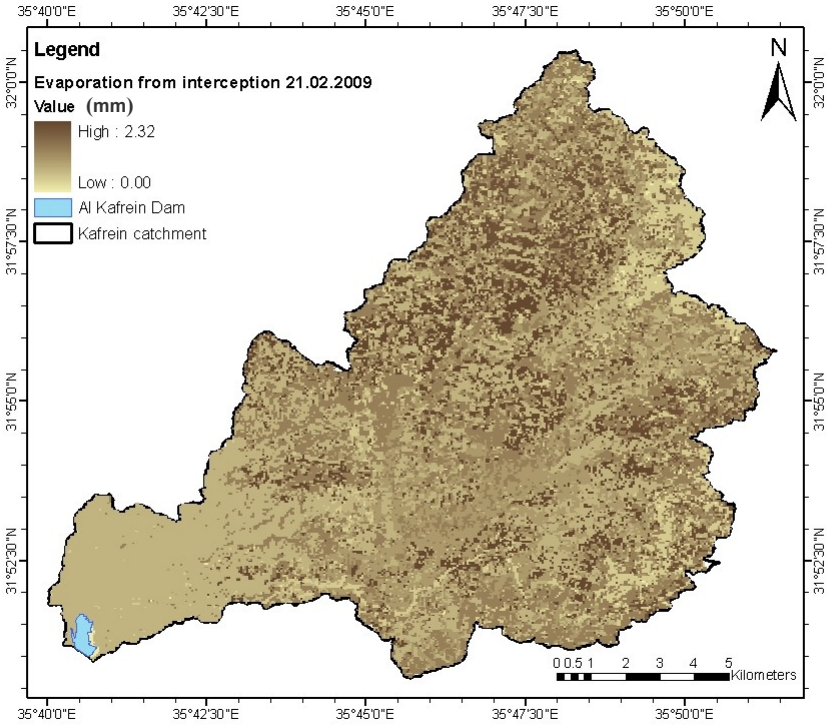

Fig. 5.48: Spatial evaporation distribution from interception in 21st Feb. 2009.

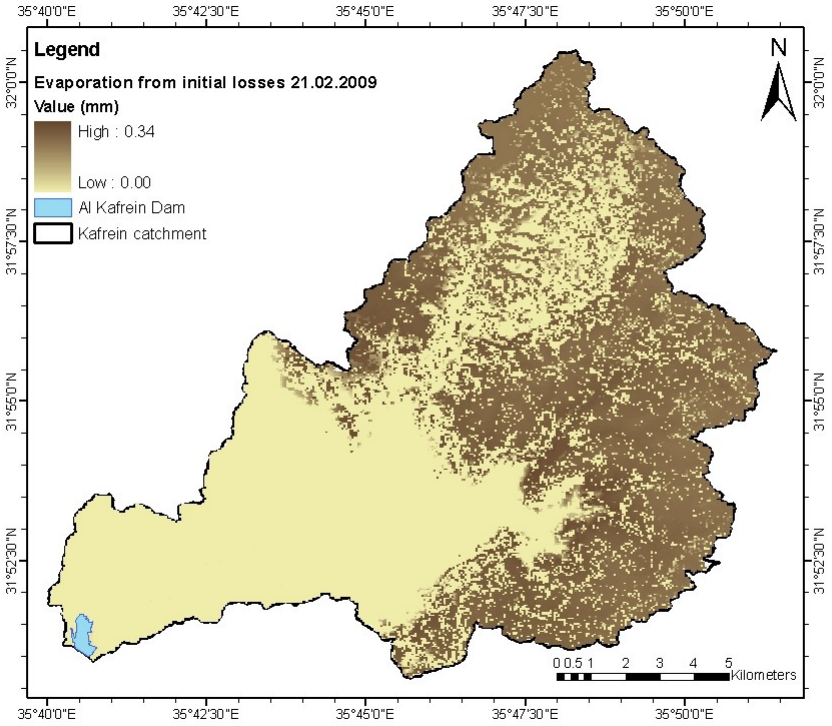

Fig. 5.49: Spatial evaporation distribution from initial losses on Feb. 21st, 2009.

Evaporation from interception is zero in urban areas (Fig. 5.48) and maximum in agricultural areas. The mean evaporation is 1.14 mm. Evaporation from bare rock areas and along the Wadi main channel, where no agriculture and sparse vegetation is found, is zero. Evaporation from initial losses increases eastward with a mean value of 0.12 mm (Fig. 5.49). The total evaporation on the 21st of February is 1.26 mm, which is a low value when compared with a mean precipitation value of 30 mm in that day, but evapotranspiration is a continuous process and most occurs during the no rain time from the initial lost water in the depression zones, soil storage, and canopy.

5.9.3 Recharge

Recharge in Wadi Kafrein occurs predominantly in the eastern and northeastern boundaries of the catchment, along the highlands where the catchment receives the most precipitation. This can be seen from the spatial distribution maps of precipitation in section 5.9.1. The recharge values are given in [mm] as a mean value for the whole catchment area, and have been simulated for everyday of the modelling period. The quantifiable recharge is directly affected by the precipitation volume, precipitation intensity, antecedent soil moisture, as well as the specific mechanism which generated the runoff.

When the soil is saturated and the generated runoff is a result of **SEOF,** the recharge is higher than storm events with high rain intensity and runoff generated by **IEOF.** For example, the precipitation during the storm event of February 21st was calculated to have a mean of 30 mm for the whole catchment. In total, this was 4.8 MCM of rain.

The fraction of total precipitation on Feb 21st, which was recharge, amounted to a mean area value of 0.8 mm for the catchment (in total: 0.13 MCM). The maximum recharge spatial value on this date was 22 mm in the upper eastern part of the catchment (Fig.5.50). During the second storm event (27.02-03.03.2009), the precipitation on February 28th was calculated to be 26 mm (in total: 4.2 MCM). This total precipitation is less than the total precipitation on Feb 21st, during the first storm event (see above).

On February 28th, the mean recharge per unit area was simulated to be 8.2 mm. which is a total catchment value of 1.3 MCM. This is ten times more than the simulated recharge with similar rainfall amount in one day (Fig. 5.51). Runoff on February 21st was mainly generated as **IEOF** while on February 28th; **SEOF** was the main runoff mechanism (section 5.9.4).

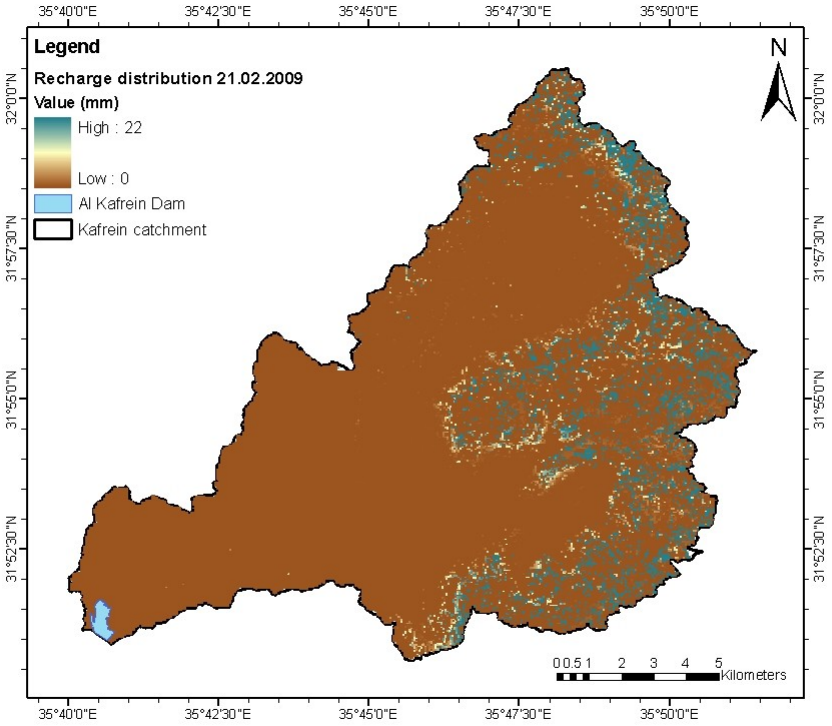

Fig. 5.50: Spatial recharge distribution on Feb. 21st, 2009.

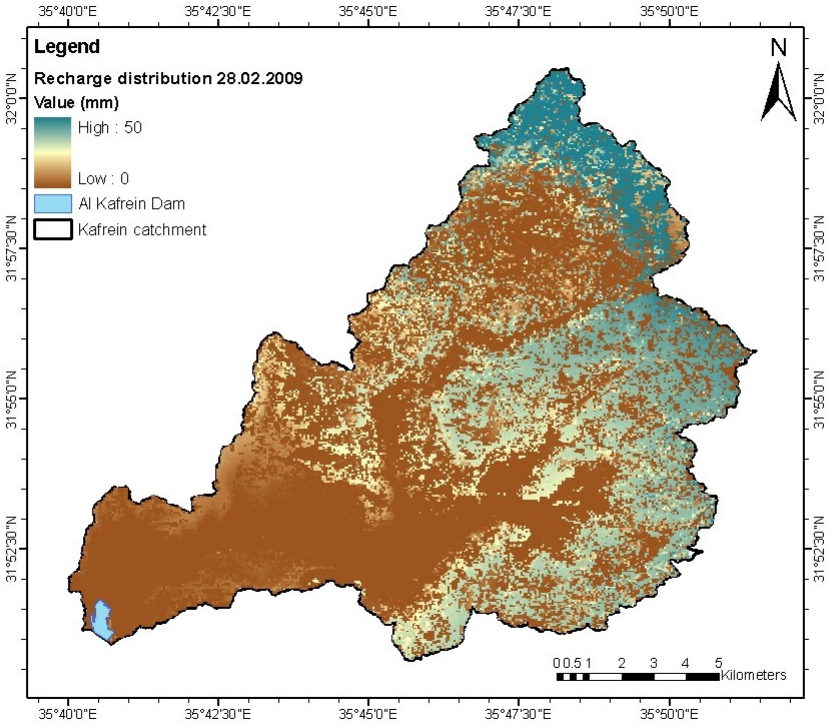

Fig. 5.51: Spatial recharge distribution on Feb. 28th, 2009.

5.9.4 Runoff generation

In earlier sections of this chapter, the methodology and results of the measured precipitation (section 5.4.1) and the measured runoff (section 5.4.3) were explained and discussed. These measurements have been used in calibrating and validating the hydrological model (section 5.7). Here, the quantitative results of the model concerning the generated runoff and the transmission losses for the runoff events, which had been used in the calibration process, will be discussed in addition to the spatial distribution of the generated runoff.

The runoff results will be presented and discussed on an event basis, in which the volumes will be given for the whole catchment area as a mean value in millimeters. The generated runoff is either a product of **IEOF** or **SEOF.** A certain volume of the generated runoff (either due to IEOF or SEOF) will be lost during the routing process which has been referred to as the **transmission losses**. Therefore, the total amount of transmission loss and the final volume of runoff, which reaches downstream, form together the generated runoff.

Measured and simulated runoff events are quantitatively given in table 5.10. Values given in table 5.10 are final runoff values while in this section; the total generated runoff (including the value of transmission losses) is discussed.

5.9.4.1 Storm event 21-22 February 2009

It has been shown in section 5.4.1 that precipitation amount was lower than average in the water year 2008/2009. As mean area rainfall, only 2.5 mm were measured over the catchment area of Wadi Kafrein in January 2009. During February and prior to the main rainfall event of 21-22.02.2009, five rainfall days were recorded with total area rainfall of 34.7 mm, out of which 22.8 mm were recorded in the 10^{th} and 11^{th} of February 2009.

The generated runoff during the 10^{th} and 11^{th} of February 2009 was mostly due to **IEOF** (98.7%) while the transmission losses presented around 44%. During the main storm event on the 21^{st} and 22^{nd} of February, 2009, a total area rainfall of 34.5 mm were recorded (around 5.6 MCM). As the runoff in the prior storm event on the 10^{th} of February was generated by **IEOF,** the actual soil storage was low with a mean area value of no more than 17 mm. Also, considering the high intensity of this storm event, it is expected that the generated runoff would be a result of **IEOF**. The model results show that 77.3% of the generated runoff was due to **IEOF** and 22.7% was due to **SEOF**. The transmission losses present 30.4% of these values.

It can be noticed from Fig.5.52, that runoff was mainly generated in the northeastern and southeastern part of the study area where urbanization is taking place. Also runoff was generated on the bare rock area in the western part near the Kafrein reservoir.

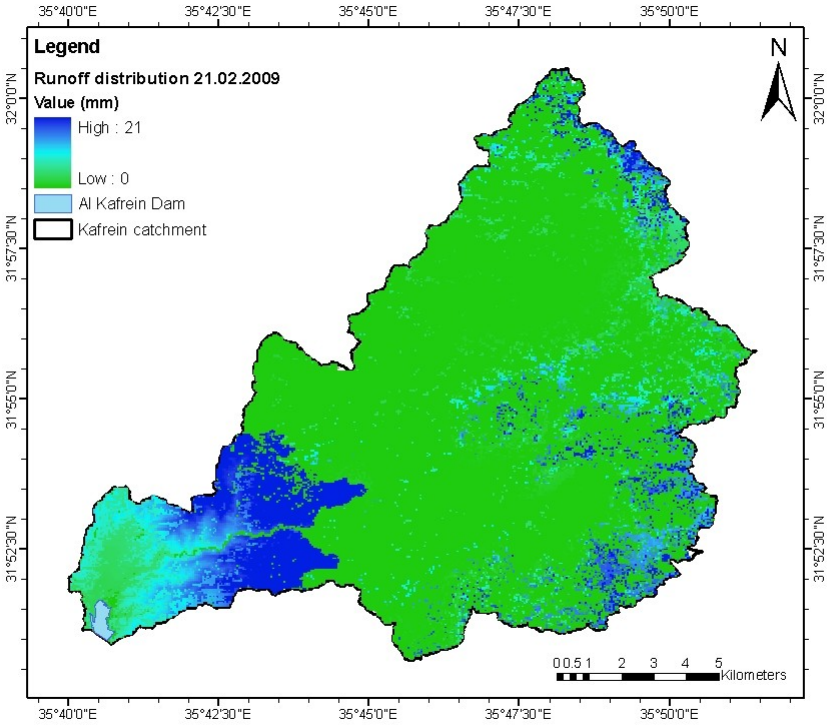

Fig. 5.52: Spatial runoff distribution on Feb. 21st, 2009.

5.9.4.2 Storm event 27 February-03 March 2009

The second storm event, which has also been used in the calibration process, had a total area rainfall of 82.4 mm (around 13.3 MCM). Out of this amount, 70 mm precipitated in the first 3 days. In this storm event, most runoff was generated due to **SEOF** in contrary to the 21-22 of February event. This is due to the antecedent soil moisture from the earlier event where 22.7% of the generated runoff was due to **SEOF**. Also, the relatively short lag time of 5 days between the two storm events contributed as well. The **SEOF** was 83% of the runoff while 17% was due to **IEOF**. The transmission losses present 25% of the generated runoff by the two mechanisms.

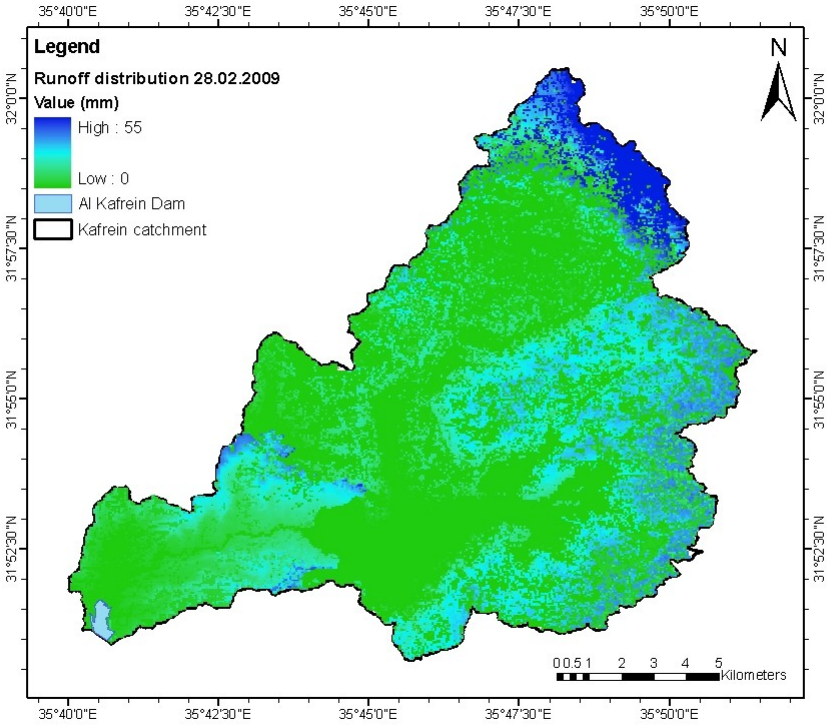

Fig. 5.53: Spatial runoff distribution on Feb. 28th, 2009.

5.9.4.3 Storm event on March 23rd, 2009

During the third storm event, on the 23rd and 24th of March, 2009, a total area rainfall of 38.7 mm (around 6.2 MCM) was recorded. This event comes almost after 3 weeks of no rain and most of the rain took place during midnight of the first day and high rainfall intensity. The runoff was generated as **IEOF** with 63.7% and 36.3% as **SEOF**. The transmission losses present 17.8% of these values.

In the western part of the study area and despite relatively low rainfall, most runoff was generated (Fig. 5.54). Similar to the first storm event, the spatial distribution of the generated runoff is mainly in the urban areas and the bare rock areas in which the infiltration rate is not high. Consequently, after a specific amount of precipitation of high intensity, these surfaces do not have the capacity to infiltrate any additional amount of rain and the runoff will be generated due to exceeding the infiltration capacity of these surfaces.

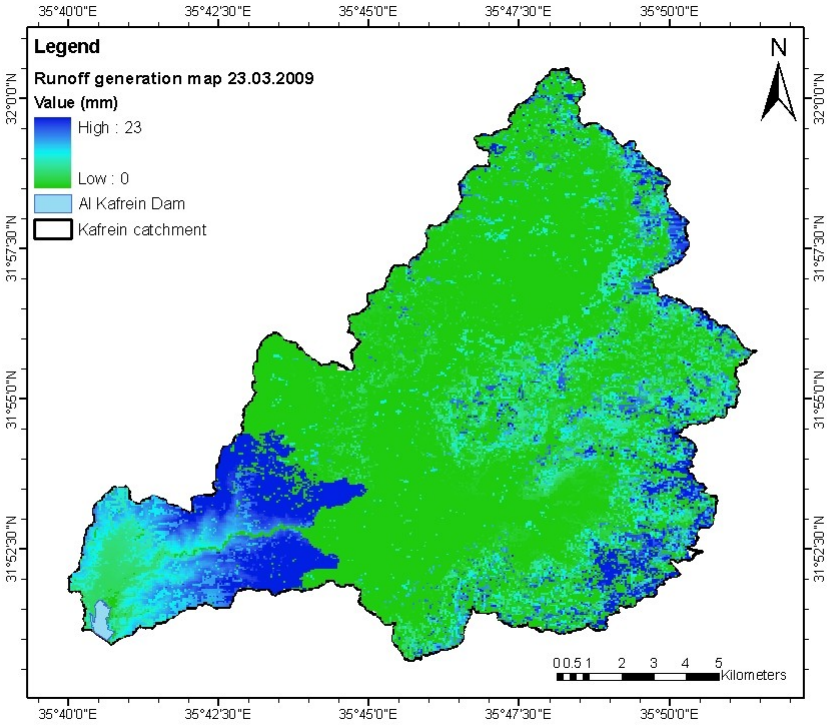

Fig. 5.54: Spatial runoff distribution on Mar. 23rd, 2009.

5.9.4.4 Runoff coefficients

The runoff coefficient is the percentage of runoff from the precipitated rainfall. The mean daily values of the generated runoff and the precipitated rainfall were used to calculate the runoff coefficients for the entire modelling period of 2007-2009. The water year 2007/2008 had low runoff coefficients, not exceeding 4% (as shown in Fig. 5.55) compared to runoff coefficients of more than 10% in the water year 2008/2009 (Fig. 5.56).

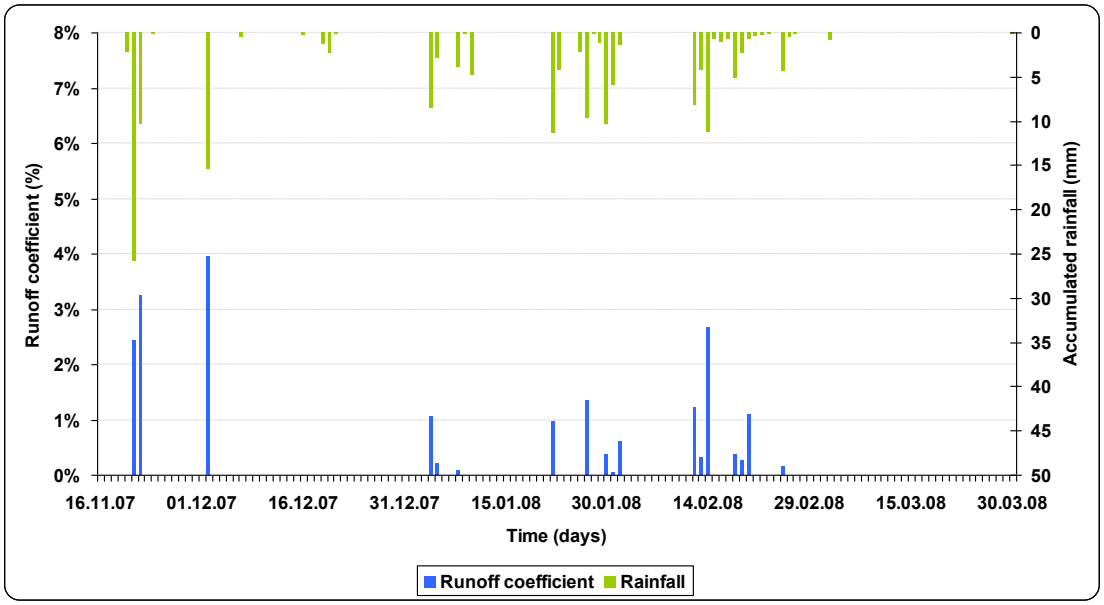

Fig. 5.55: Runoff coefficients for all events during the water year 2007/2008.

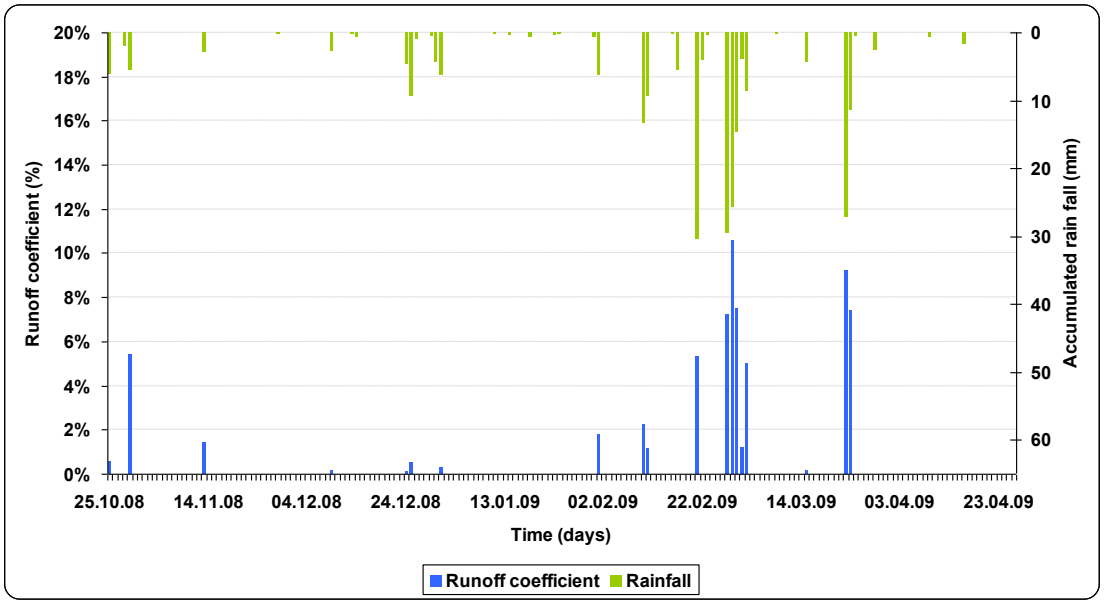

Fig. 5.56: Runoff coefficients for all events during the water year 2008/2009.

In the calibration year, 2008/2009, the second storm event of 27.02-03.03.09 had the highest runoff coefficients (Feb. 28th) with a value of 10.6%. As stated earlier, the runoff during this day was mainly generated due to saturation conditions of the soil and all the additional rain was transformed to runoff. During the third storm event on Mar. 23rd, a high magnitude of runoff was also generated (9.2%) due to the high intensity of the precipitation and prevailing infiltration excess conditions.

5.9.5 Water balance

The water balance has been calculated for the water years 2007/2008 and 2008/2009 while for the water year 2009/2010 the data was available and the modelling was conducted until the 23rd of December, 2010 (Table 5.12).

Table 5.12: Water balance of the monitored years.

Water year	Rainfall		Evapotranspiration		Recharge		Runoff		Soil storage	
	mm	MCM	%	MCM	%	MCM	%	MCM	%	MCM
2007-2008	167	26.9	90.6	24.4	7.7	2.1	3.8	1.0	0.3	0.07
2008-2009	250	40.3	77.0	31.1	18.0	7.2	5.0	2.0	0.2	0.1
2009-2010*	128	20.7	45.6	9.5	7.1	1.5	3.3	0.7	44.4	9.2

*** Until 23.12.2009**

The water balance was calculated for both water years starting from the first rainy day until the end of August of the next year, this has been done to simulate the evapotranspiration during the summer time and to calculate the soil storage and soil emptying in the summer period. Evapotranspiration was simulated on a daily basis, considering the evaporation due to interception, evaporation from initial losses, transpiration from canopy, and evaporation from soil surfaces.

Evapotranspiration in the water year 2007/2008 accounted for almost 91% of the total precipitated amount. Interception accounted for 17.9% while evaporation from initial

losses, transpiration from canopy, and evaporation from soil surfaces accounted to 33.3%, 26.9% and 21.9%, respectively. For the second water year evapotranspiration accounted for 77% of the water balance with 15.2% due to interception, 32.6% as evaporation from the initial losses, 26.6% as transpiration from canopy, and 25.6% as evaporation from soil surfaces.

In the water year 2007/2008, recharge accounted for only 7.7% of the precipitation. This low percentage can be substantiated by the dry winter, which is considered one of the driest in the record of the Jordan Meteorological Department since 1923. This dry year with only 167 mm of area rainfall had precipitation which is less than 50% of the long term annual average precipitation over Wadi Kafrein catchment. The next water year of 2008/2009 had a higher percentage of precipitation becoming recharge (18%). Around 56% of the recharge in 2008/2009 was due to the storm event of 27.02-03.03.2009, in which **SEOF** was the dominant runoff generation mechanism. This reflects the soil saturation conditions which preceded this storm event.

The generated runoff in the water year 2007/2008 accounted to 3.8% of the precipitation, which was mainly generated due to infiltration excess overland flow mechanism. 3.7% of the precipitation was runoff generated due to **IEOF** while only 0.1% was generated due to **SEOF**. The transmission losses are 24% of the generated runoff (0.25 MCM). In the following year, the generated runoff accounted to 4.96% with 2.78% as **SEOF** and 2.18% as **IEOF**. The transmission losses present 26% of the generated runoff (0.52 MCM).

The soil storage was low at the end of the water year due to persistent dry conditions. In 2007/2008, soil storage began in the second half of November, 2007 with a mean area value of 20 mm and reached its maximum value in the middle of February, 2008 with a mean area value of 55 mm (Fig. 5.57). The soil was almost fully depleted with mean values not more than 1 mm by the end of May. For the following year, the soil storage started earlier as the winter season started at the end of October, 2008 with low mean values while the maximum soil storages were up to 77 mm in the beginning of March, 2009. This is following the storm event which had much of the generated runoff due to **SEOF** runoff mechanism. Another high value of soil storages were calculated at the end of March, following the storm event on March 23rd with maximum soil storage of 79 mm as a mean value (Fig. 5.58).

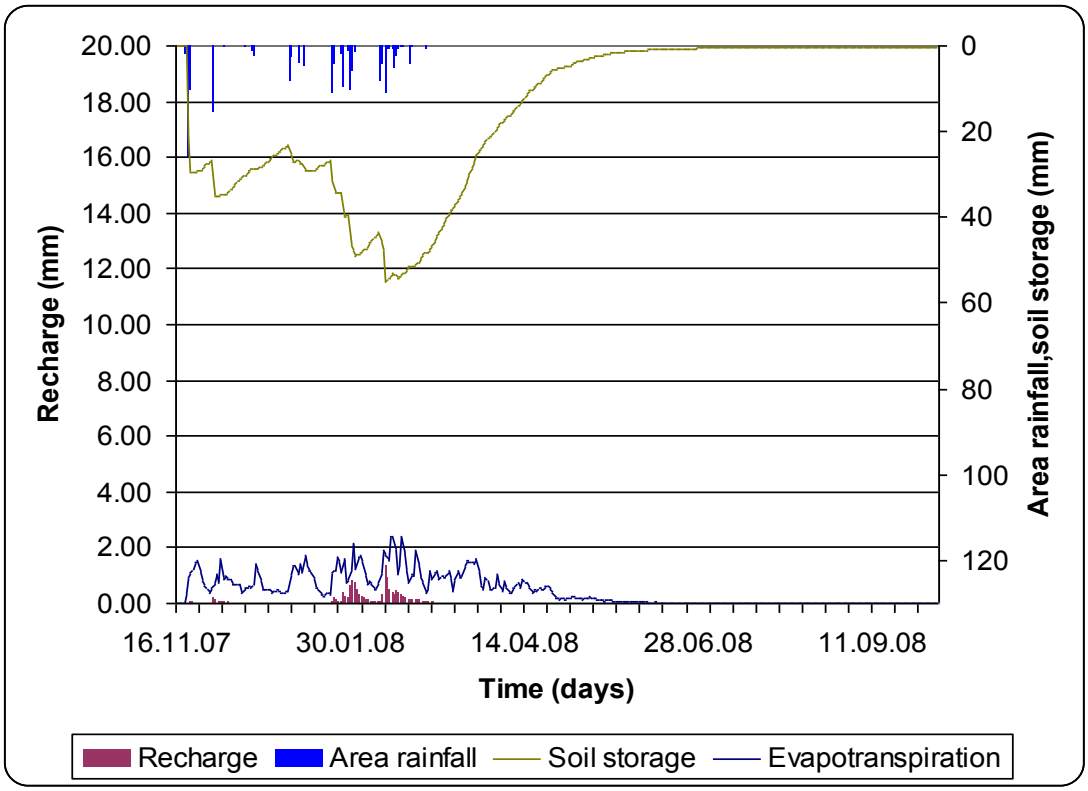

Fig. 5.57: Rainfall, recharge, evapotranspiration and soil storage amounts for the water year 2007/2008.

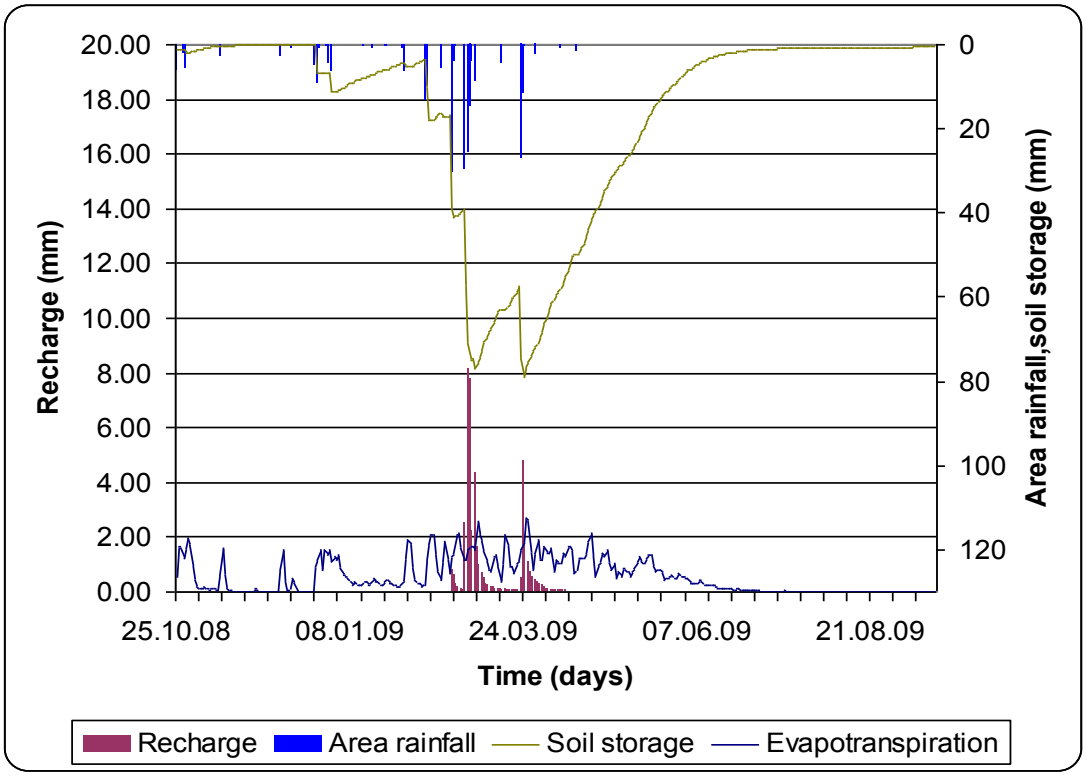

Fig. 5.58: Rainfall, recharge, evapotranspiration and soil storage amounts for the water year 2008/2009.

6 Model applications and predictions

6.1 Introduction

The topic of this Chapter is the application of the physically based and spatially distributed TRAIN-ZIN model as well as a discussion on the prediction capacity of this model. Questions pertaining to resulting model outputs and their relevance are the most pressing at this stage of the discussion. Also, the further application of the model is another pertinent issue; i.e. in which areas of research interest can the model be applied? The TRAIN-ZIN model has many advantages and further information as to why the model was selected can be found in the previous section, Model selection criteria (section 3.5).

The model has been shown to accurately simulate the hydrology of Wadi Kafrein (see section on model calibration and validation). With this model, one may also accurately predict what may happen to the hydrology of Wadi Kafrein if climate induces forcible changes to the various water balance components. Not only may the model predict the effects of climate induced changes, the model may also take catchment land/surface use changes into account. The validated TRAIN-ZIN model may be used to predict the impact of local climate change (variations in precipitation and temperature). This will be discussed in this chapter in addition to a further hydrological modelling for the water years extending from 2002 until 2007. Finally, the simulated impact of urban expansion and land use changes on the water balance components of Wadi Kafrein will be discussed.

6.2 Application One: Climatic changes and scenarios for Wadi Kafrein

Like the climate of the earth, the climate of Jordan has not been constant over geological history. As evidenced in the geological record, the part of the earth which is known today as Jordan was, during several geological periods from the early Cambrian to Lower Cretaceous, not dry land but land submerged under water (Orni and Efrat, 1971). During the late Cretaceous and the Tertiary Periods, the water of the Tythes had receded and Jordan had experienced dry continental climates. The Nubian Sandstone, which dominates the geological foundation in several locations of Jordan, is an artifact of this recession (Abed, 1983; Burdon, 1959).

The Pleistocene and Holocene Epochs had the last climatic changes that included important geological impacts. These changes, which happened during the Pleistocene and Holocene, have left important geomorphologic features on the landscape. Native ecosystems are now based around many of these features (Shehadeh, 1990).

As of now, no consensus has been reached among scientists as to the identification of what the most certain future climatic changes may be, which will be affecting Jordan and the region. Salameh (2009) studied the effect of climatic changes on surface and ground water resources in the northwestern part of Jordan. The analysis of

precipitation records has shown a general decreasing trend over the last four decades. This agrees with the climatic scenarios prepared by Pe'er and Safriel (2000) who studied the climatic changes in the region and predicted a decrease in precipitation. Hamdi et al. (2009) analyzed data from six meteorological stations distributed around Jordan to detect trends in weather parameters in Jordan. Results of this study indicated no visible positive or negative trends in the annual precipitation and maximum temperature. Bani-Domi (2005) concluded in his study that none of the precipitation series show significant deterministic and stochastic trends. The slope estimates show negative rates of change in the total annual rainfall for most of the stations, except for the stations located at high elevations. In a report prepared by the IPCC (2000) about the regional impact of climate change of the Middle East and Arid Asia, statements were made on there being no discernible trend in annual precipitation over the observed time series from 1901-1995 for the region as a whole. The only notable change, as stated by this report, was in the southwestern part of the Arabian Peninsula where there was a 200% increase in annual precipitation.

A slight increase in winter precipitation was predicted throughout the Middle East (UNEP, 1997). Taking this in consideration with the other studies, one can see clearly that predictions vary. Due to these varying conclusions on the overall trends in climate, one can expect the continued generation of different future climatic scenarios. These scenarios will be differing from one another because they will be based on differing climatic interpretations. Naturally, these scenarios differ not only because of data but also because of the type of data. The length of time series and statistical analysis procedures most likely differ. A scenario based on a data set of two years is obviously much different in scope than a data set, which spans 50-60 years or even longer.

Future climatic scenarios presented by the Intergovernmental Panel on Climate Change (IPCC) and established by the World Meteorological Organization (WMO) and United Nations Environment Program are some of the most widely accepted scenarios. Global Circulation Models (GCMs) and Regional Circulation Models (RCMs) are used by the IPCC in the creation of their future climate scenario reports.
Most decisions having to do with climate effects are made by government leaders who are educated on the predictions of GCMs. GCMs can be used to investigate possible causes of climate change and to simulate past and future climates. However, although GCMs are widely accepted, they have been criticized as to their limitations by Legates (2002). Issues are:

- An incomplete understanding of the climate system
- An imperfect ability to transform our knowledge into accurate mathematical equations
- The limited power of computers
- The models' inability to reproduce important atmospheric phenomena
- Inaccurate representations of complex natural interconnections

The scale of GCMs is not in concordance with catchment scale hydrological models, creating limitations for those interested in the link between catchment hydrology management and climate change. However, scaling procedures to downscale information from the large grid cell to the scale of the head water basins are available as discussed in Leavesley and Hay (1998). GCM-based predictions, however, are still

too uncertain to be used as the basis for effective public policy responses related to future climatic changes. GCMs can, at best, represent only a rough estimation of real world situations, with spatial resolutions no finer than regional areas of a thousand square kilometers.

Models aside, common knowledge based on observation shows that on the regional scale, the Middle East and North Africa (MENA) is one of the regions that is most vulnerable to climate change. Here exists one of the highest levels of water scarcity in the world and the majority of income and employment depend on climate-sensitive agriculture. By mid-century, per capita water availability will decrease 50% because of population growth alone, and climate change is predicted to reduce average precipitation levels by 20-30% in some parts of the region. Variability of precipitation patterns will also be increased, making water harder to manage everywhere on Earth (Cervigni et al., 2009).

The increasing variability of precipitation patterns is a pressing issue and is further compounded by the non-unanimous agreement on what exactly the effects of global climate change will be. Taking this into consideration, it is not obvious which trend the precipitation will take within the Middle East. For Jordan, the precipitation may increase or decrease in the future; no one is certain. Also, no one can say with confidence and support whether the rain events will clearly shift in terms of starting or ending of precipitation events. However, records of Jordan's climate and the World itself do show an increase in temperature (Pe'er and Safriel 2000; IPCC, 2001; Cervigni et al., 2009).

New approaches must be developed, which can overcome these limitations and which can also be used to evaluate the effect of climate change on the water balance. This is of most interest to the decision makers of the water sector in Jordan. A new approach has been developed which takes into consideration the impact of precipitation properties and temperature increase on the water balance. This development will be discussed in the coming sections.

6.2.1 Variations in rainfall amounts and intensities

In order to investigate the impact of extreme changes in precipitation amount and intensity, such as those induced by a changing global climate system, extreme years from the climate record were implemented in the model. This new method of approach is one way to overcome the problem of uncertainties in using GCMs. In this approach, the aim is not to predict climate change; rather, the aim is to investigate the impact of variations in precipitation amount and intensity using extreme years (very wet and very dry) as a boundary to predict the impact on the different water components of Wadi Kafrein catchment. Within the same line of reasoning, the impact of temperature increase on runoff generation, evapotranspiration, and recharge were also investigated, but this will be discussed subsequently.

Historical climate data from Wadi Kafrein was retrieved from the records of the Jordanian Ministry of Water and Irrigation (MWI). Daily rainfall values and intensities were analyzed for eight rainfall stations over the time span from 1980 to 2008. The spatial distribution of the stations, which are operated by the MWI, is

shown in Fig. 4.13 and 6.5 of this chapter. The data of these rain stations were used to prepare several climatic scenarios which simulate the expected precipitation patterns. The scenarios have been prepared in two steps. The first step was the scenarios being prepared based on the annual rainfall amount and the daily accumulated rainfall. The second step was daily rainfall time series of all scenarios were refined with respect to temporal resolution. This step was possible by statistical analysis of all rainfall events monitored during the period of this research (2007-2009), in which a high temporal resolution of rainfall data is available. From these rainfall events, several rainfall intensity patterns were selected and were used as an index to refine the available daily data, which did not have such a high resolution.

Figure 6.1 shows an example of the data series from one station (Wadi Es Sir Rain station). The annual rainfall amounts are from 1943 to 2008. These values have been calculated from daily data. The long term annual average is 523 mm.

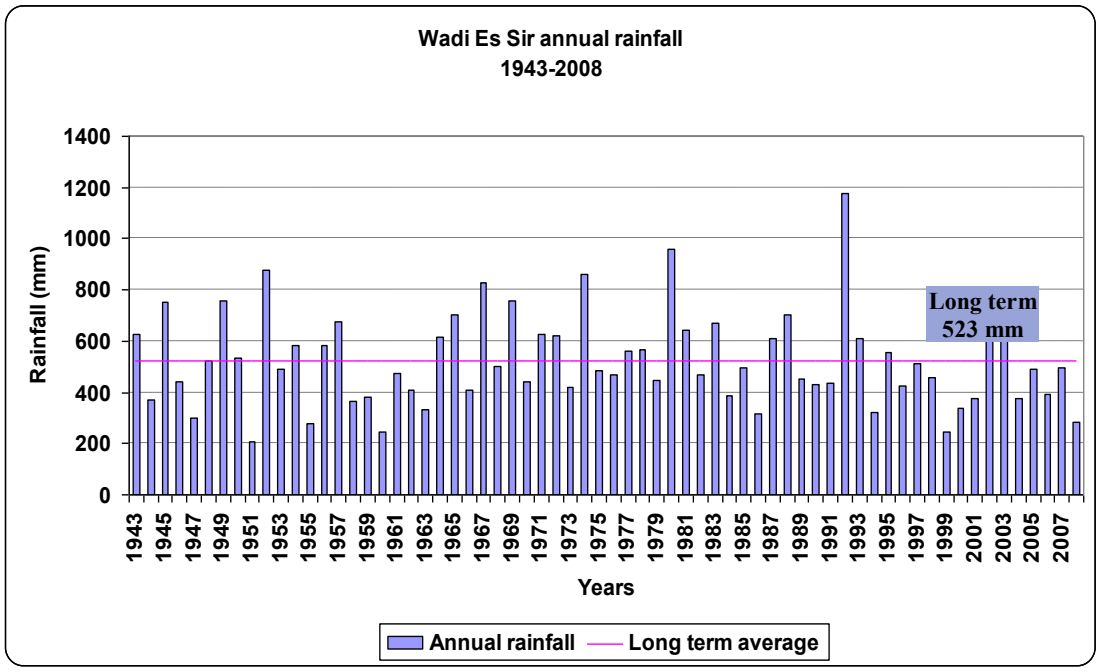

Fig. 6.1: Annual rainfall amounts for Wadi Es Sir Rain station from 1943 to 2008.

Rainfall data series are available from all stations covering the last 30 years. Records preceding the early 1980's were kept at only few of the stations. Due to this fact, the available rainfall data from 1980 to 2008 were used in the climatic scenarios. Records dating to 65 previous years were selected for the evaluation of impacts from extreme years (very wet and very dry water years). Two extreme water years, 1991/1992 and 1998/1999, which were the wettest and driest, respectively, were used for the specific years used in the scenarios. Figure 6.1 indicates that the water year 1991/1992 is the wettest year on record while the water year 1998/1999 is the second driest after the 1950/1951 year. Data on 1950/1951 were not available recorded at all rainfall stations; so in order to use the years with maximum data, the 1998/1999 water year was selected and analyzed.

6.2.1.1 Rainfall data preparation and downscaling

The annual and daily approach can be summarized as follow:

1. Daily rainfall data were acquired from all available rainfall stations (operated by MWI/Jordan), distributed between the Jordan Valley (1 station), inside the catchment area (3 stations), and around the catchment area (4 stations), see Fig. 6.5.

2. The available rainfall data were statistically analyzed for every station for the period extending from 1980 to 2008. The annual rainfall amount, number of rainy days, and rainfall depth of every day were considered.

3. Different climatic scenarios which present the possible precipitation patterns were prepared: *Wet Year* (2 scenarios), *Average Year* (1 scenario), and *Dry Year* (2 scenarios). This yielded five main scenarios as shown in Table 6.1 and graphically in Fig. 6.2.

A water year has been considered as a wet year when the annual accumulated rainfall amount of that year is higher than the long term annual average rainfall in at least 25%, while a water year is considered dry when the total accumulated rainfall of that year is less than the long term annual amount in at least 25%. So far, the annual rainfall amount was considered not the daily rainfall depth; therefore, two scenarios for every wet and dry year were considered based on two factors: *first*, number of the rainy days, *second* the daily accumulated rainfall amount (rainfall depth, mm/day). The total daily accumulated rainfall amounts of every station for the whole time series were calculated then the results were grouped as follow:

- Number of rainy days with precipitation less than 25mm/day.
- Number of rainy days with precipitation between 25 and 50 mm/day.
- Number of rainy days with precipitation between 50 and 75 mm/day.
- Number of rainy days with precipitation between 75 and 100 mm/day.
- Number of rainy days with precipitation more than 100 mm/day.

By combining the annual rainfall amount with the daily rainfall amounts (based on their statistical properties), five scenarios of water years are proposed as shown in Table 6.1. The average year has been selected in which a year with an average long term annual rainfall and an average daily rainfall characteristics. The daily rainfall amounts were calculated and analyzed for all rainfall data since 1980 until 2008 for the eight rainfall stations used in the approach.

Table 6.1: The proposed scenarios based on yearly rainfall amount and daily rainfall depth.

Annual Rain	Daily Rainfall amount	Scenario ID	Description
High	**H**igh Rainfall Depth	Scenario 1-**HH**	Wet year with high daily rainfall depth
	Low Rainfall Depth	Scenario 2-**HL**	Wet year with low daily rainfall depth
Average	**Av**erage Rainfall Depth	Scenario 3-**Avg**	Average year with average daily rainfall depth
Low	**H**igh Rainfall Depth	Scenario 4-**LH**	Dry year with high daily rainfall depth
	Low Rainfall Depth	Scenario 5-**LL**	Dry year with low daily rainfall depth

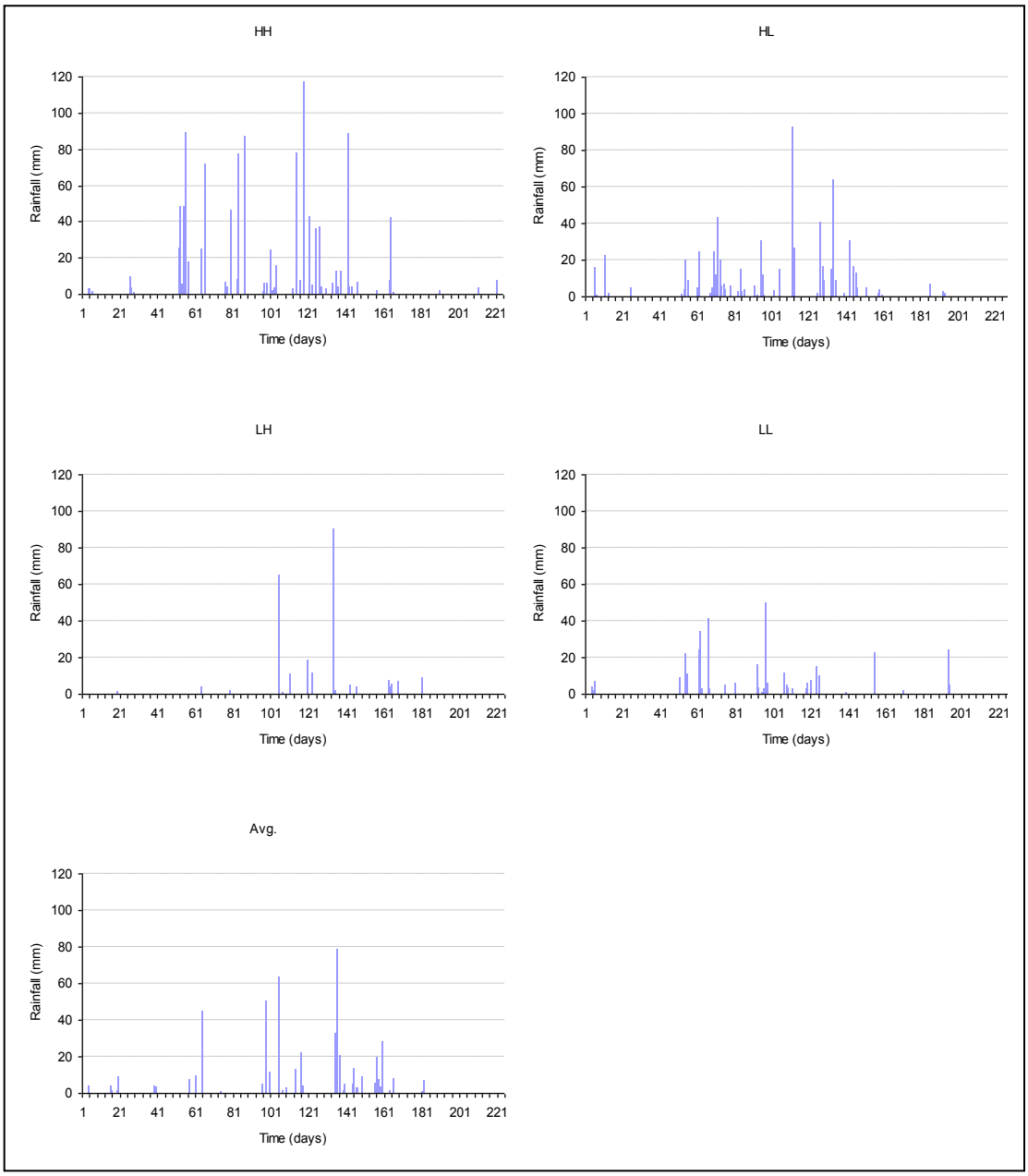

Fig. 6.2: The proposed climatic scenarios based on yearly rainfall amount and daily rainfall depth.

The available data which have been used in developing the climatic scenarios are in daily bases, but for detailed representation of runoff generation processes; a higher temporal resolution is required. Therefore; the rainfall pattern was studied from the raingauges stations which have been installed in the study area with data records from October 2007 until December 2009 and has a temporal resolution of 5 minutes. The rainfall patterns have been studied for all rainfall events with 5 minutes time step and were categorized as follow:

- Events with *high intensity* in one day: see Fig. 6.3 and 6.4a
- Events with *step wise* precipitation in one day: see Fig. 6.3 and 6.4b
- Events with *low intensity* in one day: see Fig. 6.3 and 6.4c

These patterns represent the way in which rainfall can take place, that is for the same rainfall amount the rain can fall either with high rainfall intensity within few hours (*high intensity*) or it can fall with low intensity along the day (*low intensity*) or it can be a combination between high intensity then several hours of no rain and then it rains again (*step wise*). By combining the annual scenarios presented in table 6.1 with the 5 minutes rainfall patters a total of 15 scenarios were generated as presented in table 6.2.

Table 6.2: The proposed 15 climatic scenarios based on rainfall amount and intensity.

Annual	Daily	5 Minutes	
High total amount	**H**igh Rainfall Depth	**H**igh **I**ntensity **S**cenario	**HIS**
		Step **W**ise **S**cenario	**SWS**
		Low **I**ntensity **S**cenario	**LIS**
	Low Rainfall Depth	**H**igh **I**ntensity **S**cenario	**HIS**
		Step **W**ise **S**cenario	**SWS**
		Low **I**ntensity **S**cenario	**LIS**
Average total amount	**A**verage Rainfall Depth	**H**igh **I**ntensity **S**cenario	**HIS**
		Step **W**ise **S**cenario	**SWS**
		Low **I**ntensity **S**cenario	**LIS**
Low total amount	**H**igh Rainfall Depth	**H**igh **I**ntensity **S**cenario	**HIS**
		Step **W**ise **S**cenario	**SWS**
		Low **I**ntensity **S**cenario	**LIS**
	Low Rainfall Depth	**H**igh **I**ntensity **S**cenario	**HIS**
		Step **W**ise **S**cenario	**SWS**
		Low **I**ntensity **S**cenario	**LIS**

The daily amount differs in every storm event, therefore the storm events were grouped as follow:

- Storm event with precipitation less than 25 mm per day
- Storm event with precipitation from 25-50 mm per day
- Storm event with precipitation from 50-75 mm per day
- Storm event with precipitation from 75-100 mm per day
- Storm event with precipitation more than 100 mm per day

By combining the daily storm amounts (5 groups) with the precipitation patterns (3 patterns) a 15 pattern index have been produced and the daily rainfall amounts had been downscaled to 5 minutes time step taking in consideration the daily precipitation amounts and the storm events patterns. Every storm event group has a total daily rainfall amount index, from which the given daily rainfall had been downscaled to 5 minutes time step based on the downscaling pattern index as shown in Fig. 6.3.

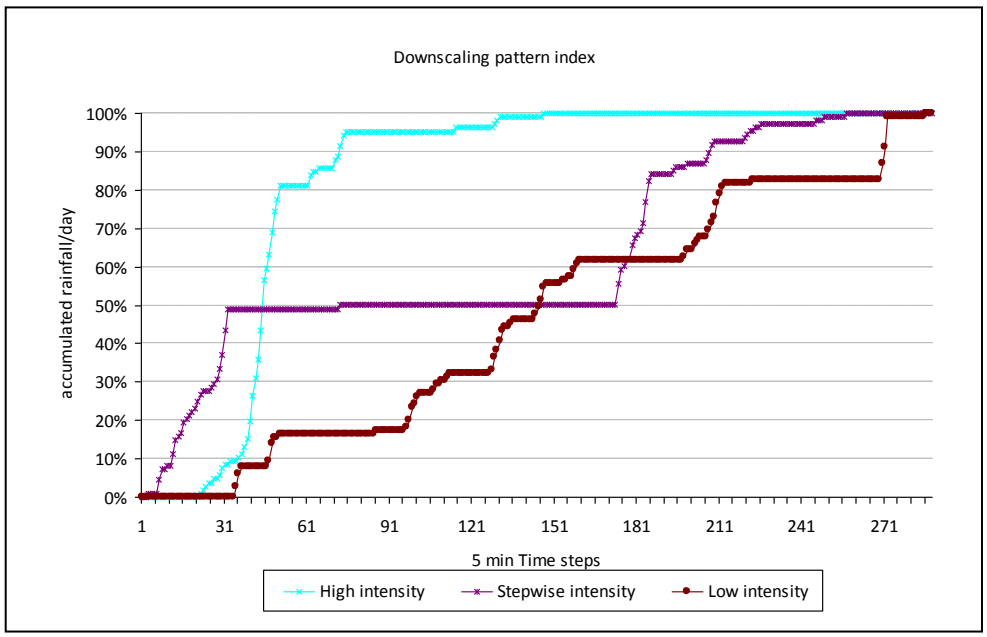

Fig. 6.3: Daily rainfall downscaling approach using 3 intensities patterns.

By considering the different rainfall intensities patterns, the same rainfall amount can fall in the same day with different intensity per same time step (i.e. 5 minutes). Figure 6.4 shows the different patterns which are proposed for the same daily rainfall amount but different amount per time step.

As the rainfall data were prepared and downscaled based on the above mentioned approach, accordingly this approach has been applied for the eight rain stations data series for the selected scenarios to be simulated. The other important data which are still required before starting the simulation are the climatic parameters (i.e.: temperature, relative humidity, solar radiation and wind speed). The climatic parameters were collected and interpolated from 5 weather stations distributed between the Jordan Valley and the high lands to the east and are discussed in the coming section.

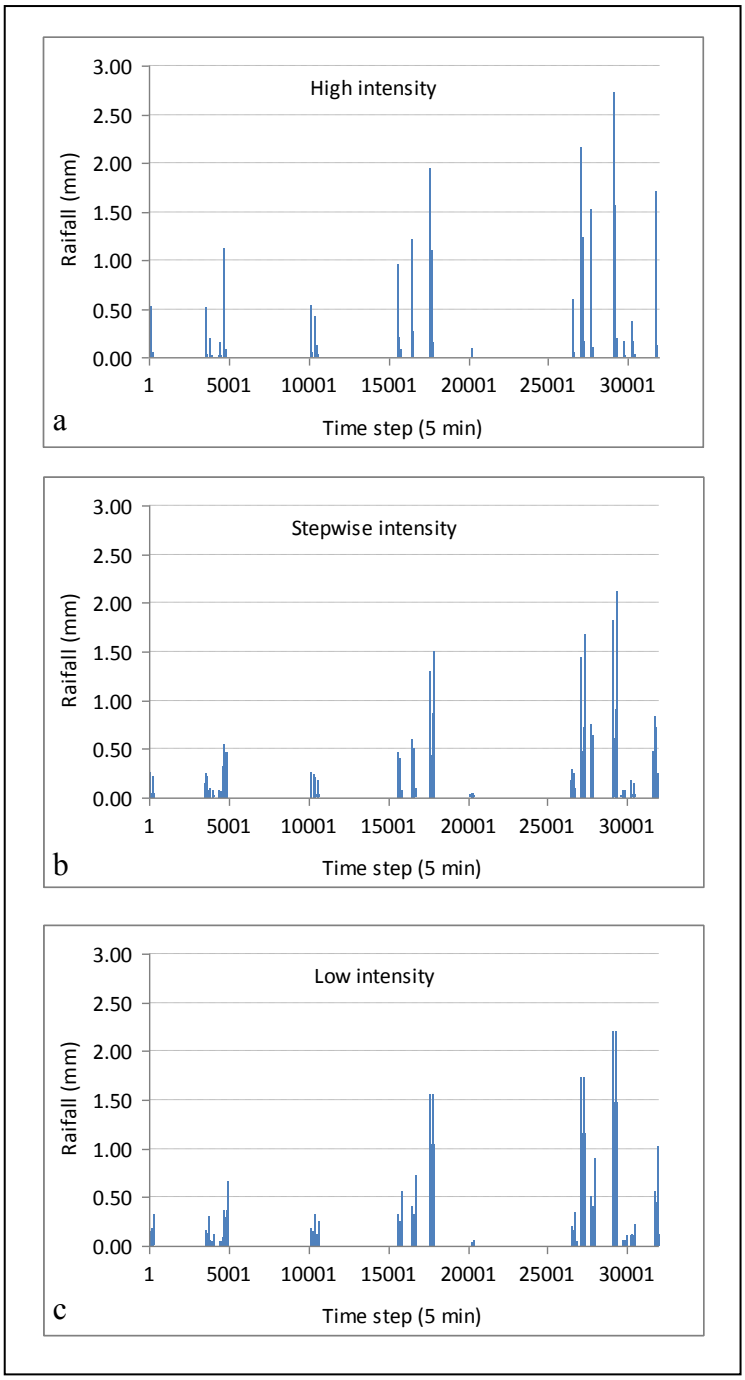

Fig. 6.4: Possible distribution patterns for similar rainfall amounts.

6.2.1.2 Climatic data preparation and interpolation

In this research a complete data set from five weather stations were prepared to be used in the proposed climatic scenarios (Table 6.3). The climatic parameters were collected from two weather stations operated by the MWI and three weather stations operated by the Jordan Meteorological Department (JMD). The spatial distribution of the raingauges and the weather stations is given in Fig. 6.5.

The weather stations are distributed between the Jordan valley in the western side and the high lands to the east of the study area. It has been considered to get the most possible available data spatially and temporally because the variations within the

catchment area of Wadi Kafrein are wide. The contradictory and huge variations within short distances require detailed and careful analysis in which the availability and quality of the data play a big role.

Table 6.3: Locations of the weather stations used in the climatic scenarios.

Station	Authority	Latitude (N)	Longitude (E)	Altitude (m)
Salt	JMD	$32^0 02`$	$35^0 44`$	796
South Shuna	MWI	$31^0 54`$	$35^0 38`$	-160
Sweileh	JMD	$32^0 00`$	$35^0 54`$	1050
Jordan University	JMD	$32^0 01`$	$35^0 53`$	980
Wadi Es Sir (NRA yard)	MWI	$31^0 57$	$35^0 51`$	900

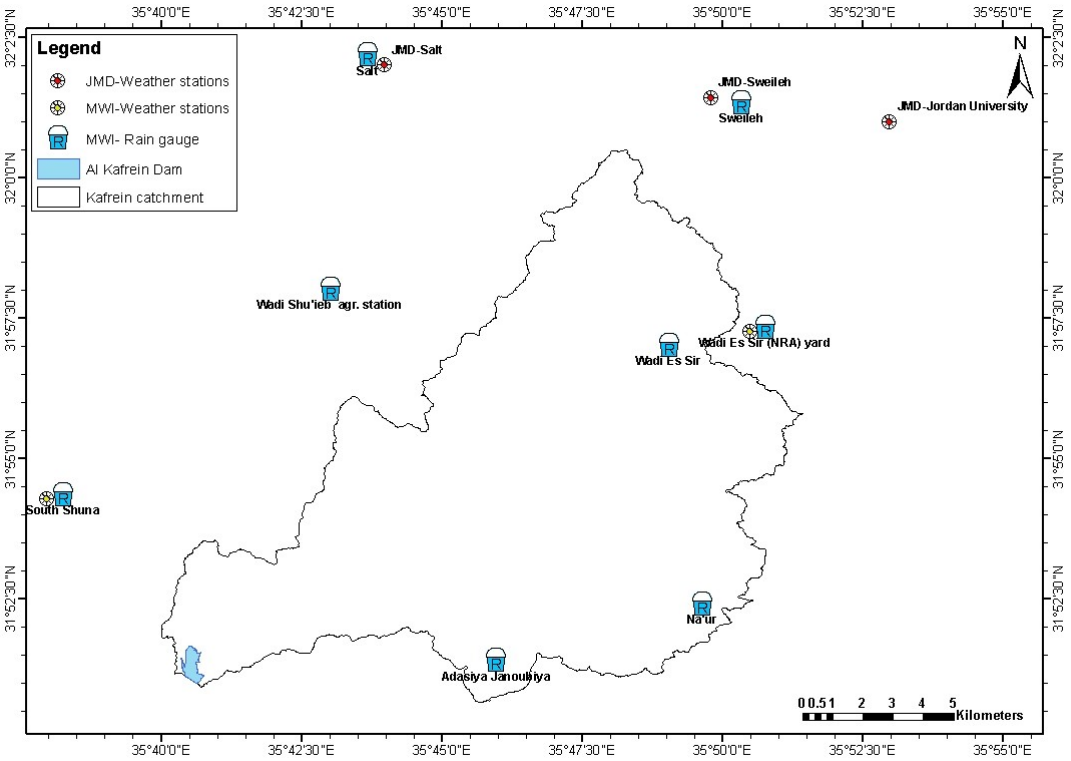

Fig. 6.5: Weather stations and raingauges used in the climatic scenarios.

6.2.2 Variations in temperature

The annual and seasonal mean (minimum and maximum) temperature variations in Jordan during the 20th century were studied by Smadi (2006). The analysis showed a significant warming trend after 1957 and 1967 for the minimum and maximum temperatures, respectively. The analysis of maximum temperatures shows a significant warming trend after the year 1967 for the summer season with a rate of temperature increase of 0.038 °C/year. Bani-Domi (2005) analyzed the trends of temperatures in Jordan and the analysis of the mean minimum and maximum temperature records for different stations which showed a warming trend for the period 1964-1999. These studies in addition to other several studies refer to an expected increase in temperature in the coming future.

Long term climatic data were acquired from the MWI for several weather stations to analyze the general trend of temperature in Jordan. As it is expected with all GCMs and RCMs a general increase in temperature is most probably the general trend to take place in the coming future.

The acquired data were available in monthly basis for the maximum, minimum and the mean temperature values. Data show a general increase trend in maximum, minimum and the mean value. As an example; the data acquired for the South Shuna station are given in Figs. 6.6-6.8 from the time period of March, 1965 until December 2008 in which an increase trend is noticed in all figures. The trends show an increase in the mean temperature value of no more than 2 °C. In this research and to simulate the effect of any future climatic increase in temperature on the water balance of Wadi Kafrein the following scenarios were prepared:

- The water year with an average scenario was selected, considering the downscaling approach which gives 3 possible distribution patterns in which the rain may fall (high intensity, stepwise intensity and low intensity), the mean temperature was increased 1°C, 2°C, and 3°C respectively for every scenario.

- Three scenarios were proposed with 1°C increase per each scenario. This has been applied for the three distribution patterns of rainfall intensity producing 9 different scenarios for the temperature increase model application.

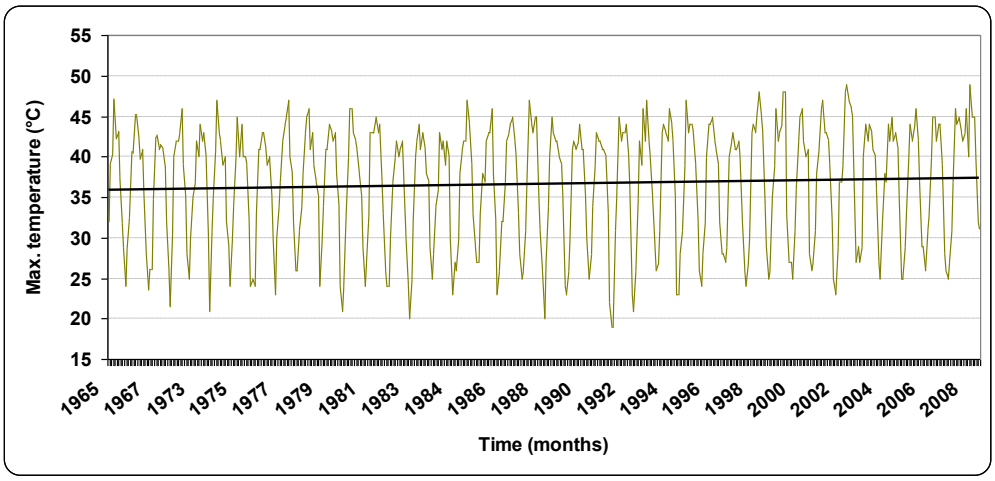

Fig. 6.6: Monthly maximum temperature in South Shuna weather station from 1965-2008.

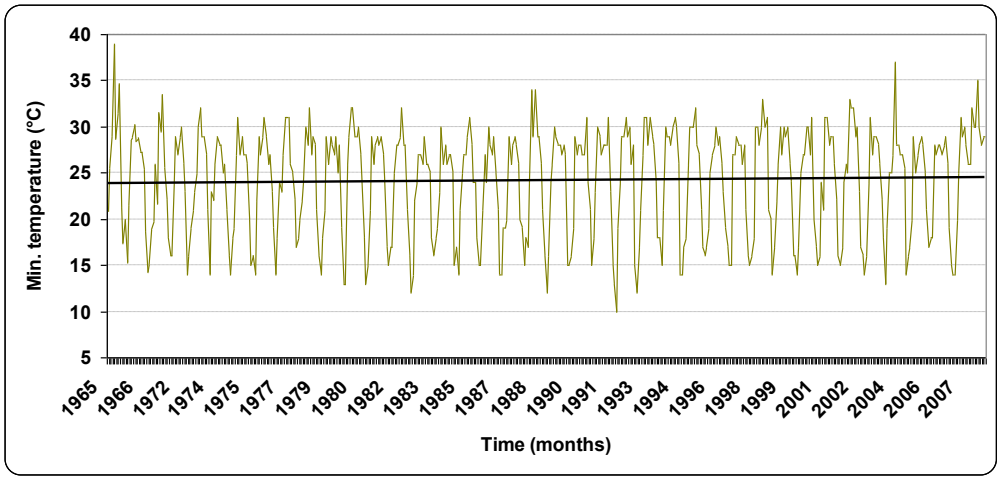

Fig. 6.7: Monthly minimum temperature in South Shuna weather station from 1965-2008.

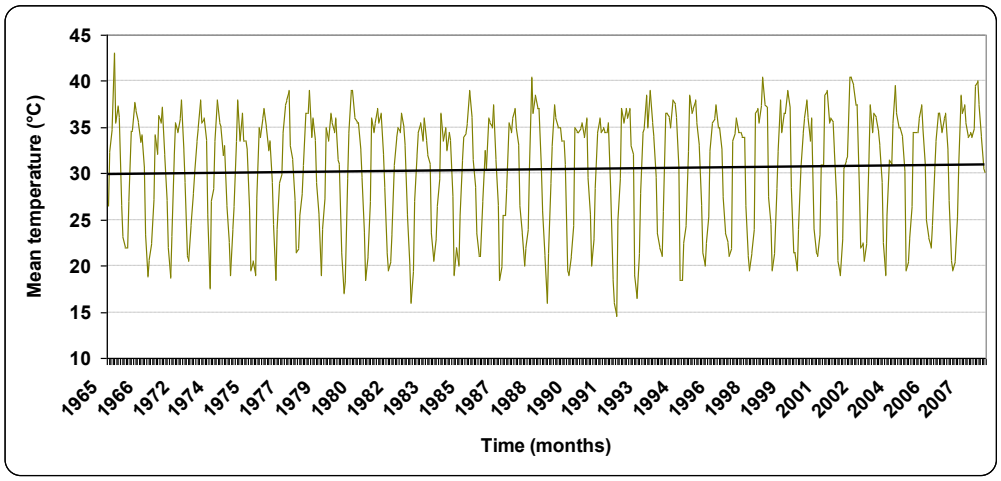

Fig. 6.8: Monthly mean temperature in South Shuna weather station from 1965-2008.

6.3 Application Two: Hydrological modelling for water years from 2002 to 2007

Since 2002, the Kafrein dam office is operating daily discharge measurements to the water before entering the dam. These data were used and the years from 2002 until 2007 were simulated to evaluate the model performance in different spatially and temporally data time series from those which were used during the study period (2007-2009). These data were acquired from the Dams Control Unit /Ministry of Water and Irrigation. The meteorological data were acquired from 5 weather stations and were spatially interpolated (Fig. 6.5). The rainfall data were acquired from eight rain stations similar to those used in the climatic scenarios. The physical properties of the study area were kept the same as those used during the calibration period. As any validation procedure only the time series of precipitation and climatological parameters were changed.

The rainfall data were collected for the same period (2002-2007) in daily basis for all rainfall stations and were spatially interpolated using the interpolation method with

elevation correction as described in section 5.6.6.1 of chapter five. The daily mean area rainfall values for the period 2002-2007 are given in Fig. 6.9. The vertical solid lines between the rainfall days were used to separate the water years from each other (i.e. only the winter season is plotted).

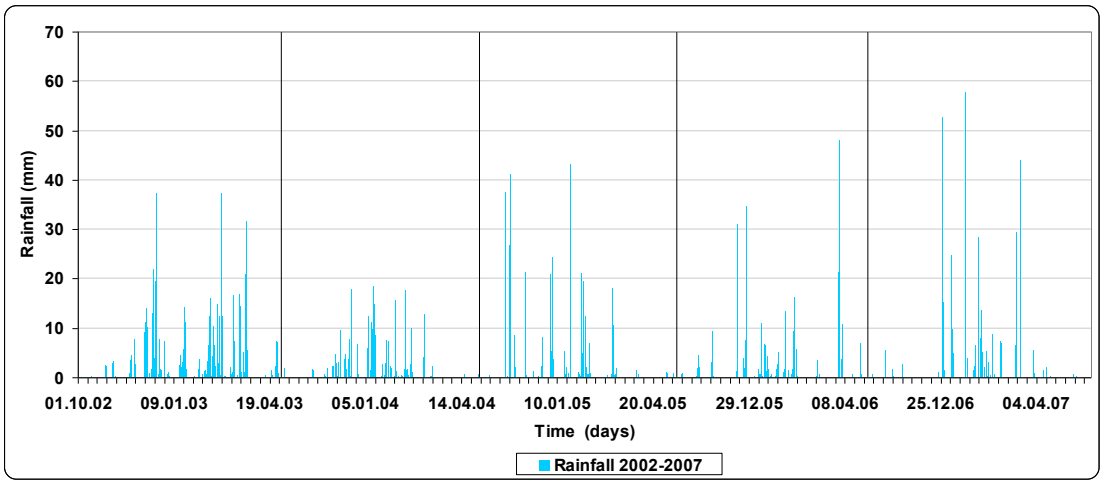

Fig. 6.9: Daily mean area rainfall for the period from 2002-2007.

The model was initially validated by runoff events during the period of the study (2007-2009) as explained in chapter five. As a source of further application of the physically based model, and to validate the model using non-stationary conditions the model was run to simulate the hydrological years extending from 2002 until 2007. Daily stream flow measurements are available downstream before the water enters the Kafrein reservoir. Data of spring discharge and the effluent of Wadi Es Sir WWTP were acquired and subtracted from the total measured daily stream flow.

A similar approach in down scaling the daily rainfall to 5 minutes to the one used in generating the climatic scenarios was used here. The difference is that after down scaling the daily precipitation to 5 minutes in the earlier mentioned three patterns, a random selection of every day was done. Meaning that every single day of the simulated years was downscaled using one pattern, either high intensity, stepwise intensity or the low intensity. This was done because in reality the storm events pattern varies from high to low intensity within the same hydrological year rather in the same day.

6.4 Application Three: Urbanization and land use changes

Land use changes, such as urbanization and agriculture are one of the most important anthropogenic influences on climate (Kalnay and Cai, 2003). Urbanization is the most powerful and most visible anthropogenic force on earth-affecting its surface, atmosphere, and seas; its biodiversity and its people. For all foreseeable future, virtually all population growth is projected to occur in urban (areas of high population concentration with high building density and infrastructure) rather than peri-urban (adjacent agricultural and undisturbed regions with low population concentration) areas (Stefanov and Netzband, 2005).

One of the most useful usages of a physically based distributed hydrological model is its ability to predict the impact of land use changes on the different hydrological components. This issue is of special interest for the decision makers and the water authorities when considering the water resources management plans.

Since the land use changes in the future are subject to a lot of uncertainty (similar to climatic changes) it is hard to predict which land cover will increase or decrease; however; there is an increase in concentration of the human population into urban areas and consequently a higher activity in construction and urbanization will most likely take place. The most prominent land use change to take place is the increase of the lands to be used for urbanization. This will result in a decrease in the other land use classes based on their relation to the present urban areas and how suitable they are to be used for urbanization.

Last census of population and housing of Jordan took place in 2004 which is done every ten years by the Department of Statistics of Jordan (DOS). The results of the 2004 census of population and housing showed an increase of buildings of 26.2% compared with 1994 and an increase of 44.7% in housing units compared with 1994 (DOS, 2004) , this is on the national scale. In Amman Governorate, the increase of buildings is 26.4% and 49.8% in the housing units compared with 1994. Also the population density increased from 47 persons /km^2 in 1994 to 60 persons / km^2 in 2004. The urban percentage has increased to 82% in 2004 compared to 78% in 1994.

In a catchment scale, the eastern boundary of the catchment area of Wadi Kafrein represents the western extent of Amman and Wadi Es Sir Cities. The cities are in a continuous expansion and it is expected to increase the urban area in Wadi Kafrein. Also the Na'ur and Aladassiya cities in the south eastern part are expanding toward west.

The urban areas expansion is expected to take place close to the present urban areas and their surroundings. To simulate the effect of urbanization expansion which is the most expected and accepted scenario for land use changes, the following approach has been followed:

- The prepared land use map (section 4.2.2 and Appendix C) and the developed soil map (section 4.2.4) were used in preparing the land use scenarios to simulate the urbanization expansion.

- The scenarios simulate an increase in the present urbanized area in all directions of 50 m up to 200 m in diameter (*LU50, LU100, LU150, and LU200*).

- The areas with slope higher than 20° were excluded as the present urbanization distribution map shows very low urban activities in steep areas more than 20°.

A base land use map has been used which presents the present situation of land use in Wadi Kafrein, and to simulate the effect of the expected future urbanization an increase in the present areas were considered of 50 meter in diameter.

A multi temporal ASTER satellite images were used to classify the land cover of Wadi Kafrein as discussed in section 4.2.2. The ASTER satellite images are very useful for arid and semi arid land cover classification as it has been demonstrated by Zhu and Blumberg (2002). The land cover map of Wadi Kafrein shows that the urban and built up areas presents 7.2% of the total catchment area of Wadi Kafrein.

In the Land Use 50 Scenario (*LU-50*), the urban area was expanded with 50 meter in all direction resulting in increase in the area occupied by urbanization from 7.2% to 11.4% from the total catchment area of Wadi Kafrein. The land use and soil maps were prepared by considering the increase in the urbanized area and the model was run to simulate the effect of urbanization on the water balance components of Wadi Kafrein. The increase in the urbanized area is shown in Fig. 6.10 for all land use scenarios (*LU-50-LU200*), in which it can be seen that the scenarios consider an urbanization expansion in the surroundings of the preset urban areas.

The increase in the urbanized area will consequently reduce the land cover of other classes as can be noticed from Fig. 6.11. The water surfaces class which occupies a small part of the catchment area represented by the Kafrein dam reservoir was not affected. On the other hand, all other land classes' areas were reduced due to the proposed urbanization expansion.

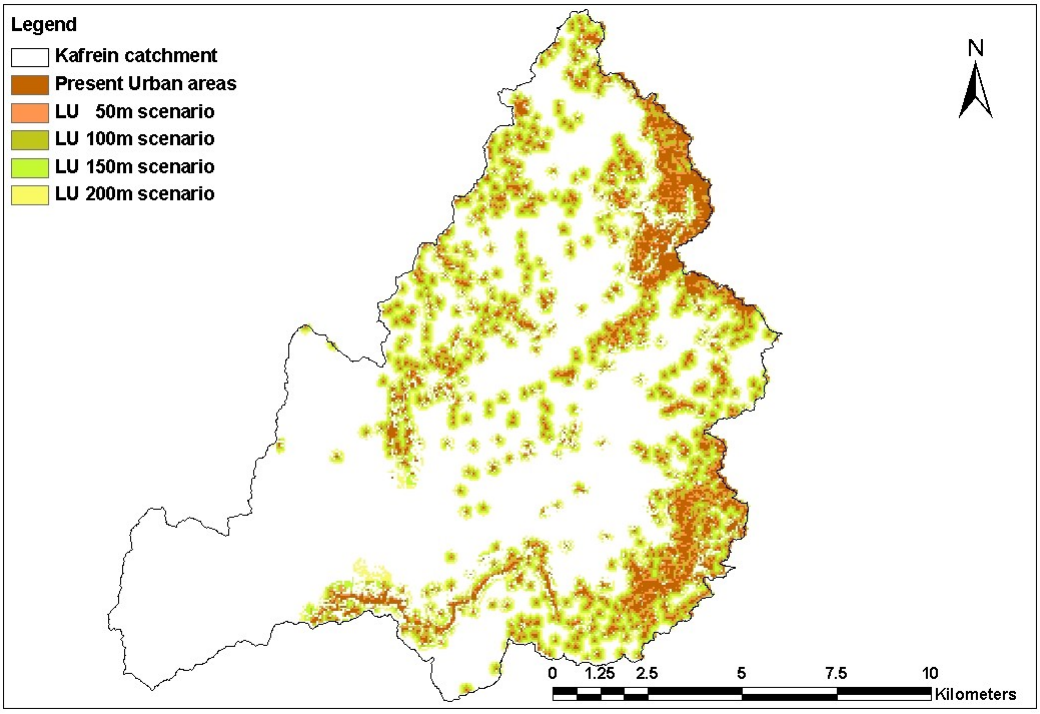

Fig. 6.10: Base map of land use and the resulted changes due to urbanization of different scenarios.

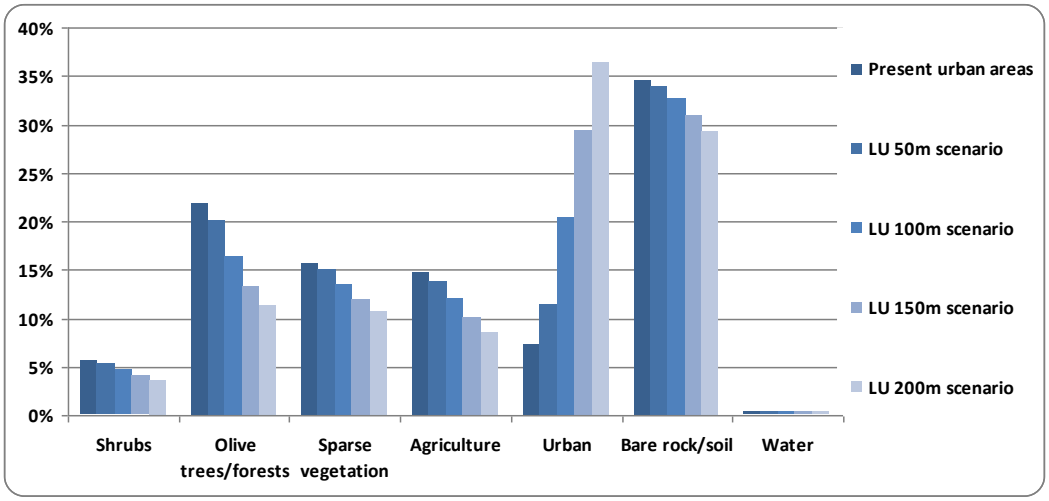

Fig. 6.11: Changes in land uses due to urbanization expansion.

6.5 Results and discussion

In earlier sections of this chapter the methodology of preparing the climatic scenarios and land use changes was explained, also the approach of time step downscaling and the further validation of the model using non-stationary conditions were discussed. In this part of the research the results will be presented and discussed with emphasis on the quantification of the water budget of Wadi Kafrein under all expected scenarios of climatic and land use changes.

6.5.1 Impact of rainfall amount and intensity on water balance

The aim of developing these climatic scenarios is to evaluate the effect of different rainfall amounts (high, low) and rainfall intensities (high, stepwise, and low) on the water budget of Wadi Kafrein. This has been prepared based on real data which include the wettest (highest rainfall amount) and driest (lowest rainfall amount) water years in the available rainfall records. Nevertheless, the rainfall division to evapotranspiration, recharge and runoff is not only affected by the annual rainfall amount but also it is highly affected by the precipitation intensity in one day or even in finer time step of minutes. For every climatic scenario year the daily rainfall was downscaled using 3 rainfall intensity patterns resulting in fifteen climatic scenarios.

The daily rainfall amounts were downscaled to 5 minutes using the 3 scenarios of *(HIS),* (*SWS)* and the *(LIS)* which are basically derived based on measured 5 minutes rainfall events during 2007-2009 as explained earlier. The recharged volume and the generated runoff are the most affected components due to the variations in rainfall intensities using the same rainfall amount of the five annual scenarios *(HL, HH, Av., LH and LL)*. The results of different scenarios using the *SWS* and *LIS* are not big when compared using the *HIS* scenario. For the same rainfall amount but with high rainfall intensities, (i.e. *HIS* scenario) the recharge volumes decreases while the generated runoff increases for the five annual scenarios.

The generated runoff is more affected by the rainfall intensity than the recharged volume because with high rainfall intensity the soil saturation conditions are not fulfilled and more rain will be diverted to runoff due to **IEOF** runoff generation process.

The generated runoff in a dry year with low rainfall depth (*LL*) did not exceed the 4.3% of the total precipitated rain while in a wet year with high rainfall depth (*HH*) the generated runoff presented 21.2% of the precipitated rainfall (Fig. 6.12). In an average year a clear increase can be noticed in the volume of the generated runoff using high intensity precipitation compared with the volumes which may generate using low or stepwise rainfall intensities as can be seen in Fig. 6.13. When rainfall precipitates in high intensities (*HIS*) more runoff will be generated due to **IEOF** as can be noticed from Fig. 6.14.

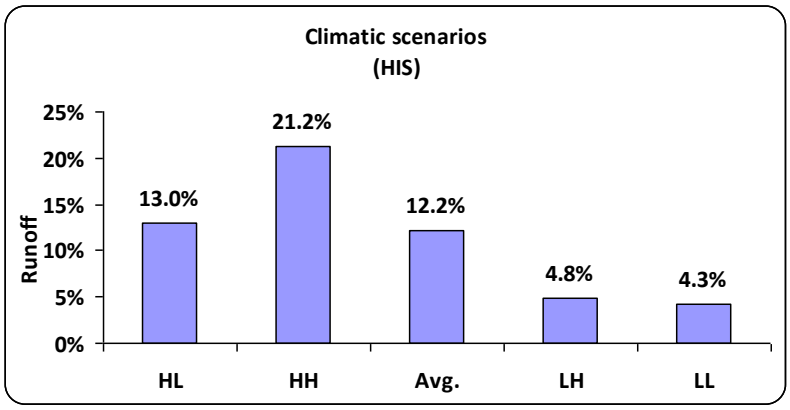

Fig. 6.12: Percentages of the generated runoff in the annual climatic scenarios.

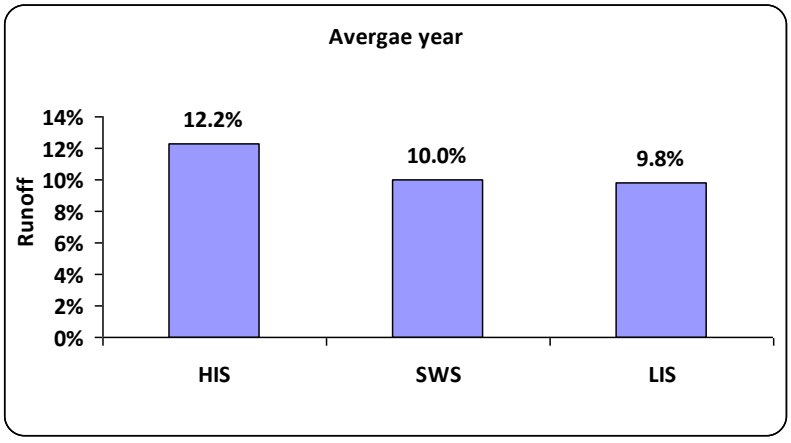

Fig. 6.13: Percentages of the generated runoff using different intensities scenarios.

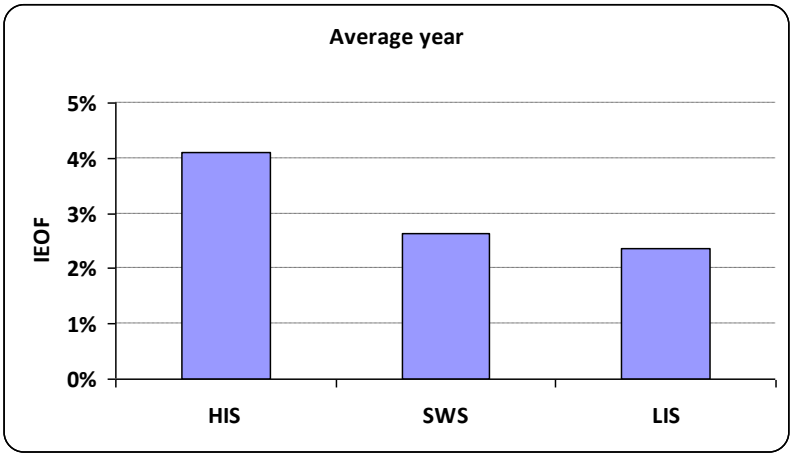

Fig. 6.14: Percentages of the generated runoff due to IEOF using different intensities scenarios.

6.5.2 Impact of temperature increase on water balance

To simulate the expected increase in temperature and to analyze its impact on the water budget, the (*Av.*) Climatic scenario year was used in the simulation. The temperature increase was considered in 3 scenarios in which the mean temperature was increased by one Celsius degree centigrade in every scenario. The temperature increase was applied considering the 3 pattern of rainfall intensities (*HIS, SWS, LIS*); as a result 9 scenarios were generated to simulate the temperature increase. By applying the *HIS* scenario lower volumes will be recharged while more runoff will be generated compared with the other two scenarios as can be noticed in Fig. 6.15 and 6.16 respectively.

The recharged volume has decreased by 1-4% due to an increase in the mean temperature of 1-3°C (Fig. 6.15). Similarly, the generated runoff has slightly decreased by 1-2.4% due to an increase in the mean temperature by 1-3°C (Fig. 6.16).

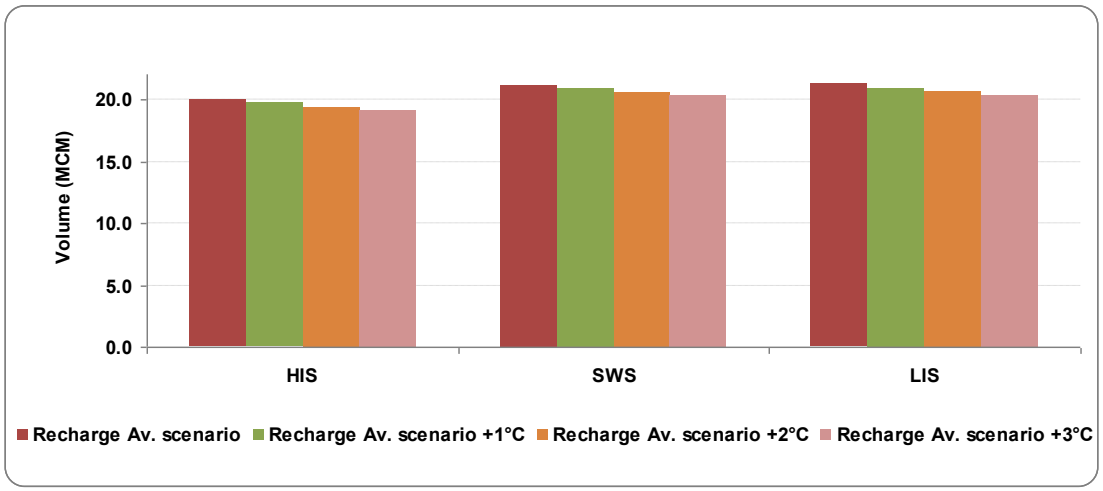

Fig. 6.15: Changes in recharge volumes due to temperature increase.

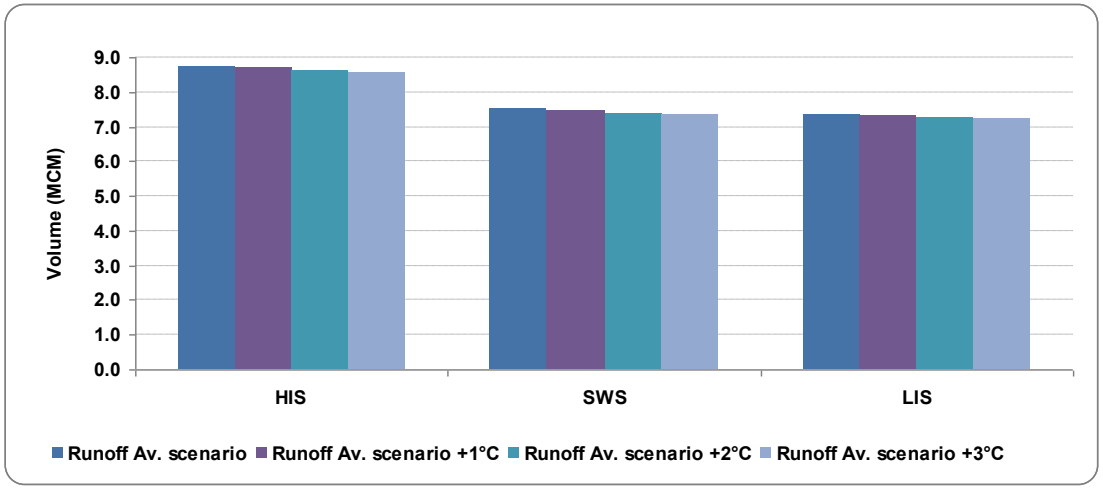

Fig. 6.16: Changes in runoff volumes due to temperature increase.

6.5.3 Impact of land use changes on water balance

Urbanization is the main anthropogenic land use change which may take place in the catchment area of Wadi Kafrein and reduce the areas which are presently covered by other classes like agriculture or forests. Consequently, this will change the water balance of Wadi Kafrein. The aim of these land use scenarios is to answer these central questions: How urbanization expansion in Wadi Kafrein would change the water balance and what will be the consequences on the recharged volumes which are the main source of water in the area and in Jordan in general, and the runoff volume which is collected by the Kafrein reservoir used for irrigation purposes?

To answer these questions, the land use map and the soil map which have been used in the calibration phase of the water year 2008/2009 were used in preparing the land use changes scenarios. The water balance was calculated for this water year and the results are presented in chapter five (section 5.9.5). To simulate the urbanization expansion, four grid maps with an increase of 50 meter in diameter for each scenario was prepared and applied for both the land use and soil maps. The results showed a slight decrease in the evapotranspiration amount and a significant decrease in the recharged volume which may reach 30% of reduction due to urbanization expansion considering the land use scenario (*LU200*) as shown in Fig. (6.17). By increasing the urbanized areas, more runoff is generated which may increase by 35% in the land use scenario (*LU200*) and an increase in the soil storage amounts is also a result of the urbanization expansion, which maybe attributed to the increase in the generated runoff volumes consequently more water is available to be stored in the soil layer. The runoff volume is the most effected component due to urbanization expansion as can be seen in Fig. (6.18).

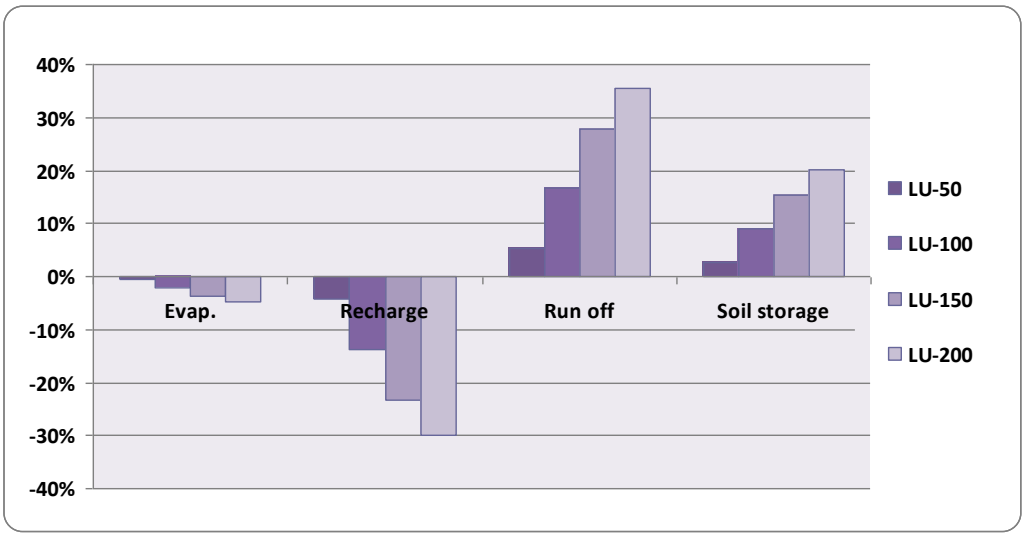

Fig. 6.17: Changes in water balance due to urbanization expansion.

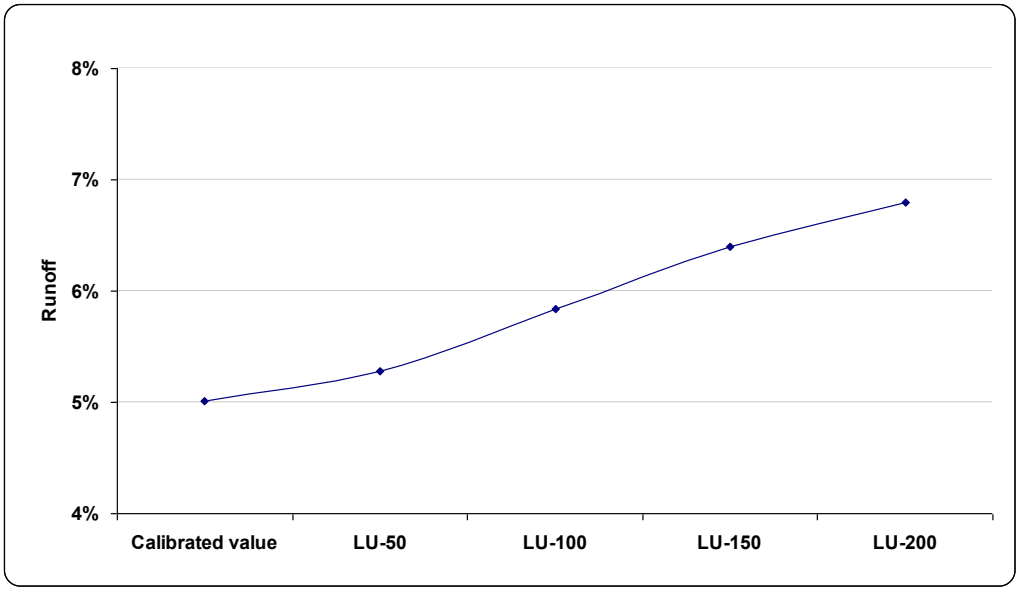

Fig. 6.18: Changes in runoff due to urbanization expansion.

6.5.4 Hydrological modelling from 2002 to 2007

The model was further validated using the available data from the Kafrein dam operation office from 2002-2007. The measured and simulated runoff was used to validate the results and is shown in Fig. 6.19. The spring discharges and the effluent from Wadi Es Sir WWTP data were not available for the water year 2006/2007. Therefore, the simulated runoff volumes of this year were not compared with the measured streamflow. Comparing with results of the previous years in which the measurements were available, the difference between the simulated runoff and the measured streamflow are within the accepted limit and are thus found to be reasonable. The water balance results of the simulated water years including the water year 2006/2007 are given in the last section where the water balances of all scenarios are discussed.

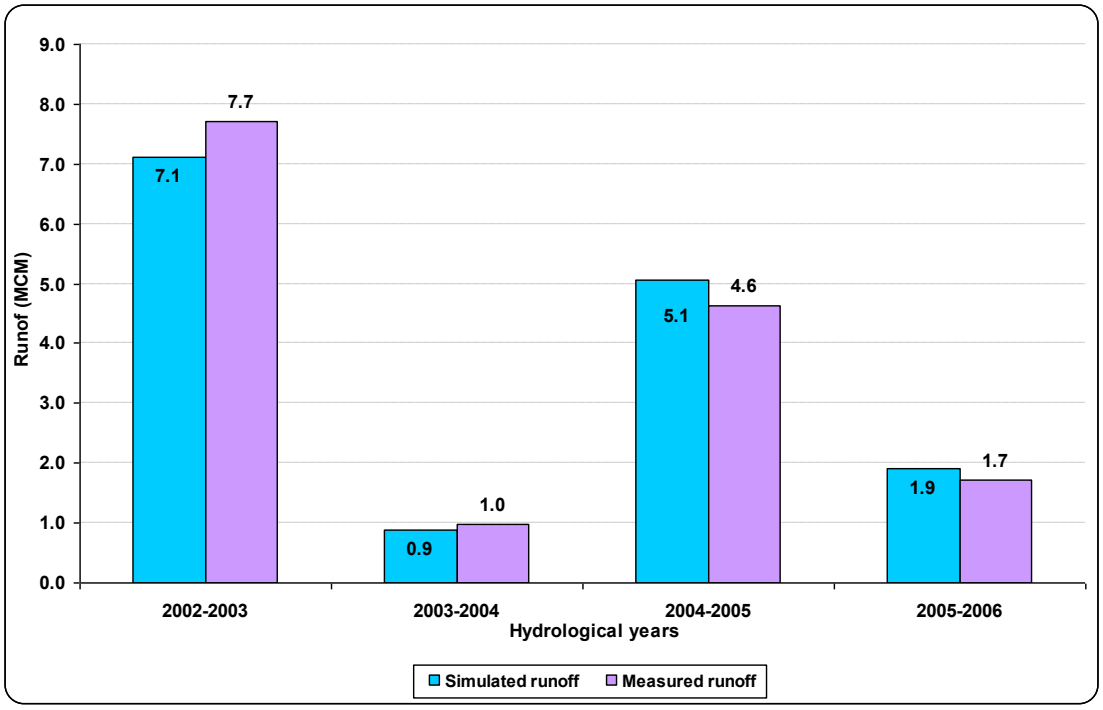

Fig. 6.19: Measured and simulated runoff volumes for the validation water years 2002-2006[1].

The simulation was done for the entire winter season (September-May) of every water year. Therefore, the soil storage is high at the end of the winter season. This, in turn, will be added to the evaporation value by the end of the summer season. The water balances of the water years 2007/2008 and 2008/2009 were calculated continuously for each entire water year (September-August) and the soil storage in the end of the winter season was found to be emptied by evaporation until the end of the water year.

It can be noticed from Fig. 6.19 that in the water year 2002/2003 relatively high volumes of runoff were generated with a measured value of 7.7 MCM. This year is considered as wet year with area rainfall of 552 mm (around 89 MCM). On the other hand, the generated runoff in the water years 2003/2004 is very low which did not reach the 1 MCM, this is related to the dry winter season in which the area rainfall did not exceed 273 mm (44 MCM) in the whole season and the daily mean area rainfall did not reach the 20 mm as can be seen in Fig. 6.9. Also, low runoff volumes were generated during the water year 2005/2006 which also has a low (1.7 MCM) area rainfall amount of 300 mm (around 48 MCM) which is less than the long term annual average precipitation over Wadi Kafrein catchment.

Stream flow measurements are taken on a daily basis by the operators of the Kafrein dam since 2002 and these data were acquired and analyzed to conduct the validation process. Figure 6.20 shows the daily hydrograph of stream flow of Wadi Kafrein from September 1st, 2002 until August 30th, 2009. The low peaks of stream flow measured during the water year 2003/2004 reflect the low rainfall amounts and consequently the low runoff values measured downstream. Also for the water year 2007/2008 which

[1] The spring discharges and the effluent from Wadi Es Sir WWTP data were not available for the water year 2006/2007, therefore; the simulated runoff amounts of this year were not compared with the measured streamflow

has been used to validate the model on an event basis witnessed low stream flow values. Both above mentioned years are considered dry while the water year 2002/2003 is considered wet which has the highest stream flow values since the daily stream flow measurements are taken.

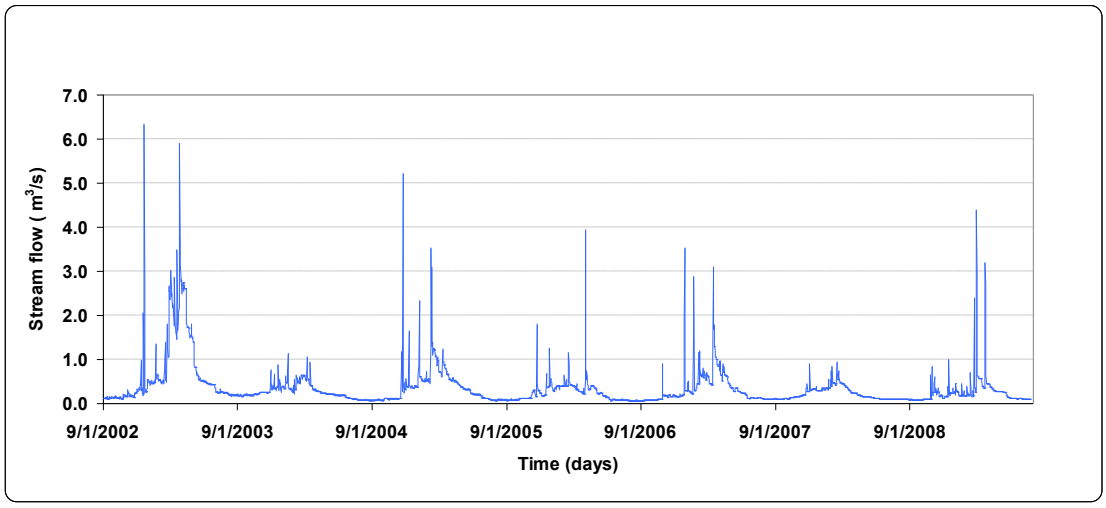

Fig. 6.20: Stream flow into Kafrein dam reservoir from 2002-2009.

6.5.5 Water balance

In a previous chapter the conduction of process oriented investigations was presented, which were based on individual rainfall and runoff events. The main runoff generation mechanisms were determined and the generated runoff and transmission losses were quantified. Also, the spatial distribution of the water balance components were given in daily time steps and the water balance was finally calculated for the entire monitoring period from 2007-2009.

Despite the importance of these process oriented investigations to the scientific research community, which help us to better understand the hydrological processes on a small scale, such investigations receive less interest by decision makers and the civil community.

In this chapter, the practical application of the developed hydrological model is given, which quantifies the water balances based on long term records of rainfall and climatic data. The detailed process oriented investigations are what the proposed water balances quantification is based on. The developed approach of the climatic scenarios aims to estimate the water balance of Wadi Kafrein for any given or projected rainfall amount and intensity. This is very important in case that for a specific year the hydrological data are not sufficient to calculate or even estimate the water balance in a proper way. Such approach is of special interest to manage the limited available water resources and for long term master plans.

The methods and models which are to be used to quantify the hydrological processes in arid and semi arid region must take into consideration the climatic differences impact on the water balance compared with those in the humid regions. The quantification of all water balance components will be given in the coming sections,

the predictive power of the developed climatic scenarios as a supportive tool for future plan water resources management will be discussed.

Two of the chosen hydrological years for climatic scenarios, namely: 1991/1992 and 1998/1999 present the wettest and the driest years in the records respectively (1980-2008). In 1991/1992 the precipitation amounts were double the long term average of almost all stations and it is the wettest years since records were available for the past 65 years back. The hydrological year 1998/1999 was very dry and as an example of Wadi Es Sir Station, it's the second driest year in the records since 1943. The long term annual average precipitation in Wadi Es Sir Station is 523 mm; the driest was recorded in 1951 with 205 mm while in 1998/1999 the total precipitation amount was 247 mm.

In order to evaluate the predictive power of the model using the developed climatic scenarios, the results of the climatic scenarios were validated by comparing them with those from the years in the study period (2007-2009) where the measured data are available in high accuracy and time step.

The hydrological year 2008/2009 was a dry year with a total area precipitation of 250 mm. This area rainfall amount is close to the climatic scenario *LL* which has an area precipitation of 279 mm. The water balance results of both years; i.e. the real measured 2008/2009 and the proposed climatic scenarios (*LL*) are given in Table 6.4. The results of the climatic scenario are close to those simulated during the calibration process for the water year 2008/2009.

Table 6.4: Validation of the climatic scenarios using the water year 2008/2009.

	Area ppt. (mm)	Evap. (MCM)	Recharge (MCM)	Runoff (MCM)	Soil storage (MCM)
LL (scenario year)	279	32.2	6.7-7.3	1.5-2.2	4-4.1*
08/09 (calibration year)	250	31.1	7.2	2	0.1

Similar comparison was done for the other year in the period of the study (2007/2008) which was compared (according to the total area precipitation amount) with the climatic year scenario *LH* (the driest scenario), Table 6.5. The values are with good agreement with those used in the calibration and validation years which present a proof of the method validity and fit to simulate the reality.

Table 6.5: Validation of the climatic scenarios using the water year 2007/2008.

	Area ppt. (mm)	Evap. (MCM)	Recharge (MCM)	Runoff (MCM)	Soil storage (MCM)
LH (scenario year)	170	17.5-17.6	2.6-2.7	1.5	5.7-5.8*
07/08 (validation year)	167	24.4	2.1	1	0.07

The higher value of evapotranspiration in the water year 2007/2008 compared with *LH* climatic scenario is due to the fact that the simulation of the former year (2007/2008) was done until the end of summer season in which the soil storage was

* Water budget was calculated during the winter season; therefore, soil storage presents the portion of rain which still not emptied from the soil layer

empted by evaporation, while in the climatic year scenario (*LL*) the simulation was done until the last rainy day.

Table 6.6 considers the results of the water balance of an average year climatic scenario (*Av.*) and the results of previous studies mostly based on empirical formulas or estimation methods such as the Curve Number (CN), (USDA, 1985).

Table 6.6: Water balance of Wadi Kafrein for an average year compared with previous studies.

	Alkhoury 2011		**Sawarieh et al., 2008**		**Salzgitter 1992**		**AGRAR and Hydrotechnik, 1977**	
	MCM	%	MCM	%	MCM	%	MCM	%
Evapotranspiration	34	49.2	46.1	80.7	-	-	-	-
Recharge	21.2	30.7	5.6	9.9	-	-	-	-
Run off	7.5	10.9	6.3	11.0	3.5	5.4	1.4	1.8
Soil storage *	6.4	9.3	-		-		-	
Area rainfall (mm)	69.1	**428**	57.1	**339.6**	65.6	**411**	75	**397**

6.5.5.1 Volume of precipitation

In the National Water Master Plan report prepared by Agrar and Hydrotechnik (1977), Wadi Kafrein catchment area is calculated to be 189 km^2, exceeding the Kafrein dam down to the Jordan Valley; therefore considering a catchment area of 161 km^2 until the Kafrein dam as considered in this study and the other above mentioned studies, the total area rainfall will be up to 63.9 MCM/a. It has been stated earlier that the climatic scenarios were prepared based on real measured data. The rainfall amounts recorded in most of the stations for the *Av.* climatic scenario are a bit higher than the long term annual average of those stations. This difference has been calculated to be 5% above the long term average. Considering this difference, the mean annual rainfall will be close to that calculated by Salzgitter (1992).

In the study of Agrar and Hydrotechnik (1977), the area rainfall was computed for each drainage area and year in terms of rainfall depth in mm and then converted into the corresponding volume of rainfall in MCM with a specially developed EDP Programme. While in the study of Salzgitter (1992), seven rainfall stations were used in calculating the average area rainfall by dividing the catchment area into Thiessen polygons. Then an isohyetal map was prepared using additional rainfall stations around the catchment. Area weighted factors were assigned to the stations. In addition, rainfall factors were developed for each station to take into account the rapid increase of rainfall with altitude and stations at the boundary of the area. Then a combined area-rainfall factor was then obtained by multiplying the area factor with the rainfall factor. These factors were used to calculate the monthly area rainfall for the Kafrein catchment which resulted in 411mm/yr as an average area rainfall. In the study of Sawarieh et al. (2008) the data of five rainfall stations were used to construct an isohyetal map, the stations are Wadi Es Sir, Wadi Es Sir NRA, Na'ur, Adasiya Janoubiya and the South Shuna station. All these stations are located in the eastern and south eastern part of the study area while the South Shuna station is located in the Jordan Valley. The rainfall stations of Sweileh, Hummar or Al Salt have higher long

* Water budget was calculated during the winter season; therefore, soil storage presents the portion of rain which still not emptied from the soil layer

term annual average rainfall and it could be that not using any of these stations located to the north and northeastern of the catchment area resulted in less rainfall volumes compared with the other studies.

It can be noticed that the calculated volume of water precipitated over Wadi Kafrein is varying based on the used method in estimation or data interpolation, and on the number and distribution of the rainfall stations used in every study. The approach of IDW with elevation correction using the high accuracy 5mx5m DEM to interpolate the daily rainfall data of eight rainfall stations was used in this research (section 5.6.6.1). It can be said that the average volume of precipitation over the catchment area of Wadi Kafrein are in the range of 65 to 70 MCM, which is a number which may vary based on the above mentioned reasons.

6.5.5.2 Volume of evapotranspiration

Evapotranspiration (ET) is the main component of the hydrological cycle in terrestrial ecosystems which is affected by the biophysical and environmental processes at the interface between soil, vegetation and atmosphere (Monteith and Unsworth, 1990; Sellers et al., 1996; Baldocchi and Meyers, 1998). By hydrological modelling it is possible to quantify the water losses by ET in the catchment area of Wadi Kafrein. Such quantification is of primary importance for survey and to manage the water resources in the catchment area of Wadi Kafrein which is extremely important due to the prevailing arid to semi arid climatic conditions and the results of the modelling can assess the available water resources.

Several models are available to calculate the ET, but historically the majority of these models were developed for well-watered agricultural crops (Stannard, 1993). It can be referred to the Penman (1948) equation as the most rigorous of these models which led to the use of the term potential evapotranspiration. The Penman equation was generalized for water-stressed crops by incorporating a canopy resistance term by Monteith (1965). This has been done to describe the effect that partially closed stomates have on ET. The Penman-Monteith (PM) Model (Monteith, 1965) assumes that canopies can be regarded as one uniform surface or big leaf to which a canopy resistance term is incorporated to determine the stomata influence on ET, (Rana et al., 1997; Allen et al., 2006; Widmoser, 2009). Nevertheless; the big leaf assumption requires that the sources of sensible and latent heat are at the same height and temperature. This requirement is met by a full canopy, or a bare soil surface, but not by a sparse canopy (Stannard, 1993), which is the general case in arid and semi arid region. Specifically in Wadi Kafrein catchment, the full canopy does not exceed 5% of the area; on the other hand the sparse vegetation presents more than 27% of the catchment area. During early growth stages crops are sparse and the big leaf assumption considered in the PM model is not valid for areas with sparse vegetation.

During the eighties of the last century several models have been evolved to address the energy balance and ET of sparse crops (e.g., Shuttleworth and Wallace, 1985; Choudhury and Monteith, 1988; Smith et al, 1988). Among these models the Shuttleworth Wallace (SW) model is very similar to the PM model in concept and in required data but it treats a sparse crop as a two-component system governed by energy balance and aerodynamic principles.

In a case study held by Stannard (1993) in the semi arid San Luis Valley, southern Calorado, the ET models of PM, SW and the modified Priestley-Tayler (PT), (Priestley and Taylor, 1972) were evaluated for suitability to be used in a sparsely vegetated, semiarid rangeland. The results showed that the PM model is significantly less accurate than either the SW or PT models. It was not surprising that the MP model is less accurate than the SW model for two reasons: *first*, the PM model big leaf assumption does not hold during dry, sunny periods, when large fraction of the sensible heat flux comes from the hot soil. *Second*, immediately after a rainfall, the PM model can not simulate the large values of bare soil evaporation, because it is exclusively a transpiration model. The results of the study showed that by using the PM model, many values of latent heat flux shortly after a rainfall are severely underestimated while the SW and PT models explicitly account for bare soil evaporation after a rainfall. Furthermore, the study results showed that during the daylight hours, the vegetation canopy is a net sink for about one-fifth of the sensible heat produced at the hot soil surface. The fact that the canopy is a sink for, rather than a source of sensible heat explains why the PM model is not acceptable for use at the semi arid San Luis Valley which also applies to other regions with similar climate and land cover. By another study held by Vorosmarty et al. (1998), their results showed that hydrological modelling is sensitive to the potential ET methods, higher in humid regions, and the SW model performs best. Federer et al. (1996) compared five methods (Thornthwaite, Hamon, Jensen-Haise, Turc, and Penman) for estimating potential evaporation for a reference surface to four methods (Priestley-Taylor, McNaughton-Black, Penman-Monteith, and Shuttleworth-Wallace) for estimating surface-dependent potential evaporation using three cover types at each of seven locations from Fairbanks, Alaska, to San Juan, Puerto Rico. They found that potential interception can only be estimated appropriately for all cover types by the SW model.

To enhance the TRAIN-ZIN model capabilities to simulate the hydrological processes in arid and semi arid region, the ET module was modified so that it is possible to use the SW model in addition to the initial PM model. Based on the above discussion, which shows the limitation of the PM model to simulate the ET in arid and semi arid regions; the SW model was found to be more convenient for the present research and has been used to simulate the ET amounts in Wadi Kafrein catchment area.

In the Study of Agrar and Hydrotechnik (1977), the potential evapotranspiration neither the class A Pan evaporation were calculated to the catchment area of Wadi Kafrein but the class A Pan evaporation was calculated to the adjacent catchment area, Wadi Shueib to be 2642 mm. In the study of Salzgitter (1992), the average monthly potential evaporation of King Hussein Nursery evaporation station in Baqa'a (around 15 km to the north east of Wadi Es Sir rainfall station) as calculated with Penman equation, and recorded with Class-A pan, was used to calculate the potential evaporation in the Kafrein catchment, a factor of 0.74 for Pan A was used. As the density of the meteorological stations in the region is very low the author considered that the potential area evaporation might be of the same order as the average evaporation at the respective stations. The Kafrein catchment evaporation was calculated to be of 1928 mm based on the above mentioned assumption. In the study of Sawarieh et al. (2008) the evapotranspiration was calculated using the empirical formula of Wundt (1937). The formula was applied to data from King Hussein Nursery evaporation station and the losses by evaporation were calculated to be around 81%. Based on measurements taken in more than two hundred catchments in

the Federal Republic of Germany, Wundt (1937, 1939) found in his studies on the relationships between the mean values of precipitation, runoff, evaporation and air temperature on the land surfaces of the earth that there exists an interrelationship between mean precipitation and mean evaporation at varying mean air temperature, these interrelation ships apply to Central and North Eurpoean conditions (Liebscher, 1972). The mean evapotranspiration for a given mean annual precipitation and mean air temperature can be taken. In the present research the SW equation using daily meteorological data from five weather stations (Table 6.3) was used to estimate the evapotranspiration in the catchment area of Wadi Kafrein and has been found to be around 58.5% from the total precipitation amount (including the soil storage amount in Table 6.6).

6.5.5.3 Volume of groundwater recharge

Groundwater recharge volumes are an important component of the water budget. Especially in the case of Wadi Kafrein, the groundwater is considered as the main water resource in the area which is also true to the whole country of Jordan. The quantification of the recharged volume is important for the short term and long term water resources management plans.

Similar to precipitation, the estimation of the recharged volume varies based on the used method in estimation or calculation. Also the recharge conditions along the Rift escarpment vary considerably due to the distribution of precipitation, conditions of evapotranspiration, slope angles, and infiltration conditions of the rock (Ali et al., 2009).

The recharge volumes calculated by Sawarieh et al. (2008) by means of the water budget concept and by using the curve number method, resulted in an average recharge volume of 5.6 MCM. In the study of MWI and GTZ (2004), a rainfall-runoff model has been developed which uses a modified Curve-Number method. The model is country wide and is raster based, each cell is 2kmx2km large. However; the country-wide approach results in the over- or under estimation for some individual catchments. The primary inaccuracy of the model is however due to the automatic procedure of spatial rainfall interpolation, therefore; results for all basins have to be carefully compared (and, if necessary corrected) with the results from other studies (MWI and GTZ, 2004). Figure 6.21 shows a recharge grid of Wadi Kafrein as calculated using the above mentioned rainfall-runoff model.

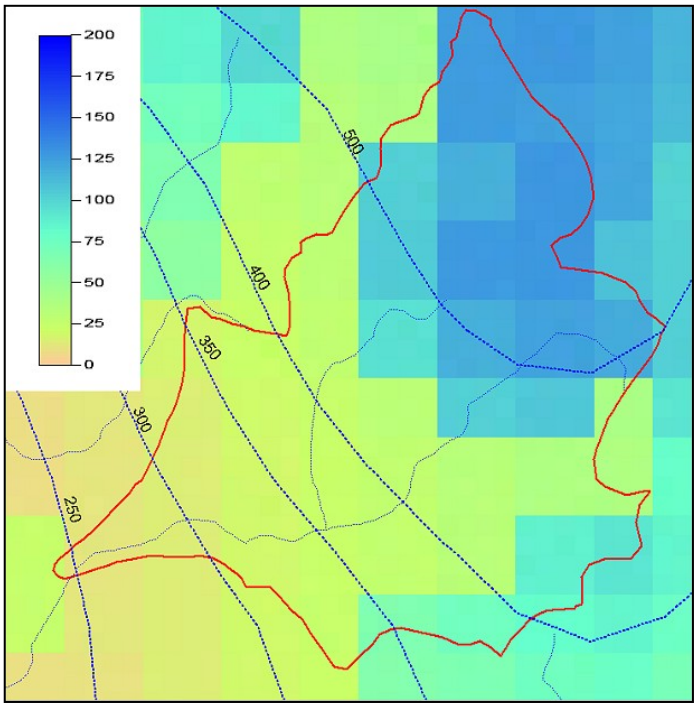

Fig. 6.21: Recharge grid in the Wadi Kafrein catchment area (MWI and GTZ, 2004). Calculated from long-term annual averages in mm; dotted lines are isohyets

The groundwater basin of Jordan Rift Side Wadis includes both the North Rift Side Wadis (W. Arab, W. Ziglab, W. Yabis, W. Kufrinja and W. Rajib) and the South Rift Side Wadis (W. Shueib, W. Kafrein and W. Hisban). The total recharge from the Jordan Rift Side Wadis has been calculated by the above mentioned model at 111 MCM/year (MWI and GTZ, 2004). The outcropping area of the deep aquifers and their catchment is restricted to some very small strips or to cliffs along the escarpment. The rocks in the crest region from Madaba (around 17 km south of Na'ur) to Amman belong to the Upper Cretaceous aquifer (section 2.5.1) and, due to the Amman flexure (section 2.4), are exposed in the northern part down to the Jordan Valley. The limestones of the upper aquifer are highly karstified and facilitate fast infiltration of rain water. In comparison with other karst regions in arid areas, the recharge to groundwater could be 60% of the yearly rainfall. Along the Jordanian Rift escarpment, recharge is reduced to 50% due to steep slopes (Ali et al., 2009).

The wide diversities within the catchment area of Wadi Kafrein in precipitation, climatic conditions and the topography presented by different steepness results in different recharge rates within the same catchment area. This can be noticed from the spatial distribution maps of recharge in the event based analysis in chapter five (section 5.9.3). Recharge zones in Wadi Kafrein are found in the eastern and upper eastern part of the study area where the limestone of the upper aquifer is highly karstified as explained earlier. The recharge volume in Wadi Kafrein is calculated to be around 21 MCM which presents 31% of the long term annual rainfall based on the *Av.* climatic scenario. As the annual rainfall of this climatic scenario is a little bit higher than the long term annual average area rainfall over Wadi Kafrein, the recharge is expected to be 2 MCM less, (see Table 6.11).

6.5.5.4 Volume of runoff

Agrar and Hydrotechnik (1977) estimated the runoff value in Wadi Kafrein to be 1.4 MCM as a long term average, while the Natural Resources Authority (NRA) gave in a two reports in 1974 a long term runoff value of 2 MCM and 1 MCM in their report of (NRA-WRD, 1974) and NRA-ID, 1974) respectively. MacDonald (1965) assigned the value of 1.4 MCM as an average runoff value. The study of Barber (1975) estimated the runoff in Wadi Kafrein of 2 MCM.

The results of the present research show that runoff in these studies was underestimated. This can be attributed to the lack of the real measured data. This has been stated clearly by Agrar and Hydrotechnik (1977) as of 60% of the catchment area of interest was un-gauged and there are not sufficient runoff measurements available to assess runoff volumes directly by runoff data analysis.

In the dry year 2007/2008 which is one of the driest years since measurements were conducted, a total runoff volume of 1MCM was recorded, and the following dry water year 2008/2009 a total volume of runoff was measured up to 2 MCM. Out of this value of 2 MCM, a total volume of 0.78 MCM was recorded only in the second runoff event between the 27th, February and 3rd of March 2009 (section 5.7.4). Also in one storm event in the 17th of December, 2009 a total volume of 0.52 MCM was measured (section 5.7.4). The Kafrein dam operational office is conducting since 2002 a daily stream flow measurements and calculates the water budget for the reservoir. As an example, during the dry year 2003/2004 the measured runoff was around 1 MCM (Fig. 6.19). Therefore; based on the measured runoff in this research and the measurements of MWI- Kafrein operational office, the value of 1 MCM or 2 MCM as a long term annual average runoff is too low and considered as underestimation of the real volumes of runoff.

It must be stated that the runoff value given in Table 6.7 refers to the generated runoff which means that it also includes the volume of the transmission losses; this was conducted in order to have the whole water balance of the catchment area. This is also true to the runoff values given in Table 6.8 and 6.9 because they are dealing with a water budget. On the other hand, for the validation years between 2002-2007 the values given in Fig. 6.19 refers to the runoff value only, without the transmission losses; because it is aimed to compare the values with the measured runoff in the downstream before it reaches the dam reservoir.

The climatic scenario which was chosen to represent an average year has a bit higher annual precipitation than the long term annual average. The simulated runoff generation value for Wadi Kafrein in an average year is 7.5 MCM. Considering only the runoff volumes which reached the downstream after the transmission losses volumes, the long term average runoff value is estimated to be around 6.4 MCM.

6.5.5.5 Predictive power of the climatic scenarios

The water balance of all climatic scenarios was calculated using the measured rainfall and climatic data and the developed downscaling approach described in section 6.2.1.1. Although the hydrological model was calibrated and validated (section 5.7 and 6.5.4), and the climatic scenarios are based on real measured rainfall and climatic

data, still the downscaling approach needs to be validated to evaluate the model predictive power to calculate the water budget for any given rainfall amount. For this purpose the water budget of the validated years 2002-2007 and the water years used in calibrating and validating the hydrological model of 2007/2008 and 2008/2009 were used and grouped based on their annual rainfall amount to be compared with the climatic scenarios. The water balance of the 15 climatic scenarios are given in Table 6.7 while the water balance of the years in which the runoff was measured and used to calibrate and validate the hydrological model are given in Table 6.8.

The **Year ID** given in Table 6.7 represents the three rainfall intensity patterns for every climatic scenario, while the **Year ID** given in Table 6.8 represents the water years used to calibrate and validate the model. The evaluation of the climatic scenarios was conducted by comparing the area rainfall of the water years in Table 6.8 with those of the climatic scenarios and based on the value of the water balance of the water years in Table 6.8 was compared with the water balance results of climatic year with similar area rainfall. The **Year ID** in Table 6.8 was given a similar color to the **Year ID** in Table 6.7 of the climatic scenarios which presents the expected range of water balance based on the area rainfall. The area rainfall of all water years is given in Table 6.9.

The water year 2002/2003 has a total area rainfall of 552 mm which is closer to the *HL-LIS* climatic scenario rather than the *HH* scenario and the results are between the two given scenarios. The water years 2003/2004 , 2005/2006 and 2008/2009 have an area rainfall of 273 mm, 300 mm, and 250 mm respectively which are close to the area rainfall of *LL* climatic scenario which has an area rainfall of 279 mm, the water years are comparable with *LL-LIS, LL-HIS* and *LL-HIS* respectively.

It can be noticed that the water year 2005/2006 has a higher recharge and runoff volumes compared with the *LL* scenario but still it is less than the *Av.* scenario values. The water year 2005/2006 has a higher area rainfall than the *LL* scenarios, therefore it is expected to have higher recharge and runoff values but still it is closer to the *LL* scenario rather than the *Av.* scenario based on the annual area rainfall. The water years 2004/2005 and 2006/2007 have an area rainfall values of 437 mm and 374 mm, respectively which are close to the *Av.-LIS* climatic scenario. Both water balance values are comparable with those resulting from the *Av.-LIS* climatic scenario. Finally the water year 2007/2008 with area rainfall of 167 mm is close to the area rainfall of *LH-SWS* climatic scenario which has an area rainfall of 170 mm.

Table 6.7: Water balance of the proposed climatic scenarios.

Year category		Year ID	Evapotranspiration (MCM)	Recharge (MCM)	Run off (MCM)	Soil storage (MCM)
Climatic scenario years		HIS	35.9	24.0	9.80	6.55
	HL	SWS	35.9	25.6	8.18	6.57
		LIS	35.6	26.0	7.71	6.57
		HIS	40.6	64.1	30.7	5.36
	HH	SWS	40.7	65.9	28.8	5.40
		LIS	40.7	65.8	28.7	5.40
		HIS	34.0	20.0	8.76	6.33
	Av.	SWS	34.0	21.2	7.52	6.36
		LIS	34.0	21.3	7.37	6.36
		HIS	17.5	2.73	1.53	5.71
	LH	SWS	17.6	2.64	1.51	5.75
		LIS	17.5	2.65	1.51	5.74
		HIS	32.2	6.73	2.18	3.96
	LL	SWS	32.3	7.21	1.48	4.08
		LIS	32.3	7.33	1.32	4.12

Table 6.8: Water budget of the calibrated and validated years from 2002-2009.

Year category	Year ID	Evapotranspiration (MCM)	Recharge (MCM)	Run off (MCM)	Soil storage (MCM)
Validation years (non stationary conditions)	2002-2003	42.5	31.0	7.94	7.74
	2003-2004	32.6	7.69	1.28	2.49
	2004-2005	32.1	25.0	5.93	7.74
	2005-2006	28.5	9.25	2.39	8.22
	2006-2007	28.5	22.3	5.30	4.26
Calibration year	2007-2008	24.4	2.08	1.04	0.066
Validation year	2008-2009	31.1	7.24	2.00	0.095

It was not surprising of having no water year which has similar water balance as the HH climatic scenario. This climatic scenario as explained earlier is based on the extreme wet year 1991/1992. Such water years are not so common in the meaning of rainfall intensities and amounts.

The results of the climatic scenarios are reasonable and can be used to estimate the water balance of any water year in which the rainfall amount is available but not the climatic data and where it is not possible to apply a hydrological model to simulate the hydrological processes. Table 6.9 shows the water balances of all scenarios and measured water years in millimeters and percentages of water components compared to the annual rainfall amount of that year.

The evapotranspiration rates range from 145 mm (around 23 MCM) up to 311 mm (around 50 MCM); these rates include the evapotranspiration from soil storage which have been shown that they are added to evapotranspiration rather than recharge. This

depends on the rainfall amount, number of the rainy days and the lag time between the events which affect the amounts of evapotranspiration. It is not likely to exceed or be less than this range.

Table 6.9: Water balance of measured and scenario water years in millimeters and percentages.

Year ID			Area rainfall	Evapotranspiration		Recharge		Run off		Soil storage	
				(mm)	(%)	(mm)	(%)	(mm)	(%)	(mm)	(%)
Climatic scenario years	HL	HIS		222.3	47.1%	148.7	31.5%	60.7	12.9%	40.6	8.6%
		SWS	472	222.6	47.1%	158.3	33.5%	50.7	10.7%	40.7	8.6%
		LIS		220.5	46.9%	161.0	34.3%	47.8	10.2%	40.7	8.7%
	HH	HIS		251.8	28.9%	396.8	45.5%	190.0	21.8%	33.2	3.8%
		SWS	872	252.1	28.9%	408.2	46.8%	178.3	20.4%	33.5	3.8%
		LIS		252.0	28.9%	407.7	46.8%	178.0	20.4%	33.5	3.8%
	Av.	HIS		210.7	49.2%	123.9	28.9%	54.3	12.7%	39.2	9.2%
		SWS	428	210.9	49.2%	131.4	30.7%	46.6	10.9%	39.4	9.2%
		LIS		210.8	49.3%	131.7	30.8%	45.6	10.7%	39.4	9.2%
	LH	HIS		108.6	63.8%	16.9	9.9%	9.5	5.6%	35.4	20.8%
		SWS	170	108.8	64.0%	16.3	9.6%	9.3	5.5%	35.6	20.9%
		LIS		108.6	63.9%	16.4	9.7%	9.4	5.5%	35.5	20.9%
	LL	HIS		199.6	71.5%	41.7	14.9%	13.5	4.8%	24.5	8.8%
		SWS	279	200.2	71.7%	44.7	16.0%	9.2	3.3%	25.3	9.1%
		LIS		200.3	71.7%	45.4	16.3%	8.2	2.9%	25.6	9.1%
2002-2003			552	263.0	47.7%	191.9	34.8%	49.2	8.9%	47.9	8.7%
2003-2004			273	202.1	74.1%	47.6	17.5%	8.0	2.9%	15.4	5.7%
2004-2005			437	198.8	48.9%	154.6	38.0%	36.8	9.0%	47.9	11.8%
2005-2006			300	176.7	59.0%	57.3	19.1%	14.8	4.9%	50.9	17.0%
2006-2007			374	176.3	47.2%	138.3	37.0%	32.8	8.8%	26.4	7.1%
2007-2008			167	150.9	90.6%	12.9	7.7%	6.4	3.9%	0.4	0.2%
2008-2009			250	192.4	77.0%	44.9	18.0%	12.4	5.0%	0.6	0.2%

As percentages of every water year, the evapotranspiration amounts range between 30% in a very wet year similar to 1991/1992, and was found to be 90% in a very dry year similar to 2007/2008.

The quantification of recharge volume is important for water resources management plans. It could range between 13 mm (around 2 MCM) up to 408 mm (around 66 MCM) in extreme wet years. The recharge presents 8% as minimum while it does not exceed the 47% of the precipitation amount.

The runoff volume is of local interest in the case of Wadi Kafrein because the water collected in the Kafrein reservoir is used for irrigation purposes in the Jordan Valley. In dry years the runoff amount could be as low as 6 mm (around 1 MCM) and in very wet years it could reach 190 mm (around 31 MCM).

6.5.5.6 Recharge and runoff assessments

Recharge assessment is of water management importance. The domestic water supply and water for irrigated agriculture in the catchment area of Wadi Kafrein depend on

groundwater. The water supply of Wadi Es Sir City in Wadi Kafrein, for example is provided by the spring discharge of Wadi Es Sir Spring (see section 2.5.2). Nevertheless, recharge varies in space and time. Similar amounts of precipitation can result in different aquifer recharge rates as a function of spatial and temporal distribution of precipitation (e.g., location of the storm core, number of wet and dry periods and also as a function of duration of wet periods) and morphoclimatic conditions (e.g., temperature, land use, vegetation, soil and rock types, and slope degree and aspect), (Sheffer et al., 2010).

Based on the validated predictive capabilities of the climatic scenarios, several recharge equations were developed to assess the recharge volumes (*Rc*) in Wadi Kafrein based on the annual rainfall amounts (*Rf*). The available data which includes the driest and wettest years in the records were included in the climatic scenarios. The developed equations are valid to assess recharge amounts with area rainfall more than 120 mm. As the very dry year 2007/2008 with lowest area rainfall of 167 mm resulted in recharge volume of 2.1 MCM (12.9 mm), it is not optimal to have any significant estimation error considering no recharge with annual rainfall less than 120 mm.

$$Rc = \begin{cases} 0.31Rf - 37.4 & 187 > Rf > 120mm.....(Eq.6.1) \\ 0.49Rf - 71 & 536 > Rf \geq 187mm.....(Eq.6.2) \\ 0.64Rf - 151.5 & Rf \geq 536mm.....(Eq.6.3) \end{cases}$$

The first condition of recharge equations (Eq. 6.1) occurred on the very extreme dry years 1998/1999 and 2007/2008 while the third condition (Eq. 6.3) occurred in the wet year 2002/2003 and the extreme wet year 1991/1992.

The case of runoff is different; runoff varies based on precipitation intensity, antecedent soil moisture, and the lag time between the storm events, in addition to other factors which can not be directly related to annual precipitation amount. As an example, in the water year 2003/2004 with annual precipitation of 273 mm, the total runoff volume was 1.3 MCM while in the water year 2008/2009 with area rainfall of 250 mm, a runoff volume of 2 MCM was measured. Based on the available data and the results of this research, a rough estimation of runoff volumes based on the area precipitation over Wadi Kafrein is given in Table 6.10.

Table 6.10: Estimations of runoff volumes based on area rainfall over Wadi Kafrein.

Area rainfall (mm)	Runoff (mm)
Rf ≤300	0-14.8
300 <Rf <450	14.9-46.5
Rf ≥ 450	>46.5

The results of this research suggest that the annual average recharge amount in Wadi Kafrein is not less than 20 MCM while the runoff amount is not less than 5 MCM per year. This indicates that previous estimations of runoff and recharge in the Wadi Kafrein were too low and evapotranspiration was too high.

7 Conclusions and future perspectives

7.1 Thesis aspects

The focus of this research is the hydrological modelling in arid and semi arid regions with emphasis on runoff generation mechanisms and transmission losses. Due to previous data scarcity and the diversity of natural conditions in the study area, a consistent reliable and up-to-date database was prepared as well as modelling tool selection criteria. After successful calibration and validation of the model, several applications were conducted concerning climatic and land use changes.

7.1.1 Rainfall-runoff modelling

The wide diversity of natural conditions within the study area requires caution in selecting the appropriate modelling tool for water balance quantification. A criterion for model tool selection was identified to choose a suitable model for the study area as discussed in chapter three.

Among other types of hydrological models, the physically based spatially distributed models are the most convenient models to simulate the hydrological processes in study areas similar to Wadi Kafrein, where spatial and temporal variations have a large impact on the hydrological processes.

The physically based spatially distributed TRAIN-ZIN model was selected to fulfill the aims of this research as it considers the spatial variations by a spatial disaggregation of the entire catchment to several sub-catchments which increases the efficiency of the model parameterization.

The long term fluxes of the individual water budget components with special focus on the vertical exchange of water at the soil-vegetation-atmosphere interface are simulated using daily and hourly climatic data while the short term horizontal water fluxes are simulated in higher resolutions of minutes for runoff routing and transmission losses. The soil layer is the intermediate surface between the two processes with interactive feedback and exchange of data in a real time.

Runoff components were well simulated using the physically based spatially distributed TRAIN-ZIN hydrological model. This has been done after rigorous calculations of the controlled catchment using reservoir mass balance equation which accounts for all terms controlling Kafrein dam reservoir storage.

The dominant parameters affecting runoff generation are the soil depth, infiltration rate, and the initial losses. Infiltration rates of different soil types in Wadi Kafrein ranged from 2mm/h in the compacted soil types represented by Ustic-Aridic transition soil moisture regime in the lower part of the study area, while the highest infiltration rates were 40 mm/h for soil types in the middle and upper part of the study area with

Xeric soil moisture regime. Initial losses are highest in agricultural areas and lowest from terrain types with bare rock or thin soil thicknesses. Soil depths range from 10 cm in the Ustic-Aridic transition soil moisture regime zones and 45 cm in the agricultural areas with Xeric soil moisture regime zones.
Transmission losses are mainly affected by channel length, channel width and by the depth of the active alluvium and the infiltration rate of the alluvium which requires intensive field measurements.

The model has been calibrated and validated using stationary and non stationary data set and does not need any further calibration. The model is capable of simulating the hydrological processes in a continuous way while runoff mechanisms and transmission losses can be simulated on an event basis in arid and semi arid regions.

7.1.2 Construction of database

The spatial and temporal resolutions of data are of critical importance in the studied catchment due to the wide heterogeneity and catchment surface diversity. The quality of hydrological models is, therefore, strongly dependant on the quality of the input data.

The detailed hydrological field measurements and instrumentations in space and time allowed the preparation of a reliable hydrological database which is of utmost importance because hydrological data are often scarce and not available in arid and semi arid catchments. The challenge of forced data scarcity was steeped off by the installation of several automatic tipping bucket raingauges and two automatic weather stations in the catchment area. Runoff measurements from the entire catchment area were made available by rigorous calculation procedures using a reservoir water balance approach. It was important to have a controlled catchment in which all incoming water can be measured to calibrate and validate the hydrological model.

The spatial disaggregation of the study area to several sub-catchments allowed a detailed determination of the spatial distribution of rainfall, evapotranspiration, runoff, and recharge zones. Monitoring and field measurements of several subwadis allowed identifying the driving forces of runoff generation and mechanism processes.

The high temporal runoff measurements in the monitored subwadis are an important issue and needs to be stressed. In arid and semi arid regions, runoff is often ephemeral, meaning that it lasts for few minutes in micro scale catchments up to several hours in meso scale catchments. The measured runoff amounts in the monitoring points downstream the subwadis lasted for few minutes in case of Infiltration Excess Overland Flow (IEOF) as main runoff generation mechanism as the case of 21st February 2009 runoff event, while it lasted for few hours in case of Saturation Excess Overland Flow (SEOF) as main runoff generation mechanism as the case of 27th February until the 3rd of March 2009 runoff event. In few cases with devastative runoff events, the storm could last few hours with IEOF as main runoff generation mechanism as the case of the 23rd of March runoff event. In all monitored subwadis, runoff measurements were set to two minutes time step to detect storm events with high temporal resolution. For the entire catchment area, hourly runoff measurements were sufficient to calibrate and validate the hydrological model.

The construction of a hydrological database using high spatial and temporal rainfall-runoff measurements and the usage of multi-temporal satellite images and innovative techniques in surveying and monitoring the Kafrein dam reservoir allowed an accurate quantification of the dam storage and accurate simulation of the hydrological processes in space and time. The importance of high time step and high spatial representation was recognized and taken into consideration as the studied area is a good example of a heterogenic arid and semi arid region.

The analysis of the thematic maps of the monitored subwadis and the measured runoff on high temporal resolution allowed the identification of the driving forces and the role of surface properties on runoff generation mechanisms and losses.

7.2 Water balance

The results of this research showed a distinctive overestimation of the evaporated amounts and a big underestimation of the diverted rainfall volumes to runoff and recharge in earlier studies. The overestimation and underestimation of the water balance components in earlier studies is related to several reasons:

- The rainfall records and the used meteorological data seemed to be insufficient for a detailed estimation for such large diversity within the catchment, including wide variations in rainfall, temperature, elevation, steepness and land use.

- The spatial distribution and the temporal resolution of the used data seemed to be insufficient to detect and quantify the hydrological processes properly as they do not cover the spatial variations and the required high temporal resolutions which are needed in such a highly variable and contradictive catchment.

- The use of inappropriate hydrological estimation methods (mainly evapotranspiration estimations methods) which are invalid for arid and semi arid regions due to their inadequacy for the prevailing climatic conditions which differ from the humid zones to which these methods were developed and can be best applied.

- The lack of using a proper tool or hydrological model which is able to analyze and quantify the hydrological processes in the catchment area under the prevailed contradictory conditions discussed earlier.

The results of this research showed a clear underestimation of the generated runoff in the catchment area of Wadi Kafrein in the available previous studies. The runoff amounts were often estimated to be around one to two million cubic meters as a long term annual average. Such volumes were recorded during dry years within the monitoring period of the present research. The results of this research estimated the long term annual average runoff to be not less than five million cubic meters. This

value is supported by the measured water budget of the Kafrein dam reservoir which has been conducted on a daily basis since 2002.

The results of the present study indicate an average annual recharge of not less than twenty million cubic meters. The long term annual average of the spring discharge in the catchment area was calculated to be around twelve million cubic meters, while the reports of the Ministry of Water and Irrigation of Jordan refers to an average abstraction from wells within the catchment area of Wadi Kafrein of around five million cubic meters. Such numbers reflect the high capabilities of the Kafrein catchment area as a recharge zone which is mainly affected by the highly karstified limestone of the upper aquifer as a result of the highly fractured and faulted zone along the Kafrein catchment.

7.2.1 Runoff generation and mechanisms

The generated runoff in arid and semi arid regions is controlled by several factors. Among others, the results of this research led to a main conclusion that the runoff generation process is mainly controlled by the physical properties of the catchment and surface characteristics. Runoff was more frequently generated and measured in the sub-Wadi (S4) in the lower part of the study area. This area has the lowest annual rainfall amounts when compared with sub-Wadis (S1-S3) in Wadi Kafrein catchment. The surface of the sub-Wadi S4 is covered by low to no vegetation and bare rocks. The catchment was spatially disaggregated to spatially homogenous sub-catchments aimed to increase the efficiency of the model parameterization. Sub-Wadi S4 is covered mainly by a terrain type 3 which is a potential source for runoff generation due to sharp slopes and low vegetation cover.

The steepness of the Wadis also has a main role in runoff generation; this has been noticed in the monitored sub-Wadi (S5) in Wadi Shueib. The detailed morphological analysis showed that around 37% of the catchment area has slopes steeper than 20° compared with other sub-Wadis (S1-S4) which have slopes steeper than 20° in the range of 10-22%. Furthermore, the highest number of runoff generation events was recorded in sub-Wadi S5 which has the smallest surface area not exceeding the 0.3 km^2. Sub-Wadi S5 has also the lowest vegetation cover leading to less interception and more rainfall water is converted to runoff. With smaller catchment areas, less runoff will be lost as transmission losses, consequently more runoff will be generated and reach the out stream of the sub-Wadi.

The land cover and soil thicknesses also have a direct effect in runoff generation. The two upper most sub-Wadis S1 and S2 receive the highest annual rainfall amounts and are located on average heights of 926 m asl and 853 m asl respectively. These two sub-Wadis recorded the lowest runoff event frequency, while in S2, runoff was never generated during the whole period of monitoring. The above mentioned sub-wadis have a Mediterranean climate with thicker soil layers and more vegetation cover. These combinations of soil thicknesses and vegetation cover led to less runoff events as they are able to absorb most of the rain.

It has been recognized that the transmission losses process is one of the most important components of the water balance of many of the arid and semi arid regions

(Hughes, 2008). The process of recharge into alluvial aquifers has been also documented (Crerar et al., 1988). In this research, transmission losses were quantified in Wadi Kafrein and the results show that transmission losses present around 18-44% of the generated runoff on an event basis while their average values ranged from 24% to 26% in 2007/2008 and 2008/2009, respectively. These values reflect the importance of this component in arid and semi arid regions.

7.3 Recommendations and perspectives

It is recommended to conduct more runoff measurements due to the importance of this water component in IWRM concepts and the benefits of this source for drinking and domestic purposes as well. Also, to improve the results of the model, it is suggested to enhance the temporal spring discharge resolution especially for the two main springs of Wadi Es Sir and Wadi Bahhath.

Further investigations are required to evaluate the amount of seepages and losses due to geological factors under the Kafrein dam reservoir. Few studies have been done in this direction while detailed studies could help effectively in evaluating the real reservoir storage and its related water components.

As the main parameters which affect the results of the hydrological model were identified in this research it is recommended to put more efforts in determining and measuring these parameters in more detail. More rigid measurements of runoff generation and transmission losses parameters are required.

Another aspect which must be considered is rainfall harvesting. A good example could be the use of the experience in King Hussein Gardens where a water harvesting project is taking place. This can be done by considering the results of this research in which the spatial distribution of recharge zones were identified and similar rainfall harvesting projects can be implemented.

The developed recharge estimation equations according to the annual precipitation are based on a forward model. Therefore, they can be further validated by considering the results of the groundwater model for Wadi Kafrein which allows the validation of the recharged amounts as simulated using the present surface water model.

The results of this research can be used to assist the decision makers and water sector managers to update the records of the available water resources in the catchment area of Wadi Kafrein and other wadis having similar climatic and morphological characteristics to Wadi Kafrein.

Since arid and semi arid regions are often lacking the accuracy of spatial and temporal hydrological parameters, it is planned to use the results of this research to be generalized to other wadis within the Lower Jordan Valley Basin which have similar climatic conditions and share similar catchment surfaces characteristics to Wadi Kafrein, where detailed measurements were made.

Publications and contributions by the author

1. **Alkhoury, W., Toll, M., Salameh, E., and Sauter M. (2009):** Rainfall-runoff relationship in microscale Wadis in a semi arid environment / a case study from Wadi Kafrein in Jordan. European Water Resources Association (EWRA) 7th International Conference, Limassol, Cyprus, June 25-27, 8 p.

2. **Alkhoury, W., Toll, M., Gunkel, A., Lange, J., and Sauter M. (2010a):** The effect of space-time variations and measurement accuracy of precipitation on hydrological modelling in arid and semi-arid regions – A case study from Jordan. Geophysical Research Abstracts Vol. 12, EGU 2010-1009-1, 2010, EGU General Assembly, Vienna, Austria, May 2-7.

3. **Alkhoury, W., Wagner, B., and Sauter M. (2010b):** Developing a soil map in a semi arid region using remote sensing-based approaches for hydrological modelling-Wadi Kafrein / Jordan. The proceedings of IWRM Karlsruhe 2010, November 24-25, 7 p.

4. **Alkhoury, W., Ziegmann, M., Frimmel, F.H., Abbt-Braun, G. and Salameh, E. (2010c):** Water quality of the King Abdullah Canal/Jordan-Impact on eutrophication and water disinfection. Toxicological & Environmental Chemistry, Vol. 92, No. 5, May 2010, 855-877.

5. **Alkhoury, W., Abu Saadah, M., Sauter M., and Salameh, E. (2011a):** Modelling the effect of land use dynamics on water resources in arid and semi arid regions using a physically based spatially distributed model. (IWRM 2011 conference, Dresden, Germany, Accepted).

6. **Alkhoury, W., Abu Saadah, M., Sauter M., and Salameh, E. (2011b):** Impact of variations in precipitation patterns and temperature increase on water resources in the semi arid region of Wadi Kafrein/Jordan. (IWRM 2011 conference, Dresden, Germany, Accepted).

7. **Menzel, L., Alkhoury, W., and Weiß, M. (2006):** Green water fluxes, irrigation water demand and environmental change in the Lower Jordan Basin GLOWA Jordan River Status Conference, Esslingen, September 19. – 21.

8. **Menzel, L., Lange, J., Gunkel, A., Alkhoury, W., and Weiß, M. (2007):** Einfluß von Klima und Bewirtschaftung auf den Wasserhaushalt im semi-ariden Einzugsgebiet des Jordan. Tag der Hydrologie 2007, Universität Rostock, 22. – 23. März.

9. **Sauter, M., Toll, Mathias, Licha, T., Rusteberg, B., Schmidt, S. and Alkhoury, W. (2009):** Sustainable and Integral Management of Available Water Resources using Innovative Technologies (SMART)-

Assessment of Water Resources and Groundwater Recharge - Zwischenbericht 3.

10. **Sauter, M., Toll, Mathias, Schmidt, S., Alkhoury, W., Rahman, M.A., Nödler, K., Licha, T., Rusteberg, B., Lange, T. and Hanf, A. (2010):** Sustainable and Integral Management of Available Water Resources using Innovative Technologies (SMART)- Assessment of Water Resources and Groundwater Recharge –Abschlussbericht- Projektphase I.

11. **Wu, Y., Wang, W., Toll, M., Alkhoury, W., Sauter, M., and Kolditz, O. (2010):** Development of a 3D groundwater model based on scarce data: The Wadi Kafrein catchment/Jordan. Environmental Earth Sciences, 16p. **(Published online: 08 January 2011).**

12. **Wu, Y., Wang, W., Toll, M., Alkhoury, W., Sauter, M., and Kolditz, O. (2010):** Development of Groundwater Model for the Arid and Semiarid Area: The Wadi Kafrein catchment/Jordan. The proceedings of the XVIII International Conference on Computational Methods in Water Resources (CMWR), Barcelona, Spain, June 21-24, 2010, 8p.

List of References

1. Abbott, M.B., Bathurst, J.C., Cunge, P.E., O'Conell, P.E. and Rasmussen, J. (1986a): An introduction to the European Hydrological system-Systeme Hydrologique Europeen, "SHE", 1: History and philosophy of a physically-based, distributed modelling system. Journal of Hydrology, Elsever Science Publishers B.V., Amsterdam, 87, pp 45-59.

2. Abbott, M.B., Bathurst, J.C., Cunge, P.E., O'Conell, P.E. and Rasmussen, J. (1986b): An introduction to the European Hydrological System-Systeme Hydrologique Europeen, "SHE", 2: Structure of a physically-based, distributed modelling system. Journal of Hydrology, Elsever Science Publishers B.V., Amsterdam, 87, pp 61-77.

3. Abbott, M.B. (1991): Hydroinformatics: information technology and aquatic environment. Avebury, Aldershot.

4. Abed, A. (1983): Paleoclimates of the upper paleistocene in the Jordan rift. Proceedings of the 2nd International Congress, Archaeol Jordan, pp. 81-94.

5. Agrar and Hydrotechnik GMBH (1977): National Water Master Plan of Jordan, Vol. 3; Surface Water Resources.

6. Ali, W., Glaser, J., Hötzel, H., lenz, S., Salameh, E., Thiel, M. and Werz, H. (2009): Groundwater conditions of the Jordan rift escarpment northeast of the Dead Sea. In (Eds): Hötzel, H., Möller, P. and Rosenthal, E.: The Water of the Jordan Valley, Scarcity and Deterioration of groundwater and its Impact on the Regional development. Springer.

7. Alila, Y. and Beckers, J., (2001): Using numerical modelling to address hydrologic forest management issues in British Columbia, Hydrol. Process. 15, 3371-3387.

8. Alkhoury, W., Toll, M., Salameh, E., Sauter M. (2009): Rainfall-runoff relationship in microscale Wadis in a semi arid environment / a case study from Wadi Kafrein in Jordan. European Water Resources Association (EWRA) 7th International Conference, Limassol, Cyprus, June 25-27, 8 p.

9. Alkhoury, W., Toll, M., Gunkel, A., Lange, J., and Sauter M. (2010a): The effect of space-time variations and measurement accuracy of precipitation on hydrological modelling in arid and semi-arid regions – A case study from Jordan. Geophysical Research Abstracts Vol. 12, EGU 2010-1009-1, 2010, EGU General Assembly, Vienna, Austria, May 2-7.

10. Alkhoury, W., Wagner, B., Sauter M. (2010b): Developing a soil map in a semi arid region using remote sensing-based approaches for hydrological modelling-Wadi Kafrein / Jordan. The proceedings of IWRM Karlsruhe 2010, November 24-25, 7 p.

11. Allen, R.G., Pereira, L.S., Raes, D. and Smith, M. (1998): Crop evapotranspiration- Guidelines for computing crop water requirements- FAO Irrigation and drainage paper 56, Rome.

12. Allen, R.G., Pruitt, W.O., Wright, J.L., Howell, T.A., Ventura, F., Snyder, R., Itenfisu, D., Steduto, P., Berengena, J., Yrisarry, J.B., Smith, M., Pereira, L.S., Raes, D., Perrier, A., Alves, I., Walter, I. and Elliot, R. (2006): A recommendation on standardized surface resistance for hourly calculation of reference ET_0 by the FAO56 Penman-Monteith method, Agr. Water Manage., 81, pp. 1-22.

13. Al Qudah, B. (2001): Soils of Jordan. In (Eds.): Zdruli, P., Steduto, P., Lacirignola, C. and Montanarella, L: Soil resources of Southern and Eastern Mediterranean countries. Bari: CIHEAM-IAMB, 2001. p. 127-141: 4 ill. 7 ref. (Options Méditerranéennes : Série B. Etudes et Recherches ; n. 34).

14. Anderson, M. and Woessner W. (2002): Applied Ground Water Modelling- Simulation of Flow and Advective Transport. London: Elsevier 381pp.

15. Andrews, I. (1992): Cretaceous and Paleogene lithostratigraphy in the subsurface of Jordan. Subsurface Geology Bulletin 5, Natural Resources Authority, Geology Directorate, Amman.

16. Arcement, G.J. and Schneider, V.R. (1989): Guide for selecting Manning's roughness coefficients for natural channels and flood plains. United Sates Geological Survey, Water Supply paper 2339. United states Government Printing office.

17. Aynekulu, E., Kassawmar, T. and Tamene, L. (2008): Applicability of ASTER imagery in mapping land cover as basis for biodiversity studies in drylands of northern Ethiopia African Journal of Ecology, Vol. 46, pp. 19-23.

18. Bailey, J.F. and Ray, H.A., (1966): Definition of Stage-discharge Relation in Natural Channels by Step-Backwater Analysis. U. S. Geological Survey Water-Supply Paper 1869-A, 34 p.

19. Baker, V.R., Kochel, R. C. And Patton, P. C. (1988): Flood Geomorphology, Wiley, New York, USA.

20. Baldocchi, D. and Meyers, T. (1998): On using eco-physiological, micrometeorological and biogeochemical theory to evaluate carbon dioxide, water vapor and trace gas fluxes over vegetation: a perspective, Agr. Forest Meteorol., 90, pp. 1-25.

21. Bandel, H. and Khoury, H. (1981): Lithostratigraphy of the Triassic in Jordan. Facies 4: pp. 1-26.

22. Bani-Domi, M. (2005): Trend Analysis of Temperatures and Precipitation in Jordan. Umm Al-Qura University Journal of Educational, Social Sciences and Humanities.Vol. 17-No.1. pp. 1-36.

23. Barber, W. (1975): An outline for Water Planning in East Jordan, NRA-WRD, Amman.

24. Bathurst, J. (1986): Physically-based distributed modelling of an upland catchment using the Systeme Hydrologique Europeen. Journal of Hydrology, 87, pp. 79-102.

25. Becker, A. and Nemec, J. (1987): Macroscale hydrologic models in support to climate research. In (Eds.): S. I. Solomon, M. Bevan & W. Hogg: The Influence of Climate Change and Climatic Variability on the Hydrological Regime and Water Resources. Proc. Vancouver Symposium, 431-445. IAHS Publ. no. 168.

26. Bender, F. (1974): Geology of Jordan. Contribution to the Regional Geology of the World. Gebrueder Borntraeger, Berlin, pp. 196.

27. Bergsma, E. (1983): Rainfall erosion surveys for conservation planning. IT Journal, 2.

28. Bergstreom, S. (1995): The HBV model, Computer Models of Watershed Hydrology. Edited by: Singh, V. P., Water Resources Publications, Highlands Ranch, pp. 443–476.

29. Betson, P. (1964): What is watershed runoff? Journal of Geophysical Research, 69. pp. 1541-1551.

30. Beven, K. (2000): Rainfall Runoff Modelling: The Primer, John Wiley & Sons, Ltd, Chichester, England.

31. Beven, K., Calver, A. and Morris, E.M. (1987): The Institute of hydrology distributed model. Institute of hydrology, report 98, Wallingford, UK.

32. Beven, K. and O'Connell, P.E. (1982): On the role of physically-based distributed modelling in hydrology. Institute of Hydrology, Wallingford, Oxon, Rep. No. 81, pp. 36.

33. Bicknell, B.R., Imhoff, J.C., Kittle, J.L., Jobes, T.H. and Donigian, A.S. (2005): Hydrological Simulation Program-Fortran (HSPF). User's Manual for Release 12.2 U.S. EPA National Exposure Research Laboratory, Athens, GA, in cooperation with U.S. Geological Survey, Water Resources Division, Reston, Virginia.

34. Birkinshaw, S.J., James, P. and Ewen, J. (2010a): Graphical User Interface for Rapid Set-up of SHETRAN Physically-Based River Catchment Model. Environmental Modelling & Software, 25, 609–610.

35. Birkinshaw, S.J. and Webb, B. (2010b): Flow pathways in the Slapton Wood catchment using temperature as a tracer. Journal of Hydrology, 383, 269-279.

36. Botkin, D.B., Estes, J.E., and MacDonald. R.B. (1984): Studying the earth's vegetation from space. BioScience, 34, pp. 508-514.

37. Bovolo, C.I., Bathurst, J.C. and Cisneros, F. (2009): Modelling the effect of forest cover on shallow landslides at the river basin scale. Ecological Engineering, doi:10.1016/j.ecoleng.2009.05.001.

38. Braca G. (2008): Stage-discharge relationships in open channels: Practices and problems. FORALPS Technical Report, 11. Universita degli Studi di Trento, Dipartimento di Ingegneria Civile e Ambientale, Trento, Italy, pp. 24.

39. Brunner, G.W. and Gorbrecht, J. (1991): A Muskingum-Cunge Channel Flow Routing Method for Drainage Networks. ASCE Journal of Hydraulics, Vol. 117, No. 5.

40. Burdon, D.J. (1959): Handbook of the Geology of Jordan, Benham and Co., Colchester. pp. 82.

41. Burges, S. J., M.S. Wigmosta, and Meena, J. M. (1998): Hydrological Effects of Land-Use Change in a Zero-Order Catchment, ASCE J. Hydrol. Eng., 3, 86-97.

42. Buttle, J. (1998): Fundamentals of small catchment hydrology. In (Eds.): Kendall, C, McDonnell, J.J.: Isotope Tracers in Catchment Hydrology, Elsevier, pp. 1-43.

43. Butts, M.B., Payne, J.T., Kristensen M. And Madsen, H. (2004): An evaluation of the impact of model structure and complexity on hydrological modelling uncertainty for streamflow prediction, Journal of Hydrology, Vol. 298, pp. 242-266.

44. Campbell, J. B. (1996): Introduction to Remote Sensing, 2nd edition. Taylor & Francis, London.

45. Carsel, R.F. and Parrish, R.S. (1988): Developing joint probability distributions of soil water retention characteristics. Water resources Research, 24, pp. 755-769.

46. Cartosat-1 Data User's Handbook, 2006. http://www.nrsa.gov.in/IRS_Documents/Handbook/cartosat1.pdf (accessed 21 April, 2008).

47. Ceballos, A. and Schnabel, S. (1998): Hydrological behavior of a small catchment in the dehesa land use system (Extremadura, SW Spain). Journal of Hydrology, pp. 210.

48. Central Water Authority, Hashemite Kingdom of Jordan (1966): Floods is Southern Jordan on 3rd November 1966. Hydrology Division, Jordan.

49. Cervigni, R., Pariente-David, S., Rigaud, K., Holten, J. and Coma Cunill, R. (2009): Addressing climate change in the Middle East and North Africa Region (MENA). MENA Knowledge and Learning, the World Bank publications, Report number 51802.

50. Choudhury, B.J. and Monteith, J.L. (1988): A four-layer model for the heat budget of homogeneous land surfaces, Q. J. R. Meteorol. Soc., 114, pp. 373-398.

51. Chow, V.T., Maidment, D.R. and Mays, L. W. (1988): Applied Hydrology. McGrew-Hill. New York, USA

52. Cournat, R. and Friedrichs, K. (1948): Supersonic Flow and Shock Waves, Interscience Publications, New York, USA.

53. Crawford, N. And Linsley, R. (1966): Digital simulation in hydrology, Stanford watershed model IV. Technical report 39. Department of Civil Engineering, Stanford University.

54. Crerar, S., fry, R., Slater, P., Van Langenhove, G., and wheeler, D. (1988): An unexpected factor affecting recharge from ephemeral river flows in SW Africa/Namibia. In: Simmers, I, and Dordrecht, Reidel D. (Eds.), Estimation of Natural Groundwater Recharge. Pub. Co., pp. 11-28.

55. Croke, B., Andrews, F., Jakeman, A., Cuddy, S. and Luddy, A. (2005): Redesign of the IHACRES rainfall-runoff model, Proceedings of the 29th Hydrology and Water Resources Symposium, Engineers Australia, February 2005.

56. Cunge, J.A. (1969): On the Subject of a Flood Propagation Computation Method (Muskigum method). Jor. Of Hydraulic Res., 7(2), pp. 205-230.

57. Cuo, L., Lettenmaier D.P., Alberti, M. and Richey J.E. (2009): Effects of a century of land cover and climate change on the hydrology of Puget Sound basin, Hydrological Processes, 23, pp. 907-933.

58. Dawdy, D.R. (1961): Depth-Discharge Relations of Alluvial Streams-Discontinuous Rating Curves. Water-Supply Paper 1498-C, U.S. Geological Survey, 16 p.

59. Deutsches Institut für Normung (1997): DIN 19682-7- Felduntersuchungen-Teil 7: Bestimmung der Infiltrationsrate mit dem Doppelringinfiltrometer. Beuth Verlag Gmbh, Berlin.

60. DHV Consultants BV & Delft Hydrulics (1999): How to establish stage discharge rating curve.New Delhi,India.

61. Diabat, A. and Abdelghafoor, M., (2004): Geological map of Amman- 3135-I, 1:50:000, The Hashemite kingdom of Jordan, Natural Resources Authority, Geology Directorate, Amman.

62. DOS, (2004): Department of Statistics, Population and Housing Census 2004. The Hashemite Kingdom of Jordan.

63. Dunne, T. (1983): Relation of field studies and modelling in the prediction of storm runoff. In (Eds): Rodriguez-Iturbe, I. and Gupta, K.: Scale Problems in Hydrology; J. Hydrol., 65.

64. Edwards, W.N. (1929): Lower Cretaceous plants from Syria and Transjordan. Annals and Magazine of Natural History, London series 10 (4), pp. 394-405.

65. Elnaqa, A. and Al-Shayeb, A. (2009): Groundwater protection and management strategy in Jordan. Water Resour. Manage. 23: 2379-2394.

66. Evans, G., Ramachandran B., Zhang Z., Bailey B. and Cheng P. (2008): An Accuracy Assessment of Cartosat-1 Stereo Image Date-Derived Digital Elevation Models: A Case Study of the Drum Mountains, Utah. The International Archives of the Photogrammetry, Remote Sensing and Spatial Information sciences. Vol. XXXVII. Part B1. Beijing.

67. Ewen, J., O'Donnel, G., Burton, A. and O'Connell, E. (2006): Errors and uncertainty in physically-based rainfall-runoff modelling of catchment change effects. Journal of Hydrology, 330, pp. 641-650.

68. FAO (1988): Food and agriculture Organization of the United Nations, Irrigation Water Management: irrigation Methods. Training manual No. 5. Water resources, development and management services-land and Water development Division, Via delle Terme de Carcalla, Rome, Italy.

69. Federer, C.A., Vörösmarty, C. and fekete, B. (1996): Intercomparison of Methods for Calculating Potential Evaporation in Regional and Global Water Balance Models, Water Resour. Res., 32(7), pp. 2315-2321.

70. Fetter, C. (1988): Applied Hydrogeology. 2nd ed. Merrill Publishing Company, Columbus, Ohio.

71. Fetter, C. (2001): Applied Hydrogeology. 4th ed. Prentice-Hall Inc. New Jersey.

72. Fischer, C. (2007): Hydrological modelling of the Water Resources in the Nahal Harod, Israel. Diploma thesis (unpublished), Institute of Hydrology, University of Freiburg, Freiburg, Germany.

73. Fleming, G. (1975): Computer simulation techniques in hydrology. Elsevier. New York.

74. Ford, D., Pingel, N. and DeVries J.J. (2002): Hydrologic Modelling System HEC-MHS, Applications Guide. US Army Corps of Engineers, Hydrologic Engineering Center, California, USA.

75. Ford, D., Pingel, N. and DeVries J.J. (2008): Hydrologic Modelling System HEC-MHS, Application Guide. US Army Corps of Engineers, Hydrologic Engineering Center, Washington, DC, USA.

76. Freeze, A. (1972): Role of subsurface flow in generating surface runoff. Upstream source areas. Water Resources Research 8 (5), pp. 1272-1283.

77. Freeze, A. (1980): A stochastic-conceptual analysis of rainfall-runoff processes on a Hillslope. Water Resources Research 16 (2), pp. 391-408.

78. Frissel, C.A., Liss, W.J., Warren, C.E. and Hurley, M.D. (1986): A hierarchical framework for stream habitat classification: viewing streams in a watershed context. Environmental Management, 10, pp. 199-214.

79. Furse, M.T., Moss, D., Wright, J.F. and Armitage, P.D. (1984): The influence of seasonal and taxonomic factors on the ordination and classification of running-water sites in Great Britain and on the prediction of their macro-invertebrate communities. Freshwater Biology, 14, pp. 257-280.

80. GEOHYTEN Corp. (1998): Geophysical investigations in the area of the Kafrein Dam. Prepared to Jordan Valley Authority, tender No. 9/98, Amman.

81. Gerits, J., De Lima J. and VAN Den Broek, T. (1990): Overland flow and erosion. In (Eds): Anderson, M. and Burt, T.: Process studies in Hillslope hydrology. John Wiley & Sons Ltd, England.

82. Gibson, P.J., Power, C.H. and Keating, J. (2000): Introductory remote Sensing: Principles and Concepts. Routledge, London.

83. GLOWA Jordan River (2006): GLOWA Jordan River project home page, http://www.glowa-jordan-river.de/Main/HomePage.

84. Goodrich, C., Williams, G., Unkrich, L., Hogan, F., Scott, L., Hultine, R., Pool, D., Coes, L. and Miller, S. (2004): Comparison of methods to estimate ephemeral channel recharge, Walnut Gulch, San Pedro River Basin, Arizona. In (Eds.): Phillips, M., Hogan, F., Scanlon, B.: Groundwater Recharge in a Desert Environment: the Southwestern United States. American Geophysical Union, Washington DC.

85. Grayson, R.B., Moore, I.D. and McHahon, T.A. (1992): Physically based hydrological modelling. 1. A terrain-based model for investigative purposes. Water Resources Research, 28(10), pp. 2639-2658.

86. Green, W. H. and Ampt, G. A. (1911): Studies on soil physics-Part 1. The flow of air and water through soils. The Journal of Agricultural Sciences, 4. pp. 1-24.

87. Green, I.R. and Stephenson, D. (1986): Criteria for comparison of single event models. Hydrological Sciences Journal, 31 (3), pp. 395-411.

88. Guentner, A. and Bronstert, A. (2004): Representation of landscape variability and lateral redistribution processes for large-scale hydrological modelling in semi-arid areas, Journal of Hydrology 297: pp. 136-161.

89. Gunkel, A. (2006): Kopplung der Modelle ZIN und TRAIN (Arbeitstitel). Dissertation zur Erlangung des Doktorgrades der Geowissenschaften Fakultät der Albert-Ludwigs-Universität Freiburg (under preparation).

90. Hagenlocher, U. and Gunkel, A. (2008): TRAIN-ZIN for Users. Institute of Hydrology, Freiburg University, Germany.

91. Hamdi, M. R., Abu-Allaban, M., Al-Shayeb, A., Jaber, M. and Momani, N.M. (2009): Climate Change in Jordan: A Comprehensive Examination Approach. American Journal of Environmental Sciences, 5 (1), pp. 58-68.

92. Harza Engineering Company in association with ArabTech. Consult. Engineers (1989): Storage facilities in the Jordan Valley – Final report on Technical, Economic and Financial Feasibility and Preliminary Design. 5 Volumes. IV parts.-Jordan Valley Authority, Amman.

93. Hendrickx, J.M., Phillips, F.M. and Harrison, J.B. (2003): Water flow processes in arid and semi-arid vadose zones. In (Ed.): Simmers, I.: Understanding Water in a dry Environment- Hydrological Processes in Arid and Semi-arid Zones. Swets & Zeitlinger B. V., Lisse, The Netherlands.

94. Herschy, R.W. (1995): Streamflow Measurement, Chapman & Hall, Second Edition.

95. Hewlett, D. and Hibbert, R. (1967): Factors affecting the response of small watersheds to precipitation in humid areas. In (Eds): Sopper E. and Lull W.: Forest Hydrology. Pergamon Press, Oxford, pp. 275-290.

96. Hillel, D. (2004): Introduction to environmental soil physics. Elsevier Science, USA.

97. HMSO (1962): Weather in the Mediterranean I: General Meteorology, 2nd ed., Her Majesty's Stationary Office, 362 p.

98. Hobler, M., Margane, A., Almomani, M. and Subah, A. (2001): Groundwater Resources of Northern Jordan. Vol. 4. Contributions to the Hydrogeology of Northern Jordan. Ministry of Water and Irrigation of Jordan (MWI) and the Federal Institute for Geosciences and Natural Resources (BGR), Advisory Services to the Water Authority of Jordan. Project No. 89.2105.8, Amman.

99. Hodgson, M.E., Jensen, J.R., Tullis, J.A. Riordan, K.D. and Archer, C.M. (2003): Synergistic Use of LIDAR and Color Aerial Photography for Mapping Urban Parcel Imperviousness. Photogrammetric Engineering & Remote Sensing. 69 (9), pp. 973-980.

100. Holmes, N. (1989): British rivers: a working classification. British Wildlife, 1, pp. 20-36.

101. Horton, R. (1933): The role of infiltration in the hydrologic cycle. Transactions of the American Geophysical Union 14.

102. Huete, A., Didan, K., Miura, T., Rodriguez, E.P., Gao, X. and Ferreira, L.G. (2002): Overview of the radiometric and biophysical performance of the MODIS vegetation indices. Remote Sensing of Environment 83 (2002) 195-213.

103. Hughes, D. (2008): Modelling semi-arid and arid hydrology and water resources: the southern African experience. In (Eds.): Wheater, H., Sorooshian, S. and Sharma, K.: Hydrological Modelling in Arid and Semi-Arid Areas. Cambridge university press.

104. Im, S., Kim, H., Kim, C. And Jang, C. (2008): Assessing the impacts of land use change on watershed hydrology using MIKE SHE. Environ. Geol. 57, pp 231-239.

105. IPCC (2000): IPCC special Report on the Regional Impacts of Climate Change, An Assessment of Vulnerability, prepared by Watson, R.T., Zinyowera, M.C. and Moss, R.H.

106. IPCC (2001): Climate Change, Synthesis Report- A Contribution of Working Groups I, II, and III to the Third Assessment Report of the Intergovernmental Panel on Climate Change. Cambridge University Press, Cambridge, United Kingdom and New York, USA, pp. 398.

107. ISO 1100-2 (1998): Measurements of liquid flow in open channels- Part 2: Determination of the stage-discharge relation.

108. Jacobsen, K., Crespi, M., Fratarcangeli, F. and Giannone, F. (2008): DEM generation with cartosat-1 stereo imagery. In (Eds.): Jeurgens, C.: Remote Sensing- New Challenges of High Resolution. Bochum.

109. Janza, M. (2009): Hydrological modelling in the karst area, Rižana spring catchment, Slovenia. Environ. Earth Sci. Springer Berlin, Germany.

110. Jensen, J. R. (2005): Introductory Digital Image Processing- A Remote Sensing Perspective. 3rd edition. Pearson Prentice Hall, USA.

111. Jensen, J. R. (2007): Remote Sensing of the Environment- An Earth Resource Perspective. 2nd edition. Pearson Prentice Hall, USA.

112. Jinlong, F., Bingfang, W. and Huiping, H. (2003): Comparative assessment of ASTER image and ETM+ fusion image for agricultural applications. Geoscience and Remote Sensing Symposium. IGARSS apos; 03. Proceedings. Volume 4, 21-25 July 2003 Page(s): 2203 – 2205.

113. Jordan Meteorological Department (2002): Jordan Climatological Handbook 2000.

114. Kalnay, E. and Cai, M. (2003): Impact of urbanization and land-use change on climate. Nature, Vol. 423, Issue 6939, pp. 528-531.

115. Kirkby, J. (1988): Hillslope runoff processes and models. J. of Hydrology, 100.

116. Klemes, V. (1986): Operational testing of hydrological simulation models, Hydrological Sciences Journal, 31, pp. 13-24.

117. Kocaman, S., Wolff, K., Gruen, A. And Baltsavias, E. (2008): Geometric validation of Cartosat-1 imagery. In Proc. 21th ISPRS Congress, 3-11 July, 2008 Beijing: International Archives of Photogrammetry, Remote Sensing and Spatial Information Sciences, Vol. 37. Part B1-3, pp. 1363-1368.

118. Kondolf, G.M., and Piégay. H. (2003): Tools in fluvial geomorphology: Problem statement and recent practice. In (Eds.): G.M. Kondolf and H. Piégay: Tools in Fluvial Geomorphology (pp. 3-22). John Wiley & Sons, New York.

119. Koussis, A.D. (1978): Theoretical estimations of flood routing parameters. Jor. Of Hydraulic Div., ASCE, 104 (HY1). Pp. 109-115.

120. Krishnaswamy, M. and Kalyanaraman, S. (2009): Indian remote Sensing satellite Cartosat-1: Technical features and data products.

http://www.gisdevelopment.net/technology/rs/techrs023.htm (accessed 23 November, 2009).

121. Kumar, A. (2006): Cartosat-1 (IRS-P5) Stereo Data Processing- A Case Study of Dehradum Area. Conference Proceedings of Map India 2006- Technical Session of Remote Sensing.

122. Kuntz, D. (2003): Soils in the Wadi Shueib catchment area and their protective potential for the Groundwater- Salt area/ Hashemite Kingdom of Jordan. Master thesis (unpublished), Department of Applied Geology, University of Karlsruhe, Germany.

123. Kutija, V. and O'Connell, P.E. (2000): Flooding and flood estimation, Water quantity and quality. University of Newcastle, UK.

124. Landsberg, H. and Schloemer, R. (1967): World climatic regions in relation to irrigation. In: R. Hagen et al. (Eds), Irrigation of Agricultural Lands. American Society of Agronomy, Wisconsin.

125. Lane, J. (1983): Transmission losses. In: SCS National engineering Handbook. US Government Print. Off., Washington, DC.

126. Lange, J. (1999): A noncalibrated rainfall-runoff model for large arid catchments, Nahal Zin, Israel. PhD thesis, Institute of Hydrology, Freiburg University, Germany.

127. Lange, J., Leibundgut, C., Greenbaum, N. And Schick, A. (1999): A noncalibrated rainfall-runoff model for large, arid catchments. Water Resources Research, Vol. 35, No. 7, pp. 2161-2172.

128. Lanini, J.L., E.A. Clark, and Lettenmaier D.P. (2009): Effects of fire-precipitation timing and regime on post-fire sediment delivery in Pacific Northwest forests, Geophys. Res. Lett., 36, L01402, doi:10.1029/2008GL034588.

129. Lavee, H., Imeson, A. and Sarah, P. (1998): The impact of climate change on geomorphology and desertification along a Mediterranean-arid transect. Land Degradation and Development 9, pp. 407-422.

130. Leavesley, G. and Hay, L. (1998): The use of coupled atmospheric and hydrological models for water-resources management in headwater basins. Hydrology, Water resources and Ecology in Headwaters, Proceedings of the Headwater' 98 Conference, Meran/Merano, Italy, April 1998). IAHS Publ. no. 248.

131. Legates, D.R. (2002): Limitations of Climate Models as predictors of climate change. National Center for Policy Analysis. Center for Climatic Research University of Delaware Newark and adjunct scholar with the NCPA.

132. Leistert, H. (2005): Modelling transmission losses; applications in the Wadi Kuiseb and the Nahal Zin. Diploma Thesis- Unpublished. Institute of hydrology, University of Freiburg, Germany.

133. Lenz, S. (1999): Hydrological investigations along Wadi al Kafrein and the Kafrein Reservoir. Diploma Thesis- Unpublished. Department of Geology, University of Karlsruhe, Germany.

134. Leung, L.R., and Wigmosta, M.S. (1999): Potential climate change impacts on mountain watersheds in the Pacific Northwest. J. Amer. Water Resour. Assoc., 35, 1463-1471.

135. Liebscher, H. (1972): A method for runoff-mapping from precipitation and air temperature data. In: World Water Balance, IAHS, Publ. 94. Vol. 1, pp. 115-121.

136. Linsley, R. K. and Franzini, J. B. (1979): Water Resources Engineering. 3rd ed. McGraw-Hill publishing company.

137. Littlewood, IG., Down, K., parker, J.R. and Post, D:A: (1997): Catchment-scale rainfall-streamflow modelling (PC version) Version 1.0-April 1997. Institute of Hydrology.

138. Lyon, J. G., Yuan, D., Lenetta, R. S. and Elvidge, C. D. (1998): A Change Detection Experiment Using Vegetation Indices. Photogrammetric Engineering & Remote Sensing. 64 (2), pp. 143-150.

139. Macdonald, M. and Partners (1964): East Bank Jordan Water Resources-Shueib and Kafrein water use study-Central Water Authority, Amman.

140. Macdonald, M. and Partners (1965): East Bank Jordan Water Resources- east Ghor Side Wadies-Central Water Authority, Amman.

141. Makhlouf, I., Abu-Azzam, H. and Al-Hiayri, A. (1996): Surface and subsurface lithostratigraphic relationships of the cretaceous Ajlun group in Jordan, Subsurface Geology Bulletin No. 8, Natural Resources Authority, Geology Directorate, Subsurface Geology Division, Amman. pp. 95.

142. Margane, A., Hobler M., Almomani M. and Subah A. (2002): Contributions to the Hydrogeology of Northern and Central Jordan. Geologisches Jahrbuch. Reihe C. The Federal Institute for Geosciences and Natural Resources (BGR). Hannover.

143. Masri, M. (1963): Report on the geology of the Amman-Zerqa area, Central Water Authority, Amman. pp. 1-74.

144. Mather, P. (2004): Computer Processing of Remotely-Sensed Images: An Introduction. 3rd ed. John Wiley & Sons, Ltd., England.

145. Mclver, D.K. and Friedl, M.A. (2002): Using Prior Probabilities in Decision-tree Classification of Remotely Sensed Data. Remote Sensing of Environment. 81, pp. 253-261.

146. McMahon, T.A. (1979): Hydrological characteristics of arid zones. Proc. Symposium on the Hydrology of Areas of Low Precipitation, Canberra, IAHS Publ. No. 128, pp. 105-123.

147. Menzel, L. (1996): Modelling canopy resistances and transpiration of grassland, Phys. Chem. Earth, 21(3), pp. 123–129.

148. Menzel L. (1997): Modellierung der Evapotranspiration im System Boden-Pflanze-Atmosphäre. Zürhcer Geographische Schriften 67, Geographisches Institut, ETH, Zurich, Switzerland, 128p.

149. Menzel L. (1999): Flächenhafte Modellierung der Evapotranspiration mit TRAIN. Potsdam-Institut für Klimafolgenforschung, Potsdam, report No. 54.

150. Menzel, L. (2007): Model based simulation of the water balance of forests on different spatial scales. In (Eds.): Feger, K.-H., Yanhui, W., Bernhofer, Ch., and Seegert: The role of forests and forest management in the water cycle Progress in Hydro Sciences and Engineering, , J., 3/2007, Dresden Water Center, Dresden, Germany, 309–319, 2007.

151. Menzel L., Teichert, E. and Weiß, M. (2007): Climate change impact on the water resources of the semi-arid Jordan region. In (Ed.): Heinonem, M.: Proc. 3rd International Conference on Climate and Water, Helsinki, pp. 320-325.

152. Menzel L., Koch, J., Onigkeit, J. And Schaldach, R. (2009): Modelling the effects of land-use and land-cover change on water availability in the Jordan River region. Adv. Geosci. 21, pp. 73-80.

153. Miller, W.A. and Cunge, J.A. (1975): Simplified equations of unsteady flow. In: (Eds.): K. Mahmood and V. Yevjevich: Unsteady Flow in Open Channels. Water Resources Pub., Ft. Collins,CO.

154. Ministry of Agriculture (1993): National Soil Map and Land Use Project- The Soils of Jordan. Level 1 Reconnaissance Soil Survey, Vol.2 Main Report, Hunting technical services Ltd., Amman, Jordan.

155. Ministry of Agriculture (1994): National Soil Map and Land Use Project- The Soils of Jordan. Level 2 Semi Detailed Studies, Vol.2 Main Report, Hunting technical services Ltd., Amman, Jordan.

156. Ministry of Public Works and Housing (1993): Raising Kafrein dam project, technical evaluation report, technical committee.

157. Mish, C. (1985): Petra. Webster's Ninth New Collegiate Dictionary. 9th ed. Springfield, MA: Merriam-Webster Inc.

158. Monteith, J.L. (1965): Evaporation and environment. In: Proceedings of the 19th Symposium of the Society for Experimental Biology, Cambridge University Press,New York, USA, pp. 205-234.

159. Monteith, J.L and Unsworth, M.H. (1990): Principles of Environmental Physics, Edward Arnold Press, London, 291 pp.

160. Montgomery, D.R. (1999): Process domains and the river continuum, Journal of the American Water Resources Association, 35, pp. 297-410.

161. Montgomery, D.R. and Buffington, J.M. (1997): Channel reach morphology in mountain drainage basins. Geological Society of America Bulletin, 109, pp. 596-611.

162. Montgomery, D.R. and Buffington, J.M. (1998): Channel processes, classification, and response potential, In (Eds): Naiman, R.J. and Bilby, R.E.: River Ecology and Management, New York: Springer-Verlag Inc., pp. 13-42.

163. Montgomery, D.R., Dietrich, W.E. and Sullivan, K. (1998): The role of GIS in watershed analysis. In (Eds.): Lane, S.N., Richards, K.S. and Chandler, J.H.: Landform Monitoring, Modelling and Analysis, Chichester: John Wiley and Sons Ltd., pp. 241-261.

164. Montzka, C., Canty, M., Kunkel, R., Menz, G. And Wenland, F. (2006): Remote sensed land cover and impervious surfaces applied in water balance modelling of a mesoscale catchment. Center for remote Sensing of land Surfaces. Proceedings of the 2nd Workshop of the EARSeL SIG on Land Use and Land Cover. Bonn, 28-30 September 2006.

165. Mudd, S. (2006): Investigation of the hydrodynamics of flash floods in ephemeral channels: Scaling analysis and simulation using a shock-capturing flow model incorporating the effects of transmission losses. Journal of Hydrology, 324, pp. 65-79.

166. MWI and GTZ (2004): Ministry of Water and Irrigation of Jordan and the German Technical Cooperation (GTZ). The National Water Master Plan, Amman-Jordan.

167. Natale, L. and Todini E. (1977): A constrained parameter estimation technique for linear models in hydrology. In (Eds): T. Ciriani, U. Maione and J. Wallis: Mathematical Models for Surface Water Hydrology, pp. 109-147, John Wiley & Sons, London.

168. NRA (1966): Natural Resources Authority, review of Spring Flow Data prior to October 1965- Technical Paper, 40, Amman.

169. NRA-ID (1975): Natural Resources Authority-Irrigation Department: Working Paper on Irrigation Development in East Jordan.

170. NRA-WRD (1975): Natural Resources Authority-Water Resources Department: Water Resources for Irrigation.

171. O'Connell, P.E. (2000): Overview of Computational Models I. Computation and Hydroinformatics, University of Newcastle, UK.

172. Onset Computer Corporation (2004): HOBO Weather Station user's Guide. Document No: 6106-E.

173. Onset Computer Corporation (2005): RG3 and RG3-M Data Logging Rain Gauge User's manual. Document No: 10241-B.

174. Orni, E. and Efrat, E. (1971): Geography of Israel. 3rd Edition, Israel University Press, Jerusalem.

175. Ortloff, C. (2005): The Water Supply and Distribution System of the Nabataean City of Petra (Jordan), 300 BC–AD 300, Cambridge Archaeological Journal 15:1, 93–109. McDonald Institute for Archaeological Research DOI: 10.1017/S0959774305000053 Printed in the United Kingdom.

176. Otto, A. and Braukmann, U. (1983): Gewässertypologie im ländlichen Raum. In: Schriftenreihe des Bundesministers für Ernährung, Landwirtschaft und Forsten. Reihe A: Angewandte Wissenschaft, Heft 288, Landwirtschaftsverlag GmbH, 61p.

177. Parker, D.H. (1970): The hydrogeology of the Mezosoic-Cainozoic aquifers of the western highlands and plateau of east Jordan, Investigation of the sandstone aquifers of east Jordan, Technical report No. 2, Unpublished report of United Nations development Project/Food and agriculture Organization project 212, 4 volumes, 424pp.

178. Parkin, G. (2000a): Calibration. In: Computation and Hydroinformatics. University of Newcastle, UK.

179. Parkin, G. (2000b): Building a model. In: Computation and Hydroinformatics. University of Newcastle, UK.

180. Patrick, E. (2002): Researching crusting soils: themes, trends, recent developments and implications for managing soil and water resources in dry areas. Progress in Physical, Geography 26(3), pp. 442-461.

181. PCI Geomatics (2006): Orthorectification and DEM extraction of Cartosat-1 imagery.

http://www.pcigeomatics.com/support/tutorials/pdf/cartosat_tutorial.pdf (accessed 24 November, 2009).

182. Pe'er, G. and Safriel, U.N. (2000): Climate Change. Israel National Report under the United Nations Framework Convention on Climate Change. Impact, Vulnerability and Adaption.

183. Penman, H.L. (1948): Natural evaporation from open water, bare soil, and grass, proc. R. Soc. London, Ser. A, 193, pp. 120-146.

184. Philip, J.R. (1983): Infiltration in one, two, and three dimensions. Procs. National Conference on Advances in Infiltration, American Society of Agricultural Engineers, St. Joseph, Mich., pp.1-13.

185. Phillips, J.V. and Ingersoll, T.L. (1998): Verification of roughness coefficients for selected natural and constructed stream channels in Arizona. United States Geological Survey Professional paper 1584.

186. Phillips, J.V., and Tadayon, S. (2006): Selection of Manning's roughness coefficient for natural and constructed vegetated and non-vegetated channels, and vegetation maintenance plan guidelines for vegetated channels in central Arizona. U.S. United States Geological Survey Scientific Investigations Report 2006–5108.

187. Pilgrim, D., Chapman, T. and Doran, D. (1988): Problems of rainfall-runoff modelling in arid and semiarid regions. Hydrological sciences-Journal-des Sciences Hydrologiques, 33, 4, pp. 379-400.

188. Ponce, V.M. and Theurer, F.D. (1982): Accuracy criteria in Diffusion routing. Jor. Of hydraulics Div., ASCE, 108(HY6). Pp. 747-757.

189. Ponce, V.M. and Chaganti, P.V. (1994): Variable-parameter Muskingum-Cunge method revisited. Journal of Hydrology, 162.pp. 433-439.

190. Powell, J. H. (1989): Stratigraphy and sedimentation of the Phanerozoic rocks in central and south Jordan, Part B Kurnub, Ajlun and Belqa Groups, Geological mapping Division Bulletin 11B, Geology Directorate, National Resources Authority, Amman.

191. Priestley, C.H.B. and Taylor, R.J. (1972): On the assessment of surface heat flux and evaporation using large-scale parameters, Month. Weather rev., 100, pp. 81-92.

192. Puigdefabregas, J., Barrio, G., Boer M., Gutierrez, L., and Sole, A. (1998): Differential responses of hillslopes and channel elements to rainfall events in a semi-arid area. Geomorphology. 23, pp. 337-251.

193. Quennell, A.M. (1951): The geology and mineral resources of (former) Transjordan, Colonial Geology and mineral resources 2, 85-115. London.

194. Rana, G., Katerji, N. and Mastrorilli, M. (1997): Environmental and soil-plant parameters for modelling actual crop evapotranspiration under water stress conditions, Ecol. Model., 101, pp. 363-371.

195. Rango, A. (1985): Assessment of remote sensing input to hydrologic models. Am. Water Resources Association. Water Resour. Bull., 21, pp 423-432.

196. Rantz, S.E. (1963): An Empirical Method of Determining Momentary Discharge of Tide-Affected Streams, U.S. Geological Survey Water Supply paper 1586-D.

197. Rantz, S.E. (1982a): Measurements and computation of streamflow, Volume 1 Measurements of Stage and Discharge, U.S. Geological Survey Water Supply paper 2175.

198. Rantz, S.E. (1982b): Measurements and computation of streamflow, Volume 2 Computation of Discharge, U.S. Geological Survey Water Supply paper 2175.

199. Rawls, W.J., Brakensiek, D.L. And Saxton, K.E. (1982): Estimation of Soil Water Properties. Transaction of the ASAE, Vol. 25, No. 5, pp. 1316-1320. Published by the American Society of Agricultural Engineers, St. Joseph, Michigan.

200. Refsgaard, J.C. (1996): Terminology, modelling protocol and classification of hydrological model codes. In (Eds.): M.B. Abbot and J.C. Refsgaard: Distributed Hydrological Modelling, pp. 17-39. Kluwer Academic Publishing. The Netherlands.

201. Refsgaard, J.C. and Abbott, M.B. (1996): The role of distributed hydrological modelling in water resources management. In (Eds.): M. B. Abbott and J. C. Refsgaard: Distributed Hydrological Modelling. pp. 1-16. Kluwer Academic Publishing. The Netherlands.

202. Refsgaard, A., Refsgaard, J.C., Jorgenson, G.H., Thomsen, R. and Sondergaard, V. (1994): A hydrological modelling system for joint analysis of regional groundwater resources and local contaminant transport. Danish Hydraulic Institute, pp. 28.

203. Refsgaard, J.C. and Storm, B. (1995): MIKE SHE. In (Ed.): Singh, V.P.: Computer Models of Watershed Hydrology, Water Resources Publications, Colorado, USA, pp. 809–846.

204. Refsgaard, J.C. and Storm, B. (1996): Construction, calibration and validation of hydrological models. In (Eds.): M. B. Abbott and J. C. Resgaard: Distributed Hydrological Modelling, pp. 41-54. Kluwer Academic Publishing. The Netherlands.

205. Renard, K., and Keppel, V. (1966): hydrographs of ephemeral streams in the Southwest. J. Hydraul. Div. ASCE 92, pp. 33-52.

206. Ritter, M. (2009): Hydrologishe Modellierung Des Extremereigness Oktober 2006 in Nahal Harod, Israel. Bachelor thesis (unpublished), Institute of Hydrology, University of Freiburg, Freiburg, Germany.

207. Rosgen, D.L. (1994): A classification of natural rivers, Catena, 22(3), pp. 169-199.

208. Running, S.W., Justice, C.O., Solomonson, V., Hall, D., Barker, J., Kaufmann, Y.J., Strahler, A. H., Heute, A. R., Muller, J. P., Vanderbilt, V., Wan, Z. M., Reillet, P. And Carneggie D. (1994): terrestrial remote Sensing Science and Algorithms Planned for EOS/MODIS. Intl. Journal of Remote Sensing. 15 (17), pp. 3587-3620.

209. RWC (2009): Royal Water Committee, Water for life, Jordan's Water Strategy 2008-2022.

210. Sabins, F. F. (1997): Remote Sensing: Principles and Interpretation. 3rd edition, W. H. freeman and Company, New York.

211. Salameh, E. (1996): Water quality degradation in Jordan (Impacts on environment, economy and future generations resources base). Amman, Jordan.

212. Salameh, E. (2009): Effects of climatic changes on surface and groundwater resources in the northwestern part of Jordan. European Water Resources Association (EWRA) 7th International Conference, Limassol, Cyprus, June 25-27, 9 p.

213. Salameh, E. and Bannayan, H. (1993): Water Resources of Jordan, Present Status and Future Potentials. Friedrich Ebert Stiftung, Amman.

214. Salameh, E. and Udluft, P. (1985): The hydrodynamic pattern of central Jordan, Geol.Jb, c38, Hannover.

215. Salas, J. (1992): Analysis and modelling of hydrologic time series. In (Ed): Maidment, D.: Handbook of Hydrology. McGraw-Hill.

216. Salzgitter Consult GMBH and Jordanian Consulting Engineer Co. JCE (1992): Studies of raising Kafrein dam- Final report on technical, economic and financial feasibility and preliminary design. Part II- main report, prepared to Ministry of Water and Irrigation - Jordan Valley Authority, Amman.

217. Sawarieh, A., Ali, W. and Wolf, L. (2008): Technical Note on Water Budget Calculations in Wadi Kafrein. University of Karlsruhe, Germany.

218. Saxton, k.E. and P.H. Willey (2006): The SPAW model for agricultural filed and pond hydrologic simulation. Pp. 401-435. In: V. P. Singh and D. K. Frevert (Eds.). Watershed models. CRC Press, Boca Raton, Florida.

219. Scharffenberg, W. and Fleming, M. (2009): Hydrologic Modelling System HEC-HMS. User's manual, Ver. 3.4. US Army Corps of Engineers, Hydrologic Engineering Center, Washington, DC, USA.

220. Scheutz, T. (2006): Prozessbasierte Niederschlags-Abflussmodellierung in einem mediterranen Kleineinzugsgebiet-Wadi Anabe, Israel. Diplomarbeit am Institut für Hydrologie, Albert-Ludwigs-Universität Freiburg i. Br.

221. Schick, A.P. (1971): A Desert flood: physical characteristics, effects on Man, geomorphic significance, human adaption- a case study in the southern Arava watershed. Jerusalem Stud. Geogr. 2, pp. 91-155.

222. Schmuge, T. (1983): Remote sensing of soil moisture with microwave radiometers. Trans. Am. Soc. Agr. Eng. 26, pp 748-753.

223. Schultz, G. (1994): Meso-scale modelling of runoff and water balances using remote sensing and other GIS data. Hydrological Sciences-Journal-des Sciences Hydrologiques, 39, 2, April 1994.

224. Schultze, F., Lewy, Z., Kuss, J. and Gharaibeh, A. (2003): Cenomanian-Turonian carbonate platform deposits in west central Jordan. Int. J. earth Sci. 92: pp. 641-660.

225. Schultze, F., Marzouk, A.M., Bassiouni, M.A.A. AND Kuss; J. (2004): The late Albian-Turonian carbonate platform succession of west-central Jordan: Stratigraphy and crises. Cretaceous Research, 25, pp. 709-737.

226. Sellers, P.J., Randall, D. A., Collatz, G.J., Berry, J.A., Field, C.B., Dazlich, D.A., Zhang, C., Collelo, G.D., and Bounoua L. (1996): A revised land surface parameterization (SiB2) for atmospheric GCMs. Part I: model formulation, J. Climate, 9, pp. 676-705.

227. Sen, Z. (2008): Wadi Hydrology. CRC Press, Tayler and Francis Group, England.

228. Shadeed, S. (2008): Up to date hydrological modelling in arid and semi arid catchment, the case of Faria catchment, West Bank, Palestine. PhD thesis, Institute of Hydrology, University of Freiburg, Germany.

229. Shawabkeh, K.F. (2001): Geological map of Karama- 3153-IV, 1:50:000, The Hashemite kingdom of Jordan, Natural Resources Authority, Geology Directorate, Amman.

230. Sheffer, N.A, Dafny, E., Gvirtzman, H., Navon, S., Frumkin, A. and Morin, E. (2010): Hydrometeorological daily recharge assessment model

(DREAM) for the Western Mountain Aquifer, Israel: Model application and effects of temporal patterns. Water Resour. Res., 46, W05510, doi: 10.1029/2008WR007607.pp. 1-16.

231. Shehadeh, N. (1990): The Climate of Jordan. 1st edition, Dar Al-Bashir, Amman-Jordan.

232. Shentsis, I. and Rosenthal, D. (2003): Recharge of aquifers by flood events in an arid region. Hydrological Processes 17 (4), pp. 695-712.

233. Sherman, L. K. (1932): Streamflow from Rainfall by the Unit Graph Method. Eng. News Rec., 108, 501-505.

234. Short, N.M. (2010): Remote Sensing Tutorial. Section 1: Image Processing and Interpretation-Morro Bay, California. The National Aeronautics and Space Administration (NASA). http://rst.gsfc.nasa.gov/

235. Shuttleworth, W. and Wallace J.S. (1985): Evaporation from sparse crops-an energy combination theory. Quart. J. R. Met. Soc. 111, pp. 839-855.

236. Simmers, I. (2003): Understanding Water in a Dry Environment, Hydrological Processes in Arid and Semi-arid Zones. A.A. Balkema Publishers.

237. Simons, P.K. (1978): The River Scene: comments on North Island Rivers. In: Proceedings of Erosion Assessment and Control conference, Christchurch, New Zealand, New Zealand Association of Soil Conservators, pp. 156-158.

238. Singh, J. (1995): Computer models of watershed hydrology. Water resources Publications.

239. Singh, V.P. (2004): Flow Routing in Open Channels: Some recent Advances. Proceedings, river Flow 2004, June 23-25, Naples-Italy.

240. Sleigh, P.A. and Goodwill. I.M. (2000): The St Venant equations. http://www.efm.leeds.ac.uk/CIVE/CIVE3400/stvenant.pdf.

241. Smadi, M. (2006): Observed abrupt changes in minimum and maximum temperatures in Jordan in the 20th century. American Journal of Environmental Sciences 2 (3). Pp. 114-120.

242. Smith, R.C.G., Barrs, H.D. and Fisher, R.A. (1988): Inferring stomatal resistance of sparse crops from infrared measurements of foliage temperature, Agric. For. Meteorol., 42, pp. 183-198.

243. Stannard, D.I. (1993): Comparison of Penman-Monteith, Shuttleworth-Wallace, and Modified Priestly-Taylor Evapotranspiration Models for Wildland Vegetation in Semiarid rangeland. Water Resources Research, Vol. 29, No. 5, pp. 1379-1892.

244. Stefanov, W.L. and Netzband, M. (2005): Assessment of ASTER land cover and MODIS NDVI data at multiple scales for ecological characterization of an arid urban center. Remote Sensing of the Environment. 99, pp. 31-43.

245. Stephenson, G.R. and Freeze, R.A. (1974): Mathematical simulation of subsurface flow contributions to snowmelt runoff, Reynolds Creek Watershed, Idaho, Water Resources Research, 10, pp. 284-294.

246. Storck, P., L. Bowling, P. Wetherbee and D. Lettenmaier, 1998: Application of a GIS-based distributed hydrology model for prediction of forest harvest effects on peak stream flow in the Pacific Northwest, Hydrol. Process., 12, 889-904

247. Storm, B. and Refsgaard, A. (1996): Distributed physically-based modelling of the entire land phase of the hydrological cycle. In (Eds.): M.B. Abbot and J.C. Refsgaard: Distributed Hydrological Modelling. Dordrecht, the Netherlands: Kluwer Academic Publishing.

248. Storm, B., Jensen, K. and Refsgaard, J. (1988): Estimation of catchment rainfall uncertainty and its influence on runoff predication. Nordic Hydrology, 19, pp. 77-88.

249. Tarboton, D. (2003): Rainfall-Runoff Processes, a workbook to accompany the Rainfall-Runoff Processes Web module. Utah State University.

250. Teimah, M. and Abu Saad, L. (1993): A study of the Ajlun and Batn el Ghoul Groups along the Ras en Naqab Escarpment- Internal report, Subsurface Geology Division, Natural Resources Authority, Amman.

251. Thompson R. (2004): Complexity, Diminishing Marginal Returns and Serial Mesopotamian Fragmentation. Journal of World Systems Research 28: 1187.

252. Thormählen, A. (2003): Hydrological modelling in a small hyperarid catchment Nahal Yael, Israel - runoff generation and transmission losses. Master thesis (unbublished), Institute of Hydrology, Freiburg University, Germany.

253. Thyer, M., Beckers, J., Spittlehouse, D., Alila, Y. and Winkler, R. (2003): Challenges in the modelling of forest and clearcut hydrologic processes at the stand level and catchment scale: Case of the Upper Penticton Creek Watershed Experiment, Water Resour. Res., in review.

254. Titarov, P.S. (2008): Evaluation of Cartosat 1 Geometric Potential. The International Archives of the Photogrammetry, Remote Sensing and Spatial Information Sciences. Vol. XXXVII. Part B1. Beijing.

255. Todini, E., and Wallis, J. (1977): Using CLS for daily or longer period rainfall-runoff modelling. In (Eds): T. Ciriani, U. Maione and J.

Wallis: Mathematical Models for Surface Water Hydrology. John Wiley & Sons. New York.

256. Tung, Y. and Asce, A. (1985): River Flood Routing By Nonlinear Muskigum Method. Jor. Of Hydraulic Engineering. Vol. 111,No. 12.

257. UNDP (1994): United Nation Development Programme, Water Reference Book for Jordan-Unpubl. Rep. No. DP/UN/JOR/87/003 prepared for MWI, Spring Flow in Jordan, Amman.

258. UNEP (1997): Global Environmental Outlook. United Nations Environmental Programme and Oxford University Press, Oxford, UK, pp. 106-115 and 201-210.

259. USDA (1975): US Department of Agriculture, Soil Taxonomy. A Basic System of Soil Classification for Making and Interpreting Soil Surveys. Agric. Handbook No 436. Soil Survey Staff, USDA Washington DC.

260. USDA (1985): US Department of Agriculture, SCS national engineering handbook, Sect. 4: Hydrology, Soil Conservation Service, USDA, Washington DC.

261. USDA (1990): US Department of Agriculture, Keys to Soil Taxonomy, SMSS. Technical Monographs Nos 18, 19. Blacksburg, Virginia.

262. USDA (1999): US Department of Agriculture, Soil Taxonomy. Agric. Handbook No 436. Soil Conservation Services, USDA Washington DC.

263. Van Genuchten, M. (1978): Numerical Solutions of the one-dimensional saturated-unsaturated flow equation. Dept. of Civil Engineering, Princeton University, New Jersey, Rep. 78-WR-09, pp. 91.

264. Van Genuchten, M. (1980): A Closed-form Equation for Predicting the Hydraulic Conductivity of Unsaturated Soils. Soil Sci. Soc. Am. J. 44. pp. 892-898.

265. VanShaar, J.R., I. Haddeland, and Lettenmaier, D.P. (2002): Effects of land cover changes on the hydrologic response of interior Columbia River Basin forested catchments, Hydrol. Process., 16, 2499-2520.

266. Vorosmarty, C.J., Federer, C.A. and Schloss, A.L. (1998): Potential evaporation functions compared on US watersheds: possible implications for global-scale water balance and terrestrial ecosystem modelling. J. Hydrol. 207, pp. 147-169.

267. WAJ (1986): Water Authority of Jordan, Spring Flow Data in Jordan prior to October 1985- Technical Paper, 51, Amman.

268. WAJ and BGR (1994): Water Authority of Jordan (WAJ) and the Federal Institute for Geosciences and Natural Resources (BGR), Ground Water Resources of Northern Jordan; Vol 3. Structural features of the main hydrogeological units in Northern Jordan, Project No. 89.2105.8, Amman.

269. WAJ and BGR (1996): Water Authority of Jordan and the Federal Institute for Geosciences and Natural Resources (BGR), Ground Water Resources of Northern Jordan; Vol 1. Rainfall, Spring Discharge and Baseflow, Part 2. Spring Discharge in Northern Jordan, Project No. 89.2105.8, Amman.

270. Wang, Q., Adiku, S., Tenhunen, J. And Granier, A. (2005): On the Relationship of NDVI with Leaf Area Index in a Deciduous Forest site. Remote Sensing of Environment. 94, pp. 244-255.

271. Wei, T.C. and McGuinness, J. L. (1973): Reciprocal squared method, a computer technique for estimating area precipitation, ARS-NC-8, U.S. Agricultural research Service, North Central Region, Coshocton, Ohio.

272. Weinmann, P.E. and Laurenson, E.M. (1979): Approximate Flood Routing methods: A review. Jor. Of Hydraulic Div., ASCE 105 (HY2). Pp. 1521-1535.

273. Werz, H., (2006): The use of remote sensing imagery for groundwater risk intensity mapping in the Wadi Shueib, Jordan. PhD thesis, Department of Applied Geology, University of Karlsruhe, Germany.

274. Wetzel, R. and Morton, D.M. (1959): Contribution a la Geologie de la Transjordanie. In L. Dubertret (editor), Notes et Memories sur le Moyen Orient, VII, pp. 95-191, Museum national d'Histoire Naturelle, Paris.

275. Wetzel, R., Morton, D.M. and Nasr, S.N. (1947): Stratigraphic sections of Jordan Valley and Dead Sea Pt. Amman: Min. Nat. Econ. pp. 1-37.

276. Wheater, H. (2008): Modelling hydrological processes in arid and semi-arid areas: an introduction to the workshop. In (Eds.): Wheater, H., Sorooshian, S. and Sharma, K.: Hydrological Modelling in Arid and Semi-Arid Areas, Cambridge University Press.

277. Wheater, H., Sorooshian S. and Sharma K. (2008): Hydrological Modelling in Arid and Semi-Arid areas. Cambridge University Press, New York.

278. Widmoser, P. (2009): A discussion on and alternative to the Penman-Monteith equation, Agr. Water Manage., 96, pp. 711-721.

279. Wigmosta, M.S. and L.R. Leung, (2001): Potential impacts of climate change on streamflow and flooding in forested basins, In (Eds.): R.C Sidle and M. Chigira: The influence of Environmental Change on

Geomorphological Hazards in Forested Areas, Centre for Agriculture and Biosciences International.

280. WMO (1980): World Meteorological Organization: Manual on stream gauging. Volume 1: Fieldwork- Volume 2: Computation of discharge, Operational hydrology Report n. 519, Geneva.

281. WMO (1986): World Meteorological Organization: level and discharge measurements under difficult conditions, Operational hydrology Report n. 24, n. 650, Geneva.

282. WMO (1994): World Meteorological Organization: Guide to hydrological practices. WMO- No. 168. 5th edition.

283. Wolfart, R. (1959): Geology and hydrogeology of the Irbid district (Hashemite Kingdom of Jordan). Bundesanstalt für Bodenforschung, Hannover.

284. Wolfart, R. (1966): Zur Geologie und Hydrogeologie von Syrien- unter besonderer Berücksichtigung der suedlichen und nordwestlichen Landesteile. Beiheft Geol. Jb. 68, 129 p, Hannover.

285. Wu, W. and Shao, G. (2002): Optimal Combinations of data, Classifiers, and Sampling Methods for Accurate Characterizations of Deforestation. Canadian Journal of Remote Sensing. 28 (4), pp. 6011-609.

286. Wundt, W. (1937): Beziehung zwischen Mittelwerten von Niederschlag, Abfluß, Verdunstung und Lufttemperatur für die Landflächen der Erde, deutsche Wasserwirtschaft, 32. Jg., H. 5 und H.6.

287. Wundt, W. (1939): Die Verdunstung von den landflächen der Erde im Zusammenhang mit der Temperatur und dem Niederschlag, Zeitschrift für angewandte Meteorologie, 56. Jg., H. 1.

288. Xevi, E., Christiaens, K., Espino, A., Sewnandan, W., Mallants, D., Sorensen, H. And Feyen, J. (1997): Calibration, Validation and Sensitivity Analysis of the MIKE-SHE Model Using the Neuenkirchen Catchment as Case Study. Water Resources Management. 11, pp 219-242.

289. Yamaguchi, Y., Kahle, A.B., Tsu, H., Kawakami, T. and Pniel, M. (1998): Overview of Advanced Spaceborne Thermal Emission and Reflection Radiometer (ASTER). IEEE Transactions on Geoscience and Remote Sensing, 36, pp. 1067-1071.

290. Yapo, P.O. Gupta, H.V. and Sorooshian, S. (1998): Multi-objective global optimization for hydrologic models, Journal of Hydrology, 204, pp. 83-97.

291. Ye, W., Bates, B.C., Viney, N.R., Sivapalan, M. and Jakemann, A.J. (1997): Performanceof conceptual rainfall-runoff models in low-yielding

ephemeral catchments. Water Resources Research, Vol. 33, pp 153-160.

292. Zachman, W.R. (1984): A river classification system: management for Minnesota's rivers. In: Proceedings of the 1984 River Recreation Symposium. October 31-November 3, Baton Rouge, Louisiana: Louisiana State University, pp. 619-627.

293. Zhao, Q., Liu, Z. Li, M., Wei, Z. And Fang S. (2009): The snowmelt runoff forecasting model of coupling WRF and DHSVM. Hydrol. Earth Syst. Sci. Discuss, 6, pp 3335-3357.available for open-access review under www.hydrol-earth-syst-sci-discuss.net/6/3335/2009.

294. Zhu, G. and Blumberg. D.G. (2002): Classification using ASTER data and SVM algorithims; The case study of Beer Sheva, Israel. Remote Sensing of Environment, 80, pp. 223-240.

295. Ziegler, A., Giambelluca, T., Sutherland, R., Nullet, M., Yarnasarn, S., Pinthong, J.,Preechapanya, P. and Jaiaree, S. (2004): Toward understanding the cumulative impacts of roads in upland agricultural watersheds of northern Thailand. Agriculture, Ecosystems& Environment 104, 145–158.

Appendixes

Appendix A
Springs in Wadi Kafrein (long term average 1980-2006)

ID No	English Name	X PNG*	Y PNG*	Altitude (m)	Aquifer	Av. Discharge (m3/hr)
AN0502	BAHHATH	226300	1146000	625	Hummar (A4)	397
AN0504	WADI EL SHITA	226100	1146800	615	Hummar (A4)	2.2
AN0510	EL KUBRA	229100	1143400	825	Hummar (A4)	4.2
AN0512	EL KASHABEH	228700	1143100	805	Hummar (A4)	0.7
AN0514	EL JAMI'	228500	1142800	800	Hummar (A4)	4.9
AN0516	EL BALAD (NA'UR)	228300	1143000	770	Hummar (A4)	5.9
AN0518	EL NASARA	228200	1143200	750	Naur (A2/A1)	16.1
AN0530	DALIYA	227400	1152400	800	Wadi Sir (A7)	17.7
AN0532	KURSI	227500	1151700	800	Wadi Sir (A7)	55.7
AN0534	WADI ES SIR	227298	1151370	715	Wadi Sir (A7)	379.7
AN0536	KHEIL	227200	1151400	715	Wadi Sir (A7)	77.9
AN0542	DEIR EL FOUQA	225000	1149200	540	Hummar (A4)	80.8
AN0544	DEIR EL TAHTA	224300	1148800	570	Hummar (A4)	124.7
AN0546	EL KHOUR	223400	1149300	580	Naur (A2/A1)	2.9
AN0550	UM FARWAH	223300	1150200	625	Hummar (A4)	3.0
AN0554	TARABIL	222800	1148100	500	Naur (A2/A1)	42.4
AN0556	EL MANAKHIR	222100	1147700	480	Naur (A2/A1)	6.0
AN0558	EL QASIR	221900	1147100	400	Naur (A2/A1)	2.4
AN0566	AIN WADI KUFREIN	222000	1143100	180	Kurnub	64.7
AN0570	ADASIYEH GHARBIYA	222000	1141000	450	Naur (A2/A1)	5.1
AN0572	ADASIYA SHARQIYA	222200	1141100	450	Naur (A2/A1)	4.5
AN0574	UM ZWEITEENEH	222800	1141800	500	Naur (A2/A1)	12.2
AN0577	AL BUHAIRA EL TEHTA	223306	1143827	184	Hummar (A4)	18.8
AN0578	AL BUHAIRA EL FOUQA	223361	1143914	184	Hummar (A4)	25.3
AN0579	AL FUQARA AL FOUQA	222646	1143369	191	Naur (A2/A1)	29.8
AN0580	AL FUQARA AL TEHTA	222599	1143299	200	Naur (A2/A1)	16.6

* Coordinates are in Palestinian grid

Appendix B
Satellite Images/ASTER

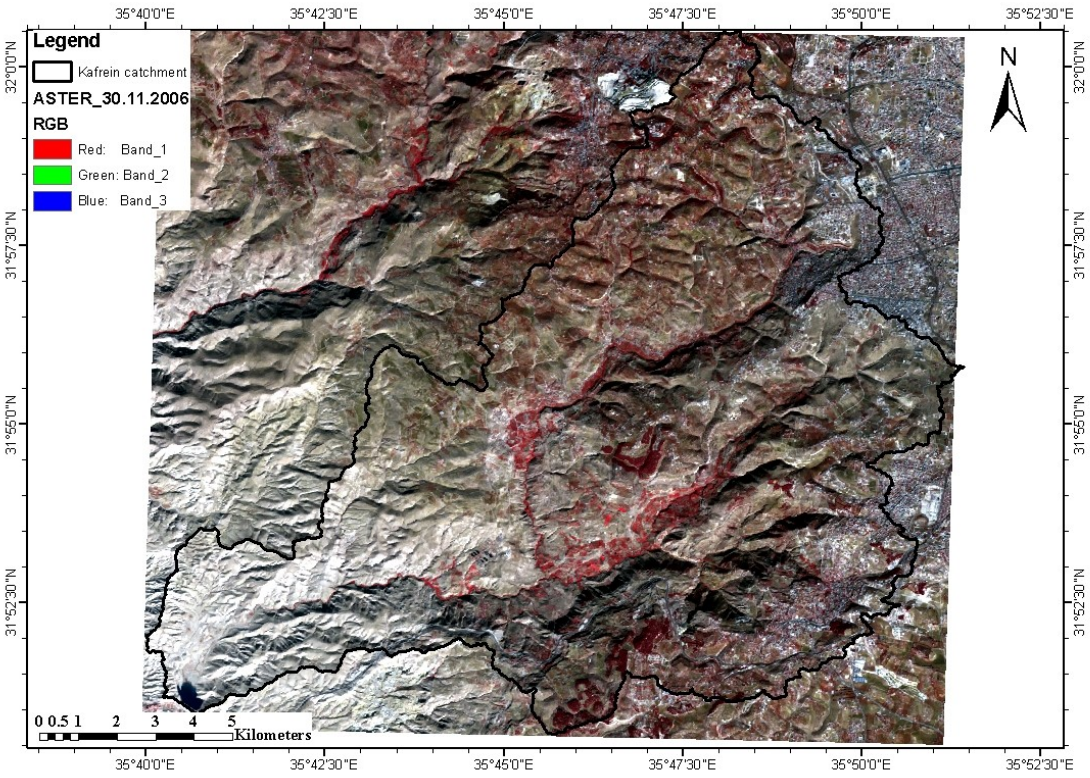

ASTER image of November 2006

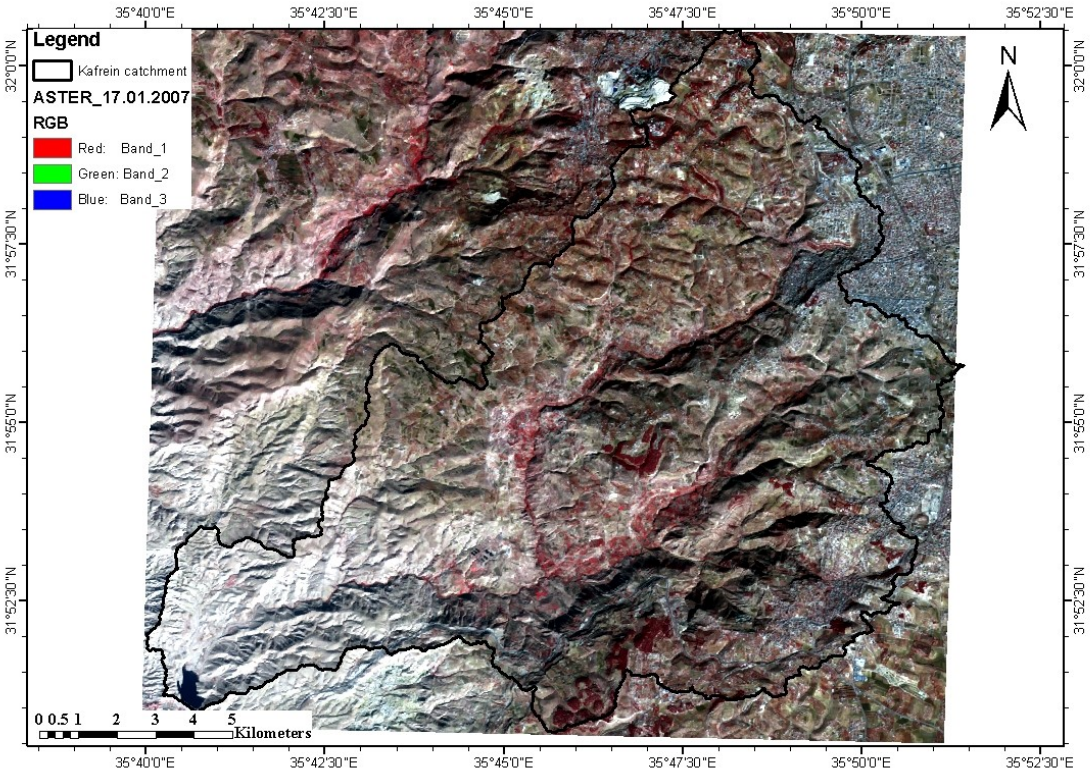

ASTER image of January 2007

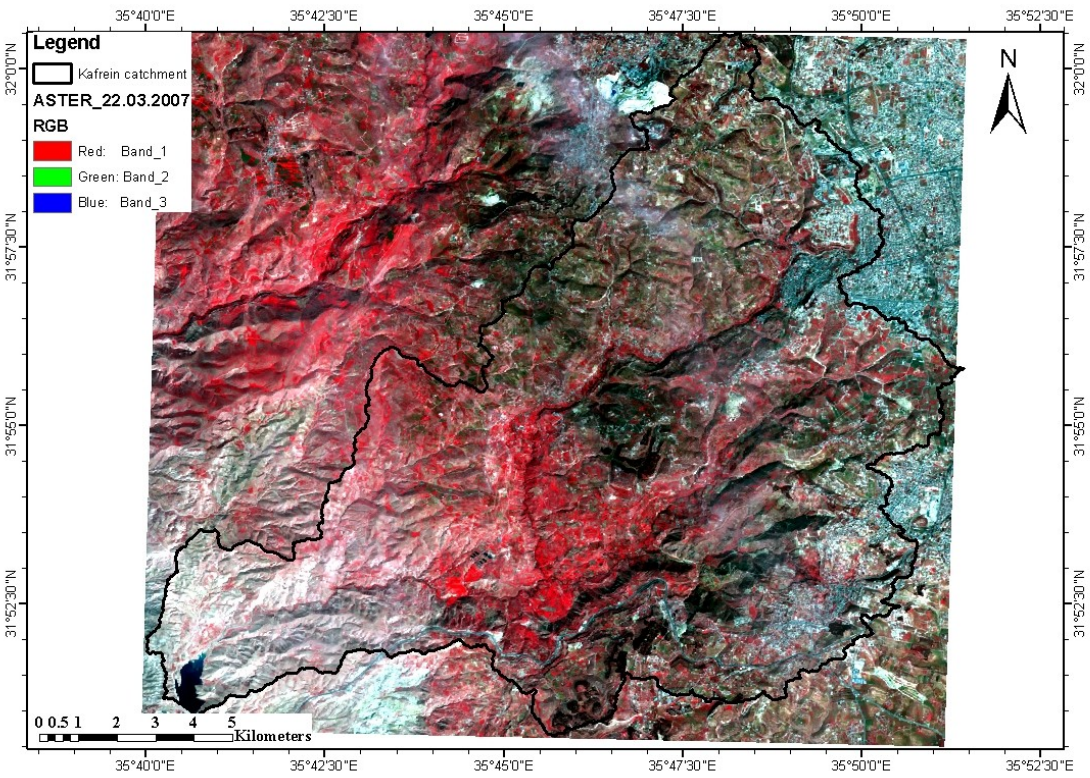

ASTER image of March 2007

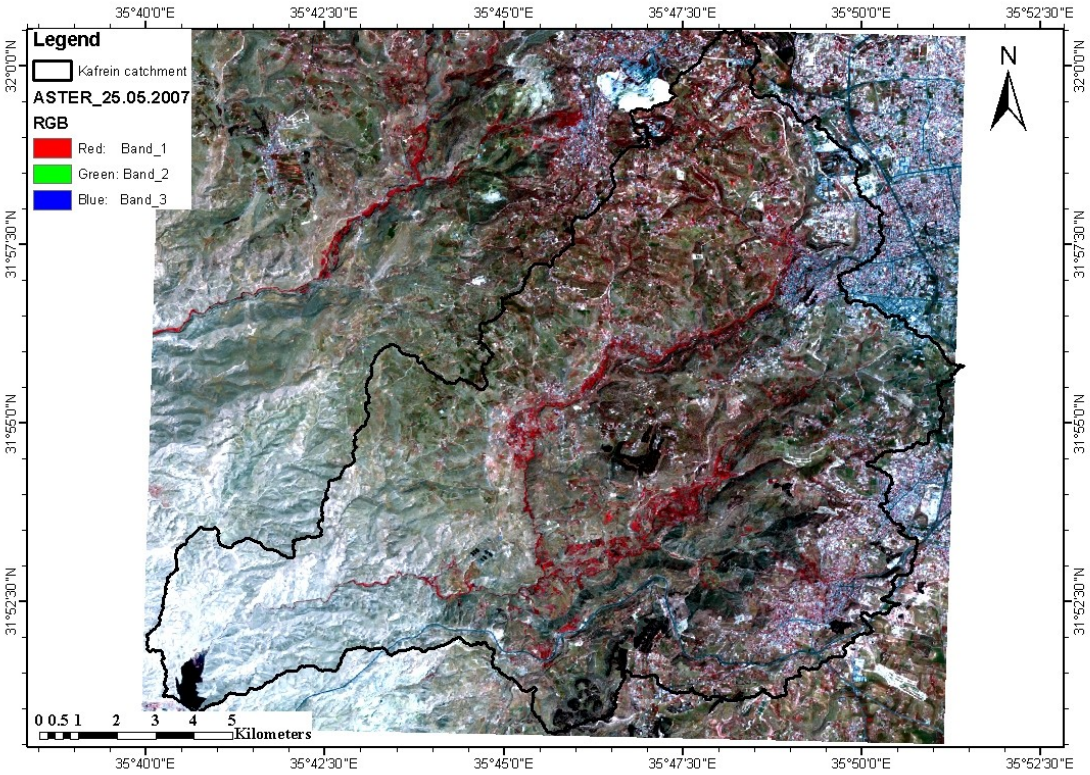

ASTER image of May 2007

Appendix C
Land Cover classification maps

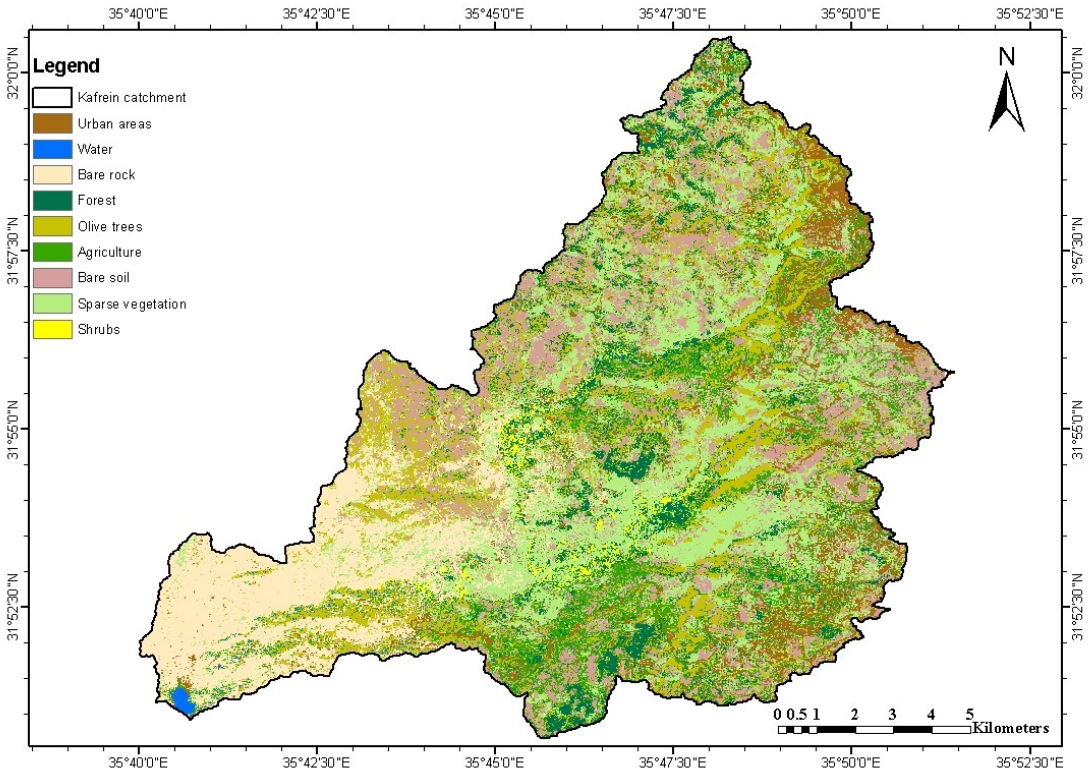

Land Cover map of November 2006

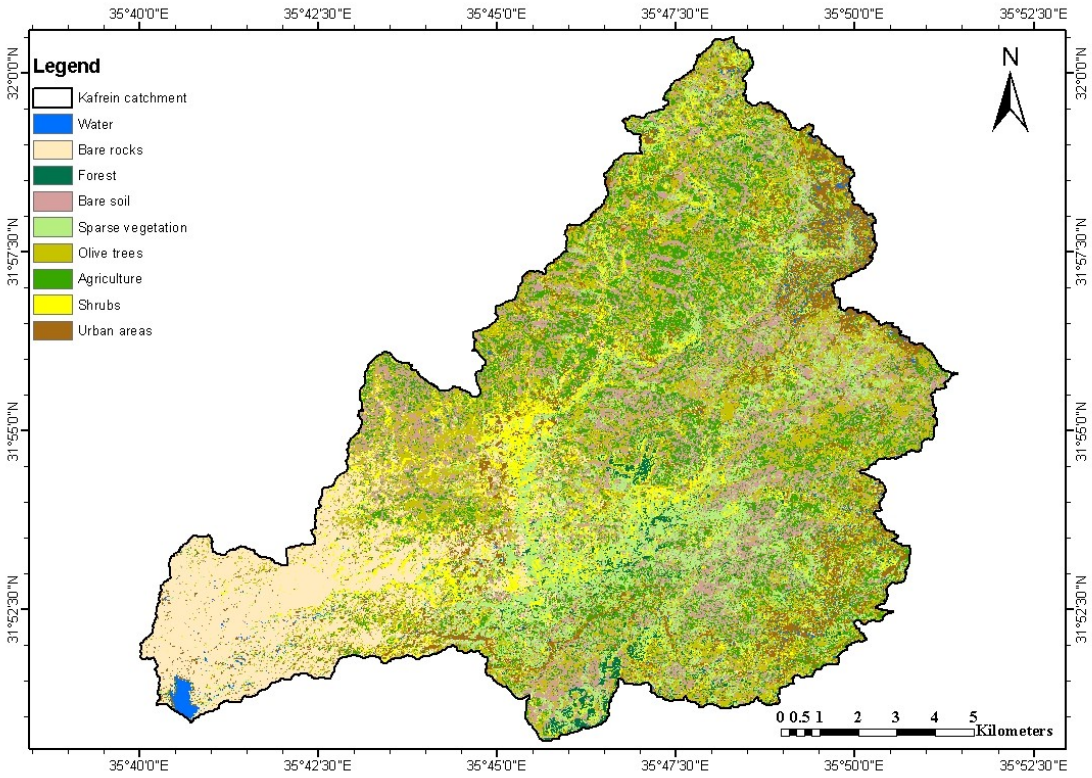

Land Cover map of January 2007

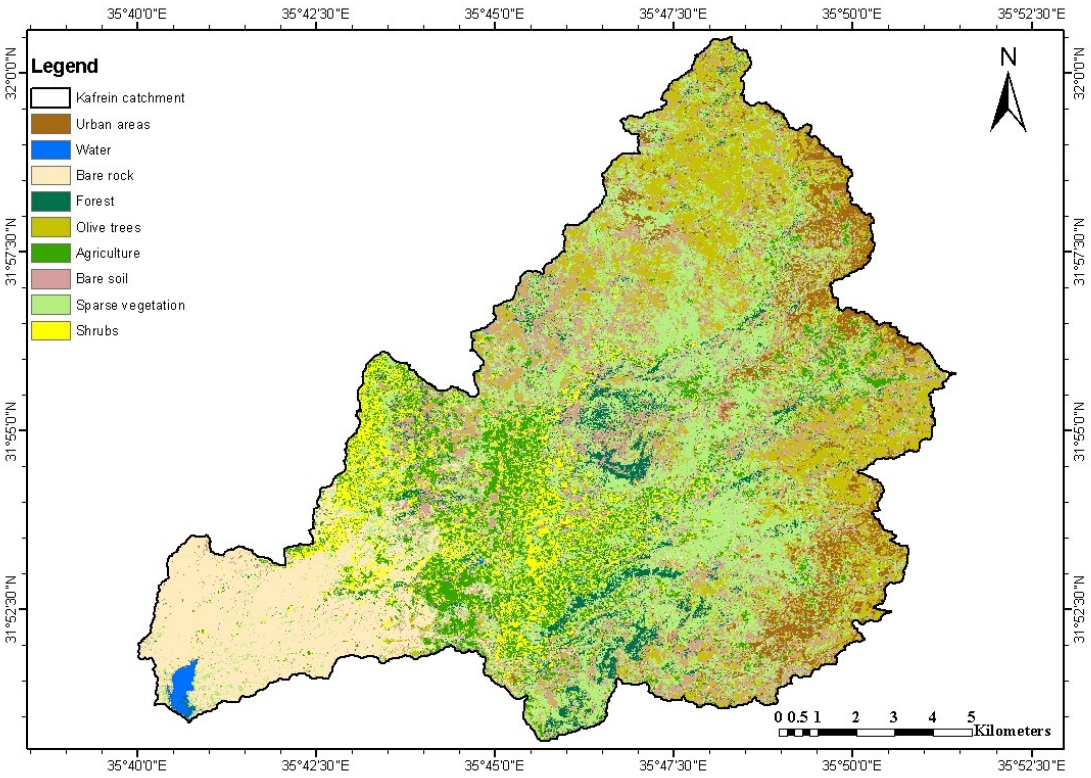

Land Cover map of March 2007

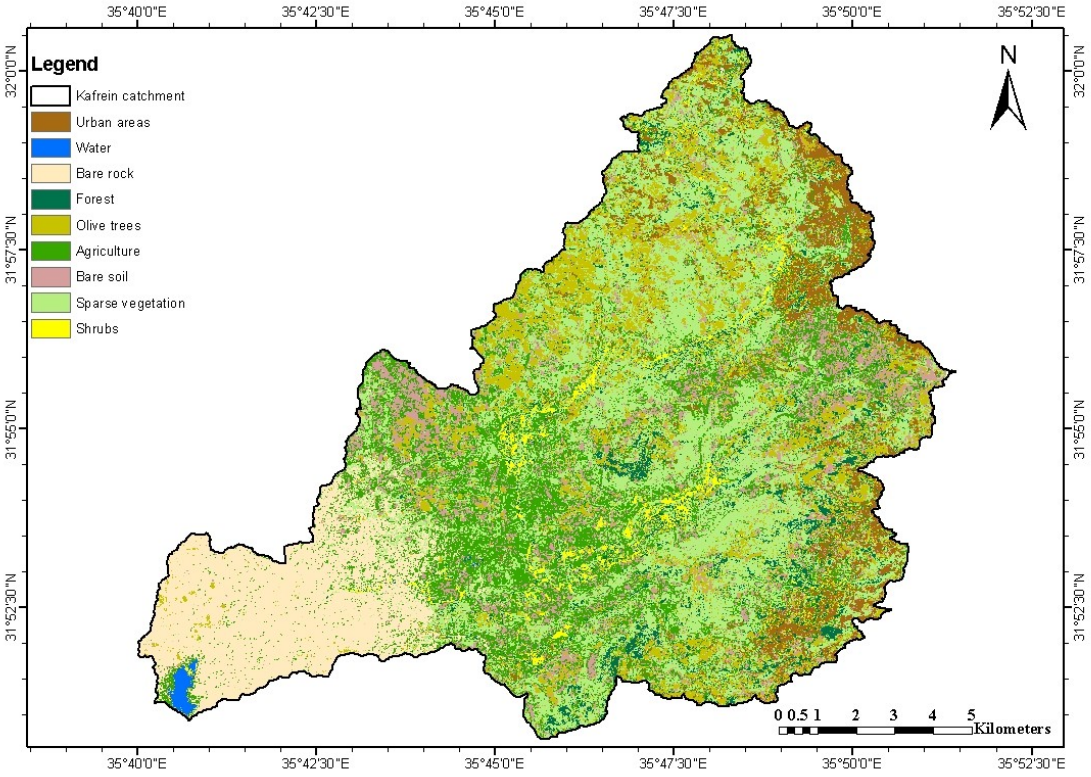

Land Cover map of May 2007

Appendix D
NDVI-DS maps

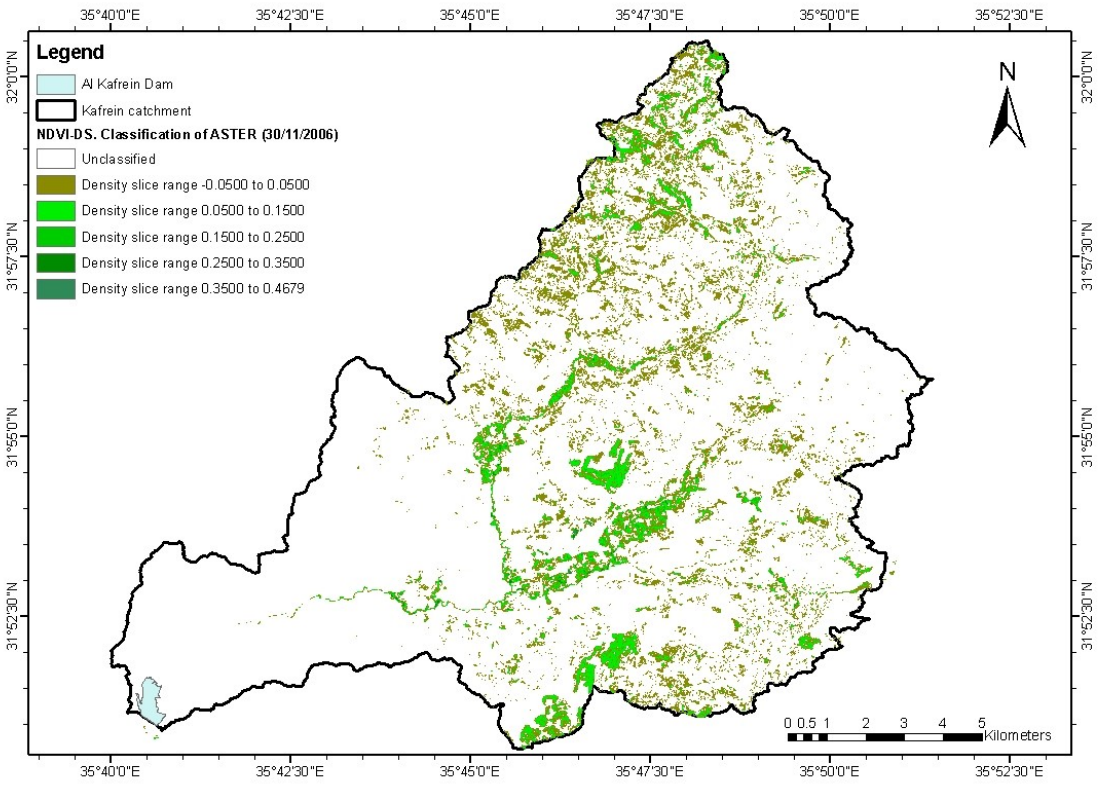

NDVI-DS map of November 2006

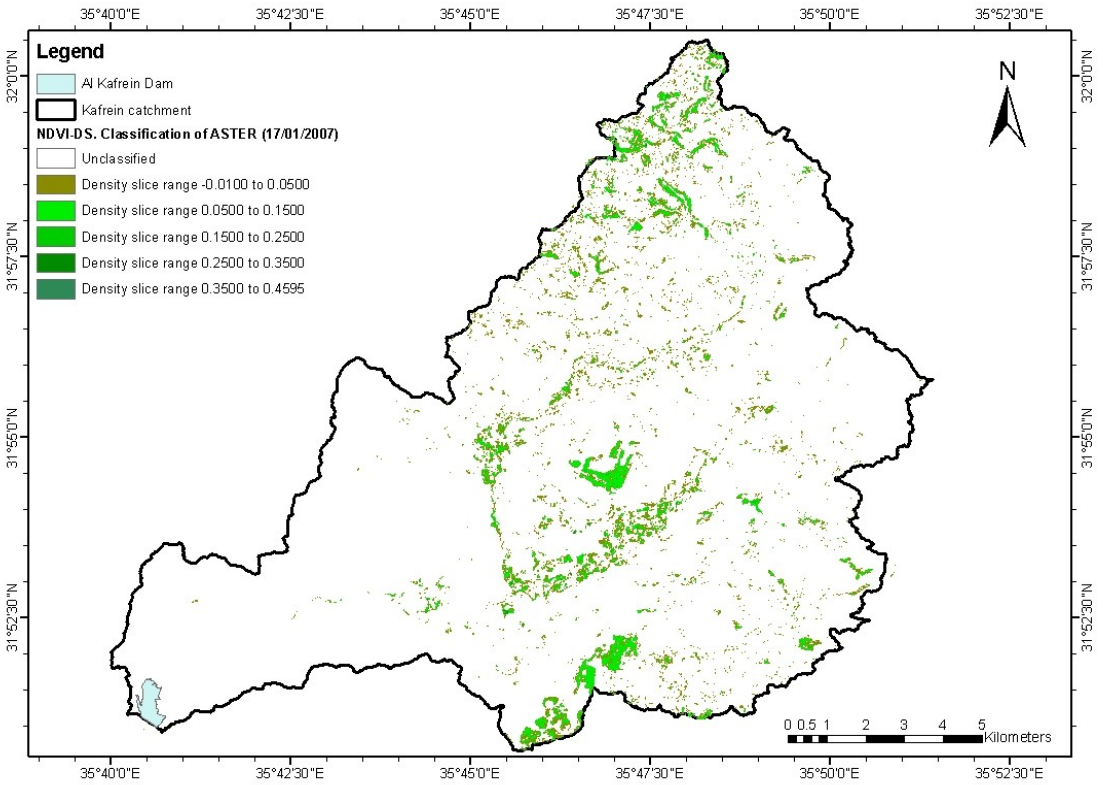

NDVI-DS map of January 2007

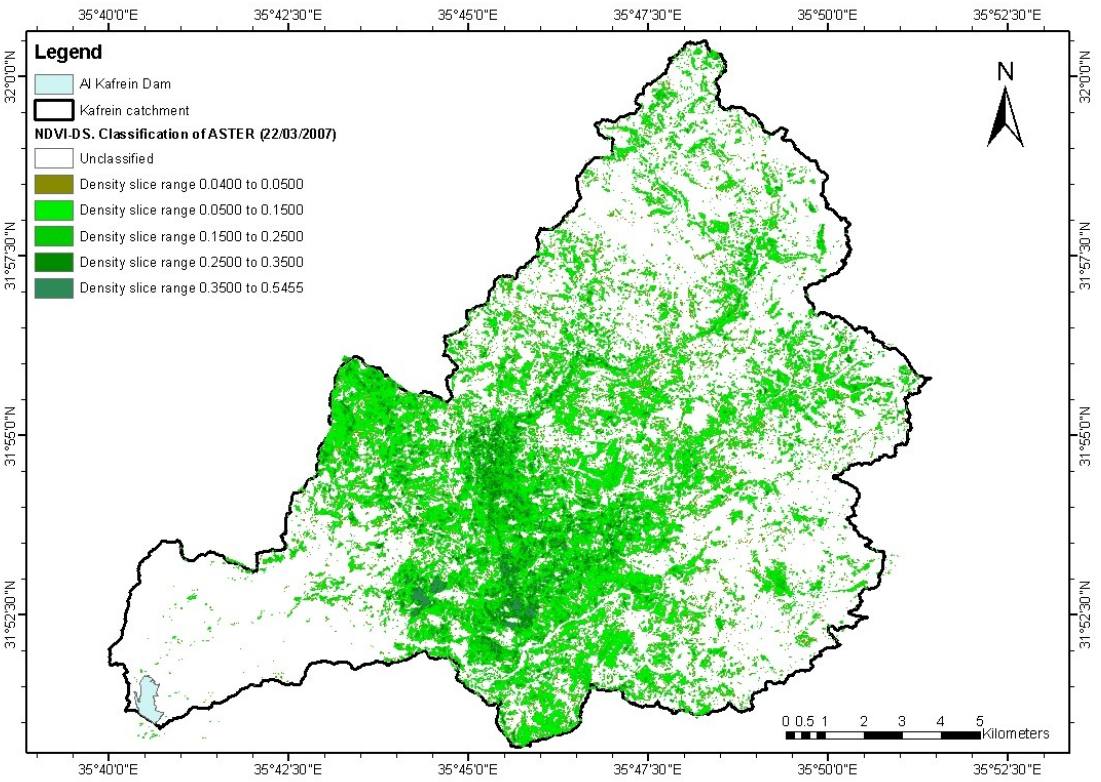

NDVI-DS map of March 2007

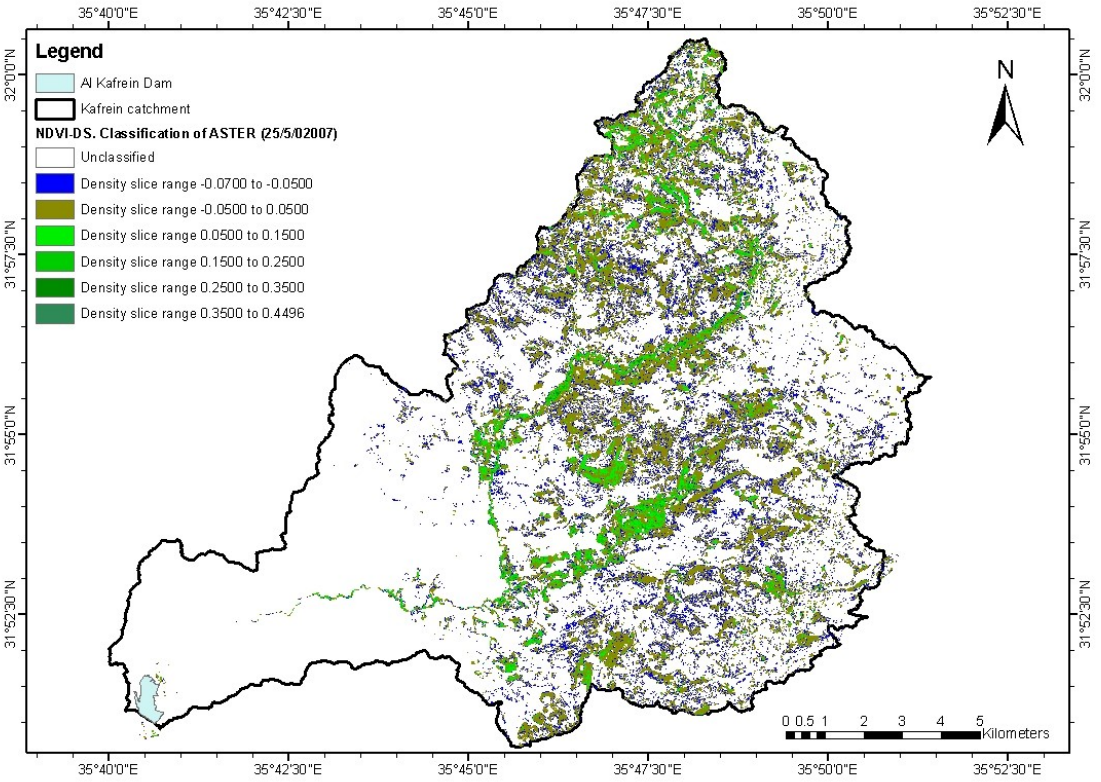

NDVI-DS map of May 2007

C.V.: William Alkhoury

Education:

Mar.2007-Mar.2011	Ph.D. student and research assistant at Geoscience Center, Department of Applied Geology, University of Göttingen, Germany.
Oct.2002–May2005	Master of Science study: Thesis title "The water constituents of King Abdullah Canal and their role in the eutrophication processes". Faculty of Graduate studies, University of Jordan, GPA (3.75 / 4).
1998–2002	B.Sc. Degree in Environmental and Applied Geology. Faculty of Science, University of Jordan, GPA (2.92 / 4).

Experience:

Mar.2006-Feb.2007	Research Assistant at the Center for Environmental System Research (CESR), University of Kassel, Germany.
Feb.2003–May2005	Teaching Assistant at the Department of Geology, University of Jordan, Jordan.
Oct.2002–Jul. 2003	Research Assistant in a project entitled: "The changes in the Dead Sea level, and its influence on the groundwater resources of its surroundings", University of Jordan. (Supervision: Prof. Elias Salameh).
May–Jul.2002	Research Assistant in a Jordanian-German project entitled: "The groundwater budget in the Jordan Valley ", two phases: 1.Electromagnetic measurements, (MAXMIN measurement). 2.Geoelectric measurements, (Supervision: Prof. Hinz Hoetzl).
Mar.–Apr.2002	Research Assistant in a Jordanian-German project entitled: "The groundwater resources of Wadi Shueib area", Hydrology and Hydrochemistry. (Glowa II Project).

Personal information:

Date of birth: 03/06/1980.
Nationality: Jordanian.
Residency: Göttingen, Germany.